NISTIR 8132

Applied and Computational Mathematics Division

Summary of Activities for Fiscal Year 2015

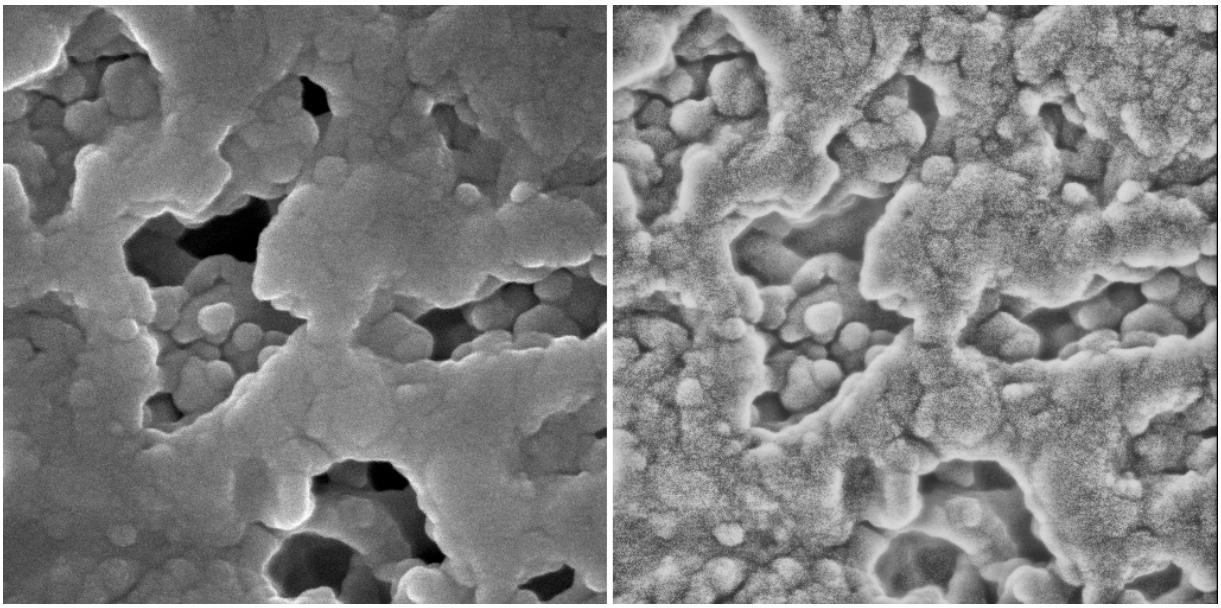

This publication is available free of charge from:
http://dx.doi.org/10.6028/NIST.IR.8132

National Institute of Standards and Technology
U.S. Department of Commerce

NISTIR 8132

Applied and Computational Mathematics Division

Summary of Activities for Fiscal Year 2015

Ronald F. Boisvert, Editor
Applied and Computational Mathematics Division
Information Technology Laboratory

This publication is available free of charge from
http://dx.doi.org/10.6028/NIST.IR.8132

May 2016

U.S. Department of Commerce
Penny Pritzker, Secretary

National Institute of Standards and Technology
Willie E. May, Under Secretary of Commerce for Standards and Technology and Director

Abstract

This report summarizes recent technical work of the Applied and Computational Sciences Division of the Information Technology Laboratory at the National Institute of Standards and Technology (NIST). Part I (Overview) provides a high-level overview of the Division's activities, including highlights of technical accomplishments during the previous year. Part II (Features) provides further details on three projects of particular note this year. This is followed in Part III (Project Summaries) by brief synopses of all technical projects active during the past year. Part IV (Activity Data) provides listings of publications, technical talks, and other professional activities in which Division staff members have participated. The reporting period covered by this document is October 2014 through December 2015.

For further information, contact Ronald F. Boisvert, Mail Stop 8910, NIST, Gaithersburg, MD 20899-8910, phone 301-975-3812, email boisvert@nist.gov, or see the Division's web site at http://www.nist.gov/itl/math/.

Cover Visualization: An image captured by a NIST scanning electron microscope (left), and an enhanced version resulting from postprocessing developed by ACMD mathematicians (right). This recently discovered technique for enhancing certain classes of imagery involves an initial adaptive histogram equalization of the image, followed by progressive Lévy fractional diffusion smoothing. For details, see page 30.

Section Visualizations: The word cloud found at the start of each Part of this document was created using Wordle, http://www.wordle.net/, using the text of this document as input.

Acknowledgements: Thanks to Lochi Orr for assisting in the compilation of Parts III and IV of this document. Thanks also to Oliver Slattery and Shahram Orandi who each carefully read the manuscript and offered many corrections and suggestions for improvement.

Contents

PART I: OVERVIEW **1**

Introduction **3**

Highlights **5**

Technical Accomplishments *5*
Technology Transfer and Community Engagement *7*
Staff News *10*
Recognition *11*

PART II: FEATURES **13**

A Strong Loophole-Free Test of Local Realism **15**

Uncertainty Quantification in Molecular Dynamics for Aerospace Polymers **18**

The Resilience of the Internet to Colluding Country Induced Connectivity Disruptions **21**

PART III: PROJECT SUMMARIES **25**

Mathematics of Metrology **27**

Computational Tools for Shape Measurement and Analysis *27*
Computation of Shape Distances *29*
Enhancement of Nanoscale Scanning Electron Microscope Imagery *30*
Molecular Movies: Imaging Femtosecond Motion during Electrochemical Transitions *30*
A Thousand-Fold Performance Leap in Ultrasensitive Cryogenic Detectors *31*
Clutter Measurements Pilot Project: Toward Evaluating Communications Spectrum Sharing Proposals *32*
Quantitative MRI *32*
Uncertainty Calculations for Building Engineering *34*
Simulation and Optimization in Cryobiology *35*
Stochastic Regression in Chemometrics *35*
Modeling Magnetic Fusion *36*
Parallel Adaptive Refinement and Multigrid Finite Element Methods *36*
Stable Explicit Time Marching in Ill-Posed Initial Value Problems for Partial Differential Equations *38*
Numerical Solutions of the Time Dependent Schrödinger Equation *41*

Advanced Materials **43**

Uncertainty Quantification in Molecular Dynamics Workflows for Aerospace Polymers *43*
Bayesian Calibration of Coarse-Grained Forces *44*
Micromagnetic Modeling *45*
OOF: Finite Element Analysis of Material Microstructures *46*
Determination of Diffusion Coefficients in Alloys *48*
Verification and Validation of Finite Element Method-based Solutions *49*
Inversion of the Abel Transform by Truncated Singular Components Method *50*

High Performance Computing and Visualization **52**

High Precision Calculations of Fundamental Properties of Few-Electron Atomic Systems *52*
Nano-structures, Nano-optics, and Control of Exciton Fine Structure with Electric and Magnetic Fields *53*
Rheology of Dense Suspensions *54*

HydratiCA: A Parallelized Numeric Model of Cement Hydration ... *58*
Network Simulation Visualization ... *60*
Image-based WebVR Graphics ... *61*
High End Visualization Software: Software Tests to Maintain System Reliability ... *62*
Optical Characterization for Advanced Immersive Displays ... *64*
Texture Compression Evaluation and Optimization ... *65*

Quantum Information ... **66**

Quantum Information Science ... *66*
Quantum Estimation Theory and Applications ... *67*
Phase Retrieval and Quantum Tomography ... *68*
Device Independently Secure Randomness from Loophole-Free Bell Tests ... *69*
Performance of Adiabatic Optimization Algorithms ... *71*
Computational Complexity of Quantum Field Theory ... *71*
Knot Theory and Quantum Physics ... *72*
One-Time Programs Using Isolated Qubits ... *72*
Post-Quantum Cryptography ... *73*
High-Speed Error Correction Codes for Quantum Key Distribution ... *74*
Towards a Quantum Repeater ... *75*
Joint Center for Quantum Information and Computer Science ... *76*

Foundations of Measurement Science for Information Systems ... **78**

Graph Theoretic Applications to Network Security and Security Metrics ... *78*
A Game Theoretic Model of Zero-Day Attack Propagation ... *79*
Security of Complex, Interdependent Systems ... *80*
Measurement Science for Systemic Risk ... *81*
Identifying the Best Nodes in a Network for Fast Communication ... *82*
Measuring Networks: Monte Carlo Sampling to Approximate the Chromatic Polynomial ... *82*
Fast Sequential Network Model Building ... *83*
An Algebraic Formulation for the Analysis and Visualization of Network Graphs ... *84*
Counting the Number of Linear Extensions of a Partially Ordered Set ... *85*
Extremal Theorems for Degree Sequence Packing and the 2-Color Discrete Tomography Problem ... *86*
Combinatorial Methods in Software Testing ... *86*
Can Micro Energy Harvesters Be Used to Power Up Wearable Sensors? ... *88*
A Study of the Energy Detection Threshold in the Body Area Network Standard CSMA/CA Protocol ... *89*

Mathematical Knowledge Management ... **92**

Digital Library of Mathematical Functions ... *92*
Visualization of Complex Functions Data ... *93*
DLMF Standard Reference Tables on Demand ... *95*
Natural Language Processing of Mathematics ... *96*
NIST Digital Repository of Mathematical Formulae ... *98*
Fundamental Solutions and Expansions for Special Functions and Orthogonal Polynomials ... *100*

PART IV: ACTIVITY DATA ... **103**

Publications ... **105**

Appeared ... *105*
Refereed Journals ... 105

Journal of Research of NIST 107
Book Chapters 107
In Conference Proceedings 108
Technical Magazine Articles 110
Technical Reports 110
Accepted *110*
In Review *111*
Presentations **112**
Invited Talks *112*
Conference Presentations *114*
Poster Presentations *116*
Web Services **117**
Software Released **117**
Conferences, Minisymposia, Lecture Series, Courses **118**
ACMD Seminar Series *118*
Shortcourses 119
Conference Organization *119*
Leadership 119
Committee Membership 119
Session Organization 120
Other Professional Activities **120**
Internal *120*
External *120*
Editorial 120
Boards and Committees 121
Community Outreach 121
Thesis Direction 122
Awards and Recognition **122**
Grants Received **122**
Grants Awarded **122**
External Contacts **122**
PART V: APPENDIX **125**
Staff **127**
Glossary of Acronyms **130**

Part I

Overview

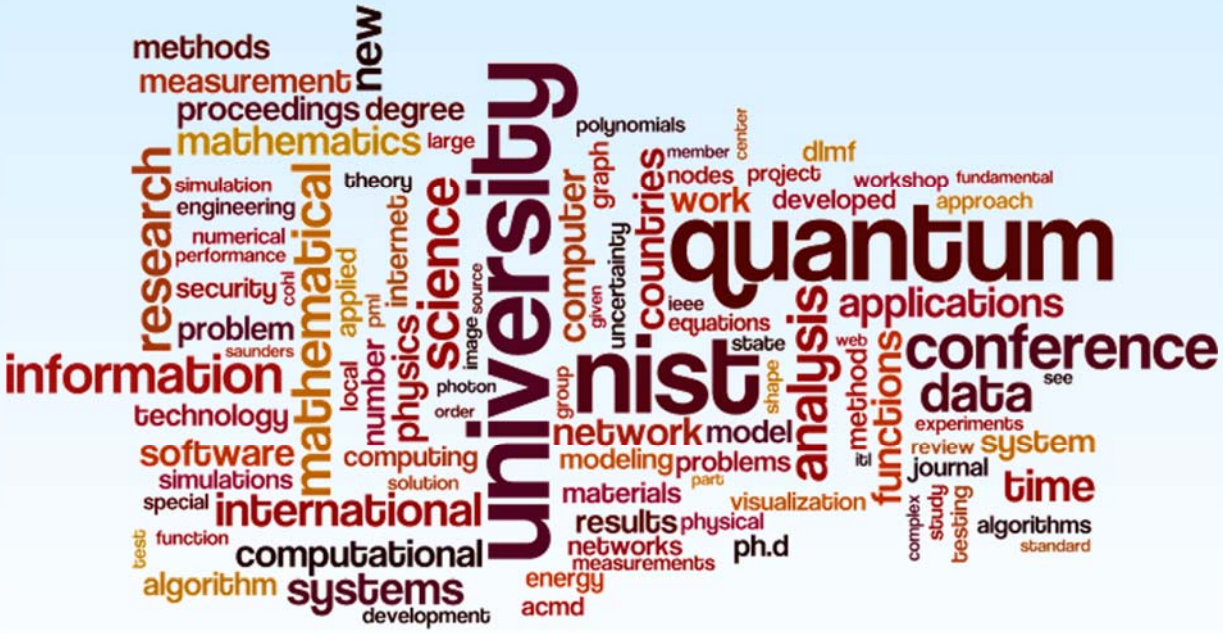

Introduction

Founded in 1901, the National Institute of Standards and Technology (NIST) is a non-regulatory federal agency within the U.S. Department of Commerce. NIST's mission is to promote U.S. innovation and industrial competitiveness by advancing measurement science, standards, and technology in ways that enhance economic security and improve our quality of life. The NIST Laboratory program is broad ranging, with research efforts encompassing physics, electrical engineering, nanotechnology, materials science, chemistry, bioscience, engineering, fire research, and information technology.

The Information Technology Laboratory (ITL) is one of seven major laboratories and user facilities at NIST. ITL's overarching goal is to maximize the benefits of information technology to society through a balanced measurement science and standards portfolio. To accomplish this, ITL seeks to

- accelerate innovation in information technology (IT) through the development and application of measurements and related technology and tools,
- develop the essential foundations of computer science, mathematics, and statistics that contribute to ITL's role in IT and measurement science broadly, and
- ensure the products of our research are available to all to promote U.S. innovation and industrial competitiveness, enhance economic security, and improve our quality of life.

The Applied and Computational Mathematics Division (ACMD) is one of seven technical Divisions in ITL. ACMD provides leadership within NIST in the use of applied and computational mathematics to solve science and engineering problems arising in measurement science and related applications. In that role ACMD staff members

- perform research and development in applied mathematics and computational science and engineering, including analytical methods, numerical and symbolic algorithms, advanced computing and communications architectures and applications, and high performance scientific visualization;
- engage in peer-to-peer collaborations in the application of mathematical and computational technologies to NIST problems;
- develop and disseminate mathematical reference data, software, and related tools; and
- work with internal groups and external organizations to develop standards, test procedures, reference implementations, and other measurement technologies for advanced scientific computation on current and future architectures.

Division staff is organized into four groups:

Mathematical Analysis and Modeling Group (*Timothy Burns, Leader*)

Performs research and maintains expertise in applied mathematics, mathematical modeling, and numerical analysis for application to measurement science.

Mathematical Software Group (*Michael Donahue, Leader*)

Performs research and maintains expertise in the methodology and application of mathematical algorithms and software in support of computational science within NIST as well as in industry and academia.

Computing and Communications Theory Group (*Ronald Boisvert, Acting Leader; Isabel Beichl and Xiao Tang, Project Leaders*)

Performs research and maintains expertise in the fundamental mathematics, physics, and measurement science necessary to enable the development and analysis of current and future computing and communications systems.

High Performance Computing and Visualization Group (*Judith Terrill, Leader*)

Performs research and maintains expertise in the methodologies and tools of high performance scientific computing and visualization for use in measurement science.

The technical work of the Division is organized into six thematic areas; these are described in the sidebar. Project descriptions in Part III of this document are organized according to these broad themes.

Division Thematic Areas

Mathematics of Metrology. Mathematics plays an important role in the science of metrology. Mathematical models are needed to understand how to design effective measurement systems, and to analyze the results they produce. Mathematical techniques are used to develop and analyze idealized models of physical phenomena to be measured, and mathematical algorithms are necessary to find optimal system parameters. Finally, mathematical and statistical techniques are needed to transform measured data into useful information. The goal of this work is to develop fundamental mathematical methods and analytical tools necessary for NIST to continue as a world-class metrology institute, and to apply them to critical measurement science applications.

Advanced Materials. Delivering technical support to the nation's manufacturing industries as they strive to out-innovate and out-perform the international competition has always been a top priority at NIST. This has also emerged as a major White House priority in recent years, in which NIST is playing an increasingly central role. Mathematical modeling, computational simulation, and data analytics are key enablers of emerging manufacturing technologies. This is most clearly evident in the Materials Genome Initiative, an interagency program with the goal of significantly reducing the time from discovery to commercial deployment of new materials through the use of modeling, simulation, and informatics. ACMD's role in advanced manufacturing centers on the development and assessment of modeling and simulation tools, with emphasis on uncertainty quantification, as well as support of NIST Laboratory efforts in such areas as materials modeling and smart manufacturing.

High Performance Computing and Visualization. Computational capability is advancing rapidly, with the result that modeling and simulation can be done with greatly increased fidelity (e.g., higher resolution and more complex physics). However, developing the requsite large-scale parallel applications remains highly challenging, requiring expertise that scientists rarely have. In addition, the hardware landscape is changing rapidly, so new algorithmic techniques must constantly be developed. We are developing and applying such expertise for application to NIST problems. In addition, computations and laboratory experiments often produce large volumes of scientific data, which cannot be readily comprehended without some form of visual analysis. We are developing the infrastructure necessary for advanced visualization of scientific data, including the use of 3D immersive environments and applying this to NIST problems. One of our goals is to develop the 3D immersive environment into a true interactive measurement laboratory.

Quantum Information. An emerging discipline at the intersection of physics and computer science, quantum information science is likely to revolutionize science and technology in the same way that lasers, electronics, and computers did in the 20th century. By encoding information into quantum states of matter, one can, in theory, exploit the seemingly strange behavior of quantum systems to enable phenomenal increases in information storage and processing capability, as well as communication channels with high levels of security. Although many of the necessary physical manipulations of quantum states have been demonstrated experimentally, scaling these up to enable fully capable quantum computers remains a grand challenge. We engage in (a) theoretical studies to understand the power of quantum computing, (b) collaborative efforts with the multi-laboratory experimental quantum science program at NIST to characterize and benchmark specific physical implementations of quantum information processing, and (c) the demonstration and assessment of technologies for quantum communication.

Foundations of Measurement Science for Information Systems. Modern information systems are astounding in their complexity. Software applications are built from thousands of interacting components. Computer networks interconnect millions of independently operating nodes. Large-scale networked applications provide the basis for services of national scope, such as financial transactions and power distribution. In spite of our increasing reliance on such systems, our ability to build far outpaces our ability to secure. Protocols controlling the behavior of individual nodes lead to unexpected macroscopic behavior. Local power anomalies propagate in unexpected ways leading to large-scale outages. Computer system vulnerabilities are exploited in viral attacks resulting in widespread loss of data and system availability. The actual resilience of our critical infrastructure is simply unknown. Measurement science has long provided a basis for the understanding and control of physical systems. Such deep understanding and insight is lacking for complex information systems. We seek to develop the mathematical foundations needed for a true measurement science for complex networked information systems.

Mathematical Knowledge Management. We work with researchers in academia and industry to develop technologies, tools, and standards for representation, exchange, and use of mathematical data. Of particular concern are semantic-based representations which can provide the basis for interoperability of mathematical information processing systems. We apply this to the development and dissemination of reference data for applied mathematics. The centerpiece of this effort is the Digital Library of Mathematical Functions, a freely available interactive and richly linked online resource, providing essential information on the properties of the special functions of applied mathematics, the foundation of mathematical modeling in all of science and engineering.

Highlights

In this section we identify some of the major accomplishments of the Division during the past year. We also provide news related to ACMD staff.

Technical Accomplishments

ACMD has made significant technical progress on many fronts during the past year. Here we highlight a few notable technical accomplishments. Further details are provided in Part II (Features) and Part III (Project Summaries).

Mathematics of Metrology. ACMD is working with scientists from the NIST Physical Measurement Laboratory (PML) to develop and analyze computational procedures for determining energies, with uncertainties, of individual photons arriving in rapid succession to transition-edge-sensor (TES) microcalorimeters for the situation in which detector nonlinearity can be neglected. Such a capability will enable more rapid characterization of energy spectra, for scientific and forensic investigations enabled by x-ray and gamma ray sources, with the exquisite energy resolution of these devices. Software implementing this capability, dubbed multi-pulse fitting, has been developed and evaluated on data collected by a 60-detector array of TES in experiments at the National Synchrotron Light Source (Brookhaven National Laboratory) as well as at NIST. The new technique, which obtains a least-squares fit of many pulses in a stream, rather than filtering pulses individually, outperforms existing record-based processing, in both energy resolution and throughput. See page 31.

Advanced Materials. While computer simulations have become a common R&D tool in many industrial settings, the demands for high-throughput can often push simulations to the limits of their validity. Motivated by these observations, ACMD staff, working with researchers at Boeing, have developed a series of uncertainty-quantification tools for molecular dynamics simulations of thermoset polymers, a key component of carbon-composites used by the aerospace industry. Such tools are meant to assess the validity and predictive power of simulations; thus, our analysis helps industrial engineers know when and to what extent their models are useful for decision-making. Details of this analysis applied to molecular dynamic predictions of the glass-transition temperature have been accepted for publication. See page 18.

High Performance Computing and Visualization. ACMD completed a major upgrade of its Immersive Visualization Environment (IVE) hardware, known as a Cave Automatic Virtual Environment (CAVE), this year. The IVE hardware underwent a major upgrade providing a significant improvement in visual quality. The new IVE has a larger display area and greater graphics resolution. It is also brighter and has greater contrast. In addition, it has a three-way host display switch that allows the selection of one of three computers to be the CAVE host at the touch of a button. This capability provides for a primary, backup and experimental host to be available to run applications as needed. Full flexibility of video routing allows easy selection of special case configurations. System reliability for the CAVE is very important. Included with the hardware procurement, a custom software component for self-monitoring of the hardware was specified and delivered. Combined with existing system tests it is now possible to run automated tests nightly to confirm correct operation of many CAVE subsystems and components. While certain tests require human observation, the automated self-test software provides a high level of confidence for ongoing system availability. See page 62.

We are using the ACMD CAVE to provide insight in a variety of ongoing NIST projects, including

- Flow of suspensions in pipe systems composed of spherical particles in a fluid matrix, with application to the pumping of concrete and slurries. See page 54.
- Complex chemical kinetics, with application to cement hydration. See page 58.
- Spatial distribution of spins in semiconductor nano-scale systems such as quantum dots, with application to the understanding and control of optical properties. See page 53.

Mathematical Knowledge Management. ACMD took important steps this year to ensure the future vitality of the Digital Library of Mathematical Functions (DLMF) project. The DLMF is an online resource on the properties of the special functions of applied mathematics[1]. In particular, a restructuring of the management of the project was undertaken in order to ensure active maintenance and development of the DLMF for the future. In addition, a new set of Senior Associate Editors, who will advise NIST management on the future evolution of the project, was put in place. On November 9-10, 2015 the Senior Associate Editors assembled at NIST to discuss the possibility of a second edition of the DLMF with significant new content and features. Finally, Associate Editors were identified for each existing DLMF chapter. They will work with the DLMF Mathematics Editor in responding to user queries about current chapter content, as well as developing minor updates. For further details, see page 92.

Quantum Information. Quantum theory has properties that seem surprising and strange from the perspective of classical physics and everyday intuition. The most profound divide between classical physics and quantum physics is that classical physics obeys the principle of local realism, but quantum physics does not. Since the mid 1960s, when John Bell proposed an experimental test of this property, physicists have performed a series of experiments suggesting violation of local realism, but all have suffered from loopholes, and thereby have not definitively ruled out this principle. This year ACMD researchers participated in a loophole-free test of local realism, rejecting the hypothesis that the universe obeys local realism with a very high level of statistical significance and ending a decades long quest of foundational physics. This work has received a great deal of attention, including being named as number nine in the top 25 science stories of 2015 by *Science News*. See page 15.

NIST and the University of Maryland (UMD), with the support and participation of the Research Directorate of the National Security Agency/Central Security Service (NSA/CSS), inaugurated a new joint venture, the Joint Center for Quantum Information and Computer Science (QuICS) on October 31, 2014. Scientists at the center will conduct basic research to understand how quantum systems can be effectively used to store, transport and process information. QuICS has quickly established itself as a substantial research presence in quantum information science. Newly recruited to the UMD Computer Science Department, Andrew Childs, a well-known quantum information theorist, began his tenure as QuICS Co-Director in November. Two postdocs given the distinction of Hartree Postdoctoral Fellows, as well as two additional outstanding postdoctoral researchers, also began their tenures in the fall of 2014; others have since joined. QuICS Fellows have recruited a total of 11 graduate students into the Center. The technical work of QuICS has also seen a strong start, with 65 papers submitted for publication in calendar 2015 alone. QuICS has indeed made an impressive start. See page 76.

Foundations of Measurement Science for Information Systems. ACMD staff have developed an efficient algorithm for estimating the coefficients of the chromatic polynomial $P(G,x)$. P gives the number of colorings of a graph G as a function of the number of colors x. The chromatic polynomial is a fundamental metric for the characterization of abstract networks. As such it plays an important role in scheduling and assignment problems, such as the allocation of frequencies to communications providers. In addition, it has a role in graph analytics as applied to big data, as well as to the q-state Potts model in statistical physics, because it gives a measure of graph or network invariants. Computing P is known to be #P hard, in general. Division staff devised wo algorithms to estimate the coefficients of the chromatic polynomial of a graph. We have compared our methods with other approximation methods and found we have more accuracy in less time. A technical article has been submitted for publication. See page 82.

This year ACMD, working with the NIST Computer Security Division and the Army Research Laboratory, completed a study of an internet weakness which has been long suspected, but rarely studied quantitatively. This weakness takes the form of the potential of colluding countries deliberately inhibiting Internet access of other countries. In this study, we analyzed the scenario in which a group of countries disconnect two other countries, isolate a set of countries from the Internet, or break the Internet into non-communicative clusters. We find that despite the potential for these attacks, the Internet as a whole has become increasingly resilient over the period of examination from 2008 to 2013. However, the gains in

[1] http://dlmf.nist.gov/

robustness and resilience are primarily concentrated in well-connected countries, which form an extremely resilient core. See page 21.

Technology Transfer and Community Engagement

The volume of technical output of ACMD remains high. During the last 18 months, Division staff members were (co-)authors of 49 articles appearing in peer-reviewed journals, 44 papers in conference proceedings, and 16 published in other venues. Ten additional papers were accepted for publication, while 30 others are undergoing review. Division staff gave 46 invited technical talks and presented 42 others in conferences and workshops.

ACMD continues to maintain an active website with a variety of information and services, most notably the Digital Library of Mathematical Functions, though legacy services that are no longer actively developed, like the Guide to Available Mathematical Software, the Matrix Market, and the SciMark Java benchmark still see significant use. During calendar year (CY) 2015, the division web server satisfied more than 5.5 million requests for pages during more than 1.1 million user visits. Another indication of the successful transfer of our technology is references to our software in refereed journal articles. For example, our software system for nano-magnetic modeling (OOMMF) was cited in 163 such papers published in CY 2015 alone; see page 45.

Members of the Division are also active in professional circles. Staff members hold a total of 13 editorial positions in peer-reviewed journals. For example, ACMD faculty appointee Dianne O'Leary serves at Editor-in-Chief of the *SIAM Journal on Matrix Analysis and Applications.* Staff members are also active in conference organization, serving on 17 organizing/steering/program committees. Of note, ACMD played an important role as sponsor or (co-)organizer of several significant events this year, including the following:

- *Dynamics of and on Networks*[2]. Santa Fe Institute, NM. December 1-5, 2014.

  A NIST grant provided partial funding for this event. This workshop moved beyond the static structure of networks to understand two kinds of dynamics: dynamics "of" a network, where the topology changes over time, and dynamics "on" a network, where the topology is fixed on relevant timescales, and discrete or continuous variables on nodes and edges evolve.

- *Reinventing the Grid: Designing Resilient, Adaptive and Creative Power Systems*[3]. Santa Fe Institute, NM. April 13-17, 2015.

  A NIST grant provided partial funding for this event, whose goal was to catalyze collaborations and new approaches to address fundamental questions surrounding the evolution of electricity service. It gathered together experts in electric power and ecological systems, along with local Santa Fe Institute experts. In addition, we included members of the global "Maker" movement to motivate creative thinking about energy problems. We also had significant industry involvement, with participants from local utilities and solar power companies.

- *13th International Symposium on Orthogonal Polynomials, Special Functions and Applications* (OPSFA-13)[4]. NIST, Gaithersburg, MD. June 1-5, 2015. (D. Lozier, Co-Organizer and H. Cohl, Member of the Program Committee).

  Only the second instance of this biennial conference to be held in North America, the meeting was co-sponsored by ACMD and the Society for Industrial and Applied Mathematics (SIAM). Conferences in this series provide a forum for mathematicians, physicists, computational scientists, and application scientists in other fields to communicate recent research results on mathematical functions that play an essential role in analytical and computational investigations in all areas in science

[2] http://www.santafe.edu/gevent/detail/science/1739/

[3] http://www.santafe.edu/gevent/detail/science/1953/

[4] http://www.siam.org/meetings/opsfa13/

and engineering. The OPSFA community provides the technical basis for the NIST Digital Library of Mathematical Functions (DLMF), an online source of reference information on this topic. Some 200 attendees from 34 countries participated in this event. The symposium featured 10 invited plenary lectures, 22 organized minisymposia of 4-12 talks each, as well as 8 contributed paper sessions. Three ACMD staff members made technical presentations.

- *Conference on Intelligent Computer Mathematics* (CICM)[5]. Washington, DC. July 13-17, 2015. (B. Miller and A. Youssef, Co-Organizers)

  The 8th such conference in the series, and the first to be held in the US, CICM brought together researchers who seek to advance the use of computers and communication systems in mathematical research. During the week-long event, more than 65 participants from 15 countries shared recent advances on such topics as digital mathematical systems and libraries, mathematical knowledge management, and automated theorem proving. Three ACMD staff members made technical presentations. The proceedings of the conference have appeared as volume 9150 in the Springer series Lecture Notes in Artificial Intelligence.

- *Workshop on Uncertainty Quantification in Materials Modeling*[6], Purdue University, West Lafayette, IN. July 28-31, 2015. (A. Dienstfrey and P. Patrone, Co-Organizers)

  Organized into six half-day sessions, each of which included a background tutorial followed by hands-on computational exercises, the event provided working scientists with exposure to techniques and tools for assessing the results of computational simulations in materials science, thus reflecting an important goal of the Materials Genome Initiative. The 40 participants included staff from a variety of academic and industrial institutions.

- *Numerical Reproducibility at Exascale*[7], at SC15[8], Austin, TX. November 20, 2015. (M. Mascagni and Walid Keyrouz, Co-Organizers)

  A cornerstone of the scientific method is experimental reproducibility. As computation has grown into a powerful tool for scientific inquiry, the assumption of computational reproducibility has been at the heart of numerical analysis in support of scientific computing. With ordinary CPUs, supporting a single, serial, computation, the ability to document a numerical result has been a straightforward process. However, as computer hardware continues to develop, it is becoming harder to ensure computational reproducibility, or to even completely document a given computation. This workshop explored the current state of computational reproducibility in high performance computing, and sought to organize solutions at different levels.

- *Inference on Networks: Algorithms, Phase Transitions, New Models and New Data*[9], Santa Fe Institute, NM, December 14-18, 2015.

  A NIST grant provided partial funding for this event. Networks provide a rigorous representation for both modeling and understanding the structure and function of complex systems. Over the past 10 years, researchers working in statistical inference and statistical physics have developed powerful new algorithms for understanding network data, and have revealed new phenomena in the behavior of these algorithms. This workshop brought together experts in network science, statistical inference, and statistical physics to present recent advances in inference on networks and to organize future efforts on developing a deeper mathematical understanding of probability on networks, message-passing algorithms, and random matrices, on developing new models to handle new sources of rich data, and on applying these ideas to key questions in complex systems.

[5] http://cicm-conference.org/2015/cicm.php?event=&menu=general
[6] http://www.ima.umn.edu/2014-2015/SW7.28-31.15/
[7] http://www.nist.gov/itl/ssd/is/numreprod2015.cfm
[8] The International Conference for High Performance Computing, Networking, Storage and Analysis, http://sc15.supercomputing.org/
[9] http://www.santafe.edu/gevent/detail/science/2154/

Service within professional societies is also prevalent among our staff. For example, Barry Schneider served as Chair of the Division of Computational Physics of the American Physical Society (APS). Geoffrey McFadden serves as Member-at-Large of the Council of the Society for Industrial and Applied Mathematics (SIAM). Faculty appointee Michael Mascagni is a Member of the Board of Directors of the International Association for Mathematics and Computers in Simulation (IMACS). Ronald Boisvert continues to serve as a member of the Publications Board of the Association for Computing Machinery (ACM). Staff members are also active in a variety of working groups. For example, Ronald Boisvert and Andrew Dienstfrey serve as members of the International Federation for Information Processing (IFIP) Working Group 2.5 on Numerical Software, Donald Porter is a member of the Tcl Core Team, Bruce Miller is a member of W3C's Math Working Group, and Sandy Ressler is a member of the Web3D Consortium. Barry Schneider represents NIST on the High End Computing (HEC) Interagency Working Group of the Federal Networking and

Table 1. *Undergraduate and graduate student interns in ACMD.*

Name	From	Program		Mentor	Topic
Achim, Tudor	Stanford U.	G	NPSC	J. Terrill	Analysis of cement hydration data with artificial intelligence tools
Baume, Michael	U. of Maryland	G	DGR	S. Jordan	Analysis of quantum algorithms
Chen, Weijan	Washington U. St Louis	G	FGR	X. Tang	Quantum memory technology
Hadiji, Hedi	Ecole Polytechnique, Sophia Antipolis	G	FGR	M. Mascagni	Probabilistic techniques for solving partial differential equations
Jablonski, Kim	Jacobs U. Bremen	G	FGR	B. Miller	Mathematical knowledge management
Keith, Adam	U. of Colorado Boulder	G	PREP	E. Knill	Quantum measurement analysis
Kohlhause, Lukas	Jacobs U. Bremen	G	FGR	B. Miller	Mathematical knowledge management
Mayer, Karl	U. of Colorado Boulder	G	PREP	E. Knill	Protocols for quantum optics
Peng, Bo	Washington U. St Louis	G	FGR	X. Tang	Generation of correlated photon pairs in on-chip high-q WGM resonators
Schubotz, Moritz	Technische U. Berlin	G	FGR	H. Cohl	Digital Repository of Mathematical Formulae project development
Van Meter, James	U. of Colorado Boulder	G	PREP	E. Knill	Quantum measurement of space-time
Wills, Peter	U. of Colorado Boulder	G	PREP	E. Knill	Statistical analysis for quantum info
Zhang, Guohao	UMBC	G	DGR	J. Terrill	Scientific visualization
Zhang, Lizhong	ISIMA, France	G	FGR	S. Langer	Software development for OOF3D
Zhao, Henan	UMBC	G	DGR	J. Terrill	Scientific visualization
Berger, Isabelle	George Washington U.	U	SURF	H. Cohl	CAS search and verification for orthogonal polynomial generating functions
Dang, Thinh	American University	U	SURF	H. Cohl	Fundamental solutions for PDEs on Riemannian manifolds of constant curvature
Davis, Kyle	The College of NJ	U	SURF	S. Ressler	Integrating Oculus VR headset with Web 3D graphics and Leap motion tracker
Jackson, Alauna	Bowie State U.	U	SURF	J. Terrill	Integrating Oculus VR headset with Web 3D graphics and Leap motion tracker
Park, Zoe	Georgetown U.	U	SURF	B. Cloteaux	Software for graph theory algorithms
Rabiega, Daniel	Millersville U. PA	U	SURF	M. Mascagni	Computing solutions to problems in materials science using Monte Carlo methods
Traini, Catherine	Hood College	U	SURF	H. Cohl	CAS search and verification for orthogonal polynomial generating functions
Weller, Ryan	U. of Colorado Boulder	U	SURF	S. Langer	Software development for OOF3D
Youssef, Raef	UMBC	U	SURF	J. Terrill	Integrating Oculus VR headset with Web 3D graphics and Leap motion tracker
Zimmerman, Jason	Millersville U. PA	U	SURF	J. Terrill	Integrating Oculus VR headset with Web 3D graphics and Leap motion tracker

Legend *G Graduate student* *U Undergraduate*
PREP Professional Research Experience Program (Boulder)
FGR Foreign Guest Researcher
NPSC National Physical Sciences Consortium Fellow
DGR Domestic Guest Researcher
SURF Summer Undergraduate Research Fellowship

Table 2. *High school interns in ACMD.*

Name	From	Program	Mentor	Topic
Agrawal, Neil	Poolesville HS	SVP	H. Cohl	Literature search for formula proofs in the Zeta Functions Chapter of the DLMF
Agrawal, Nina	Poolesville HS	SVP	H. Cohl	Literature search for formula proofs in the Zeta Functions Chapter of the DLMF
Americianaki, Yusuf	Quince Orchard HS	SVP	H. Cohl	MediaWiki development for DRMF
Cohen, Hannah	Magruder HS	SVP	H. Cohl	Literature Search in DLMF
Gandla, Divya	Poolesville HS	SVP	H. Cohl	Digital Repository of Mathematical Formulae
Kapoor, Yash	Clarksburg, HS	SVP	H. Cohl	Mathematical formula research
Madhu, Shraeya	Poolesville HS	SVP	H. Cohl	Digital Repository of Mathematical Formulae
Nair, Sean	Montgomery Blair HS	SVP	H. Cohl	Dual Bessel function definite integrals using the method of integral transforms
Psurek, Aleksander	Thomas S. Wootton HS	SHIP	J. Terrill	Immersive Visualizations
Shah, Akash	Northwest HS	SHIP	H. Cohl	Mathematical formulae interface and search tools
Sharma, Ankita	Poolesville HS	SVP	H. Cohl	Digital repository of mathematical functions
Xu, Wenqing	Montgomery Blair HS	SVP	H. Cohl	Generalizations of generating functions of q-hypergeometric orthogonal polynomials
Zhou, Sabrina	Montgomery Blair HS	SVP	H. Cohl	Digital Repository of Mathematical Formulae Seeding and Development
Zou, Cherry Ying	Poolesville HS	SVP	H. Cohl	Digital repository of mathematical functions
Zou, Claude	Poolesville HS	SVP	H. Cohl	Incorporation of semantics in LaTeX expressions

Legend *HS High school* *SHIP Summer High school Internship Program* *SVP Student Volunteer Program*

Information Technology Research and Development (NITRD) Program. Further details can be found in Part IV of this report. For further details, see Section IV, Activity Data.

Staff News

The past year saw a few staffing changes. Among these are the following.

Arrivals

Peter Bierhorst joined ACMD on January 15, 2015 as a NIST Fellow Postdoc working with Manny Knill. Peter received a Ph.D. in mathematics from Tulane University in 2014. At NIST Peter is performing research in quantum information theory, focusing on statistical analysis of quantum experiments.

Paul Patrone, who works in the areas of material modeling and uncertainty quantification, joined ACMD's Mathematical Analysis and Modeling Group on August 24, 2015. Paul received a Master's degree in Applied Mathematics (2012) and a Ph.D. in physics (2013) from the University of Maryland. He was most recently an Industrial Postdoc at the Institute for Mathematics and its Applications at the University of Minnesota. As part of that program, he spent a year working at the Boeing Company in Seattle, where he worked on uncertainty quantification in the modeling of aerospace composites

Lochi Orr joined ACMD on December 14, 2015 to provide administrative support to the Mathematical Analysis and Modeling Group and the Mathematical Software Group. Lochi, who has a degree in Criminal Justice, was most recently employed by the Drug Enforcement Administration in Baltimore.

Departures

Yvonne Kemper, who began a stay in ACMD as a NIST National Research Council (NRC) Postdoctoral Associate in December 2013, moved on in July 2015 to a second postdoc position in the Mathematics

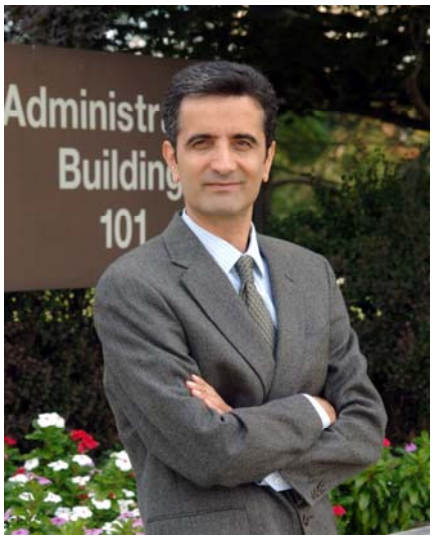

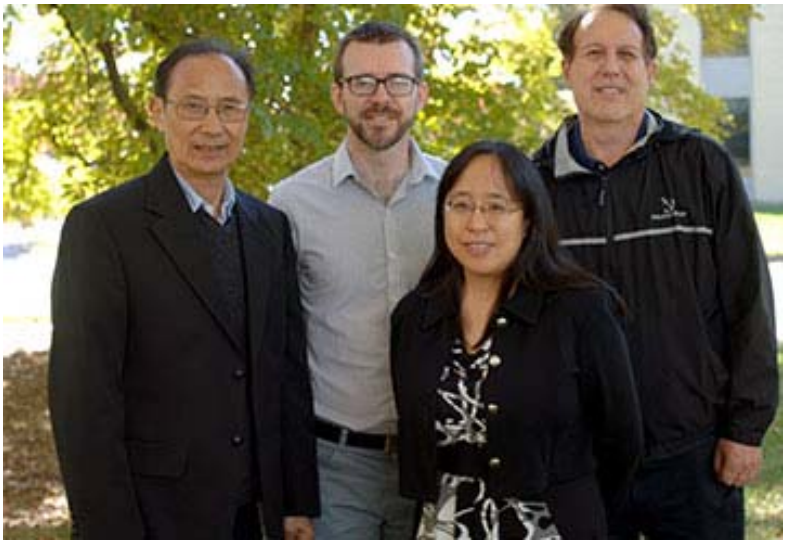

Figure 1. *2015 Department of Commerce Bronze Medal winners from ACMD. Left: Kamran Sayrafian. Right: Xiao Tang, Oliver Slattery, Paulina Kuo and Barry Hershman.*

Department at the University of Vienna. She received a Ph.D. in mathematics from the University of California at Davis in 2013, where she wrote a thesis on structural measurements of simplicial complexes and convex polytopes. At NIST she worked with Isabel Beichl on methods for approximating the chromatic polynomial.

In August 2015 **James Shook**, an NRC Postdoctoral Associate in ACMD since 2011, took a permanent position in the NIST Computer Security Division. While in ACMD James worked with Isabel Beichl and others on problems in combinatorics and graph theory.

Students

During FY 2015 ACMD was able to support the work of 42 student interns, including 15 graduate students, 10 undergraduates, and 15 high school students. See Table 2 and Table 1 for a complete listing.

ACMD staff members are quite active in the education of graduate students, serving both as Ph.D. advisers and as members of thesis committees. For a complete list, see page 120.

Recognition

Division staff garnered a number of professional recognitions during the past year. These are described below.

Manny Knill was honored with the 2015 Samuel Wesley Stratton Award "for pioneering research in the field of quantum information science and engineering." The Stratton Award, one of the most prestigious awards conferred by NIST, was first presented in 1962. It is granted for outstanding scientific or engineering achievements in support of NIST objectives.

Kamran Sayrafian received a 2015 Department of Commerce (DOC) Bronze Medal "for leadership in the advancement of body-area network technologies that will enable innovations in personal health care delivery and telemedicine." Examples of his current research work in this area can be found on pages 88 and 89.

Barry Hershman, **Paulina Kuo**, **Oliver Slattery** and **Xiao Tang** also received a 2015 DOC Bronze medal this year. They were cited "for the development of upconversion single photon detectors and spectrometers for use in quantum information research and measurement science." The team's current work on quantum communications is described on page 75.

Figure 2. *Yi-Kai Liu describes his work on one-time memories in the isolated qubits model at the annual QCrypt Conference.*

In the fall of 2014, **Raghu Kacker** received a Department of Commerce Silver Medal "for enabling unprecedented levels of software reliability through development of innovative software testing methodologies and tools." The medal recognizes the accomplishments of the combinatorial testing project whose current activities are described on page 86. D. Richard Kuhn of the ITL Computer Security Division was a joint honoree.

ACMD staff members and associates garnered three of the five annual ITL awards presented in 2015:

- *Outstanding Contribution to ITL:* **Scott Glancy,** for technical and analytical excellence in the advancement of quantum tomography and its application to quantum optics experiments with light and microwaves.
- *Outstanding Journal Paper:* **James Sims**, for excellence in research and exposition in the paper "Hylleraas-Configuration-Interaction Nonrelativistic Energies for the 1 S Ground States of the Beryllium Isoelectronic Sequence," which was published in the Journal of Chemical Physics in 2014.[10]
- *Outstanding Conference Paper:* **Yi-Kai Liu**, for excellence in research and exposition in the paper "Single-Shot Security for One-time Memories in the Isolated Qubits Model," which was published in the Proceedings of the 34th Annual Cryptology Conference held in Santa Barbara, CA in August 2014.[11]

Finally, in December 2015, Oliver Slattery, a member of ACMD's quantum communications team, was awarded a Ph.D. degree in physics from the University of Limerick in December 2015.

[10] http://dx.doi.org/10.1063/1.4881639
[11] http://dx.doi.org/2010.1007/978-3-662-44381-1_2

Part II

Features

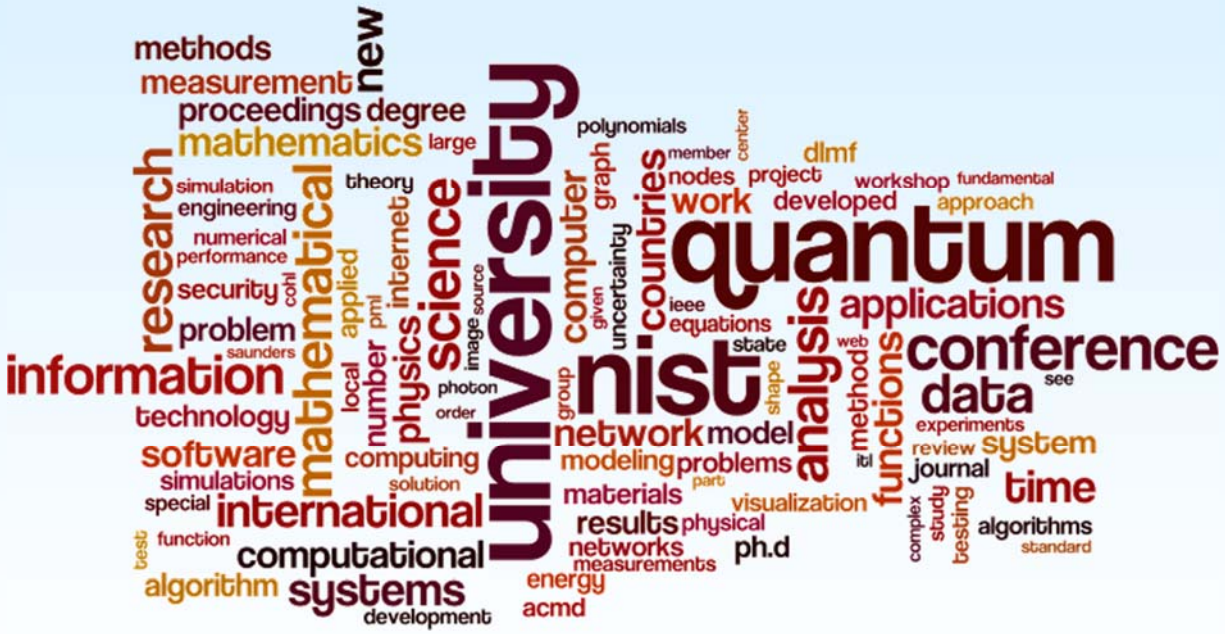

A Strong Loophole-Free Test of Local Realism

Quantum theory has properties that seem surprising and strange from the perspective of classical physics and everyday intuition. These include unavoidable randomness, systems existing in superpositions of states, and entanglement between systems. The most profound divide between classical physics and quantum physics is that classical physics obeys the principle of local realism, but quantum physics does not. This divide was discovered by John S. Bell in 1964 [1]. Since then, physicists have performed a series of experiments suggesting violation of local realism, but all have suffered from loopholes, and thereby have not definitively ruled out this principle. This year ACMD researchers participated in a loophole-free test of local realism, rejecting the hypothesis that the universe obeys local realism with a very high level of statistical significance and ending a decades long quest of foundational physics [2].

Scott Glancy

Compared with the world of our everyday experience, quantum theory may seem strange. Objects can exist simultaneously in two configurations. This is known as a *superposition* of states. For example, a photon can exist in an equal superposition of horizontal and vertical polarizations, which we write as $|H\rangle+|V\rangle$. Measurements performed on objects in superpositions give random results, but superpositions are fundamentally different from familiar probabilities because they can take negative (or even complex) values. We say that multiple objects in a correlated superposition are *entangled*. For example, the two-photon entangled state $|HH\rangle-|VV\rangle$ has 50 % probability that both are horizontal and 50 % probability that both are vertical. If one of the photons is measured to be horizontal, the state of the other photon immediately collapses to $|H\rangle$, even if they are separated by a great distance[12]. These features have inspired pithy quotes[13] seemingly endless philosophical debate, the invention of paradoxes, experiments realizing paradoxes, resolutions of the paradoxes, and the science of quantum information theory.

During the early development of quantum theory in the late 1920's, a small group of physicists speculated that the apparently fundamental randomness might be explained by a system of *hidden variables*. If we were able to measure the hidden variables, we would be able to predict with certainty all measurement outcomes, but unfortunately the hidden variables are forever hidden from us. If hidden variable theory were true, then we could attribute many of the strange features of quantum mechanics and its paradoxes to hidden processes that would better conform to our everyday intuitions.

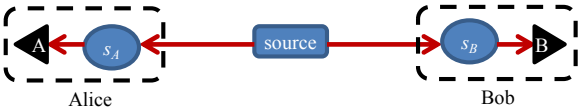

Figure 3. *Basic diagram of an experiment to test local realism. A source sends a pair of particles to measurement stations "Alice" and "Bob." They randomly choose measurement settings s_A and s_B, which determine what property of the particles Alice and Bob measure. They obtain measurement results A and B. If the particles obey the principle of local realism, the probability distribution of (s_A, s_B, A, B) is constrained by Bell inequalities. The experiment is designed to observe violation of one of the inequalities. In our experiment, the source makes entangled photon pairs, which travel to Alice and Bob along optical fibers. Alice and Bob choose an angle along which to measure the photons' polarization, and detect the photons with high efficiency superconducting-nanowire single-photon detectors.*

To illustrate, consider the entangled photon pair $|HH\rangle-|VV\rangle$. If both photons were measured to be horizontal, the hidden variable explanation would be that they had both been horizontal, and the measurement only revealed this fact. According to this perspective, a process that is thought to create the entangled state $|HH\rangle-|VV\rangle$ is actually a process that sometimes creates two H photons and at other times creates two V photons. Hidden variable theories obey the principle of *realism*, according to which the results of all possible measurements exist as hidden variables before the measurements occur. The measurements reveal the hidden variables. According to the theory of relativity, the hidden variables should obey a further principle of *local realism,* which says that each particle carries its own hidden variables with results of all possible measurements that might be performed on that particle, and the hidden varialbes of separated particles can communicate with one another no faster than the speed of light.

John S. Bell's great discovery was that one can perform experiments to test whether the universe obeys the principle of local realism. A basic diagram of such an experiment is given in Figure 3. A source creates a pair of particles (photons in our experiment) and sends them to two separated laboratories, labeled "Alice" and "Bob". Alice and Bob each randomly choose one of two measurements to make on the particle and then measure the particle. In our experiment, the two choices are to (1) measure polarization along the horizontal/vertical axes or (2) measure polarization along a slightly rotated pair of axes. Bell proved that if the particles obey local realism, the probability distribution of measurement results

[12] Whether this collapse is a real physical process or a mathematical manipulation is still a subject of heated debate among physicists.

[13] E.g., "God does not play dice." and "spooky action at a distance"

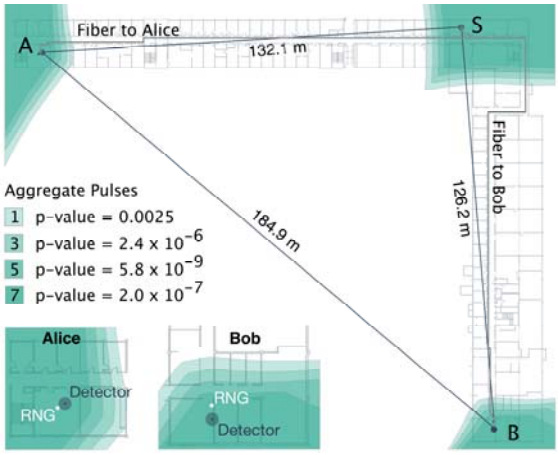

Figure 4. *Locations of source (S), Alice (A), and Bob (B) in NIST Building 1 of the Boulder campus. The shaded regions represent extremely conservative uncertainty regions for the locations of the source, Alice, and Bob. If all three are actually located within regions of a given shading, then the corresponding p-value for local realism applies. The bottom left of the figure shows expanded views of Alice's and Bob's labs specifying the locations of their random number generators (RNG) and detectors.*

must obey a set of inequalities (the *Bell inequalities*). However, Bell also showed that if the source makes entangled particles, then quantum theory predicts that the measurement probabilities can violate these inequalities.

Bell's work provided a clear outline for an experiment to test local realism (and local hidden variable theory) in the laboratory. Since then many research groups have performed various experiments to test local realism. However, previous experiments have all allowed means by which a local realistic system could (at least in principle) appear to violate the Bell inequality being tested. We say that such experiments contain *loopholes*. The three most technically challenging loopholes have been (1) the measurement inefficiency loophole, (2) the communication loophole, and (3) weak-analysis loopholes. While some past experiments have closed some (but not all) of these loopholes, no experiment had closed all loopholes until this year.

Measurement Inefficiency Loophole. If the efficiency of transmission and measurement of the entangled particles is less than 2/3, even quantum systems are unable to violate Bell's inequalities. To demonstrate violation, past experiments have simply discarded all events in which two particles were not detected, implicitly assuming that the measurement probabilities for detected particles is the same as the probabilities for lost particles. However, that assumption may not be strictly true, and one can engineer local realistic systems that can show Bell inequality violation for the subset of detected particles. This loophole was first closed in an experiment performed by NIST's Ion Storage Group in 2001 [3]. To close the measurement inefficiency loophole in our experiment, we used high efficiency superconducting nanowire single-photon detectors, developed in NIST's PML [4]. We also engineered the source to produce entangled photons that could efficiently enter optical fibers for transmission to the Alice and Bob measurement stations.

Communication Loophole. If information about Alice's random measurement choice reaches Bob before he completes his measurement (or vice-versa), a local realistic system could use that information to produce correlations between measurement results that in the absence of communication would be impossible for local realistic systems. To be certain that communication is impossible, we locate Alice and Bob ≈130 m from the source and perform the measurements so quickly that a signal traveling at the speed of light cannot travel from Alice to Bob or vice versa before the measurement is complete. The locations of the labs within NIST Building 1 of the Boulder campus are shown in Figure 4. High-speed photon detectors, electronics, and random number generators were developed to complete the measurements in the allowed time.

Weak Analysis Loophole. A test of the hypothesis of local realism deserves a rigorous statistical analysis of the experimental data. However, previous experiments have been analyzed using methods that required the invocation of assumptions about the data that were unjustified and, in some cases, false. These assumptions have introduced loopholes that would allow local realistic systems to appear to violate a Bell's inequality or to inflate the statistical significance of a violation. Often it has been impossible to interpret reported results as clear statements about statistical significance or probabilities. For several years, ACMD researchers have been developing methods to calculate *p*-values[14] for tests of local realism [5-10]. We have removed assumptions that the data from the experiment is independent and identically distributed, that the violation of the inequality is normally distributed, and others, so that no analysis loopholes remain. Only the null hypothesis of local realism is tested. For this experiment, ACMD researchers also designed rigorous data collection and analysis protocols and performed various consistency checks.

Several data sets were recorded during the NIST experiment, the best of these yielded a *p*-value of 5.8×10^{-9}, which is the probability that a local-realistic system would violate the Bell inequality by as much as we observed in our experiment or more. Similar experiments were performed this year at the Technical University of Delft [11] and at the University of Vienna [12]. Together these experiments firmly refute the hypothesis that our universe obeys the principle of local

[14] a measure of statistical significance

realism and confirm fundamental predictions of quantum mechanics.

NIST's experimental apparatus that was testing local realism will soon have a new job: generation of secure random numbers. Just as no local-realistic system can mimic the data from the experiment, no hacker can control or predict the experimental record (provided that the random number generators Alice and Bob use for their measurement choices are secure). Such a source of secure, unpredictable random numbers can be used for various cryptographic tasks or incorporated into NIST's Randomness Beacon[15].

References

[1] J. S. Bell, On the Einstein-Podolsky-Rosen Paradox, *Physics* **1** (1964), 195-200.

[2] L. K. Shalm *et al.*, A Strong Loophole-free Test of Local Realism, *Physical Review Letters* **115** (2015), 250402.

[3] M. A. Rowe, D. Kielpinski, V. Meyer, C. A. Sackett, W. M. Itano, C. Monroe, and D. J. Wineland, Experimental Violation of a Bell's Inequality with Efficient Detection, *Nature* **409** (2001), 791-794.

[4] F. Marsili, V. B. Verma, J. A. Stern, S. Harrington, A. E. Lita, T. Gerrits, I. Vayshenker, B. Baek, M. D. Shaw, R. P. Mirin, and S. W. Nam, Detecting Single Infrared Photons with 93 % System Efficiency, *Nature Photonics* **7** (2013), 210–214.

[5] Y. Zhang, S. Glancy, and E. Knill, Asymptotically Optimal Data Analysis for Rejecting Local Realism, *Physical Review A* **84** (2011), 062118.

[6] Y. Zhang, S. Glancy, and E. Knill, Efficient Quantification of Experimental Evidence Against Local Realism, *Physical Review A* **88** (2013), 052119.

[7] P. Bierhorst, A Rigorous Analysis of the Clauser–Horne–Shimony–Holt Inequality Experiment When Trials Need Not Be Independent, *Foundations of Physics* **44** (2014), 736-761.

[8] E. Knill, S. Glancy, S. W. Nam, K. Coakley, and Y. Zhang, Bell Inequalities for Continuously Emitting Sources, *Physical Review A* **91** (2015), 032105.

[9] P. Bierhorst, A Robust Mathematical Model for a Loophole-Free Clauser–Horne Experiment, *Journal of Physics A: Mathematical and Theoretical* **48** (2015), 195302.

[10] B. G. Christensen, A. Hill, P. G. Kwiat, E. Knill, S. W. Nam, K. Coakley, S. Glancy, L. K. Shalm, Y. Zhang, Analysis of Coincidence-Time Loopholes in Experimental Bell Tests, *Physical Review A* **92** (2015), 032130.

[11] B. Hensen *et al.*, Loophole-free Bell Inequality Violation Using Electron Spins Separated by 1.3 Kilometres, *Nature* **526** (2015), 682–686.

[12] M. Giustina *et al.*, Significant-Loophole-Free Test of Bell's Theorem with Entangled Photons, *Physical Review Letters* **115** (2015), 250401.

Participants

Peter Bierhorst, Scott Glancy, Emanuel Knill (ACMD); Kevin J. Coakley (NIST ITL); Michael S. Allman, Joshua C. Bienfang, Shellee D. Dyer, Thomas Gerrits, Carson Hodge, Adriana E. Lita, Camilla Lambrocco, Alan L. Migdall, Richard P. Mirin, Sae Woo Nam, Lynden K. Shalm, Martin J. Stevens, Edward Tortorici, Varun B. Verma, Michael A. Wayne (NIST PML); Carlos Abellàn, Waldimar Amaya, Morgan W. Mitchell, Valerio Pruneri (The Barcelona Institute of Science and Technology, Spain), Bradley G. Christensen, Daniel R. Kumor, Paul G. Kwiat (University of Illinois at Urbana-Champaign); William H. Farr, Francesco Marsili, Matthew D. Shaw, Jeffrey A. Stern (Jet Propulsion Laboratory); Deny R. Hamel (University of Moncton, Canada); Thomas Jennewein, Evan Meyer-Scott, Yanbao Zhang (University of Waterloo, Canada)

[15] http://www.nist.gov/itl/csd/ct/nist_beacon.cfm

Uncertainty Quantification in Molecular Dynamics for Aerospace Polymers

In the past two decades, computer simulations have become a common R&D tool in the aerospace industry. While this strategy holds promise, the high-throughput demands of industry can extend simulations toward the limits of their validity. Motivated by these observations, we have developed a series of uncertainty-quantification tools for molecular dynamics simulations of thermoset polymers, a key component of carbon-composites used by the aerospace industry. Broadly speaking, such tools are meant to assess the validity and predictive power of simulations; thus, our analysis helps industrial engineers know when and to what extent their models are useful for decision-making purposes. Details of this analysis applied to molecular dynamic predictions of the glass-transition temperature have been accepted for publication. We anticipate that our analysis can be extended to other material properties and simulation techniques. Industrial stakeholders are actively using our methods, some of which have recently been incorporated into commercial software packages.

Andrew Dienstfrey and Paul Patrone

In the commercial aerospace industry, advances in computer simulations and modeling have led to a dramatic paradigm shift in how airplanes are designed and manufactured. From a macroeconomic perspective, the motivations for this are clear: every dollar spent on simulations yields as much as a $9 return-on-investment by informing decision-making, reducing excess testing, and therefore decreasing development times and costs [1,2]. Thus, industrial researchers are increasingly considering ways to integrate simulations more fully into the aerospace design process.

Materials science has been identified as a key area where advances in computer modeling are needed [1,3]. The principal drivers for this are threefold: (i) new materials are becoming market drivers in several industrial sectors; (ii) computers are now sufficiently powerful that scientists can consider tailoring materials *in silico* to meet specific needs [1,4]; and (iii) the complex, many-body simulations required to model such advanced materials are still relatively new and require exhaustive verification and validation of their predictions [1,3].

To understand the interplay of these facts, it is sufficient to learn from the success of the Boeing 787 Dreamliner. Built from more than 50 % advanced and composite materials by weight, the 787 boasts significantly improved fuel efficiency that reduces operating costs for airline carriers by up to 6 % [5]. Eyeing the economic implications of rising oil prices and the savings promised by the 787, potential customers in 2006 all but forced the other global airline manufacturers to invest billions in similar composite manufacturing techniques [7]. Research engineers quickly realized that new materials were the catalyst driving this change, and the market was soon to be saturated with current-generation composites. Thus, recent efforts have focused on reducing time-to-market of next-generation materials as a means to retain competitive advantage. Simulation-based search for new materials is seen as a key tool for enabling this *materials-by-design* paradigm [7].

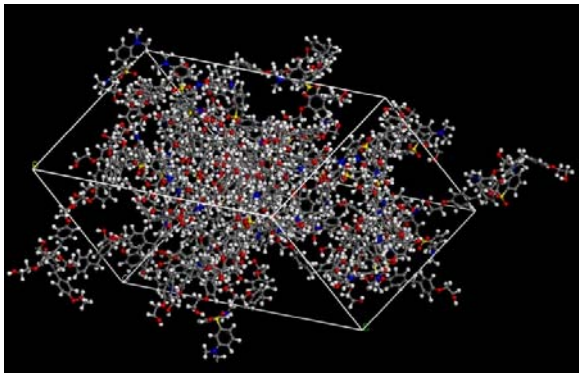

Figure 5. *Unit cell showing cross-linked polymer system (33DDS and BisF) containing 2000 atoms. Molecular dynamics evolves all atoms by Newtonian dynamics using a potential model to compute inter-atomic forces.*

From a practical standpoint, this strategy must confront the complexity of aerospace composites. Such materials are not monolithic entities, but rather a compound mixture of many subcomponents. Modern thermoset resins, for example, can include more than 10 distinct monomer types, which are mixed in varying proportions to balance trade-offs in end-product performance. The flexibility offered by this combinatorially large design space reflects both the immense potential and difficulty associated with designing polymer systems.

To address these difficulties, aerospace and other composite-based industries are turning to molecular dynamic (MD) simulations as a means of balancing accuracy and throughput [1,3]. Broadly speaking, MD simulations integrate Newton's equations of motion forward in time for large, many-body particle dynamics problems. A representative system is shown in Figure 5. For crosslinked polymers used in aerospace composites, the success of MD is largely due to its ability to

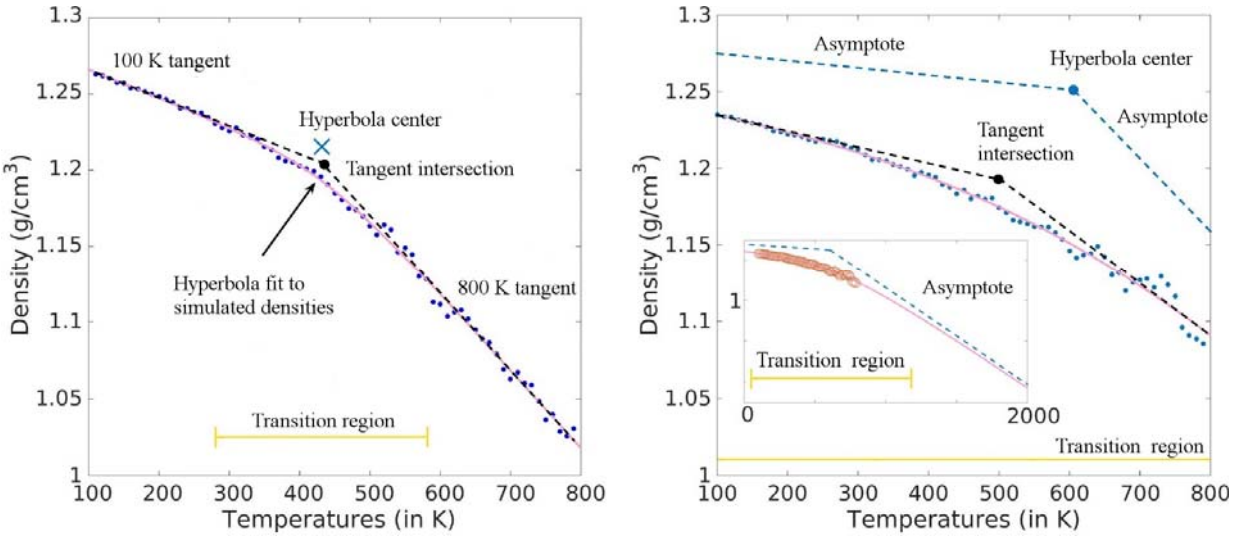

Figure 6. *Comparison of density-temperature data for two different amine-cured epoxies. T_g is typically computed as the intersection temperature of two lines fit to the low and high temperature asymptotic regimes. Using hyperbolas, we test for the existence of such regimes by comparing the data to asymptotes. The left plot shows a system in which the data clearly samples asymptotic behavior, corresponding to temperatures outside of the transition region. The right plot shows a dataset that does not sample asymptotic behavior.*

describe the evolution of complex molecular conformations which govern bulk mechanical properties. Such level of detail, however, comes at a price.

For one, the length and time scales of MD simulations are vastly different than their physical counterparts. A representative sample of bulk material has a mass of a few grams, and thereby consists of $O(10^{23})$ atoms. Relevant time-scales range from dynamic responses of $O(10^{-5})$ seconds, to aging processes taking place over the many-year lifetime of a component. By comparison, current high-end MD simulations treat at most $O(10^{6})$ atoms for $O(10^{-8})$ seconds. This huge discrepancy in scales is a cause for concern.

A separate issue arises from the opposite end of the length spectrum, namely the details of the interatomic force-fields that complete Newton's equations. While such forces could, in principle, be derived from quantum mechanical considerations, this approach is not widely practiced. Instead, a large variety of parameterized interatomic force-fields have been designed for diverse material classes and purposes. These phenomenological interactions model interatomic bonds, bond and torsional angles between bonded triplets, and long-range electrostatic and van der Waals forces in order to approximate the force on each of the atoms in a system.

In light of these fundamental concerns it may appear remarkable that atomistic simulations such as MD are at all informative of bulk system behavior. However, a counter-balancing is provided in that the bridge from atomic to macroscale is built on ensemble averages of atomistic dynamics. Such statistics have the effect of smoothing out fine scale details of the interatomic force-fields, and return average bulk-scale properties with variances that decay proportional to the inverse system size. Therein lies the theoretical prospects for the value of the MD enterprise.

In light of these observations, a key task in any MD-based R&D activity is to assess confidence in simulations so as to render their predictions more informative for decision making. The growing field of uncertainty quantification (UQ) provides a useful foundation from which to develop and analyze such techniques. In the following we describe research results completed in FY 2015 toward this goal.

Uncertainty quantification for glass-transition. Building upon work from FY 2014, we developed a systematic UQ workflow to assess data arising from MD simulations of the glass-transition temperature T_g. This quantity is both an important property for engineers[16] that is also difficult to model; thus it represents a useful proving ground upon which to develop UQ methods

We begin by addressing the question: Is simulated data consistent with the definition of T_g? In particular, it is common practice to estimate T_g by extrapolating to the intersection of two fit-lines characterizing the low and high-temperature asymptotic behavior of density-temperature curves. Deciding what constitutes "asymptotic behavior" at these extreme temperature regions is left to the modeler, and hence widely disparate estimates of T_g are possible from hard-to-decide cases. Motivated by this, we implemented a non-linear regression analysis that estimates a hyperbola model for the entire density-

[16] It determines, for example, the temperature at which a wing becomes soft.

temperature dataset, thereby eliminating the need for supervised intervention and data sub-setting. As an added benefit, the resulting hyperbola model may be analyzed further to determine whether asymptotic regimes are manifest in the simulation data; see Figure 6. Thus we present a systematic approach to resolve what was previously left open to user skill.

Additionally, we developed a pooling analysis that estimates bias in the T_g predictions by iteratively resampling from collections of datasets. Importantly, such approaches can indicate when simulations are too small to yield property estimates that are converged as a function of system size.

Finally, we quantified the total uncertainty in the simulation-based "measurements" of T_g as the combination of two principal contributions. One represents the dispersion due to the uncertainty of the non-linear regression determined in the first phase of the analysis. This contribution is estimated using a parameterized bootstrap Monte Carlo technique. The second characterizes the dispersion between multiple independent simulations of the identical physical system. Physically, this second contribution is meant to capture the dispersion due to small system sizes and, thus, limited sampling of polymer cross-linking statistics as well as possibilities for metastable dynamical equilibrium resulting from local minima in the energy landscape. From the statistical perspective our uncertainty analysis is closely-related to that which is obtained in metrological key-comparison studies [8]. To the best of our knowledge this is the first time that such a metrology approach has been applied to the uncertainty analysis of simulation-based data.

Details of this work are provided in a publication that is currently under review [9]. Industrial stakeholders are also using this workflow in their simulation protocol, and the software company Schrodinger has incorporated elements of our analysis into their commercially available MD simulation package. Future directions include (i) generalizing our analysis to more mechanical properties of interest, and (ii) developing additional analysis tools for quantifying the extent to which a finite simulation samples the network structure of bulk materials.

In addition to this analysis, we continued outreach to the broader computational materials science community as part of the Materials Genome Initiative. In particular, from July 28–July 31 2015, in collaboration with the Institute for Mathematics and its Applications (IMA), Air Force Research Lab and Purdue University we organized an IMA Hot Topics Workshop on Uncertainty Quantification in Materials Science at Purdue's nanoHUB. This workshop is described elsewhere in this annual report. Response to the workshop was positive, and a follow-up is scheduled to be held at IMA in February 2016.

References

[1] G. Goldbeck, *The Economic Impact of Molecular Modelling: Impact of the Field on Research, Industry, and Economic Development.* Goldbeck Consulting Ltd., St. John's Innovation Centre, Cambridge, United Kingdom, 2012.

[2] E. C. Joseph, C. Ingle, C. Meunier, S. Conway, G. Cattaneo, and N. Martinez, A Strategic Agenda for European Leadership in Supercomputing: HPC 2020 — IDC Final Report of the HPC Study for the DG Information Society of the European Commission, September 2010.

[3] A. Dienstfrey, F. R. Phelan Jr., S. Christensen, A. Strachan, F. Santosa and R. F. Boisvert, Uncertainty Quantification in Materials Modeling, *JOM* **66**:7 (2014), 1342-1344.

[4] S. Christensen and J. Senger, Distortional Matrix of Epoxy Resin and Diamine, U.S. Patent 7,985,808 B2, filed April 23, 2010, issued July 26, 2011.

[5] J. Ostrower, Boeing's Key Mission: Cut Dreamliner Costs, *The Wall Street Journal,* June 10, 2014, B1.

[6] D. Gates, Airplane Kingpins Tell Airbus: Overhaul A350, *Seattle Times*, March 29, 2006.

[7] J. Cotton, R. J. Glamm, D. M. Rosenbladt, E. Pripstein and S. Christensen, "Integrated Computational Materials Engineering Needs for Aerospace," TMS ICME Conference, Colorado Springs, CO, June 3, 2015.

[8] A. Rukhin, Weighted Means Statistics in Interlaboratory Studies, *Metrologia* **46**:3 (2009), 323-331.

[9] P. N. Patrone, A. Dienstfrey, A. R. Browning, S. Tucker and S. Christensen, Uncertainty Quantification in Molecular Dynamics Studies of the Glass Transition Temperature, *Polymer* **87** (2016), 246-259.

Participants

Andrew Dientfrey, Paul Patrone (ACMD); Stephen Christensen, Andrea Browning, Sam Tucker (The Boeing Company)

The Resilience of the Internet to Colluding Country Induced Connectivity Disruptions

The apparent robustness of Internet networking hides underlying weaknesses. In this work, we have revealed a class of such weaknesses in the form of colluding countries deliberately filtering out other countries. For this we have analyzed the scenario in which a group of countries disconnect two other countries, isolate a set of countries from the Internet, or break the Internet into non-communicative clusters. We find that despite the potential for these attacks, the Internet as a whole has become increasingly resilient over the period of examination from 2008 to 2013. However, the gains in robustness and resilience are primarily concentrated in well-connected countries, which form an extremely resilient core. Our study suggests that the less connected countries form new links largely with well-connected countries, and not to each other, maintaining the centrality of the well-connected countries in the paths between the less connected countries on the fringe. Because of this, the resilience of these less connected countries has not increased significantly over the time period studied. The result is that a small set of countries is able to isolate significant portions of the Internet or to divide it up into clusters. Individual well connected countries are often able to unilaterally isolate network dependent neighbors. These weaknesses could be addressed through a focus on establishing links between poorly connected countries. This would move the poorly connected countries away from dependence on the infrastructure of more highly connected countries.

Assane Gueye

The Internet was designed to be robust to disruption due to the failure of specific networks or routers [1]. However, events have empirically demonstrated that despite this design, single points of failure (e.g., the digging up of a fiber optic cable, or the cutting of a submarine line by a ship anchor) are capable of disconnecting entire countries from the rest of the internet [2]. In this study [3], we examine the capability for deliberate disruption or filtering enacted on inter-country network routes. In particular, we examine to what extent a group of colluding countries can disrupt Internet connectivity for other countries by evaluating three Internet connectivity security questions:

1. *Cutting Pairwise Communications:* What is the minimal number of colluding countries required to prevent two other countries from communicating?
2. *Country Isolation:* What is the maximal number of countries that can be cut off from the Internet by a group of colluding countries?
3. *Non-Communicative Clusters:* Into how many non-communicative clusters can a group of colluding countries divide the Internet?

These questions are modeled as countries completely cutting off routes to other countries. While this certainly can be done, we use this approach to model a large class of attacks (possibly as yet undiscovered) whereby selective traffic along country-to-country routes may be maliciously handled.

To evaluate these three questions, we created an interconnectivity map of the worldwide Internet routing infrastructure, aggregated at the level of individual countries. We did this by using data provided by the Cooperative Association for Internet Data Analysis (CAIDA)[17]. CAIDA has a worldwide monitoring network that provides an approximate topological map of the Internet at the Internet Protocol (IP) layer. It then uses the RouteViews[18] Border Gateway Protocol (BGP) data to collapse the IP topology into a map of autonomous systems (ASs), approximately the set of Internet Service Providers. The worldwide monitoring network has a number of monitors that have evolved from 33 in 2008 to 89 in 2013,[19] with some being added, others retired, but with 24 monitors being active in all years.

The collected data consists of AS connectivity from 2008 to 2013 inclusive, with links between the ASs. In using the data, we first model all direct links as bidirectional since, for our experiments, we are concerned about the capability to transmit data as opposed to currently policy-based directionality of traffic flow. We then used the AS-to-country mappings to aggregate the AS nodes into country nodes where edges represent inter-country connectivity. This mapping assigns ASs to their country of registration despite the physical location of the ASs servers. One aspect of this approach that deserves special attention is the existence of multinational ASs (MOAs) which have points of presence (PoPs) within multiple countries and sometimes in different continents. For our work, we map MOAs to their home country (i.e., country of registration), which implies that a MOA is required to implement Internet filtering laws

[17] http://www.caida.org/

[18] http://www.routeviews.org/

[19] 42 in 2009, 54 in 2010, 59 in 2011, and 65 in 2012

or government directives from their home country regardless of the physical location of the routers they own. The rationale for this approach comes from the legal literature: "the home country may also have laws that attempt to regulate business activities of the company that are conducted outside the home country" [4].

For each year, we generate two inter-country connectivity graphs. The first graph is created by using the information provided by all monitors for that year. This graph is useful for evaluating bounds on the resilience of a particular year. However, the addition of new monitors with new vantage points, as well as the retiring of old monitors, means that the visible portions of the routing graph vary significantly from year-to-year, independent of changes in the underlying routing graph itself. This makes it difficult to reliably compare the resilience between different years. To enable year to year comparisons, we generate a second graph by restricting the discovered routes to those visible to a set of 24 monitors that were active in all six years of our evaluation.

As a result, we get two undirected graphs for each year. For each graph, the nodes represent the countries with presence in the CAIDA data and the links between two nodes represent a connection between an AS registered in the first country and an AS registered in the second. We then use graph theory tools to evaluate the three questions stated above.

Cutting Pairwise Communications. The communications of two countries, s and t, are considered prevented or cut if the ASs registered to s cease having connectivity the ASs registered to t. To evaluate the cutting of pairwise communications, we iterate over all pairs of countries (s,t) that are not adjacent and determine the minimum, maximum, and mean node connectivity. The node connectivity calculation determines the minimum number of nodes required to disconnect the graph such that s and t end up in separate components.

Country Isolation. A country is considered cut off from the Internet or isolated if the ASs registered to that particular country cease having connectivity to the largest remaining connected component of the global Internet. In the country isolation problem, we would like to know the maximal number of countries that can be cut off from the Internet (i.e., the largest remaining connected component) by a group of k colluding countries. For fixed k, this problem is known to be in general NP-hard [5]. As a consequence, we resort to heuristic algorithms to find approximate solutions. To evaluate country isolation, we iteratively increase the size k of the set of colluding countries and, at each iteration, use our heuristic algorithms to choose a specific set of country nodes that (approximately) maximizes the number of isolated countries.

Non-Communicative Clusters. The Internet is considered to be broken into non-communicative pieces if the ASs registered to a group of countries are connected while being disconnected from the rest of the Internet. In our country graph, there will be multiple isolated clusters (possibly consisting of just single nodes) after removing the colluding nodes. In this non-communicative clusters problem, the goal of the colluding countries is to maximize the number of non-communicative clusters. This is similar to country isolation except that instead of optimizing on the number of isolated countries, the algorithms must optimize on the number of isolated clusters. We use the same set of algorithms to compute an approximate solution. As in the previous case, to evaluate non-communicative clusters, we iteratively increase the size k of the set of colluding countries and, at each iteration, we use our algorithms to choose a specific set of country nodes that maximizes the number of non-communicative clusters.

The algorithms are iterative in nature and greedily exploit well-known features of the network. In the first one, we iteratively remove the node with the maximum degree in the remaining graph as well as all edges that are incident to it. In a second one, we iteratively remove the node whose deletion maximizes the number of non-communicative clusters. In a third approach, we iteratively remove the nodes that bisect the current largest cluster in the most even way. For our empirical results,

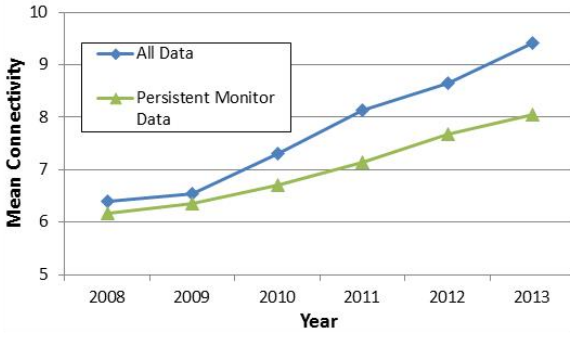

Figure 7. *Mean Number of Collaborating Countries Needed to Disconnect a Pair of Countries.*

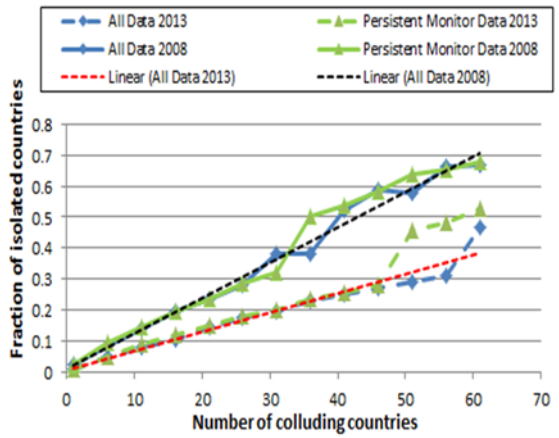

Figure 8. *Improvement in Robustness: Comparing 2008 to 2013.*

each data point is analyzed by all approaches but only the result that best optimizes the relevant security question is kept. Thus, each presented curve in our analysis is made up of answers from all approachess, representing our best available approximation of the true NP-hard answer.

Results. Overall, our experiments have shown that the Internet as a whole is becoming more resilient to colluding country induced connectivity disruptions.

Considering cutting pairwise communications, the data shows that it is quite feasible for groups of colluding countries to block communications between pairs of countries, although this is becoming more difficult to implement over time. For all years and both data sets (the one using all monitors and the one using one the 24 persistent monitors), the minimum pairwise connectivity was 1. This indicates that given the routes visible through the CAIDA dataset, there always exists some country that by itself can disconnect some other pair of countries. However, some non-adjacent pairs of countries are extremely hard to disconnect. As shown in Figure 7 on the "all data" line, in 2013 there were non-adjacent pairs of countries that required collusion between a minimum of 68 countries in order to disconnect them. Furthermore, the data from the set of persistent monitors shows an increasing trend over time.

With regard to country isolation, we observe a linear increase in the number of isolated countries as the number of colluding countries increases from 1 to around 60. This is the case for both data sets for all years. However, the rate of increase diminishes over time indicating that the Internet has become more resilient over the years. This is shown in Figure 8 which compares years 2008 and 2013. Another way to see this improvement in robustness is to ask: how many colluding countries does it take to isolate a fraction of *x* % of the Internet? Figure 9 shows that over time, more countries need to collude in order to cut off the same fraction of countries from the Internet. However, these increases are for larger percentages of the countries. The "cost" of isolating just 10 % of the countries in the Internet is small and relatively stable. This indicates that the Internet is still sensitive to colluding attacks, and suggests that a fringe set of countries are not receiving the benefits of increased robustness.

Finally, the analysis of the *number of non-communicative clusters* shows a linear increase in the number of clusters as more countries collude for each year and each data set. However, similar to the previous case, the rate of increase diminishes over time indicating that the Internet has become more resilient since 2008. This is confirmed with the plots of Figure 10 which shows the number of colluding countries needed to separate the network in differing numbers of connected components. With both data sets, the trend is that, over time, more countries are required to collude in order to separate the

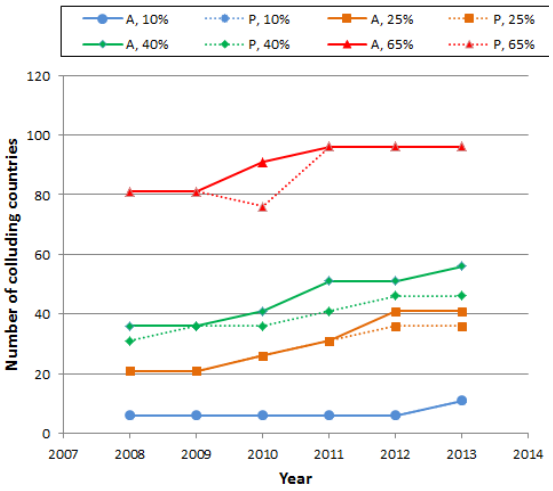

Figure 9. *Number of Colluding Countries Needed to Isolate a Fraction x % of the Nodes as a Function of the Year. "A, 10 %" in the Legend, means that the plot is done using the entire data set, and the fraction of isolated nodes is 10 %; "P" indicates that only the persistent monitor data is used.*

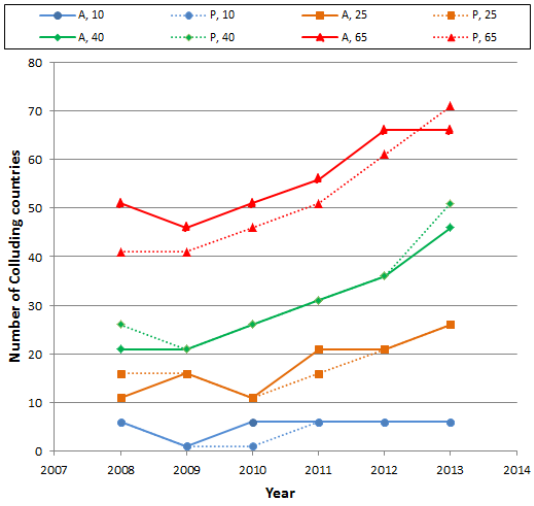

Figure 10. *Number of Colluding Countries Needed to Divide the Network into x Clusters as a Function of the Year. "A, 10" in the Legend, means that the plot is done using the entire data set and the number of clusters is 10; "P" indicates that only the persistent monitor data is used.*

Internet into some predetermined number of non-communicative clusters for approximately 25 clusters or more. For smaller isolated clusters, the number of required countries remains relatively constant.

A point of commonality among these three findings is that they involve the smallest grouping of target countries in our experiment, where those countries were the least connected ones in the country-based AS graph. This suggests that, for these most vulnerable countries (that are most easily cut off from the Internet using the fewest colluding countries), their robustness has not noticeably increased over the time period of our analysis. This appears to be due to the fact that the majority of

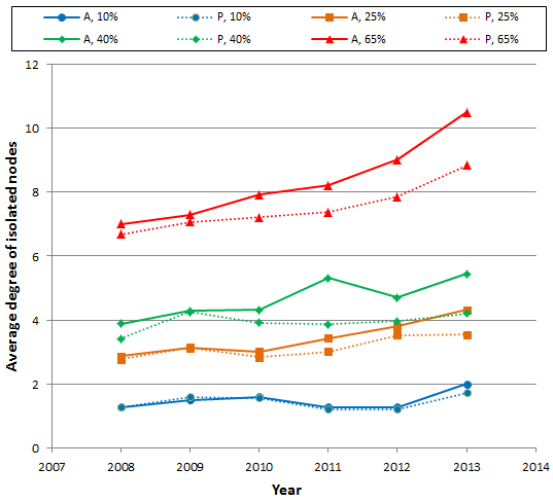

Figure 11. *Average Degree of Isolated Nodes per Year. "A, 10 %" in the Legend, means that the plot is done using the entire data set, and the fraction of isolated nodes is 10 %; "P" indicates that only the persistent monitor data is used.*

new edges observed in the country AS graph had at least one endpoint on a country that was already highly connected. This "rich get richer" phenomenon has been observed in other networks [6], and suggests that countries that cannot offer significant connectivity to potential partners will have difficulty obtaining sufficient communicating partners to ensure the robustness of their connectivity to the rest of the Internet.

Figure 11 shows the average degree of the isolated nodes per year when some specific percentage of the countries in the Internet are being isolated. Note that, when just 10 % of the countries are isolated, the average degree of the isolated countries is less than 2. As the size of the set of isolated countries increases, the average degree of the isolated nodes also increases. In addition, while the degree of the isolated nodes for 10 % isolation appears relatively constant with respect to year, the degree increases sharply for later years when examining the isolation of 65 % of the nodes in the graph, supporting the hypotheses that the majority of new links are being formed to the most densely and robustly connected nodes.

These weaknesses could be addressed through a focus on establishing links between poorly connected countries (e.g., through grants to poorer countries or through collaboration between coalitions of physically adjacent countries). This would move the poorly connected countries away from dependence on the infrastructure of the more highly connected countries. It would also move the Internet as a whole towards a more resilient architecture through the provision of alternate geographically diverse pathways.

Future Work. This study on the security of country connectivity graphs is the first of its kind and thus a large amount of related work remains to be explored. Most if not all of the data needed is already publicly available from the CAIDA data sets. One could model all the PoPs on the Internet and their connectivity and analyze how an attacker could take out sets of PoPs to damage the Internet. Another approach could be, instead of mapping ASs to their country of registration, to map the PoPs underlying the ASs to the countries in which they physically reside. This would enable one to model countries nationalizing the Internet infrastructure within their physical boundaries to see what harm could be done. An alternative approach could be to rerun our experiments without modeling all edges as bidirectional. This would show the amount of damage colluding countries could do prior to any possible policy changes implemented by the ASs. Lastly, one could look at specific geographic regions comprising poorer countries to evaluate ways to improve their Internet resilience, as in [7].

References

[1] W. Willinger and J. Doyle, Robustness and the Internet: Design and Evolution, Chapter 10 in *Robust Design, a Repertoire of Biological, Ecological, and Engineering Case Studies* (E. Jen, ed.), Oxford University Press, 2005.

[2] A. Chang, Undersea Cables Are Actually More Vulnerable Than You Might Think[20], Wired, April 3, 2013.

[3] P. Mell, R. Harang and A. Gueye, The Resilience of the Internet to Colluding Country Induced Connectivity Disruptions, in *Proceedings of the Workshop on Security of Emerging Networking Technologies* (SENT), San Diego CA, February 8, 2015.

[4] J. Hawkinson, Guidelines for Creation, Selection, and Registration of an Autonomous System (AS)[21], Internet Engineering Task Force, RFC 1930, March 1996.

[5] T. Bui and C. Jones, Finding Good Approximate Vertex and Edge Partitions is NP-hard, *Information Processing Letters* **42**:3 (1992), 153-159.

[6] A.-L. Barabási and R. Albert, Emergence of Scaling in Random Networks, *Science* **286**:5439 (1999), 509-512.

[7] A. Gueye, P. Mell, D. Banse and Y. Congo, On the Internet Connectivity on Africa, in *Proceedings of the 7th EAI International Conference on e-Infrastructure and e-Services for Developing Countries*, Cotonou, Benin, December 15-16, 2015.

Participants

Assane Gueye, Peter Mell (NIST ITL), Richard Harang (Army Research Laboratory)

[20] http://www.wired.co.uk/news/archive/2013-04/3/vulnerable-undersea-cables

[21] http://tools.ietf.org/html/rfc1930

Part III

Project Summaries

Mathematics of Metrology

Mathematics plays an important role in the science of metrology. Mathematical models are needed to understand how to design effective measurement systems, and to analyze the results they produce. Mathematical techniques are used to develop and analyze idealized models of physical phenomena to be measured, and mathematical algorithms are necessary to find optimal system parameters. Finally, mathematical and statistical techniques are needed to transform measured data into useful information. The goal of this work is to develop fundamental mathematical methods and analytical tools necessary for NIST to continue as a world-class metrology institute, and to apply them to critical measurement science applications.

Computational Tools for Shape Measurement and Analysis

Günay Doğan
Javier Bernal
Charles R. Hagwood (NIST ITL)

The main goal of this project is to develop efficient and reliable computational tools to detect geometric structures, such as curves, regions and boundaries, from given direct and indirect measurements, e.g., microscope images or tomographic measurements, as well as to evaluate and compare these geometric structures or shapes in a quantitative manner. This is important in many areas of science and engineering, where the practitioners obtain their data as images, and would like to detect and analyze the objects in the data. Examples are microscopy images for cell biology or micro-CT (computed tomography) images of microstructures in material science. In Fiscal Year (FY) 2015, we made advances in the following specific components of this project.

Shape energies for image segmentation. Image segmentation is the problem of identifying objects or regions and their boundaries in given images. Our approach to segmentation is to design shape energies incorporating image data and shape regularity criteria modeling specific segmentation scenarios. The shape, a curve or a surface, is the free variable in these energies, and we aim to compute optimal shapes minimizing these energies. In this approach, we start with suboptimal initial curves, and iteratively deform them towards the right object boundaries in the images (see Figure 12 for an example). Günay Doğan has been implementing, and continued to develop a selection of shape energies effective for image segmentation. These are:

1. The Geodesic Active Contour model, used to detect region boundaries characterized by high image gradients (see [1]);
2. A region-based multiphase segmentation shape energy (see [2]), which can decompose the image into homogeneous regions each defined with a distinct mean intensity value (a common scenario in material microstructures); and
3. An anisotropic boundary energy, which improves detection of concave regions by aligning curve normals with extended image gradient fields.

Faster shape optimization. Realizing the iterative shape optimization solution for the segmentation in an effective manner requires a well-thought design and integration of multiple critical ingredients. A central piece is the discretization of the shape, ensuring good resolution of data and geometry without too much computational overhead. To reduce computational cost, we also need to reduce the number of iterations needed to reach optima. For this, Günay Doğan has been developing shape-Newton algorithms and customized stopping criteria, and his recent work demonstrating the efficiency gains for the multiphase segmentation energy was published in [3]. He has also been working with researchers from George Mason University to leverage coarse-to-fine discretizations to further reduce computational cost, and to increase likelihood of finding global minima.

Automation of image segmentation. Many users of our segmentation software are not expected to have a background or experience in image processing. Therefore, it is very important to make the segmentation algorithms as automated as possible for these users. Realistically, almost all algorithms solving any significant data problems require some, and possibly many, parameters to be set, typically by a domain expert. For example, a traditional implementation of the Geodesic Active Contour model requires an edge indicator function to be defined from the image by setting a smoothing parameter and an edge contrast parameter. The edge indicator function is integrated over a curve to define the shape energy, and the energy may not work out if good parameter values are not used in the definition. Then the shape energy is minimized by taking a specified number of steps at specified step sizes, requiring two more parameters governing the iterations, and depending on their values, the iterations may take too long or terminate prematurely. There are additional parameters in the discretization of the geometry and related differential geometry as well. One can easily see

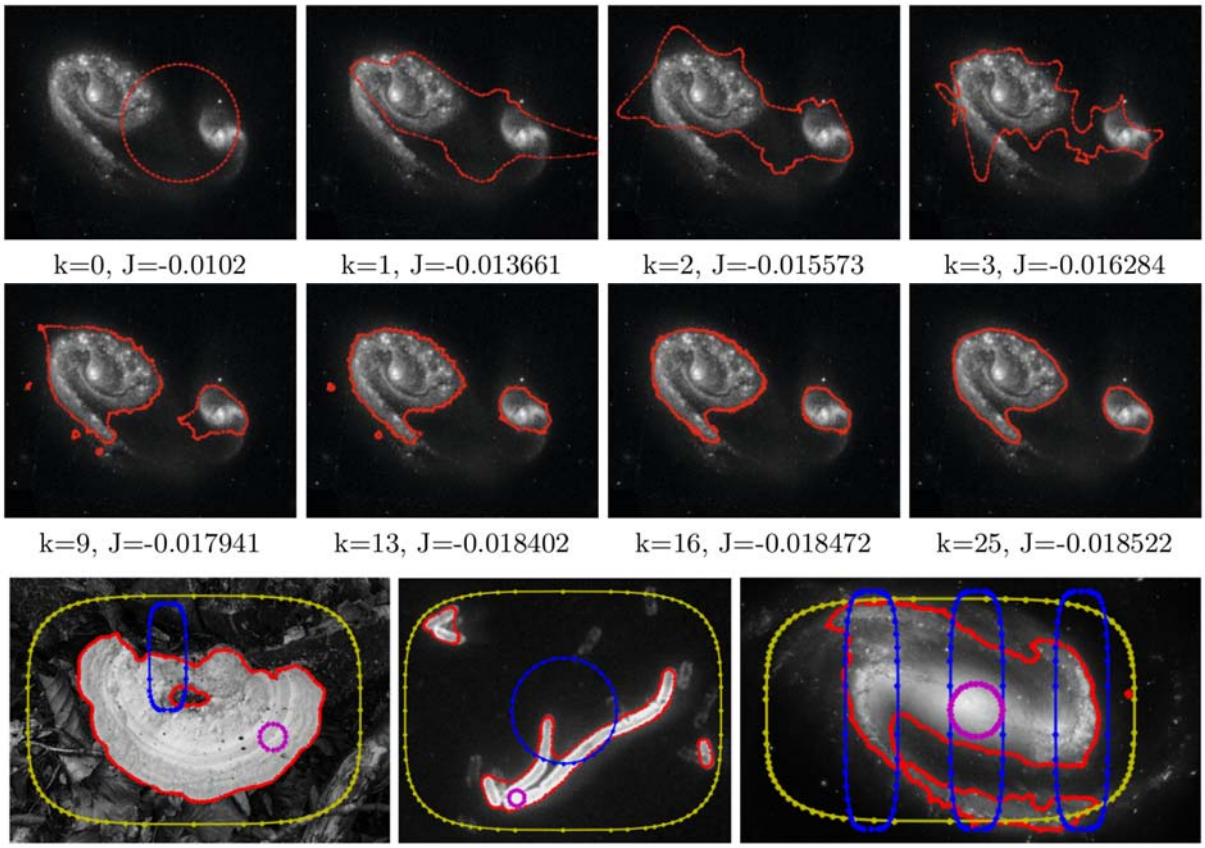

Figure 12. *Example of the energy (denoted J at iteration k) minimization process used to detect objects by iteratively deforming curves, shown in the top two rows. The bottom row shows detected boundaries (red) in different images, starting from different initial curves (blue, yellow, magenta).*

that it is too much to expect of a user, a material scientist, for example, to make good choices under varying imaging scenarios without expert help. For this reason, Günay Doğan has been developing heuristics and algorithmic principles to set such parameters automatically in the shape energies and the shape optimization procedures.

Meshing segmented images. An important use of our segmentation algorithms is for analysis of material microstructure images with the finite element software OOF (see page 46). This requires a computational mesh capturing the geometric features of the microstructure, based on its segmentation. We have previously developed a meshing algorithm that extracts the grain boundaries from a segmented image, and returns a triangulation matching these boundaries. We improved this algorithm by developing smoothing and coarsening algorithms for the boundaries. This results in more natural-looking and compact boundary curves. We then use it to generate high-quality triangulations with fewer elements than the previous version of the algorithm.

Computing shape distances. We have been working with Javier Bernal and Charles Hagwood to develop efficient numerical algorithms to compute an elastic shape distance (dissimilarity score) between 2D shapes. Our shape distance algorithm resulted in up to two orders of magnitude speed gains for large curves, due to its subquadratic running times (in contrast with the cubic asymptotic complexity of the original elastic shape distance algorithm). We have recently developed a fast curve alignment algorithm that runs in $O(N \log N)$ time (down from quadratic time complexity), further improving the efficiency of our shape distance algorithm. Details of this work are described in a separate section on computation of shape distances.

[1] V. Caselles, R. Kimmel, G. Sapiro, Geodesic Active Contours, *in International Journal of Computer Vision* **22**:1 (1997), 61-79.

[2] G. Doğan, An Efficient Curve Evolution Algorithm for Multiphase Image Segmentation, in *Proceedings of the 10th International Conference on Energy Minimization Methods in Computer Vision and Pattern Recognition* (EMMCVPR'15), Hong Kong, January 2015.

[3] G. Doğan, An Efficient Curve Evolution Algorithm for Multiphase Image Segmentation, in *Proceedings of the 5th International Conference on Scale Space and Variational Methods in Computer Vision* (SSVM'15), Bordeaux, France, May 2015.

Computation of Shape Distances

Günay Doğan
Javier Bernal
Charles R. Hagwood (NIST ITL)

In many engineering and scientific applications, experts are interested in comparing shapes of objects quantitatively, making inferences based on the shape similarity or dissimilarity. Examples of such applications are morphological analysis of cells or cell colonies in biology, and object recognition in computer vision. Often such applications involve large data sets, and this motivates the need for fast shape analysis algorithms.

The shape of an object is unlike typical data descriptors, such as feature vectors, or matrices. These are finite-dimensional quantities, which exist in simple vector spaces, whereas mathematical shapes are abstract entities existing on infinite-dimensional Riemannian manifolds. This introduces challenges in both the representation of shapes and computation of shape dissimilarities or shape distances for statistical analyses.

In this work, we have been developing fast algorithms to compute elastic shape distances between given 2D closed curves, based on the square root velocity function (SRVF) formalism of Srivastava et al. [1]. The resulting elastic shape distance is a useful shape dissimilarity metric that matches our intuitive understanding of shapes. It is invariant to scaling, rotation and translation, and it is robust to moderate changes in local features of the shapes. However, it is computationally very expensive. The original algorithm in [1] has cubic asymptotic time complexity with respect to N, the number of the curve nodes, and slows down considerably when N is increased beyond a few hundreds.

The main challenge of this computation is to minimize a mismatch energy so as to optimally match the SRVF representations of two given curves. The variables of this minimization are the rotation angle and the starting point for optimal alignment of the curve shapes, and a reparameterization function defined on the curve to enable elastic matching of curve features. Previously, we developed an iterative optimization algorithm that performed this minimization in subquadratic running times; see Figure 13 which demonstrates the speed gains by our algorithm. The key ingredients of this algorithm were our fast dynamic programming and nonlinear constrained optimization procedures. We presented this algorithm in the premier computer vision conference CVPR'15 [2].

More recently, we improved the efficiency of our algorithm even further. We developed a fast alignment algorithm for closed curves, matching their starting points and rotation angles in O(N log N) time using the Fast Fourier Transform, as opposed to the naïve algorithm with quadratic time complexity [3].

We are currently working on the dynamic programming component of our algorithm. Although this algorithm is very fast in practice, its asymptotic time complexity is quadratic. Our preliminary results show that we will be able to reduce this to linear time complexity. This will enable us to handle very large curves without performance degradation, making it very suitable for large-scale shape statistics studies.

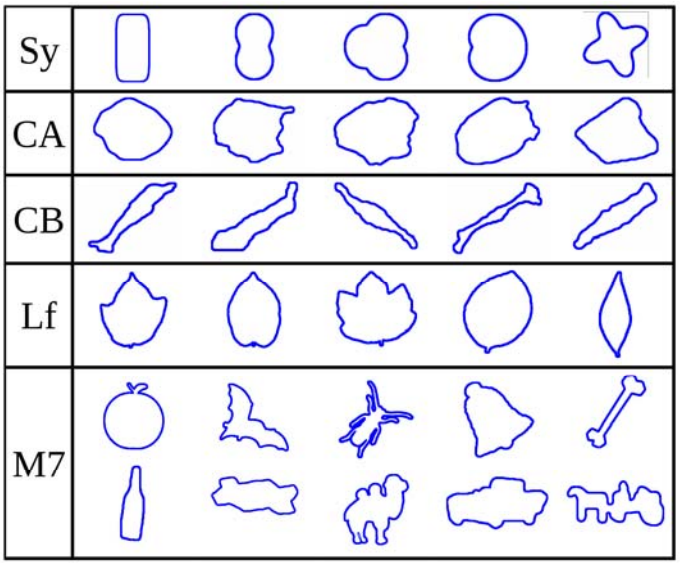

	Matrix Size	Prev. Algo.	New Algo
Synthetic (Sy)	6×6 = 36	1 h	12 min
Cells (CA&CB)	10×10 = 100	2.5 h	4.5 min
Leaves (Lf)	75×75 = 5625	129 h	12.5 h
MPEG7 (M7)	100×100 = 10^4	240 h	38.5 h

Figure 13. *An order of magnitude in speed-up by our new algorithm computing pairwise shape distance matrices for different shape data sets for N=256.*

[1] Srivastava, E. Klassen, S. Joshi and I. Jermyn, Shape analysis of elastic curves in Euclidean space, *IEEE Transactions on Pattern Analysis and Machine Intelligence* **33:7** (2011) 1415-1428.

[2] G. Doğan, J. Bernal and C. R. Hagwood, A Fast Algorithm for Elastic Shape Distances between Closed Planar Curves, in *Proceedings of the IEEE Conference on Computer Vision and Pattern Recognition* (CVPR'15), Boston, MA, June 2015.

[3] G. Doğan, J. Bernal and C. R. Hagwood, FFT-based Alignment of 2d Closed Curves with Application to Elastic Shape Analysis, in *Proceedings of the 1st International Workshop on Differential Geometry in Computer Vision for Analysis of Shapes, Images and Trajectories* (DiffCV'15), Swansea, United Kingdom, September 2015.

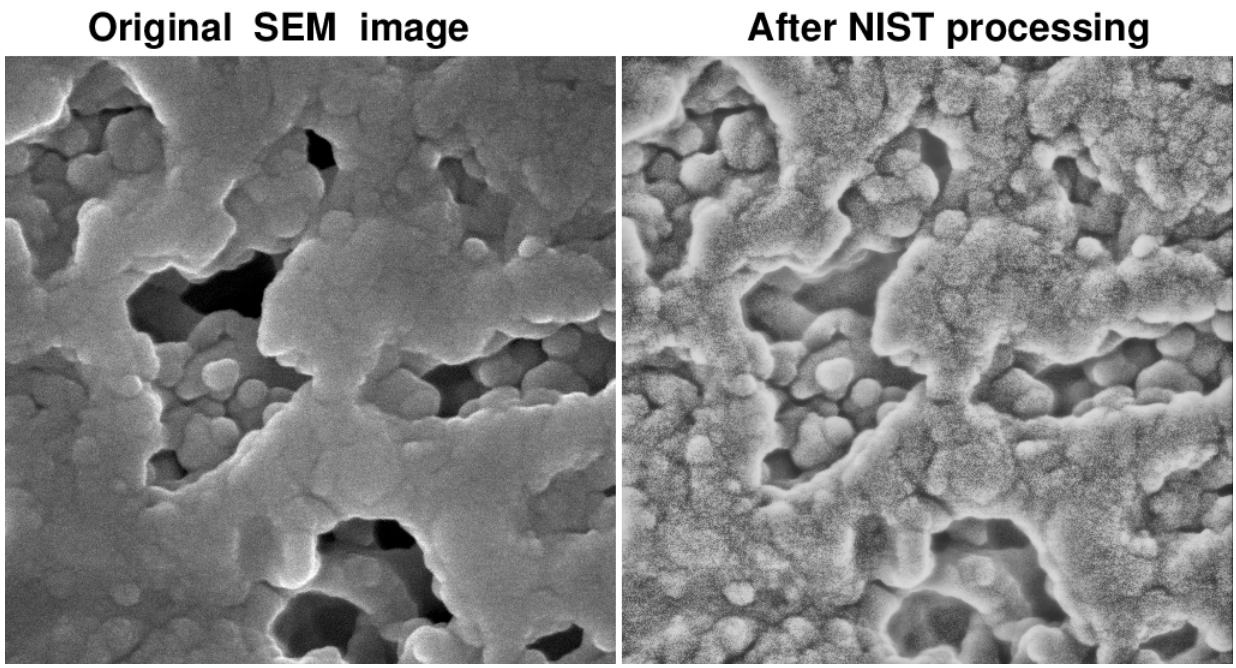

Figure 14. *Useful enhancement of nanoscale SEM image using technique discussed in References [1] and [2].*

Enhancement of Nanoscale Scanning Electron Microscope Imagery

Alfred S. Carasso
Andras E. Vladar (NIST PML)

A recently discovered powerful technique for enhancing Helium Ion Microscope (HIM) imagery [1], involves an initial adaptive histogram equalization of the image, followed by progressive Lévy fractional diffusion smoothing. This particular two stage method had previously been developed for enhancements of forensic latent fingerprints [2]. Interactive Data Language (IDL) software is provided in [1] that can implement this method. Surprisingly, this approach is usually *not helpful* in a wide variety of commonly occurring images, such as face images, astronomical images, or medical images. However, the method has recently been found useful on certain types of scanning electron microscope (SEM) images as illustrated in Figure 14.

This development is highly significant in nanoscale microscopy, as there is now considerable interest in low dose, low landing energy SEM imaging, which typically produces very noisy images. Useful enhancement of such imagery may now be feasible using the above NIST technique.

[1] A. S. Carasso and A. E. Vladar, Recovery of Background Structures in Nanoscale Helium Ion Microscope Imaging, *Journal of Research of the NIST* **119** (2014), 683-701.

[2] A. S. Carasso, A Framework for Reproducible Latent Fingerprint Enhancements, *Journal of Research of the NIST* **119** (2014), 212-226.

Molecular Movies: Imaging Femtosecond Motion during Electrochemical Transitions

Bradley Alpert
Joel Ullom (NIST PML)
Chris Cromer (NIST PML)
Ralph Jimenez (NIST PML)

Vital to the development of next-generation nanomaterials, including photovoltaics and industrial catalysts, is an understanding gained through measurement of electron release, transport, and transfer in engineered nanostructures. This project, completed this year after five years of support by a NIST Innovations in Measurement Science (IMS) grant, achieved the first time-resolved x-ray emission and time-resolved x-ray absorption measurements with a table-top laboratory set-up. The apparatus enables experiments to capture the motion of electrons, atoms, and molecules on femtosecond time scales and with picometer spatial resolution.

The combination of table-top x-ray lasers, a dramatic recent breakthrough developed at JILA[22], with

[22] JILA is a joint physics institute of the University of Colorado at Boulder and NIST. See https://jila.colorado.edu/

transition-edge sensor (TES) microcalorimeter spectroscopy, intensively developed and refined in the Quantum Electronics and Photonics Division, enables these new measurement capabilities. The integration of these components, accompanied by a significant increase in detector array sizes, to achieve large increases in temporal and spatial resolution while maintaining extraordinary TES energy resolution, continues to demand new data modeling and processing techniques. These techniques will overcome current limitations by

- resolving temporal overlap in photon detection while achieving energy resolution of temporally isolated arrivals,
- improving efficiency in elimination of low-frequency background noise, and
- extending multiplexing and reducing cross talk in extracting the signals from 0.1 K to room temperatures.

Wiener filtering, long used among astronomers for estimating amplitudes of pulses of known shape contaminated with noise of known frequency content, is suitable for measuring isolated pulses. Novel processing approaches have been developed, characterized, and are being extended, that rely on this knowledge but are suitable for overlapping pulses.

Analysis efforts this year (1) successfully completed development of a processing method, dubbed multi-pulse fitting, applicable when pulses are poorly separated in time but small enough to allow neglect of detector response nonlinearity, and (2) achieved initial success in treating nonlinear detector response by a modified method of independent component analysis (ICA), which exploits entropy minimization.

Multi-pulse fitting relies on a linear detector response model in which the signal is a superposition of pulses of a single shape and various amplitudes, noise coloring (i.e., its frequency dependence) is corrected, and by a pulse-height to photon energy calibration curve that corrects for deficiencies of this model. This method performs quite well, with low pulse rejection and low deterioration in energy resolution with increasing pulse rate, up to about 100 counts per second per detector, provided photon energies are a modest fraction of the level that saturates the detector.

Detector nonlinear response, significant at higher photon rates and at energies approaching those that saturate the detectors, remains a challenge, but promising results have been achieved by detector characterization through minimization of the entropy of a measured spectrum. This approach uses a calibration source with highly localized spectral features, often present in spectra of interest, to establish calibration curves that separate the effect of detector residual energy from energy of a new arrival. The method, based on information theory, is under active development.

[1] J. W. Fowler, B. K. Alpert, W. B. Doriese, D. A. Fischer, C. Jaye, Y. I. Joe. G. C. O'Neil and D. S. Swetz, J. N. Ullom, Microcalorimeter Spectroscopy at High Pulse Rates: a Multi-Pulse Fitting Technique, *Astrophysical Journal Supplement Series* **219** (2015), 35.

[2] J. W. Fowler, B. K. Alpert, W. B. Doriese, Y. I. Joe, G. C. O'Neil, J. N. Ullom and D.S. Swetz, The Practice of Pulse Processing, *Journal of Low Temperature Physics*, to appear.

A Thousand-Fold Performance Leap in Ultrasensitive Cryogenic Detectors

Bradley Alpert
Joel Ullom (NIST PML)
Lawrence Hudson (NIST PML)
Terrence Jach (NIST MML)

Small arrays of ultrasensitive cryogenic detectors invented and developed at NIST have driven breakthroughs in x-ray materials analysis, nuclear forensics, and astrophysics. They have played a part in prominent international science collaborations in recent years. Despite these successes, NIST's existing cryogenic sensor technology is inadequate for new applications such as in-line industrial materials analysis, energy resolved x-ray imaging, and next-generation astrophysics experiments, which all require faster sensors, much larger arrays, or both. Last year, new support from the NIST Innovations in Measurement Science (IMS) was awarded to develop both of these capabilities in pursuit of 1000-fold increase in sensor throughput, through completely new sensor readout technique (microwave multiplexer) enabling much larger detector arrays and through major new, higher throughput, processing capabilities.

A major project connected to the NIST IMS effort is HOLMES [1], now underway in Italy to measure the mass of the electron neutrino. This experiment, which will use NIST-developed microcalorimeters, superconducting quantum interference device (SQUID) amplifiers, and microwave multiplexer readout, relies on extreme statistics for the spectrum produced by the decay of ^{163}Ho. A principal source of error for microcalorimeter characterization of this spectrum is expected to be due to undetected near-simultaneous ^{163}Ho decay events (pile-ups). Improvements in processing that would allow better detection of nearly coincident pulse pairs could radically alter the design space for the detectors of the experiment.

Alpert this year conducted simulations and developed a novel pile-up detection algorithm using NIST detector response models [2], that convinced the Italian team, led by Angelo Nucciotti, to consider a region of the detector design space (for a slower pulse rise) previously believed unusable for HOLMES. The resulting detectors will have reduced pulse rise (or arrival time)

distortion and the readout electronics specifications will be less extreme, enabling arrays containing more detectors and therefore potentially higher statistics and more precise characterization of the neutrino mass.

[1] B. Alpert, M. Balata, D. Bennett, M. Biasotti, C. Boragno, C. Brofferio, V. Ceriale, D. Corsini, P.K. Day, M. De Gerone, R. Dressler, M. Faverzani, E. Ferri, J. Fowler, F. Gatti, A. Giachero, J. Hays-Wehle, S. Heinitz, G. Hilton, U. Kőster, M. Lusignoli, M. Maino, J. Mates, S. Nisi, R. Nizzolo, A. Nucciotti, G. Pessina, G. Pizzigoni, A. Puiu, S. Ragazzi, C. Reintsema, M. Ribeiro-Gomes, D. Schmidt, D. Schumann, M. Sisti, D. Swetz, F. Terranova and J. Ullom, HOLMES: The Electron Capture Decay of ^{163}Ho to Measure the Neutrino Mass with sub-eV Sensitivity, *European Physics Journal C* **75**:3 (2015), 112.

[2] B. Alpert, E. Ferri, D. Bennett, M. Faverzani, J. Fowler, A. Giachero, J. Hays-Wehle, M. Maino, A. Nucciotti, A. Puiu, D. Swetz and J. Ullom, Algorithms for Identification of Nearly-Coincident Events in Calorimetric Sensors, *Journal of Low Temperature Physics*, to appear.

Clutter Measurements Pilot Project: Toward Evaluating Communications Spectrum Sharing Proposals

Bradley Alpert
Chriss Hammerschmidt (NTIA)
Robert Johnk (NTIA)
Sarah Streett (NIST ITL)
Jack Wang (NIST ITL)

The joint NIST-NTIA Center for Advanced Communications (CAC) and the NIST Communications Technology Laboratory (CTL) will develop the scientific and engineering capacity and experience for technical assessment of spectrum sharing and commercialization proposals. Components of this expertise are already present in the NIST Electromagnetics Division, Physical Measurement Laboratory, the DOC Public Safety Communications Research (PSCR), National Telecommunications and Information Administration (NTIA), and their collaborative research relationships in measurement and modeling within NIST and NTIA.

Kent Rochford, who leads CAC and CTL, suggested in April, 2014, that the researchers (listed above) begin a collaboration to form an initial research bridge between NIST and NTIA. Following a successful effort by Alpert and Wang for preliminary assessment of the uncertainty of in-building Long Term Evolution (LTE) cell phone path-loss surveys by Johnk, presented by Johnk at the PSCR Public Safety Broadband Stakeholder Conference, June, 2014, NTIA Institute for Telecommunication Sciences (ITS) lead Hammerschmidt proposed a one-year pilot project to assess communications disruption due to environmental clutter (buildings, vegetation, power lines, etc.). Its objectives have been (1) collect representative clutter measurement data in support of ongoing rulemakings such as the 3.5 GHz Joint Working Group, (2) perform statistical analysis on these data and determine uncertainties, (3) refine the measurement methods in preparation for a comprehensive data collection program, and (4) provide measurement data to support refinement of existing propagation models.

Lack of experience of the researchers in evaluating uncertainties of communications channel losses, including those due to clutter, has prompted a flurry of initial activity to establish the project's direction. In particular, early surveys have suffered from (1) lack of repeatability due to position uncertainty and limited comparability between nominally identical surveys, (2) large discrepancy, even in uncluttered areas, between path loss surveys and those expected from the ITS Irregular Terrain Model (ITM) of path loss, and (3) lack of a survey of environmental clutter, to serve as a potential independent, predictive variable.

Several field surveys, around Boulder, in Denver, and in San Diego were conducted by the ITS researchers during the past year. The NIST team evaluated the procedures and made recommendations toward isolating different sources of variability and causes of discrepancy between path losses predicted by the ITM and those observed in the surveys. These sources include precise receiving antenna location and velocity, detailed terrain and obstacle shapes as obtained through LiDAR and other surveys, moving scatterers, transmitting and receiving antenna characterization, and temperature, humidity, and time of day factors. More work is needed to demonstrate consistent, repeatable surveys, develop more reliable propagation models, and enable predictions with characterized uncertainty.

A report for the pilot project is in preparation.

Quantitative MRI

Zydrunas Gimbutas
Andrew Dienstfrey
Stephen Russek (NIST PML)
Katy Keenan (NIST PML)
Karl Stupic (NIST PML)
Michael Boss (NIST PML)

Magnetic resonance imaging (MRI) is maturing as a quantitative biomedical imaging technology. For example, imaging facilities routinely report tumor volumes in units of mm^3, blood perfusion in units of ml g^{-1} min^{-1}, apparent diffusion coefficient in mm^2 s^{-1}, and temperature in K. However, as of a few years ago the use of International System (SI) units for these technologies was potentially unwarranted as SI traceability chains

Figure 15. *NIST-Developed MR system phantom. In addition to geometry, biomedical quantities such as proton density, $T_1(\mathbf{r})$, and $T_2(\mathbf{r})$ are defined and characterized by independent means. How accurate are MR-based measurements of these quantities in research and clinical settings?*

supporting these MRI measurement modalities were unclear if not non-existent. More recently NIST and partner institutions have made substantial investments to develop such traceability chains. In the medical community, standard reference artifacts are referred to as phantoms and, in particular, NIST now supports several phantoms providing SI-traceable calibration standards for MRI scanners. One such phantom is shown in Figure 15.

MRI is governed by solutions to the Bloch-Torrey equation

$$\frac{d\mathbf{M}}{dt} = \gamma \mathbf{M} \times \mathbf{B} - \frac{M_x \hat{\mathbf{x}} + M_y \hat{\mathbf{y}}}{T_2} + \frac{(M_0 - M_z)\hat{\mathbf{z}}}{T_1} + D\nabla^2 \mathbf{M}$$

Here, the quantities of medical interest are the tissue-dependent relaxation times T_1, T_2 and the effective diffusion coefficient D which reflects a combination of tissue porosity and anatomical structure. **B** is the forcing magnetization which is further resolved as a sum of gradient and radio-frequency (RF) terms. Finally, the gyromagnetic ratio, γ, is a physical constant and **M** is the magnetic moment arising from collections of nuclear spins.

Broadly speaking, a magnetic resonance measurement consists of a preparation stage in which **M** is preferentially aligned along a fixed axis. This is followed by a sequence of RF pulses, represented in the **B** term above, which rotate **M** by nominal amounts following the dynamics of the Bloch-Torrey equations. Ultimately, the component of **M** lying transverse to a receiver coil is detected as the primary measurement signal. Sequences of RF pulses, distinguished with respect to timing, duration, and orientation, have the effect of emphasizing distinct terms in the Bloch-Torrey equations. Thus, the MR community speaks of weighted images such as T_1, T_2, and diffusion-weighted images. Our goal is to transform this qualitative, pictorial understanding into a quantitative analysis returning in vivo, volumetric parameter maps, traceable to the SI units.

Restricting attention to quantitative T_2 analysis, a specifically designed sequence of RF pulses is delivered such that the signal in each voxel may be modeled as a simple exponential decay,

$$s(\mathbf{r}, t) = C\exp\left(-\frac{t}{T_2(\mathbf{r})}\right). \qquad (1)$$

A series of MR scans of the NIST T_2 array is shown in Figure 16. Each sphere in this array is filled with a prescribed concentration of $MnCl_2$ solution resulting in a nominal true value of T_2. The grayscale values representing MR signal intensity should obey the exponential model (1) with the addition of measurement noise. Recently ACMD staff wrote a computer code to perform the non-linear inversion which takes noisy samples of (1) as input, and returns an estimate of $T_2(\mathbf{r})$. Furthermore, an uncertainty estimate is derived from a parametric bootstrap, Monte Carlo analysis. This Monte Carlo uncertainty analysis was found to be within a reasonable factor of the lower-bounds on uncertainty determined by unbiased, Cramer-Rao theory. Preliminary results are promising, demonstrating the ability to quantify T_2 using the NIST MR scanner with relative expanded uncertainties ranging from 10 % – 20 %. Further attempts to reduce this uncertainty revealed systematic intensity signals that were not noticed previously in this experiment. We are currently performing further studies to identify the sources of these signals.

This T_2 analysis workflow is being developed as a paradigm for a large, cross-site, multi-modal quantitative MRI phantom study being conducted by NIST in collaboration with several external stakeholders. In this study, NIST-designed phantoms are being circulated and imaged using tightly prescribed scanning protocols. The quantities to be analyzed include: T_1, T_2, proton density, 3D geometric distortion, geometric resolution, and slice profile. Currently there is inadequate understanding of the degree to which these quantities can be measured in clinical MR settings independent of variability in location, time, and scanner device. Stable recovery in the presence of such variables is critical for longitudinal studies necessary to provide new quantitative foundations for diagnosis, treatment, and long-term monitoring of a variety of medical conditions such as Alzheimer's, traumatic brain injury, and stroke. We will initiate detailed analysis of the round robin study in 2016. External collaborators include the Department of Veterans Affairs, the National Institutes of Health, and

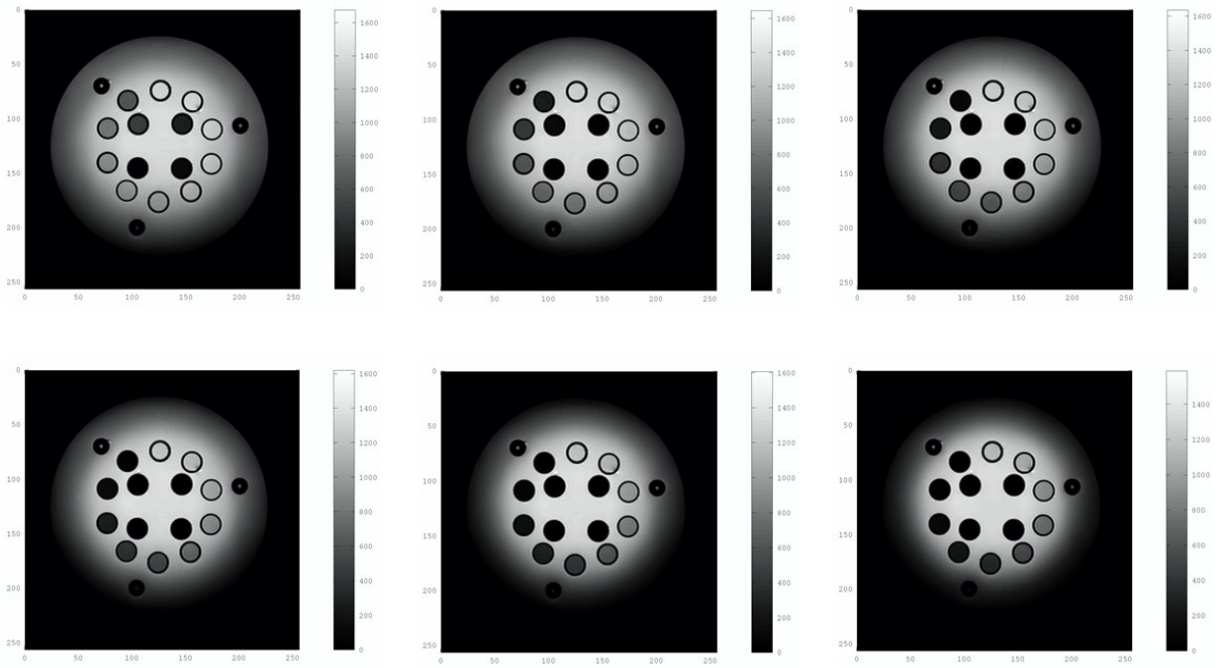

Figure 16. *MR scan of NIST T_2 array. Each sphere is loaded with $MnCl_2$ solution of different concentrations resulting in a known collection of true T_2 values. The signal intensity progresses from light to dark following an exponential decay law as in Equation 1.*

a standards subcommittee of the International Society of Magnetic Resonance in Medicine, which in turn, contains several academic centers as members. We hope to report on this work in the coming year.

[1] H.-L. Cheng, *et al.*, Practical Medical Applications of Quantitative MR Relaxometry, *Journal of Magnetic Resonance Imaging* (2012) **36**, 805-824.

Uncertainty Calculations for Building Engineering

Anthony Kearsley
Lisa Ng (NIST EL)
Andy Persily (NIST EL)

Calculating flow within confined building spaces is an important problem. Unhealthy flow can jeopardize human health and welfare, and may even lead to mortality and extreme cases. Flow simulation and modeling is also particularly crucial when energy efficiency is a focus of building specifications. Such is the case with the Net-zero house built here at NIST.

One important flow calculation involves, essentially, balancing flow from different zones within the house, and doing so based on measured quantities, and therefore uncertainties. The problem can be formulated in terms of *tracer analysis* where a tracer injection, say G, at some instance in time is measured, which gives rise to a concentration response, call it C, and a change in concentration as a function of time, say C'. These three quantities associated with a collection of zones measured at some instant in time determine an *instantaneous* data set. Given n zones, the data set (C, C', G) are three $n \times n$ matrices. In this case, an energy balance is sought such that our matching variables, say W, should have row sums that vanish. In practice, one may want to impose simple bounds on the elements w_{ij} of W. Taken together a solution to

$$C\, W^{\mathsf{T}} = T$$

is sought, where T is the tracer rate matrix, a sum of tracer injection G and an injection correction accumulation term, $k\, C'$, where k is a constant zone specific constant. Loosely speaking, T is a matrix of tracer rates. This problem is further complicated in that a solution W is sought that (approximately) solves the equation above (and satisfies constraints not specified here) but is also subject to measurement errors. In short, an approximate solution W and estimated uncertainties are needed.

This year we managed to solve the above equation with small uncertainties associated with each of the measurements. We did so by solving a constrained output-least-squares formulation of the problem together with an augmented Lagrangian technique to impose the constraints, mostly simple bounds. A local Newton-method was formulated and employed to estimate worst case estimates and were found to be within the domain of validity.

Simulation and Optimization in Cryobiology

Anthony Kearsley
Daniel Anderson (George Mason University)
James Benson (Northern Illinois University)

Mathematical modeling is playing an ever increasing role in the understanding cells, tissues, and organs undergoing cryopreservation. The frequency and variety of uses of these models is increasing almost daily. Cryopreservation procedures permit cells to be stored indefinitely using extremely cold temperatures to suspend all metabolic activities. Cryoprotectants are the chemical foundation of cryobiology as they prevent cellular damage during the freezing process. After proper freezing, cells should be able to be stored for an indefinite amount of time. This can be done, for example, by immersing them in liquid nitrogen, an extremely cold fluid with an approximate temperature of -196 ºC. Cryoprotectants must be removed later during the thawing process and slowly the water balance in the cell can be restored, and normal activity in the cell should return. Procedures exist for the freezing of single cells, tissue comprised of many cells, and entire organs. Size, amount of cytoplasm (or fluid), and structural complexity change the freezing procedures employed. For example, cells with less cytoplasm, like sperm cells, are generally considered to be less difficult to freeze than those cells with more cytoplasm, like eggs. Slow freezing or equilibration has been successfully employed to freeze and store a wide range cells but research is ongoing to optimize the cryobiology of cells.

In a series of recent review papers, [1-3] we have examined from first principles the thermal transport, mass transport and solidification processes of an externally-cooled ternary mixture that surrounds a biological cell. We have established a thermodynamic framework suitable for cryobiological applications through the identification of various forms for the Gibbs Free Energy for chemical systems and forms for chemical potential gradients used in the definition of chemical fluxes and also reviewed choices for chemical composition variables. We have developed the bulk transport models as well as their coupling to both phase-change (solidification) boundaries and the semi-permeable cell membrane; detailed equations in the bulk and at the boundaries were given for multi-species systems. We have conducted a thorough study of the partial differential equations and coupled boundary conditions specific for a spherical cell geometry surrounded by a ternary solution. Solutions to this free-boundary problem were compared to related models in cryobiology that assume spatial uniformity of thermal and chemical fields in the cell and surrounding fluid. One of our more complicated models adds a solidification front encroaching upon the cell and effects generated by the associated confinement of the fluid and cell. To our knowledge we are the first to study this scenario. Our future work [4] seeks to describe the solution strategies and numerical methods for this multiple free-boundary problem as well as related control problems.

[1] D. M. Anderson, J. D. Benson and A. J. Kearsley, Foundations of Modeling in Cryobiology—I: Concentration, Gibbs Energy, and Chemical Potential Relationships, *Cryobiology* **69** (2014) 349–360.

[2] D. M. Anderson, J. D. Benson and A. J. Kearsley, Foundations of Modeling in Cryobiology—II: Heat and Mass Transport in Bulk and at Cell Membrane and Ice-Liquid Interfaces, in preparation.

[3] D. M. Anderson, J. D. Benson and A. J. Kearsley, Foundations of Modeling in Cryobiology—III: Heat and Mass Transport in a Ternary System, in preparation.

[4] D. M. Anderson, J. D. Benson and A. J. Kearsley, Numerical Solution of Inward Solidification of a Dilute Ternary Solution towards a Semi-Permeable Spherical Cell, in preparation.

Stochastic Regression in Chemometrics

Anthony Kearsley
John Curry (NIST PML)
William Wallace (NIST MML)

Stochastic differential equations (SDE) can be used to model complex phenomenon including modelling noise in chemometrics spectroscopy. Previously our research demonstrated that a stochastic regression model can be used to successfully separate signal from noise in very important chemical spectra (arising in forensics, health science, etc.). Spectra can be decomposed into additive contributions from signal and from estimated noise. With an eye towards developing this mathematical machinery into a method for analyzing patterns in chemical spectra we investigated the mean-square stability of a stochastic differential equation developed specifically to predict a decomposition of chemical spectra into noise and signal. Making an assumption of multiplicative noise, we observed fascinating numerical behavior that suggests that the stochastic regression suggested earlier [1] may be even more effective at identifying spectral structure than previously expected.

If one considers a traditional θ-method applied to a deterministic problem, it was shown by Saito and Mitsui [2] that the deterministic A-stability property of the θ-method does not carry through to the mean-square context in general. In fact, they rigorously demonstrated a condition under which unconditional stability holds. This suggests an identifiable point which one can compute precisely where unconditional stability is lost. This can be thought of as an $A(\alpha)$ stability result.

We sought to use this result to determine in our stochastic regression where the ratio of noise and signal coefficients actually *loose stability*. Intuition suggests that these points would indicate structures of interest, say a peak, a trough or an inflection point. A few differences exist between our work in [1] and the more general work (e.g., [3]). We regress on the variation in a signal, not the actual signal position. Secondly, we have a linear deterministic term not present in the *standard* SDE model. We have identified very promising but perplexing numerical results that suggest the work presented in [1] does a better job of predicting structures of interest than it should when applied to a collection of data taken from an *electrospray* experiment. We plan to continue our study of SDE analysis as a chemical structure prediction method.

[1] A. J. Kearsley, Y. Gadhyan and W. E. Wallace, Stochastic Regression Modeling of Chemical Spectra, *Chemometrics and Intelligent Laboratory Systems* **139** (2014), 26-32.

[2] Y. Saito and T. Mitsui, Stability Analysis of Numerical Schemes for Stochastic Differential Equations, *SIAM Journal of Numerical Analysis* **33** (1996), 2254–2267.

[3] D. J. Higham, An Algorithmic Introduction to Numerical Simulation of Stochastic Differential Equations, *SIAM Review* **43** (2001), 525-546.

Modeling Magnetic Fusion

Geoffrey McFadden
Antoine Cerfon (New York University)

A future source of commercial energy may be based on the controlled fusion of a hot plasma of hydrogen isotopes that is confined by a strong magnetic field. Quite often a toroidal geometry is envisioned in which the ions fuse to form helium and release energetic neutrons. A number of computational methods to model such magnetic fusion devices have been developed by researchers at New York University (NYU) and elsewhere to allow effective numerical simulations of the most essential features of modern tokomak and stellarator experiments.

G. McFadden and colleagues at NYU completed a benchmarking exercise to compare the simulation results produced by a number of codes that are in use by the fusion community [1,2]. The benchmark is based on the DIII-D tokomak experiment at General Atomics in San Diego, California. The benchmarking exercise was organized by researchers at the Princeton Plasma Physics Laboratory and Oak Ridge National Laboratory.

G. McFadden and colleagues at NYU are currently modeling the linear stability of a plasma in an annular configuration with an axial distribution of current. In this study the results of a conventional magnetohydrodynamic (MHD) model are compared with those from a more complicated model that includes effects of particle transport. This results in a non-self-adjoint eigenproblem in which the (complex) eigenvalue enters in a nonlinear fashion, requiring a non-standard numerical treatment. The study should be useful in highlighting limitations of the continuum MHD models that are widely used to predict the performance of fusion devises.

[1] A. Reiman, A. Cerfon, G. McFadden, et al., Tokamak Plasma High Field Side Response to an $n = 3$ Magnetic Perturbation: A Comparison of 3D Equilibrium Solutions from Seven Different Codes, *Nuclear Fusion* **55** (2015) 063026.

[2] P. R. Garabedian and G. B. McFadden, Design of the DEMO Fusion Reactor Following ITER, *Journal of Research of the National Institute of Standards and Technology* **114** (2009) 229-236.

Parallel Adaptive Refinement and Multigrid Finite Element Methods

William F. Mitchell
Marjorie A. McClain
Eite Tiesinga (NIST PML)
Paul Julienne (NIST PML)
John Villarrubia (NIST PML)
Garnett Bryant (NIST PML)
Michael Gullans (NIST PML)

http://math.nist.gov/phaml

Finite element methods using adaptive refinement and multigrid techniques have been shown to be very efficient for solving partial differential equations (PDEs). Adaptive refinement reduces the number of grid points by concentrating the grid in the areas where the action is, and multigrid methods solve the resulting linear systems in an optimal number of operations. Recent research has been with *hp*-adaptive methods where adaptivity is in both the grid size and the polynomial order of approximation, resulting in exponential rates of convergence. W. Mitchell has been developing a code, PHAML (for Parallel Hierarchical Adaptive MultiLevel), to apply these methods on parallel computers. The expertise and software developed in this project are useful for many NIST laboratory programs, including material design, semiconductor device simulation, the quantum physics of matter, and simulation of scanning electron microscopes.

We have continued to expand the forms of *hp*-adaptivity available in PHAML. We implemented a new strategy this year due to Bürg and Dörfler which solves a local residual problem on a small patch of elements for each of the candidate refinements to determine which candidate is most effective. We also extended four of

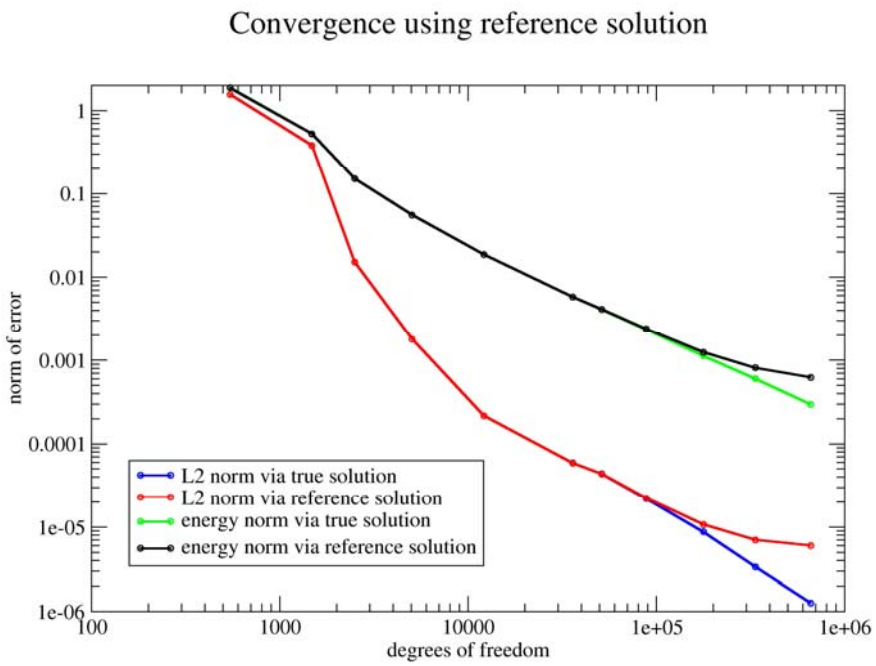

Figure 17. *Convergence of a finite element solution as measured by using a reference solution vs. using the true solution.*

the *hp*-adaptive strategies, as well as *p*-adaptivity, to the 3D code. We used PHAML to perform a numerical experiment to address the question of how large of a polynomial degree is worthwhile in *hp* and high order finite elements, and what type of refinement is best in different situations. The study showed that with low accuracy requirements, *h*-adaptive refinement with elements of degree 3 or 4 is sufficient, but with high accuracy requirements it is best to use *hp*-adaptivity up to degree 10. We have created a web site[23] to make available a collection of standard benchmark PDEs that are suitable for bench-marking and testing adaptive mesh refinement algorithms and error estimators. We continue to add new PDEs to this collection to cover additional problem characteristics. We also completed the implementation of a reference solution module and added a reference solution to one problem in the collection for which the exact solution is unknown. We performed a study to assess whether or not one can use a reference solution as the "true" solution for determining the norm of the error of a less accurate solution, examining convergence rates, determining the accuracy of an *a posteriori* error estimate, etc. As shown in Figure 17, the reference solution is an excellent substitute for the true solution until the norm of the error is about a factor of 2 or 4 larger than the norm of the error of the reference solution.

There are three major collaborative efforts with PML that apply PHAML to their physical models. In a collaboration with Eite Tiesinga and Paul Julienne, we are using PHAML to study the interaction of atoms and molecules held in an optical trap. We are using a 3D model to calculate the bound states, scattering properties and dynamics of two interacting dipolar molecules. Figure 18 illustrates the type of wave functions that come from these calculations. The large lobes are due to the optical trap, and the small lobes in the center are due to the atom-atom interaction with the orientation due to the dipole moment. We are also looking into the use of absorbing (non-reflecting) boundary conditions on the surface of an ellipsoid removed from the domain. We have performed calculations to examine how the energy levels are effected by the eccentricity of the ellipsoid.

We are also collaborating with John Villarrubia to apply PHAML to the modeling of scanning electron microscope images of samples that contain a mixture of conducting and insulating regions. John has a code, JMONSEL[24], that models electron scattering in materials, secondary electron production, and detection. We have coupled this code with PHAML which performs the finite element analysis to determine the electric fields that affect the image. This year we extended PHAML to handle several situations that arise in John's models but were not previously supported by PHAML. These include interior Dirichlet constraints which come from a grounded piece of metal in the sample, floating constraints which come from a charged piece of metal in the interior of the sample, and duplicate face elements at the interface of two materials. We have also begun to experiment with mesh adaptivity. We are developing a new physics-based error estimate that reflects the amount of error in an electron's path as it passes through an element, rather than the error in the electric potential in that element.

Our collaboration with Garnett Bryant applies PHAML to the simulation of quantum dot structures. Nanoscale semiconductor quantum dot structures can be

[23] NIST Adaptive Mesh Refinement Benchmark Problems, http://math.nist.gov/amr-benchmark

[24] Java Monte Carlo Simulation of Secondary Electrons

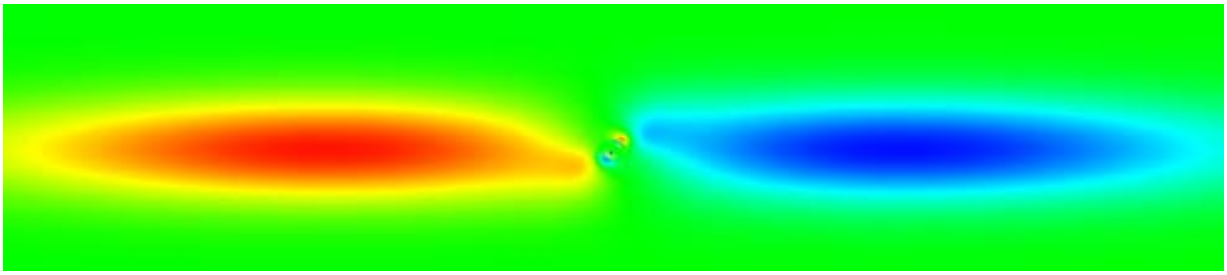

Figure 18. *The x-z plane slice of a wave function from a simulation that combines an optical trap, atom-atom interaction and dipole moment.*

modified, controlled, and manipulated by applied electric fields that arise from the local strain in the quantum dots. In this collaboration we are using PHAML to determine these applied fields and potentials down to the scale of the quantum dots. This year we interfaced PHAML with Garnett's existing codes that describe these quantum dot structures. With one of Garnett's post-docs, Michael Gullans, we have begun to use PHAML to model a single plasmon SET-donor-graphene device, which has applications to on-chip photodetection, optical signal processing and quantum computing with CMOS compatible devices.

Future work will continue to enhance PHAML with additional capabilities, robustness and efficiency, implement and study some recently proposed *hp*-adaptive strategies, complete the extension of PHAML to 3D problems, continue the development of the adaptive mesh refinement benchmark suite, and continue collaborations that use PHAML to solve NIST applications.

Relevant recent references are provided in [1-8].

[1] W.F. Mitchell and M.A. McClain, A Comparison of *hp*-Adaptive Strategies for Elliptic Partial Differential Equations, *ACM Transactions on Mathematical Soft*ware **41**:1 (2014), 2 (39 pages).

[2] W.F. Mitchell, How High a Degree is High Enough for High Order Finite Elements? Proceedings of the 2015 International Conference on Computational Science, *Procedia Computer Science* **51** (2015), 246–255.

[3] W.F. Mitchell, 30 Years of Newest Vertex Bisection, in review.

[4] W.F. Mitchell and M.A. McClain, "Performance of *hp*-Adaptive Strategies for Elliptic Partial Differential Equations," International Conference on Numerical Analysis and Applied Mathematics, Rhodes, Greece, September 2014.

[5] W.F. Mitchell, "NIST AMR Benchmarks," poster, SIAM Conference on Computational Science and Engineering, Salt Lake City, UT, March 2015.

[6] W.F. Mitchell, "Using Space Filling Curves to Find an Element That Contains a Given Point, SIAM Conference on Computational Science and Engineering," Salt Lake City, UT, March 2015.

[7] W.F. Mitchell, "How High a Degree is High Enough for High Order Finite Elements?" International Conference on Computational Science (ICCS), Reykjavik, Iceland, June 2015.

[8] W.F. Mitchell, "30 Years of Newest Vertex Bisection," 13th International Conference of Numerical Analysis and Applied Mathematics (ICNAAM), Rhodes, Greece, September 2015.

Stable Explicit Time Marching in Ill-Posed Initial Value Problems for Partial Differential Equations

Alfred S. Carasso

There is a great deal of current interest in effective numerical methods for solving multidimensdional, nonlinear, ill-posed initial value problems in partial differential equations. In environmental forensics, ill-posed time-reversed parabolic equations are widely used in locating sources of groundwater contamination [1-2]. In geophysics, thermal convection in the Earth's mantle is the principal heat and mass transport mechanism. Numerical computation of the ill-posed time-reversed thermal convection problem is an active research topic, seeking to reconstruct temperature profiles in the Earth's interior in the geological past [3-4]. Numerous other significant applications of ill-posed problems are discussed in [5-7].

However, computation of ill-posed initial value problems presents formidable difficulties. Conventional stepwise time-marching schemes, whether explicit or implicit, are necessarily unconditionally unstable, and result in explosive noise amplification. Recently, in a major breakthrough [8-9], a method was discovered that can stabilize explicit marching schemes by applying easily synthesized linear smoothing operators at each time step to quench the instability. Smoothing operators $S = \exp\{-\varepsilon\, \Delta t\, (-\Delta)^p\}$, based on positive real powers of the negative Laplacian $(-\Delta)$, can be realized efficiently on rectangular domains using fast Fourier transform (FFT) algorithms. Such stabilization leads to a distortion away from the true solution. However, that error is often small enough to allow for useful results in many problems of interest. This new approach opens the door to relatively easy and useful computation of some previously intractable nonlinear problems, and it provides a useful

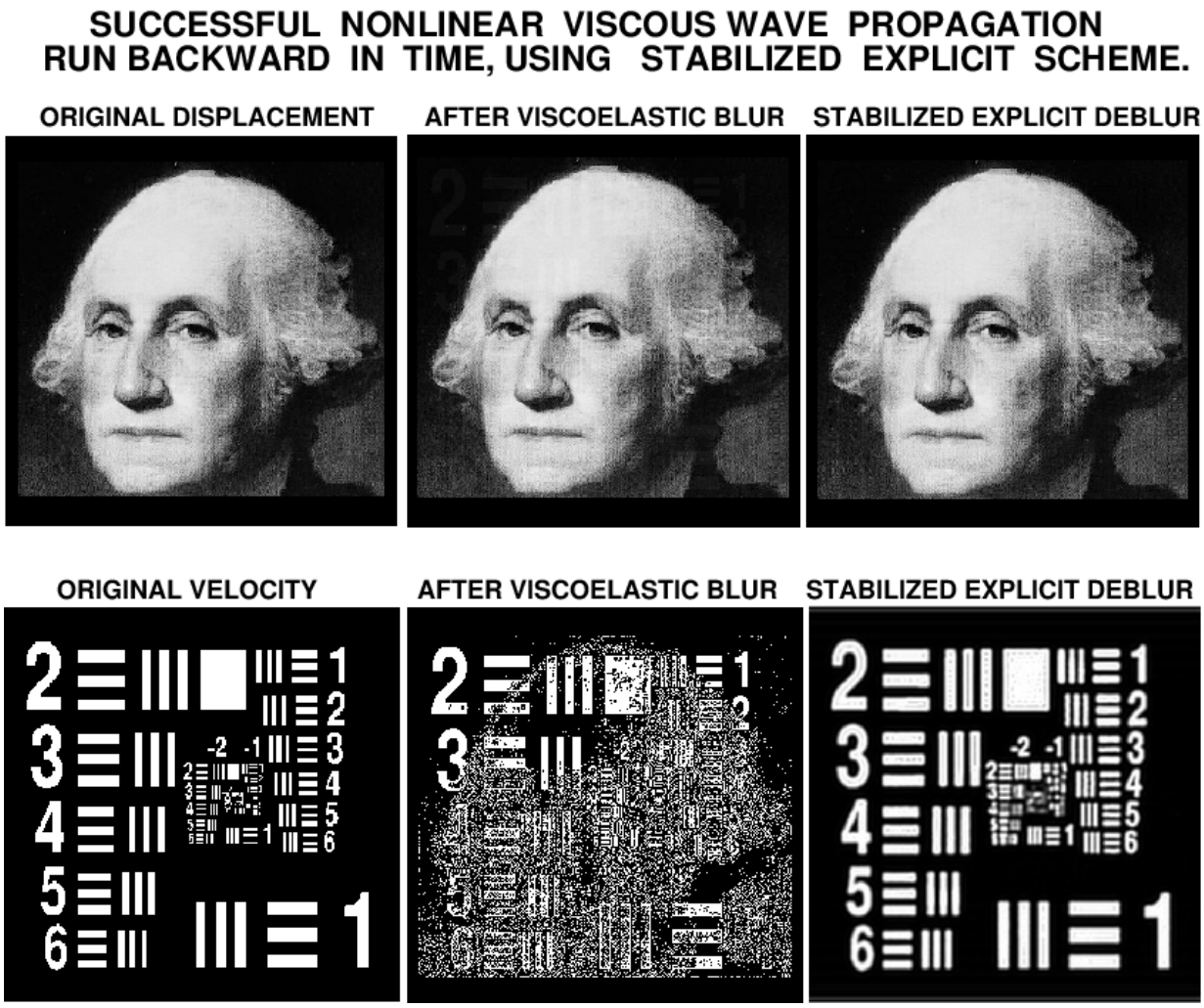

Figure 19. *Successful backward recovery in nonlinear viscous wave equation applied to 512 × 512 images. With initial displacement and velocity shown in the leftmost column, nonlinear viscous wave equation was solved numerically forward in time up to a positive time T. This produced the images shown in the middle column. These data were then used as input in the time-reversed FFT-Laplacian stabilized explicit scheme discussed in [9] to produce the deblurred images shown in the rightmost column.*

complement to the quasi-reversibility method [6], whose formulation is primarily oriented toward linear problems.

Viscous wave equation. An instructive survey of prototypical ill-posed initial value problems is given in [6]. With positive constants a, b, the classical linear viscous wave equation $w_{tt} - 2a\Delta w_t - b\Delta w = 0$ is discussed in [6], and shown to be ill-posed backward in time. In [9], a more general nonlinear version of the same equation is considered in a rectangular region. A stabilized explicit scheme is then developed and analyzed for the time-reversed problem, and shown to lead to almost best-possible results in the canonical linear self adjoint case. Eight bit gray scale 512 × 512 pixel images provide ideal test problems for inverse reconstruction algorithms, and several such images are used in [8-9]. An example of successful nonlinear backward in time viscous wave reconstruction is shown in Figure 19. With initial displacement and velocity shown in the left most column, a nonlinear viscous wave equation was solved numerically forward in time up to some positive time T, resulting in the images in the middle column. Using the middle column as input data at time T, the stabilized explicit scheme discussed in [9] was run backward in time to produce the images in the rightmost column. This example is not tractable by the quasi-reversibility approach discussed in [6], owing to the nonlinearity. Moreover, even in the linear case, the quasi-reversibility method involves the addition of higher order differential operators, and the use of implicit schemes to march backward in time. With large multidimensional arrays, such implicit schemes would require a computationally intensive solution of the resulting algebraic systems of difference equations at each time step. This difficulty is avoided in the present explicit approach.

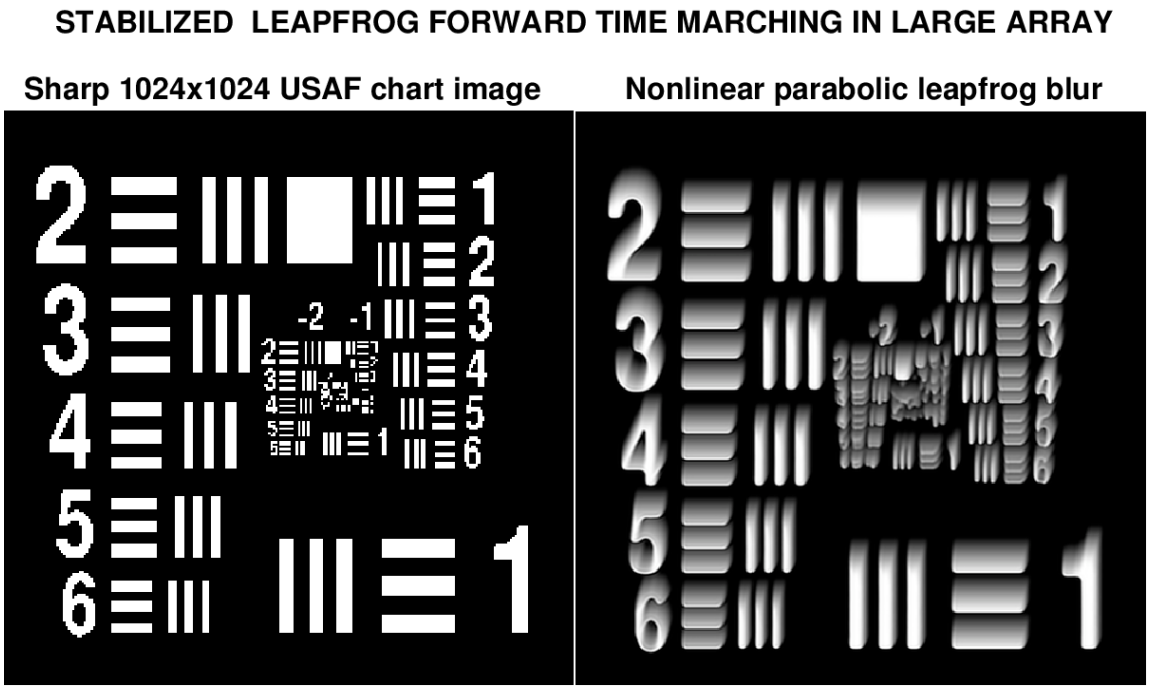

Figure 20. *Relatively painless second order accurate stabilized explicit leapfrog computation in well-posed forward nonlinear parabolic equation applied to 1024 × 1024 image. Second order accuracy using Crank-Nicholson implicit scheme would require solution of nonlinear system of difference equations of order 10^6 at each time step.*

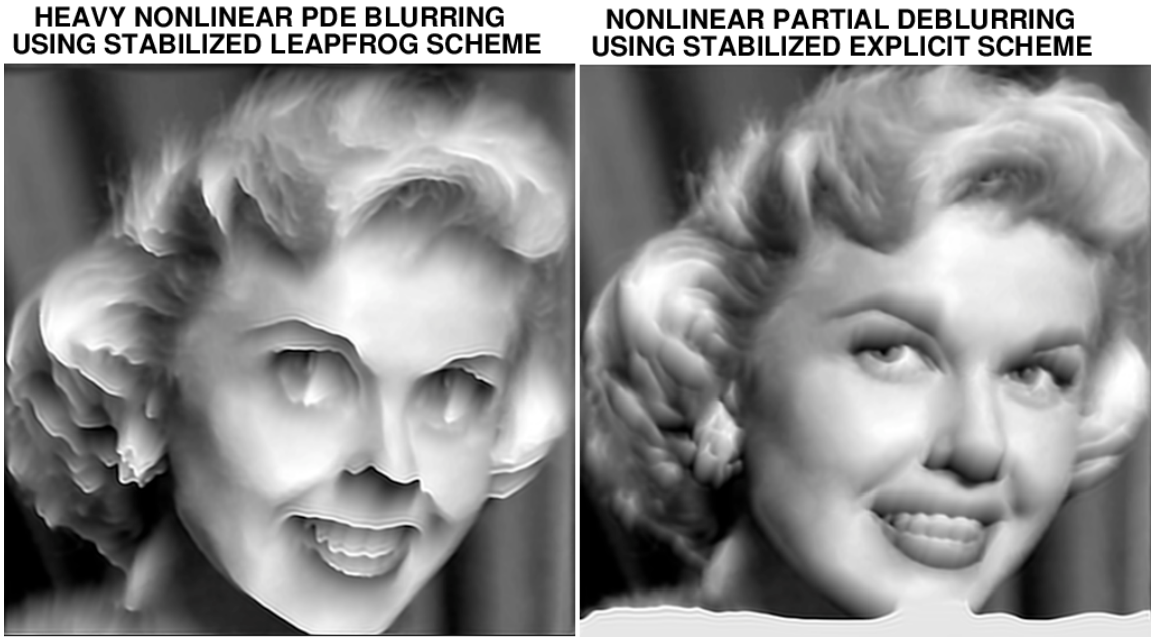

Figure 21. *Accurate nonlinear parabolic blurring of 512 × 512 Doris Day image is easily achieved with the stabilized leapfrog scheme. However, backward leapfrog recovery fails here, while useful reconstruction is provided with the backward pure explicit scheme in [8].*

Stabilizing the leapfrog scheme in parabolic equations. One hundred years ago, L. F. Richardson introduced second order accurate explicit centered time differencing, and used such a "leapfrog" scheme in his failed attempt at numerical weather prediction. However, while highly desirable, the leapfrog scheme is unconditionally unstable in well-posed forward parabolic equations. Using an approach similar to that used in [8], stabilization of the leapfrog scheme was achieved

for an important class of second order nonlinear parabolic equations. An example of a relatively painless second order accurate stabilized explicit leapfrog computation, in a well-posed forward nonlinear parabolic equation applied to 1024 × 1024 image, is given in Figure 20. To obtain the equivalent accuracy using the Crank-Nicholson implicit scheme would necessitate the solution of a nonlinear system of difference equations of order 10^6 at each time step. Surprisingly, the stabilized leapfrog scheme is much less well-behaved backward in time than is the less accurate pure explicit scheme in [8]. In Figure 21, the nonlinearly distorted Doris Day image, computed accurately by the forward stabilized leapfrog scheme, cannot be deblurred by the backward leapfrog scheme. Useful reconstruction is feasible however, with the backward pure explicit scheme in [8].

Future directions. Future work will consider other irreversible systems of partial differential equations such as coupled sound and heat flow, and thermoelasticity. An approach to problems in nonrectangular regions, based on enclosing that region in a larger rectangle, is being considered. Also, the anomalous behavior backward in time in the stabilized leapfrog scheme will be reexamined, and possibly mitigated.

[1] J. Atmadja and A. C. Bagtzoglou, State of the Art Report on Mathematical Methods for Groundwater Pollution Source Identification, *Environmental Forensics* **2** (2001), 205-214.

[2] T. H. Skaggs and Z. J. Kabala, Recovering The History of a Groundwater Contaminant Plume: Method of Quasi-Reversibility, *Water Resources Research* **31** (1995), 2669-2673. DOI 10.1029/95WR02383

[3] Ismail-Zadeh *et al*., Three Dimensional Forward and Backward Numerical Modeling of Mantle Plume Evolution: Effects of Thermal Diffusion, *Journal of Geophysical Research* **111** (2006) B06401. DOI 10.1029/2005JB003782

[4] A. Ismail-Zadeh *et al*., Numerical Techniques for Solving the Inverse Retrospective Problem of Thermal Evolution of the Earth Interior, *Computers and Structures* **87** (2009), 802-811.

[5] M. M. Lavrentiev, Some Improperly Posed Problems of Mathematical Physics, Springer-Verlag, New York, 1967.

[6] R. Lattès and J. L. Lions, The Method of Quasi-Reversibility, American Elsevier, New York, 1969.

[7] K. A. Ames and B. Straughan, Non-Standard and Improperly Posed Problems, Academic Press, New York, 1997.

[8] A. S. Carasso, Stable Explicit Time Marching in Well-Posed or Ill-Posed Nonlinear Parabolic Equations, *Inverse Problems in Science and Engineering*, 2015. DOI 10.1080/17415977.2015.1110150

[9] A. S. Carasso, Stable Explicit Stepwise Marching Scheme in Ill-Posed Time-Reversed Viscous Wave Equations, *Inverse Problems in Science and Engineering*, 2016, to appear.

Numerical Solutions of the Time Dependent Schrödinger Equation

Barry I. Schneider
Klaus Bartschat (Drake University)
Xiaoxu Guan (Louisiana State University)

We have been collaborating for a number of years to develop numerically robust methods for solving the time dependent Schrödinger equation. Although the approaches that have been developed are quite general, the applications to date have concentrated on describing the single and double ionization of electrons exposed to intense, ultrafast, laser radiation. These attosecond (10^{-18} sec) pulses provide a new window to study electronic motion in atoms and molecules on their natural timescale. To put this in context, the motion of electrons responsible for chemical binding and electron transfer processes in nature, have a characteristic timescale of about 100 attoseconds. (It takes an electron 152 attoseconds to go around the hydrogen atom).

Such processes can only be described using time dependent quantum mechanics and, where appropriate, need to be coupled to Maxwell's equations to describe macroscopic phenomena. At the end of the day, we wish to image quantum phenomena with sub-femtosecond temporal and sub-Angstrom spatial resolution, eventually producing "molecular movies" of this motion in much the same way as it is done in molecular dynamics simulations of heavy particle processes. The basic methodology as applied to atoms and simple diatomic molecules has been described in [1-3,5-10], and [4] provides a detailed review of the work. The essential aspects have been

- development of the finite element discrete variable method (FEDVR) to spatially discretize the coordinates of the electrons, and
- use of the short iterative Lanczos method to propagate the wavefunction in time.

The method has been efficiently parallelized using the message passing interface (MPI), MPI and scales linearly with the size of the FEDVR basis. Large scale calculations have been performed on a number of atoms and molecules using resources provided by the National Science Foundation (NSF) Extreme Science and Engineering Discovery Environment (XSEDE). The group has received a competitively awarded allocation of more than 8 million service units for the current fiscal year.

Intel Co-Processor Study. During the past year, the group has concentrated its efforts porting the code to the Intel Phi co-processors and studying the behavior of the code as a function of the work allocated to the main Xeon node and the Intel Phi cores. The study was done using the Compiler Assisted Offload mode. In that approach, compiler directives are inserted into the code to

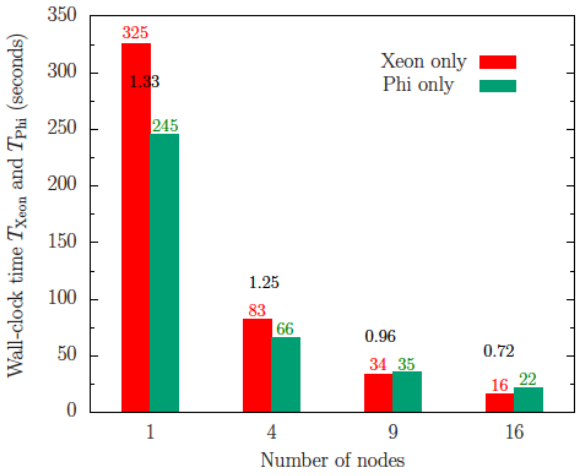

Figure 22. *Comparison of benchmark code on Xeon and Intel Phi processors.*

direct the most time consuming part of the computation to the Intel Phi co-processors.

For the current application we studied the structured, sparse matrix-vector multiplies required to solve the Schrödinger equation at the next time step. In all of the tests, only a single MPI task was launched on any Xeon node consisting of 16 (20) cores. Then various numbers of threads are launched on either the Xeon host or the Intel Phi. The Xeon node is allowed to host up to 16 (20) OpenMP threads. The Intel Phi can host up to 250 threads. Only a single Intel Phi card per Xeon node was employed in all of the tests. We did not examine the case where some threads executed on the Xeon cores and some on the Intel Phi. The results are summarized in Figure 22. Thus we can see that for one or two nodes, the ability to launch 250 threads on the Intel Phi enables a performance gain. But, by nine nodes its essentially a tie and by sixteen nodes, the Xeon nodes are outperforming the Phi co-processor. Essentially, what we are seeing is a tradeoff between the larger speed of the Xeon cores and the larger number of threads that can be launched on the Phi. Clearly, sixteen Xeon nodes performing 256 OpenMP tasks is better than sixteen nodes performing 4000 OpenMP tasks on the Phi. It is also important to remember that there are communication costs associated with moving data from the Phi back to the host that are not present when working entirely on the host.

Hybrid Gaussian-FEDVR Code. We have begun a study to employ a mixed basis of Gaussian functions at short range and FEDVR functions at long range to extend our methods to complex polyatomic molecules. This approach has several important advantages over using a single basis over all of space. First, the use of nuclear centered Gaussians preserves the local atomic symmetry around each nucleus and avoids the poor convergence of using a single-center FEDVR basis at all distances. Second, once the electron is far enough away from the nuclear cusps, a single center expansion converges quickly and importantly, can represent the electrons out to very large distances using an approach that is very amenable to domain decomposition. The major issue is to compute the one and two electron integrals between the two types of basis functions. This is currently under active investigation.

[1] J. Feist, S. Nagele, R. Pazourek, E. Persson, B. I. Schneider, L. A. Collins and J. Burgdörfer, Nonsequential Two-Photon Double Ionization of Helium, Physical Review A **77**, 043420 (2008).

[2] X. Guan, K. Bartschat and B. I. Schneider, Dynamics of Two-photon Ionization of Helium in Short Intense XUV Laser Pulses, *Physical Review A* **77** (2008), 043421.

[3] X. Guan, K. Bartschat and B. I. Schneider, Two-photon Double Ionization of H_2 in Intense Femtosecond Laser Pulses, *Physical Review A* **82** (2010), 041407.

[4] B. I. Schneider, J. Feist, S. Nagele, R. Pazourek, S. Hu, L. Collins and J. Burgdörfer, Recent Advances in Computational Methods for the Solution of the Time-Dependent Schrödinger Equation for the Interaction of Short, Intense Radiation with One and Two Electron Systems, in *Dynamic Imaging, Theoretical and Numerical Methods Series: CRM Series in Mathematical Physics* **XV** (A. Bandrauk and M. Ivanov eds.), 2011

[5] X. Guan, E. Secor, K. Bartschat and B. I. Schneider, Double-slit Interference Effect in Electron Emission from H_2^+ Exposed to X-Ray Radiation, *Physical Review* A **85** (2012), 043419.

[6] X. Guan, K. Bartschat, B. I. Schneider and L. Koesterke, Resonance Effects in Two-Photon Double Ionization of H_2 by Femtosecond XUV Laser Pulses, *Physical Review A* **88** (2013), 043402.

[7] J. Feist, O. Zatsarinny, S. Nagele, R. Pazourek, J. Burgdörfer, X. Guan, K. Bartschat and B. I. Schneider, Time Delays for Attosecond Streaking in Photoionization, *Physical Review A* **89** (2014), 033417.

[8] X. Guan, K. Bartschat, B. I. Schneider, and L. Koesterke, Alignment and pulse-duration effects in two-photon double ionization of H_2 by femtosecond XUV laser pulses, *Physical Review A* **90** (2014), 043416.

[9] B. I. Schneider, L. A. Collins, X. Guan, K. Bartschat and D. Feder, Time-Dependent Computational Methods for Matter Under Extreme Conditions, *Advances in Chemical Physics* **157**, Proceedings of the 240 Conference: Science's Great Challenges, Volume 157, (A. Dinner, ed.), John Wiley and Sons, 2015.

[10] B. I. Schneider, X. Guan and K. Bartschat, Time Propagation of Partial Differential Equations Using the Short Iterative Lanczos Method and Finite-Element Discrete Variable Representation, *International Advances in Quantum Chemistry*, to appear.

Advanced Materials

Delivering technical support to the nation's manufacturing industries as they strive to out-innovate and outperform the international competition has always been a top priority at NIST. This has also emerged as a major White House priority in recent years, in which NIST is playing an increasingly central role. Mathematical modeling, computational simulation, and data analytics are key enablers of emerging manufacturing technologies. This is most clearly evident in the Materials Genome Initiative, an interagency program with the goal of significantly reducing the time from discovery to commercial deployment of new materials through the use of modeling, simulation, and informatics. ACMD's role in advanced manufacturing centers on the development and assessment of modeling and simulation tools, with emphasis on uncertainty quantification, as well as support of NIST Laboratory efforts in such areas as materials modeling and smart manufacturing.

Uncertainty Quantification in Molecular Dynamics Workflows for Aerospace Polymers

Paul Patrone
Andrew Dienstfrey
Stephen Christensen (The Boeing Company)
Andrea Browning (The Boeing Company)
Sam Tucker (The Boeing Company)

In computational chemistry, molecular dynamics (MD) simulations are becoming a key tool for the discovery of next-generation materials [1-2]. For crosslinked polymers used in aerospace composites, this success is largely due to the ability of MD to describe the evolution of complex molecular conformations, which typically govern bulk mechanical properties. Such levels of detail, however, come at a price: MD simulations can only model at most $O(10^6)$ atoms, 17 orders of magnitude less than the bulk systems one usually wishes to study. In many cases, this discrepancy has led to considerable uncertainties in the resulting predictions, and consequently there is growing need for methods that assess the quality of simulated data.

Building upon work from FY 2014, we developed a systematic uncertainty quantification (UQ) workflow to assess data arising from MD simulations of the glass-transition temperature T_g. This quantity is both an important property for engineers (since it determines, e.g., the temperature at which a wing becomes soft) that is also difficult to model; thus it is a useful proving ground upon which to develop UQ methods. Details of our work are provided in a publication that is currently under review [3]. Industrial stakeholders are also using this workflow in their simulation protocol, and the software company Schrodinger has incorporated elements of our analysis into their commercially available package. We briefly summarize our main ideas here.

The workflow proceeds in two stages. Without computing uncertainties, the first stage of the analysis assesses whether data is of sufficient quality to be used for property estimation. We begin by addressing the question: is simulated data consistent with the definition of T_g? In particular, it is common practice to estimate T_g by extrapolating to the intersection of two fit-lines characterizing the low and high-temperature asymptotic behavior of density-temperature curves. Motivated by this, we implemented a hyperbolic regression analysis for determining whether data exhibits such asymptotic behavior. Additionally, we developed a pooling analysis that estimates bias in the T_g predictions by iteratively resampling from collections of datasets. Importantly, such approaches can indicate when simulations are too small to yield property estimates that are converged as a function of system size.

Given a collection of datasets that are of sufficient quality, the second stage of the analysis estimates T_g and its uncertainties. We propose to model the output of the i^{th} simulation via

$$T_{g,i} = \bar{T}_g + N(0,\sigma_i^2) + N(0,y^2)$$

where $N(0,X)$ is a normal random variable with mean zero and variance X, ${\sigma_i}^2$ is a within-simulation noise associated with thermal fluctuations and limited time averaging of the i^{th} MD simulation, and y^2 is a between-simulation uncertainty quantifying the extent to which a finite-size simulation undersamples the crosslinked network and relevant molecular conformations. Estimation of the ${\sigma_i}^2$ proceeds for each dataset individually by a noise-sampling process akin to parametric bootstrap analysis. Given these, we then estimate y^2 and $\bar{T}_g$ via maximum likelihood analysis. Interestingly, this approach leads to a weighted-mean estimator of the form

$$\bar{T}_g \approx \left[\sum_i \frac{1}{y^2+{\sigma_i}^2}\right]^{-1} \sum_i \frac{T_{g,i}}{y^2+{\sigma_i}^2}$$

which is frequently used in key comparison studies of fundamental constants. Related quantities can be derived for uncertainties in this estimator. Future directions for our work include (i) generalizing our analysis to more mechanical properties of interest, and (ii) developing additional analysis tools for quantifying the

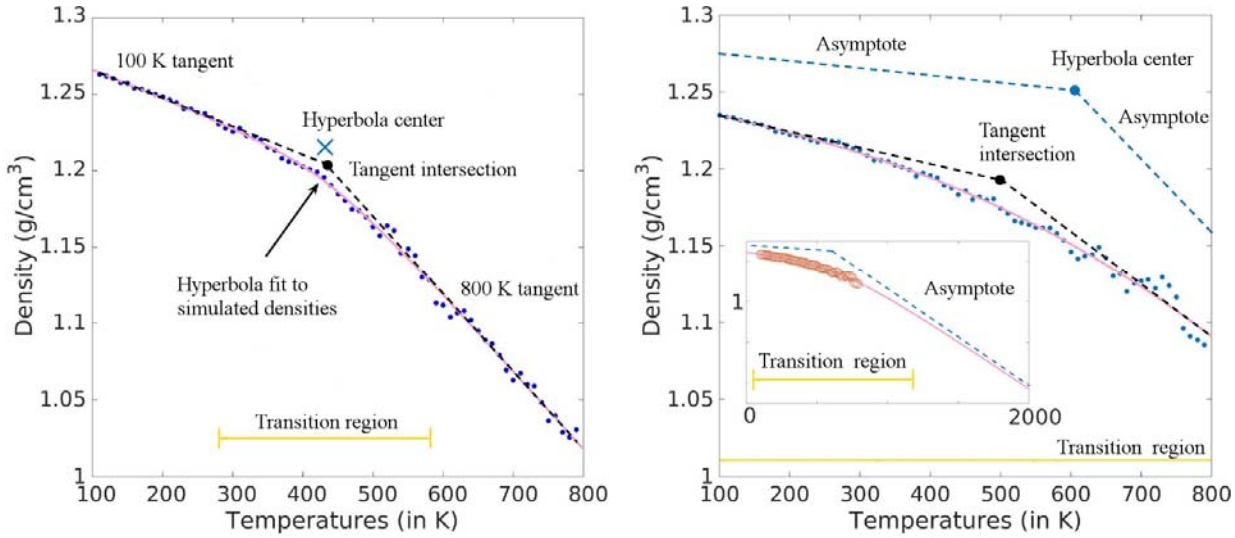

Figure 23. *Comparison of density-temperature data for two different amine-cured epoxies. Tg is typically computed as the intersection temperature of two lines fit to the low and high temperature asymptotic regimes. Using hyperbolas, we test for the existence of such regimes by comparing the data to asymptotes. The left plot shows a system in which the data clearly samples asymptotic behavior, corresponding to temperatures outside of the transition region. The right plot shows a dataset that does not sample asymptotic behavior.*

extent to which a finite simulation undersamples the network structure of bulk materials.

In addition to the MD-polymers applications, we continued outreach to the broader computational materials science community as part of the Materials Genome Initiative. In particular, from July 28 – July 31 2015, we ran a Hot Topics Workshop on Uncertainty Quantification in Materials Science at Purdue University in collaboration with Air Force Research Lab, the Institute for Mathematics and Its Applications (IMA), and Purdue's nanoHUB. The main goal of this workshop was to provide a hands-on venue for materials scientists in industry and academia to learn UQ methods. Over three days, six speakers gave three one hour lectures plus computer tutorials to roughly 40 participants, nearly a third of whom were from industry. The last day of the workshop was devoted to short talks on hot-topics and open problems in UQ of materials science. Response to the workshop was positive, and a follow-up is scheduled to be held at IMA in February 2016.

[1] S. Christensen, J. Senger. 2010. Distortional matrix of epoxy resin and diamine. U.S. Patent 7,745,549 B2, filed December 20, 2006, issued June 29, 2010.

[2] S. Christensen, J. Senger. 2011. Distortional matrix of epoxy resin and diamine. U.S. Patent 7,985,808 B2, filed April 23, 2010, issued July 26, 2011.

[3] P. N. Patrone, A. Dienstfrey, A. R. Browning, S. Tucker and S. Christensen, Uncertainty Quantification in Molecular Dynamics Studies of the Glass Transition Temperature, *in review.*

Bayesian Calibration of Coarse-Grained Forces

Paul N Patrone
Thomas Rosch (NIST MML)
Frederick Phelan (NIST MML)

In recent years, the high-throughput capabilities of molecular dynamics (MD) have attracted the interest of companies involved in materials research and development. In such settings, simulations are beginning to accelerate materials insertion, given their ability to rapidly search design spaces for novel systems that warrant further experimental study [1]. While it is generally agreed that this procedure can significantly reduce material development costs, however, a key theme has repeatedly emerged from practical implementations thereof: in order to be useful for commercial applications, computational models require techniques that can rapidly calibrate inputs and assess uncertainties in simulated predictions [2].

In the context of coarse-grained (CG) MD, this theme has proven to be especially germane. In particular, high-throughput applications require the ability to rapidly customize the level of coarse-graining for arbitrary systems across a range of state points (e.g. temperatures); inexpensive and robust calibration techniques are thus critical for enabling this degree of flexibility. Often, the key input to be determined is the CG interparticle force field $f(r; q)$ as a function of separation r and state-point q. Many techniques have been developed to compute these functions from thermodynamic considerations of atomistic systems. However,

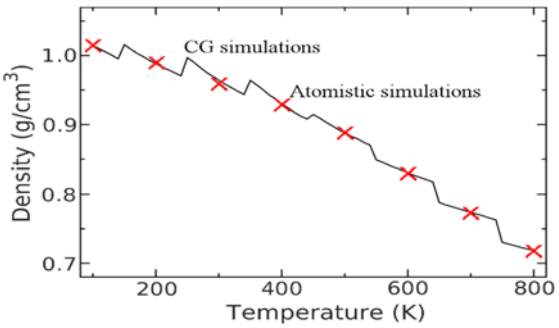

Figure 24. *Density-temperature data comparing atomistic simulations of polystyrene with their coarse-grained counterparts. Red x are simulated results from atomistic MD. At each temperature, we used the force-matching algorithm [4] to estimate CG forces at T=100 K, 200 K, …, 800 K. For a fixed force computed at an anchor point T_i, we then simulated CG densities at 10 K intervals in the domain [T_i – 50 K, T_i + 40 K] (black line). The densities exhibit sharp jumps when the force curve changes. Such behavior is unphysical for systems like polystyrene and indicates that a given f is unsuitable for simulating the density outside of a small window around the temperature at which it was calibrated.*

such methods typically draw information from a limited number of state-points, and the resulting forces can yield incorrect predictions for even small changes away from the calibration conditions (see Figure 24). Thus, the following question remains an important open problem: is there a general and inexpensive method for calibrating $f(r; q)$ so that a CG simulation yields the same predictions as a corresponding atomistic simulation on a large interval of state-points? In this project, we developed a coarse-graining workflow, based on ideas from numerical analysis and Bayesian probability, for addressing this problem. The main steps in our workflow are

- building a statistical model to describe the target predictions against which to calibrate the CG forces;
- constructing a prior probability for the forces via a combination of standard CG techniques and interpolation; and
- correcting the prior probability distribution via a Bayesian algorithm that uses functional derivatives of the CG simulations to systematically update the forces.

Importantly, these functional derivatives are inexpensive to approximate, given that CG simulations are orders of magnitudes faster than MD. As a result, we were able to show that our workflow overcomes the difficulties of generating transferable forces by rapidly and robustly calibrating priors constructed from non-robust and cheap interpolations of forces in state space. Using polystyrene as a test case, we also demonstrated that our approach can calibrate forces over a 700 K range so that they yield a target density-temperature curve to within statistical error.

Results of this work are detailed in a paper that has been submitted for publication [3]. Future directions for this work include showing that Bayesian approaches can be used to simultaneously calibrate multiple material properties, and developing uncertainty quantification techniques for the iterative Boltzmann inversion method of coarse-graining.

[1] C. Li and A. Strachan, Molecular Scale Simulations on Thermoset Polymers: A Review, *Journal of Polymer Science, Part B*, **53** (2014), 103–122.

[2] A. Dienstfrey, F. R. Phelan Jr., S. Christensen, A. Strachan, F. Santosa and R. Boisvert, Uncertainty Quantification in Materials Modeling, *The Journal of the Minerals, Metals, and Materials Society (JOM)* **66** (2014), 1342-1344.

[3] P. N. Patrone, T. W. Rosch and F. R. Phelan Jr., Bayesian Calibration of Coarse-Grained Forces: Efficiently Addressing Transferability, *in review.*

[4] S. Izvekov, G. A. Voth, Multiscale Coarse-graining of Liquid-state Systems, *The Journal of Chemical Physics,* **123** (2005), 134105.

Micromagnetic Modeling

Michael Donahue
Donald Porter
Robert McMichael (NIST CNST)
June Lau (NIST MML)

http://math.nist.gov/oommf/

Advances in magnetic devices such as recording heads, field sensors, spin torque oscillators, and magnetic nonvolatile memory (MRAM) are dependent on an understanding of magnetization processes in magnetic materials at the nanometer level. Micromagnetics, a mathematical model used to simulate magnetic behavior, is needed to interpret measurements at this scale. ACMD is working with industrial and academic partners, as well as with colleagues in the NIST Cenetr for Nanoscale Science and Technology (CNST), Materials Measurement Laboratory (MML), and Physical Measurement Laboratory (PML), to improve the state-of-the-art in micromagnetic modeling.

Michael Donahue and Donald Porter in ACMD have developed a widely used public domain computer code for doing computational micromagnetics, the Object-Oriented Micromagnetic Modeling Framework (OOMMF). OOMMF serves as an open, well-documented environment in which algorithms can be evaluated on benchmark problems. OOMMF has a modular structure that allows independent developers to contribute extensions that add to the basic functionality of OOMMF. OOMMF also provides a fully functional micromagnetic modeling system, handling both two and three-dimensional problems, with sophisticated extensible input and output mechanisms. In FY 2015 alone, the software was downloaded more than 6000 times, and

use of OOMMF was acknowledged in more than 185 peer-reviewed journal articles. OOMMF has become an invaluable tool in the magnetics research community.

Key new developments over the last year include the following.

- Major reworking of non-uniform memory access (NUMA) aware memory use along with threading improvements to support simulations size of more than 100 million spins.
- Demonstration test of a one billion spin simulation. Using this enhanced capability, completed several simulations of archetype magnetization structures at 0.1 nm spatial resolution. Current work involves analyzing these calculations to make a quantitative determination of how computation error relates to spatial resolution.
- Released OOMMF version 1.2a6 in Sept. 2015[25].
- Began collaboration with staff at the nanoHUB project[26] of Purdue University to add OOMMF to the collection of software tools available to run on their online service.

OOMMF is part of a larger activity, the Micromagnetic Modeling Activity Group (muMAG), formed to address fundamental issues in micromagnetic modeling through two activities: the development of public domain reference software, and the definition and dissemination of standard problems for testing modeling software. ACMD staff members are involved in development of the standard problem suite as well. A new standard problem 5, adapted from [1], addressing the proper calculation of the spin torque transfer effect was released[27] in September, 2014. New solutions to standard problem 4 were also released[28]. Ongoing work includes the production of standard problem 5 solutions for submission, and development of new standard problems.

In addition to the continuing development of OOMMF, the project also does collaborative research using OOMMF. Continued collaboration with the University of California, San Diego on porting OOMMF calculations to massively parallel graphical processing units (GPUs) has produced an article for publication. Collaboration with the University of Maryland has demonstrated nanoscale control over magnetic anisotropy in a trans-critical Permalloy thin film via strain-mediated coupling to ferroelectric domains in $BaTiO_3$, a degree of control helpful in the aim to make compact and efficient memory devices. The ACMD micromagnetic project produced one invited talk [2], one conference presentation [3], and three manuscripts submitted for publication [4-6] this past year.

[1] M. Najafi, et al., Proposal for a Standard Problem for Micromagnetic Simulations including Spin-Transfer Torque, *Journal of Applied Physics* **105** (2009), 113914-113921.

[2] M. J. Donahue, "An Introduction to Micromagnetic Modeling", March 15, 2015, Orlando, Florida. Part of the short course *Characterization Techniques for Magnetic Materials* offered in advance of the annual meeting of The Minerals Metals and Materials Society.

[3] M. J. Donahue, "Implementation of a localized fourth order demagnetization tensor," 59th Annual Magnetism and Magnetic Materials, November 5, 2014, Honolulu, HI.

[4] S.W. Fackler, M.J. Donahue, T. Gao, P.N.A. Nero, S.-W. Cheong, J. Cumings, and I. Takeuchi, Locally Controlled Magnetic Anisotropy in Transcritical Permalloy Thin Films using Ferroelectric $BaTiO^3$ Domains, *Applied Physics Letters* **105** (November 2014), 212905.

[5] S. Fu, W. Cui, M. Hu, R. Chang, M.J. Donahue, and V. Lomakin, Finite Difference Micromagnetic Solvers with Object Oriented Micromagnetic Framework on Graphics Processing Units, *IEEE Transactions on Magnetics*, to appear.

[6] S. Mitropoulos, V. Tsiantos, K. Ovaliadis, D. Kechrakos, and M. Donahue, Stiff Modes in Spin Valve Simulations with OOMMF, *Physica B*, to appear.

OOF: Finite Element Analysis of Material Microstructures

Stephen A. Langer
Andrew C.E. Reid (NIST MML)
Günay Doğan
Shahriyar Keshavarz (Theiss Research)
Faical Yannick Palingwende Congo
Lizhong Zhang

http://www.ctcms.nist.gov/oof/

The microstructure of a material is the (usually) complex ensemble of polycrystalline grains, second phases, cracks, pores, and other features occurring on length scales large compared to atomic sizes. The Object-Oriented Finite Elements (OOF) Project, a collaboration between ACMD and MML, is developing software tools for analyzing real material microstructure. OOF uses data from a micrograph of a real or simulated material to compute the macroscopic behavior of the material via finite element analysis. The OOF user loads images into the program, assigns material properties to the features of the image, generates a finite element mesh that matches the geometry of the features, chooses which

[25] http://math.nist.gov/oommf/software-12.html

[26] http://nanohub.org/

[27] http://www.ctcms.nist.gov/~rdm/std5/spec5.xhtml

[28] http://www.ctcms.nist.gov/~rdm/std4/spec4.html

physical properties to solve for, and performs virtual experiments to determine the effect of the microstructural geometry on the material. OOF is intended to be a general-purpose tool, applicable to a wide variety of microstructures in a wide variety of physical situations.

There are two versions of OOF, OOF2 and OOF3D, freely available on the OOF website. OOF2 starts with two dimensional images of microstructures and solves two dimensional equations, assuming that the material being simulated is either a thin freely suspended film or a slice from a larger volume that is unvarying in the third dimension (generalizations of plane stress and plane strain, respectively). OOF3D starts with three dimensional images and solves equations in three dimensions.

OOF is used by academic, industrial, and government users world-wide, although exact numbers are hard to obtain. OOF2 was downloaded 2500 times this year, but those numbers are suspect, because OOF3D was downloaded an unbelievable 15000 times. OOF3D was downloaded to 1157 unique IP addresses. Discounting the 10 sites (all Chinese) that downloaded it more than 1000 times, a reasonable guess is that the number of actual downloads is in the thousands for both programs.

Most of the year's progress was on code development for future releases. However, two papers appeared, one on OOF's graphical user interface (GUI) testing procedure [1], and one on applying OOF to a problem in planetary geology [2], and two new versions of the programs were released. OOF2 version 2.1.12 included parallel computation in parts of the program (but only when run on Linux) and bug fixes. OOF3D 3.0.1 fixed a number of bugs from the initial 3D release.

OOF development this year was divided into a number of efforts. Yannick Congo added to the OOF3D test suite, and moved the OOF2 source control from a local Concurrent Versioning System (CVS) repository to the NIST GitHub repository[29]. He also added improvements to the OOF3D GUI. Lizhong Zhang replaced Yannick Congo during the year. He has been optimizing OOF2 by finding and fixing inefficient serial code, and by converting serial code to parallel. Ryan Weller, a SURF student from the University of Colorado, added three dimensional graphics widgets to OOF3D. Many operations in OOF3D are easier if the user can use a mouse to define, move, or rotate objects in three dimensions. This is fundamentally different from the equivalent operations in OOF2 simply because 3D movement can't be represented in a straight forward manner on a 2D computer screen. Ryan implemented a compound widget composed of a plane and an arrow, which is perpendicular to the plane. Clicking and dragging the arrow head rotates the arrow and plane around the point where they meet. Clicking and dragging the plane moves it in its normal direction (along the arrow). Clicking and dragging while pressing the control key moves the arrow on the plane, changing the rotation point. The widget can be used to define clipping planes, or to delimit sets of selected pixels or mesh elements.

Andrew Reid and Shahriyar Keshavarz, a new MML post-doc and an expert on plasticity, have been working on adding crystal plasticity modeling to OOF. A significant component of this is that the crystal-plastic constitutive rules really do not make sense to implement outside of a large-strain displacement scheme, so the first order of business is to add this capability to OOF. Shahriyar's participation has helped the rest of the developers gain an outsiders perspective on the material property applications programming interface (API) in OOF, which is less accessible and well-structured than initially believed, making the gaps in the existing documentation more important to remedy. A review and documentation update of the property API is now underway in parallel with the implementation of crystal plasticity. OOF's highly-valued generality of scope will be retained, and this process will yield a very general large-strain and large-displacement extension framework applicable across the full range of constitutive laws OOF can implement.

Günay Doğan has been developing algorithms to automate segmentation and meshing of microstructure images. His focus has been multiphase images, which consists of multiple regions, each approximated by a distinct average value, and images in which the regions are separated by well-defined high-gradient boundaries. He improved his previous segmentation-to-meshing algorithm, so that it would produce smoother and coarser boundaries resulting in more compact triangulations for finite element analysis. He also improved several components of the shape optimization algorithm used for multiphase segmentation and edge-based segmentation for better performance and usability. Although much of the development effort went into increasing the efficiency with Newton-type optimization, better step size selection and stopping criteria, computational efficiency is not the sole issue for a typical OOF user. The user usually does not have much image analysis experience, and thus can be overwhelmed by the multiple choices required to achieve acceptable results with a given segmentation algorithm. For this reason, Günay developed principles and approaches to set parameters and initialization methods, and incorporated them into the segmentation code (more details can be found in the section on Computational Tools for Shape Measurement and Analysis). Currently, he is working on interfacing the code with OOF, so that the segmentation software can be invoked from OOF, and can be used to analyze images loaded into OOF workspace.

Steve Langer began the year fixing bugs and adding missing features to OOF3D, but spent most of the year redesigning and reimplementing the algorithm used to

[29] http://www.github.com/usnistgov

compute the volume of the intersection of a tetrahedral finite element with a group of voxels (3D pixels). This is used to compute the homogeneity of an element with respect to the various material properties that have been assigned to the voxels. The homogeneity calculation is at the heart of OOF3D's mesh adaptation methods, which construct a mesh that is a good approximation to the geometry of a microstructure. The calculation is subtler than it first appears. The homogeneity calculation must be done quickly, so it's not possible to consider each voxel individually. Instead, all voxels with a given material type are grouped, and the faces of the aggregate voxel group are determined. Finding the intersection of these faces with an element is the difficult step, because round-off error can lead the program to make the wrong decision about whether a point is inside or outside the tetrahedron, or about the ordering of two points on the perimeter of a polygon. The round-off problem arises when the nodes of the element lie on or near a boundary between two types of voxels, and the mesh adaptation methods unfortunately work to *increase* the frequency of these cases, because they maximize the homogeneity of the elements.

One approach tried this year was to use thresholds and sloppy arithmetic to determine when points coincided. It was discovered that different thresholds were needed in different situations, and that no single set of threshold values would work in all situations. A new approach is being developed that will avoid the round-off error problem by retaining more topological information about each intersection point.

[1] S. A. Langer, A. C. E. Reid, F. Y. Congo, R. Lua and V. .R. Coffman, gtklogger: A Tool for Systematically Testing Graphical User Interfaces, NIST TN 1862, Aug 2015.

[2] J. L. Molaro, S. Byrne and S.A. Langer, Grain-scale Thermoelastic Stresses and Spatiotemporal Temperature Gradients on Airless Bodies, Implications for Rock Breakdown, *Journal of Geophysical Research: Planets* **120**:2 (2015), 255-277.

Determination of Diffusion Coefficients in Alloys

Geoffrey McFadden
Anthony Kearsley
James Filliben (NIST ITL)
William Boettinger (NIST MML)
Carelyn Campbell (NIST MML)
Kil-Won Moon (NIST MML)
Robert Sekerka (Carnegie Mellon University)

A common technique for the measurement of alloy diffusion coefficients is through the analysis of diffusion couples. A diffusion couple consists of two long homogeneous solid samples, each of differing alloy

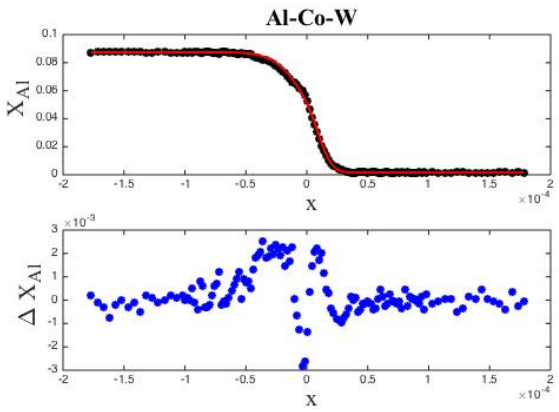

Figure 25. *Top: Concentration (mole fraction of Aluminum in a ternary Aluminum-Cobalt-Tungsten alloy) versus distance (in meters) in a diffusion couple. The initial junction was at x=0. The black points are experimental data, and the solid red curve is a numerical solution to the ODE using a diffusion coefficient with three degrees of freedom that is chosen to fit the data. Bottom: Difference between the ODE solution and the experimental data versus distance.*

compositions, which are joined together to form a single sample with discontinuous concentration profiles. At high enough temperatures significant inter-diffusion may occur, allowing the concentrations profiles to relax in time. After a long enough time, this diffusion process would eventually lead to a homogeneous sample. At intermediate times the sample may be quenched to low temperatures, halting the diffusion process, and the spatial distribution of the resulting concentration profiles can be measured in detail. The time of measurement is ideally chosen so that the diffusion process is confined to the vicinity of the initial junction, leaving the far ends of the sample undisturbed at their initial concentrations. An example is shown in Figure 25. Fick's law relates the flux of solute to the instantaneous concentration gradients at each point; the constants of proportionality are known as diffusion coefficients, which are generally functions of the local concentration at each point. The experimental determination of the diffusion coefficients is the goal of the project. Under the right conditions the diffusion couple can be modeled as a one-dimensional sample of infinite extent in each direction. The diffusion process is then modeled as a system of diffusion equations for the individual concentrations. For the idealized initial conditions there is a similarity solution due to Boltzmann in which the concentrations depend on the single independent coordinate $(x-x_0)/t^{1/2}$, where x_0 is the position of the initial discontinuity, and t is the elapsed time. Under this change of variables, the diffusion equations reduce to coupled nonlinear ordinary differential equations (ODEs) with far-field boundary conditions given by the initial concentrations in each sample. An inverse approach to the determination of diffusion coefficients is then to compare numerical solutions of the ODEs with the experimentally measured profiles, iterating on the diffusion coefficients to minimize the

difference. Typically, we assume a low-order power series for the concentration dependence of the diffusion coefficients, using the polynomial coefficients as the unknowns in minimizing the error. An example of the resulting fit is shown in Figure 25. More general representations for the concentration dependence are also useful, as motivated by thermodynamic arguments.

In some cases, an analytical approach can be used to obtain direct relations between the diffusion coefficients and the concentration profiles. For example, an appropriate integration of the ODEs produces a direct relation between the solute flux at a point and specific integrals of the concentration profiles. We have recently extended analyses of this type that pertain to single phase binary alloy systems to the more general case of multiphase, multicomponent systems [1].

[1] R. F. Sekerka, G. B. McFadden and W. J. Boettinger, Analytical Derivation of the Sauer-Freise-den Broeder Flux Equation for Multicomponent Multiphase Diffusion Couples with Variable Molar Volume, in preparation.

Verification and Validation of Finite Element Method-based Solutions

Jeffrey T. Fong
James J. Filliben (NIST ITL)
N. Alan Heckert (NIST ITL)
Stephen Freiman (NIST MML)
Li Ma (NIST MML)
Ward Johnson (NIST MML)
Stephen Russek (NIST PML)
Karl Stupic (NIST PML)
Katherine Keenan (NIST PML)
Pedro V. Marcal (MPACT Corp.)
Robert Rainsberger (XYZ Scientific)

The finite element method (FEM) and the mathematics of the verification and validation (V&V) of its computational results [1, 2] have been of interest to engineers and scientists since the 1960s. Difficulties in "correct" modeling and "accurate" computing for large-scale practical problems involving complex geometry and uncertainty in governing equations and physical parameters have created a need to develop efficient methods and subsequently recommended practices of FEM V&V. The availability of many commercial FEM codes that are increasingly user-friendly has complicated the problem of answering the fundamental question, "is the FEM result correct, and what are its confidence bounds?" By considering every FEM solution as the result of a numerical experiment and by using a combination of three mathematical methods, we have developed a new approach to the V & V of FEM.

Errors and uncertainties in FEM modeling and computing are known to originate from at least seven sources: (1) Numerical algorithm of approximation for solving a system of partial differential equations with initial and boundary conditions; (2) the choice and design of the finite element mesh and element type; (3) the choice of when to stop computing before verification; (4) the uncertainty in the geometric parameters; (5) the uncertainty in the physical and material property parameters; (6) the uncertainty in the loading parameters, and (7) the uncertainty in the choice of a correct model. Examples of developing local and global validation metrics for specific classes of problems in scientific computing not using FEM have appeared in the literature (see, e.g., [3, 4]). Using a fractional factorial orthogonal two-level design of experiments [5], we addressed in a 2008 paper [6] the FEM uncertainty problem for sources (4), (5), and (6). To address source (3), we used a nonlinear least squares algorithm and a mathematical function named the logistic distribution (after Verhulst [7]), that allows a user to fit a sequence of FEM solutions of increasing mesh density such that a "plateau" is predicted as the right horizontal asymptote representing the extrapolated solution at "infinite" degrees of freedom (see Figure 26, and [8]). To address sources (1) and (2), we recently expanded our 2008 experimental design [6] to check the "robustness" of the FEM platform and element type in a new design involving both continuous and discrete factors. Source (7) is, of course, addressed by experiments.

[1] O. C. Zienkiewicz and R. L. Taylor, *The Finite Element Method, Volume 1: The Basis*, 5th edition, Butterworth-Heinemann, 2000.

[2] W. L. Oberkampf and C. J. Roy, *Verification and Validation in Scientific Computing*, Cambridge University Press, 2010.

[3] M. F. Barone, W. L. Oberkampf and F. G. Blottner, Validation Case Study: Prediction of Compressible Turbulent Mixing Layer Growth Rate, *AIAA Journal* **44**:7 (2006), 1488-1497.

[4] W. L. Oberkampf and M. F. Barone, Measures of Agreement Between Computation and Experiment: Validation Metrics, *Journal of Computational Physic*s **217** (2006), 5-36.

[5] G. E. P. Box, W. G. Hunter and J. S. Hunter, *Statistics for Experimenters*, 1st edition, Wiley, 1978.

[6] J. T. Fong, J. J. Filliben, N. A. Heckert and R. deWit, Design of Experiments Approach to Verification and Uncertainty Estimation of Simulations based on Finite Element Method, in *Proceedings of the Conference of the American Society for Engineering Education*, June 22-25, 2008, Pittsburgh, PA, AC2008-2725.

[7] P. F. Verhulst, Recherches Mathematiques sur la Loi d'Accroissement de la Population," [Mathematical Research into the Law of Population Growth Increase], 1845, re-published in *Nouveaux Memoires de l'Academie Royaledes Sciences et Belles-Lettres de Bruxelles* **18** (2013), 1-42.

[8] J. T. Fong, J. J. Filliben, N. A. Heckert, P. V. Marcal, R. Rainsberger and L. Ma, Uncertainty Quantification of

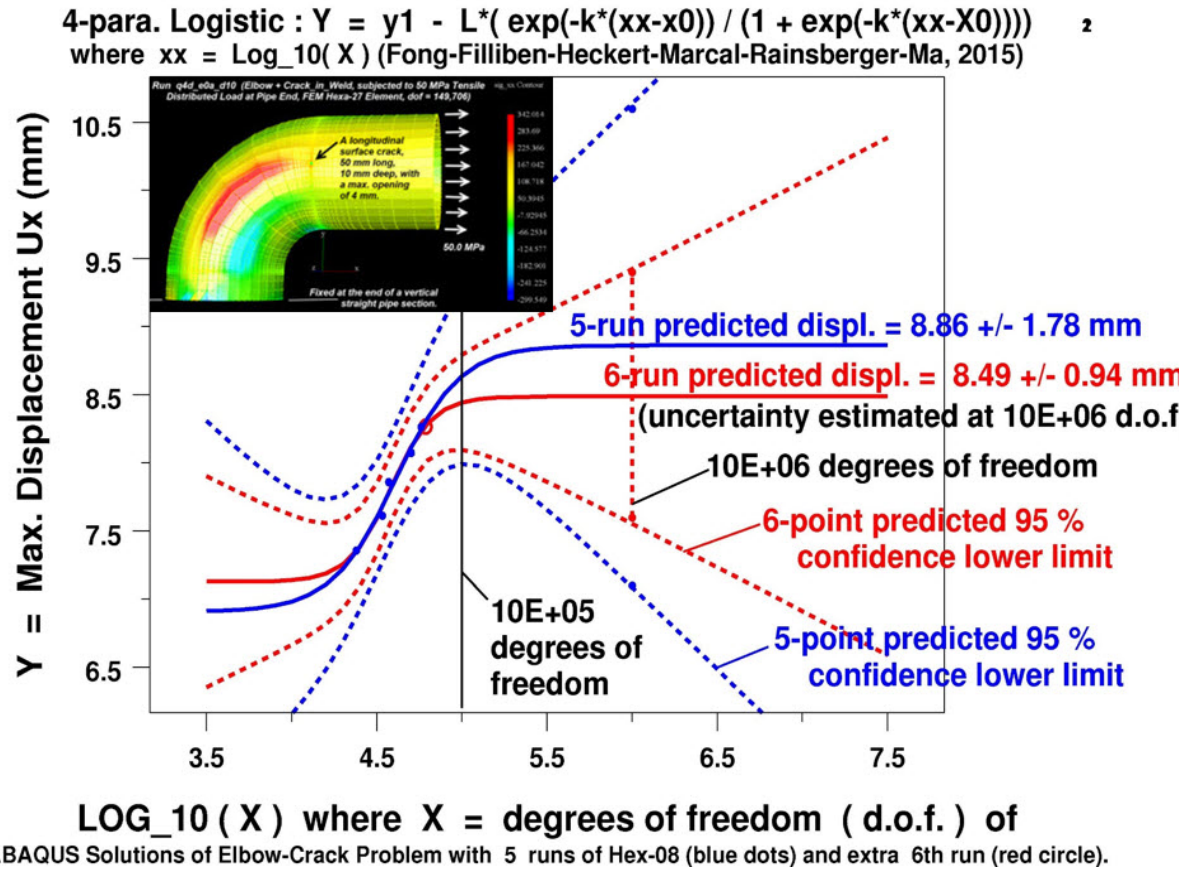

Figure 26. *Extrapolation of coarse finite element solutions to finer meshes with larger degrees of freedom.*

Stresses in a Cracked Pipe Elbow Weldment using a Logistic Function Fit, a Nonlinear Least Squares Algorithm, and a Super-Parametric Method, *Procedia Engineering* **130** (2015), 135-149. DOI: 10.1016/j.proeng.2015.12.183

Inversion of the Abel Transform by Truncated Singular Components Method

Timothy J. Burns
Bert W. Rust

Despite many years of study, the determination of accurate constitutive response models for the flow stress in materials for finite-element simulations of high-speed machining operations remains a difficult unsolved problem. Most attempts to model the material response have been based on direct methods that fit compression test data of small samples of the material of interest to a given highly nonlinear constitutive response model. The main problem with this approach has been that the conditions under which compression tests can be performed are not nearly as extreme as the actual conditions that are present in a typical high-speed machining operation [1], so that a machining process simulation using the nonlinear material response model necessarily requires huge extrapolations in order to simulate the cutting conditions.

One area of machining research in which significant progress has been made in the past few years has been in the measurement of the 2D temperature distribution on the chip–tool interface using infrared thermography. In particular, Menon and Madhavan [2] have reported high accuracy temperature measurements during high-speed machining of a titanium alloy, using single wavelength thermography with an instrumented transparent tool. For their experimental cutting conditions, they have obtained a 1D temperature distribution as a function of distance along the rake face of the tool, along an internal cross section of the chip–tool interface, with an estimated uncertainty of less than 1 %. Motivated by this work, we have been investigating a new approach to the problem of estimating flow stress in machining that is based on an inverse method. By finding an asymptotic solution of a convection-diffusion problem that models the flux of heat into the chip and the tool during a cutting experiment, the temperature distribution along the tool face can be shown to satisfy Abel's equation, a Volterra

integral equation of the first kind with a weakly singular kernel, convolved with the flow stress [3]. Inversion of this Abel transform provides an estimate of the distribution of flow stress in the chip material near the tool-chip interface.

Because the temperature data are discrete and experimentally determined, estimation of the flow stress by inversion of the Abel transform under these circumstances is an ill-posed problem. This year, we have shown that the Truncated Singular Components Method (TSCM) of Rust [4], [5], which has been successfully used to find approximate numerical solutions of Fredholm integral equations of the first kind with noisy data, can also be applied to find approximate numerical solutions of the Abel equation [6]. The basic idea is to discretize the integral equation, and obtain an overdetermined system of linear equations, that is perturbed by the measurement errors, which are assumed to be samples from a univariate normal distribution, as is typically the case. Using methods that have been developed for the statistical analysis of time series, we treat the discrete problem as a linear regression problem. The key idea is to use the singular value decomposition of the matrix of the system to separate signal from noise in the data, prior to obtaining an estimate of the desired solution of the integral equation. A paper on this work is in preparation.

[1] S. P. Mates, R. L. Rhorer, E. P. Whitenton, T. J. Burns and D. Basak, A Pulse-Heated Kolsky Bar Technique for Measuring Flow Stress of Metals Subjected to High Loading and Heating Rates, *Experimental Mechanics* **48** (2008), 799–807.

[2] T. Menon and V. Madhavan, Infrared Thermography of the Chip-Tool Interface through Transparent Cutting Tools, in *Proceedings of the North American Manufacturing Research Institution/SME*, Ann Arbor, MI, June 2014.

[3] T. J. Burns, S. P. Mates, R. L. Rhorer, E. P. Whitenton and D. Basak, Inverse Method for Estimating Shear Stress in Machining. *Journal of Mechanics and Physics of Solids* **86** (2016), 220–236.

[4] B. W. Rust, Truncating the Singular Value Decomposition for Ill-Posed Problems, NIST IR 6131, July 1998.

[5] B. W. Rust and D. P. O'Leary, Residual Periodograms for Choosing Regularization Parameters for Ill-Posed Problems, *Inverse Problems* **24** (2008), 034005 (30 pages). DOI:10.1088/0266-5611/24/3/034005.

[6] T. J. Burns and B. W. Rust, "Estimation of Shear Stress in Machining by Approximating the Solution of a Volterra Integral Equation of the First Kind," ASME 2015 Applied Mechanics and Materials Conference, McMAT2015, Seattle, WA, June 2015.

High Performance Computing and Visualization

Computational capability is advancing rapidly, with the result that modeling and simulation can be done with greatly increased fidelity (e.g., higher resolution, more complex physics). However, developing the requisite large-scale parallel applications remains highly challenging, requiring expertise that scientists rarely have. In addition, the hardware landscape is changing rapidly, so new algorithmic techniques must constantly be developed. We are developing and applying such expertise for application to NIST problems. In addition, computations and laboratory experiments often produce large volumes of scientific data, which cannot be readily comprehended without some form of visual analysis. We are developing the infrastructure necessary for advanced visualization of scientific data, including the use of 3D immersive environments and applying this to NIST problems. One of our goals is to develop the 3D immersive environment into a true interactive measurement laboratory.

High Precision Calculations of Fundamental Properties of Few-Electron Atomic Systems

James Sims
Stanley Hagstrom (Indiana University)
Maria B. Ruiz (University of Erlangen)

http://www.nist.gov/itl/math/hpcvg/atomic.cfm

NIST has long been involved in supplying critically-evaluated data on atomic and molecular properties such as the atomic properties of the elements contained in the Periodic Table and the vibrational and electronic energy level data for neutral and ionic molecules contained in the NIST Chemistry WebBook. Fundamental to this endeavor is the ability to predict, theoretically, a property more accurately than even the most accurate experiments. It is our goal to be able to accomplish this for few-electron atomic systems.

While impressive advances have been made throughout the years in the study of atomic structure, at both the experimental and theoretical levels, information on atomic energy levels remains scarce, especially for highly ionized atoms. The availability of high precision results tails off as the state of ionization increases, not to mention higher angular momentum states. In addition, atomic anions have more diffuse electronic distributions, thus representing more challenging computational targets than corresponding ground states.

In the past two decades, there have been breathtaking improvements in computer hardware as well as innovations in mathematical formulations and algorithms, leading to "virtual experiments" becoming a more and more cost-effective and reliable way to investigate chemical and physical phenomena. Our contribution in this arena has been undertaking the theoretical development of our hybrid Hylleraas-CI (Hy-CI) wave function method to bring sub-chemical accuracy to atomic systems with more than two electrons. Our Hy-CI method has been employed to explore its utility for both three electron lithium systems and the four electron beryllium (Be) atom. In the case of lithium, we have computed four excited states of the lithium atom two orders of magnitude more accurately than has been done before [1].

At the four electron level, to get truly accurate chemical properties, such as familiar chemical electron affinities and ionization energies, it is important to get close to the nanohartree level we achieved for the three election atom, a significantly more difficult problem for four electrons than for three. By investigating more flexible atomic orbital basis sets and better configuration state function filtering techniques to control expansion lengths, we have been able to successfully tackle the four electron case. Progress to date has included computing the non-relativistic ground state energy of not only beryllium, but many members of its isoelectronic series to 8 significant digit accuracy. With the results from our calculations, and a least squares fit of the calculated energies, we have been able to compute the entire beryllium ground state isoelectronic sequence [2].

The next step to enabling the calculation, not just for the ground singlet S symmetry of the beryllium atom and other members of its isoelectronic sequence, but higher angular momentum states as well, is to complete the process of making the four electron integrals, the real bottleneck at the 4 and more electron level, as efficient as possible, as well as modifying the codes to be able to compute the energy levels of the Be atom for states of different spin, angular momentum and N quantum number than the ground state.

The first part of this code revision has been completed and a paper on the mathematical and computational science issues involved in doing Hy-CI four electron integrals published [3]. We are currently doing a calculation on the first excited Be state of singlet S symmetry and plan to do three or four more states of the same symmetry. Then our plans are to modify the code to handle triplet spin, and treat non-S angular momentum states as well by generalizing our angular

momentum projector, currently limited to S states, to handle states of any angular momentum symmetry. This will enable the calculation of higher angular momentum states of the four electron atom and its ions.

[1] J. S. Sims and S. A. Hagstrom, Hy-CI Study of the 2 Doublet S Ground State of Neutral Lithium and the First Five Excited Doublet S States, *Physical Review A* **80** (2009), 052507.

[2] J. S. Sims and S. A. Hagstrom, Hylleraas-configuration-interaction Nonrelativistic Energies for the Singlet S Ground States of the Beryllium Isoelectronic Series Up through Z = 113, *Journal of Chemical Physics* **140** (2014), 224312.

[3] James S. Sims and Stanley A. Hagstrom, Mathematical and Computational Science Issues in High Precision Hylleraas-Configuration Interaction Variational Calculations: III. Four-electron Integrals, *Journal of Physics B: Atomic, Molecular and Optical Physics* **48** (2015), 175003.

Nano-structures, Nano-optics, and Control of Exciton Fine Structure with Electric and Magnetic Fields

James S. Sims
Wesley Griffin
Judith Terrill
Garnett W. Bryant (NIST PML)
Jian Chen (UMBC)
Henan Zhao (UMBC)

http://www.nist.gov/itl/math/hpcvg/nanohpc.cfm
http://www.nist.gov/itl/math/hpcvg/nanovis.cfm

Research and development of nanotechnology, with applications ranging from smart materials to quantum computation to biolabs on a chip, has been identified as a national priority. Semiconductor nanoparticles, also known as nanocrystals and quantum dots (QDs), are one of the most intensely studied nanotechnology paradigms. Nanoparticles are typically 1 nm to 10 nm in size, consisting of 10^3 to 10^6 atoms. Precise control of particle size, shape and composition allows one to tailor charge distributions and control quantum effects to obtain properties completely different from the bulk or from small clusters. As a result of quantum confinement effects, nanoparticles act as artificial atoms, with discrete electronic spectra that can be exploited as light sources for enhanced lasers, discrete components in nanoelectronics, qubits for quantum information processing, and ultrastable fluorescent labels for biosensors to detect pathogens and to do cell biology.

We are working with the NIST Physical Measurement Lab (PML) to develop computationally efficient large scale simulations of such nanostructures, and also to develop immersive visualization techniques and tools to enable analysis of highly complex computational results of this type. In particular, electrical, mechanical, and optical properties of semiconductor nanocrystals and quantum dots are studied. In the most complex cases this entails modeling structures with on the order of 10^6 atoms. High performance computational and visualization tools are critical for obtaining the throughput necessary for systematic, comprehensive study.

As device sizes in silicon (Si) electronics continues to decrease, devices are rapidly approaching the atomic scale where a change in only a few atoms can make a significant change in device performance. At the same time, the ability to make Si nanodevices with only a few, deterministically placed dopant atoms opens the possibility to create quantum information processing devices with these structures. We are currently participating in a program which aims to make, characterize, and model both traditional and quantum Si devices at this few-dopant atom limit. Atomistic modeling must be used.

We are currently extending our tight-binding atomistic modeling codes to consider Si structures with just a few dopant atoms. This requires an extension to Si, developing and implementing models for dopants, and including the effects of potentials provided by gates, sources and drains. Work is underway to develop codes that provide the needed potentials, develop the visualization tools needed for these simulations, and develop the parallelization methods needed to ensure that the atomistic tools remain computationally tractable.

As part of a continuing NIST grant award, Jian Chen and Henan Zhao of UMBC have developed a desktop visualization tool for the numerical simulation output in close cooperation with NIST PML collaborator Garnett Bryant. The tool employs a novel visualization technique developed last year [1]; a paper describing this new technique is currently in review [2]. Figure 27 is a snapshot from the current version of the tool. The tool has gone through several iterations as Bryant has applied the tool to existing datasets. As part of this iterative process, we designed and validated a coloring approach that generates a perceptually uniform scale where colors at equal parameter distance have an equal perceived color difference. We coupled this with an orientation clustering to show the cosine distances among vectors. Orientation of the spatial distribution is an important metric since it determines how to understand and engineer spin control. The cosine distance provided faster understanding of the 3D structure. We also developed shape clustering methods to automate visual pattern finding in orientations, and implemented user-controllable cutting planes and regions of interest.

[1] J. Chen, H. Zhao, W. Griffin, J. Terrill and G. Bryant, Validation of Split Vector Encoding and Stereoscopy for Quantitative Visualization of Quantum Physics Data in Virtual Environment, poster, IEEE Virtual Reality (VR2015), Arles France, March 23-27, 2015.

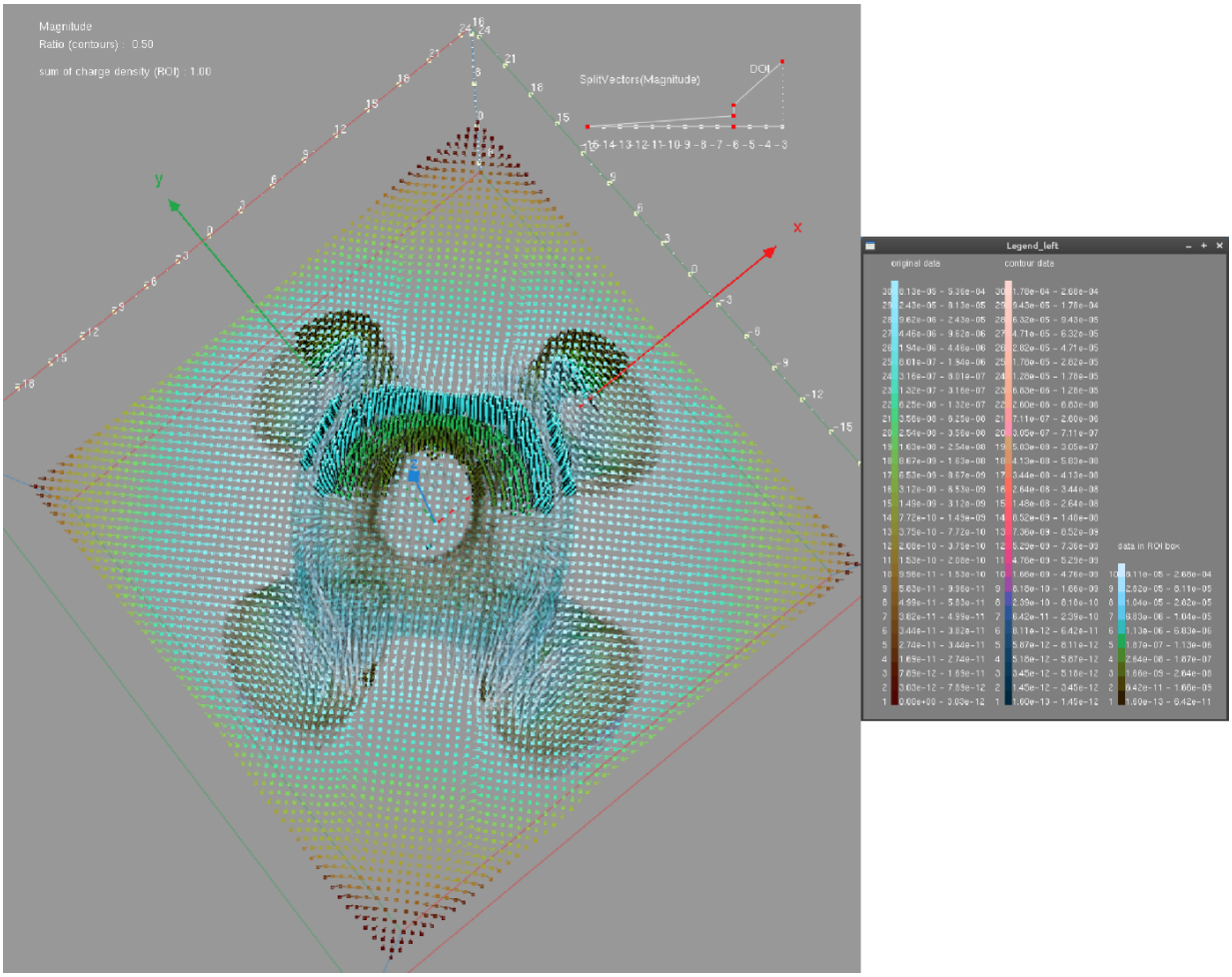

Figure 27. *Visualization of a nanostructure composed of Indium-Arsenic. Clustering is based on magnitude and the legend indicates the clustering. The structure of the data is clearly seen as a "tabletop" with four legs. The Split Vector encoding technique ensures that all of the data is visible, even though the range of magnitudes is from 10^{-16} to 10^{-3}.*

[2] H. Zhao, G. Bryant, W. Griffin, J. Terrill and J. Chen, Validation of Split Vector Encoding and Stereoscopy for Quantitative Visualization of Quantum Physics Data, in review.

Rheology of Dense Suspensions

William George
Judith Terrill
Steven Satterfield
John Hagedorn
Marc Olano
Nicos Martys (NIST EL)
Chiara Ferraris (NIST EL)
Pascal Hebraud (CNRS/IPCMS)

Understanding the mechanisms of dispersion or agglomeration of particulate matter in complex fluids, such as suspensions, is of importance in many industries such as pharmaceuticals, coatings, and construction. These fluids are disordered systems consisting of a variety of components with disparate properties that can interact in many different ways. Predicting the flow of such systems is challenging, requiring very large-scale simulations. In collaboration with scientists in NIST's Engineering Laboratory (EL), we have developed an application, called QDPD (quaternion-based dissipative particle dynamics), which is capable of performing large-scale simulations of dense suspensions [1]. This simulator uses a modified version of the dissipative particle dynamics technique [2] for the simulation of Newtonian fluids, and the smoothed particle hydrodynamics technique (SPH) [3] for the simulation of non-Newtonian fluids.

QDPD is highly parallel and has been shown to efficiently scale up to 128 000 processors when running on the US Department of Energy (DOE) supercomputer Mira (IBM Blue Gene/Q) at the Argonne National Laboratory Leadership Computing Facility. Our goal is to

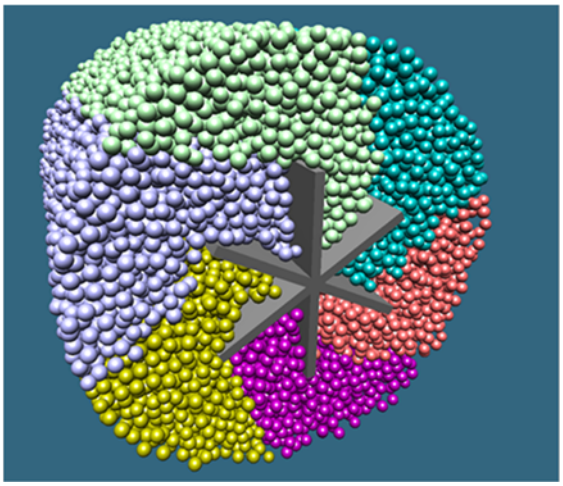

Figure 28. *A snapshot from a QDPD simulation of a proposed mortar SRM in a 6-blade rheometer with a view from the bottom of the rheometer. From this view, the blades are rotating clockwise. The suspended spheres are color-coded by their starting section.*

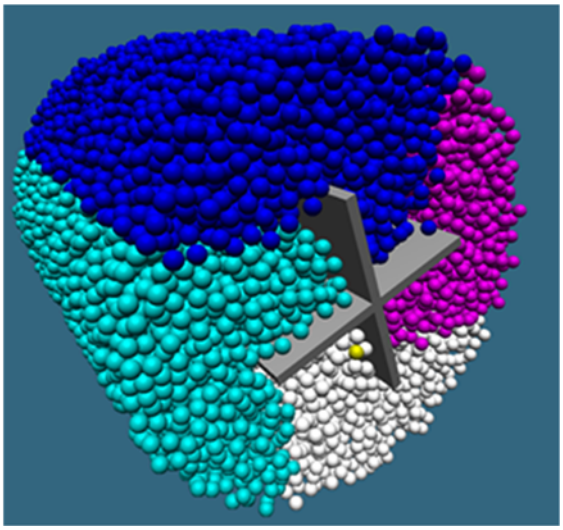

Figure 29. *A snapshot from a QDPD simulation of a proposed mortar SRM in a 4-blade rheometer. This is a view from the bottom of the rheometer. From this view, the blades are rotating clockwise. The suspended spheres are color-coded by their starting quadrant.*

advance our understanding of the flow properties of a specific material, fresh concrete, a dense suspension composed of cement, water, sand, and rocks. We are using this code for two projects: a study of vane rheometers and flow in a pipe system.

Vane Rheometers. We are currently using this computational approach in the development of standard reference materials (SRMs) for the calibration of vane rheometers used to measure the flow properties of fresh concrete. Figure 28 and Figure 29 show snapshots of our rheometer simulations of the proposed mortar SRM in a vane rheometer. While concrete flow measurements, using different concrete rheometers, can be found to correlate, they usually do not provide identical absolute values. This is a consequence of the complex flow patterns that develop in the rheometer combined with the non-Newtonian behavior of the mortar or concrete. This results in complex local stress and strain/strain rate fields that make it difficult to express measurement data in terms of fundamental rheological parameters. By modeling the flow of an SRM in a vane rheometer, we are able to predict what should be measured by an experimentalist. Furthermore, we design our simulations to map out many details of the local flow, such as stress/strain fields in 3D, in order to provide insight into the process. Most research on suspensions has made the simplifying assumption that the matrix fluid, that is, the fluid supporting the suspended particle, is Newtonian. With the use of high-performance computing, we have been able to simulate suspensions with non-Newtonian fluid matrices, which includes most suspensions of interest to industry.

Our simulations have demonstrated that the viscosity versus shear rate curves for suspensions having various volume fractions can be collapsed onto a single universal curve parameterized by the properties of the underlying non-Newtonian matrix fluid [4]. This, along with other results from our studies, has advanced our understanding of the flow of dense suspensions [5-6].

Building on this research, we have begun using simulation in the design process for new standard reference

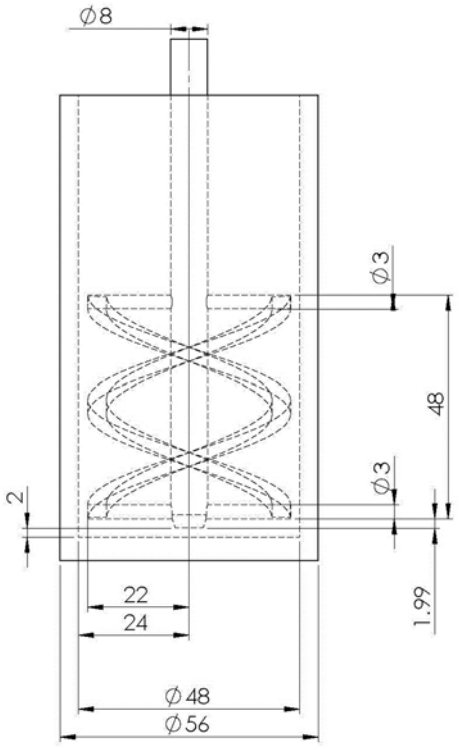

Figure 30.. *A design drawing for a proposed "double-helix" rheometer blade.*

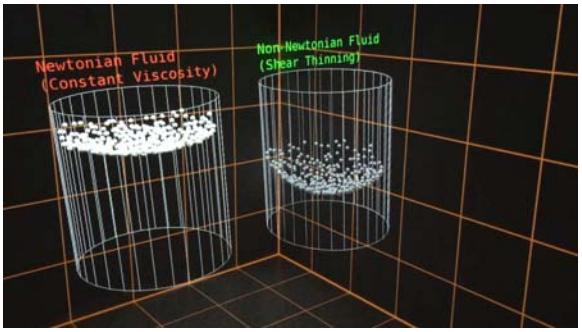

Figure 31. *One layer is isolated for a visual speed comparison during animation of the simulation data.*

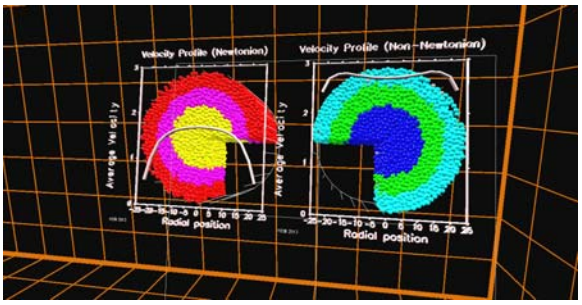

Figure 32. *Velocity profile plots show velocity of the solids near the pipe wall is much greater for shear thinning (non-Newtonian) case.*

materials (SRMs) which will be used for calibrating mortar and concrete rheometers. See Figure 28 and

Figure 29. The first such SRM will be mortar, which should be completed in 2016, followed by concrete a year later.

To support our study, we submitted a proposal for supercomputer time to the DOE Advanced Scientific Computing Research (ASCR) Leadership Computing Challenge (ALCC), in February 2015. This resulted in an award of 50 million CPU-hours of supercomputer time on the IBM Blue Gene/Q, Mira, at the Argonne Leadership Computing Facility. Mira, currently ranked 5th on the Top 500 list of supercomputer installations,[30] will enable us to perform high fidelity simulations.

Our simulations in 2016 will focus on the design of the blades within the rheometers. The current typical design, with 4 or 6 flat blades, has been shown to be sub-optimal [7-8] and other blade designs are under consideration. We will modify our simulator to study newly proposed blade designs, such as the "double-helix" blade shown in Figure 30.

Flow in Two Pipe Systems. We have also investigated another flow geometry of interest to industry, a pipe/channel system. Flows of suspensions through such systems are important for a wide variety of applications, including pumping of concrete and slurries, microfluidic devices, and biological systems. Many computational experiments were required to develop a model of the forces between the wall of the pipe and the suspended inclusions, as well as the forces between the matrix fluid and the pipe. Although these simulations on the NIST cluster, Raritan, are still underway, initial results of this study have been submitted for presentation at the International Concrete Sustainability Conference (SCC2016) scheduled for May 2016 [9]. A more complete report will be published once all of our pipe-flow simulations have been completed.

A critical part of the understanding of the two pipe system is visualization of the results in the NIST Cave Automatic Virtual Environment (CAVE). Specifically, a CAVE application was created for comparison of Newtonian and non-Newtonian fluids. Two pipe flow data sets, one Newtonian and one non-Newtonian, produced by numerical simulations are displayed and analyzed. The capabilities of the NIST 3D environment are used to do a side by side comparison of a Newtonian matrix fluid and a non-Newtonian shear thinning matrix fluid; see Figure 31. Animation controls allow simulation time to be played forward/backward at full or single step speeds. One layer can be isolated and displayed to visually compare the velocity of the two simulations. Quarter sections of both pipe flows may be turned on and off to reveal the inner data (flow); see Figure 32. Interactive sliders provide flexibility for side by side comparison at almost any position (side-by-side, overlapping, over/under, front/back). User controlled navigation through the 3D space provides viewing from any point of view. The virtual models can be scaled from hand held objects to human (and larger) sizes.

The immersive environment has an interactive clipping plane tool, which behaves like a "data windshield". It cuts away the data elements between the user and the clipping plane. For this project an analysis capability was added to this data probe. While the user explores the flowing particles with the clipping tool, average velocity of the simulated flow is extracted and displayed to the user as an *xy* line plot. By creating a line plot, it may be positioned on the clipping tool making it visible to the natural line of sight. The view is somewhat like a heads-up-display or *virtual* augmented reality. The numerical analysis represented by the line plot can be easily studied in the context of the corresponding physical location. The plot is dynamically updated corresponding to both the simulation time step (frame number) and the *z* layer position used to compute average velocity. A novel line plot algorithm was created consisting of 3D line segments in virtual 3D space. This type of object is also known as a *wire-frame* model. Additionally, to draw numerical values, a pure stroke font was needed. The Hershey fonts, originally developed in 1967 were utilized for the stroke font. The

[30] http://www.top500.org

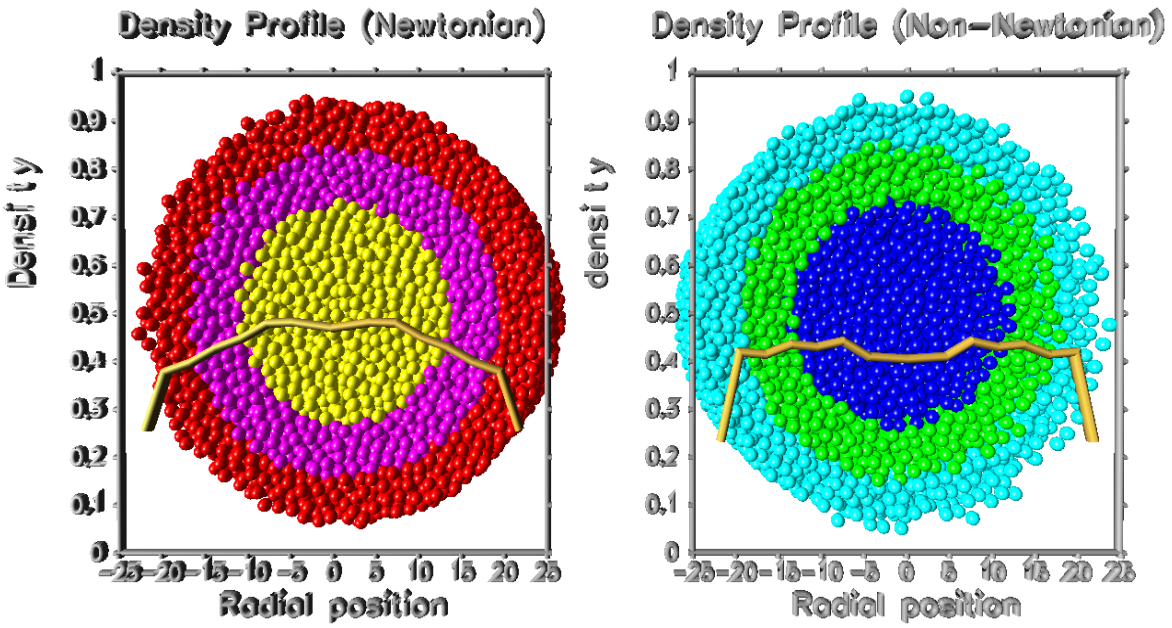

Figure 33. *Density profile plots show he density of the solids is greater near the central axis of the tube.*

xy plot wire frame geometry used to render the velocity vs radius plot is generally sparse enough to allow viewing of both the analysis and the underlying geometry.

Results. Several results are clearly indicated in the analysis and visualization of the simulation data.

- The shear thinning system flows much more quickly than the Newtonian system; see Figure 31.
- The velocity of the solids near the pipe wall is much greater for shear thinning (non-Newtonian); see Figure 32.
- For both fluid types, the solid density is greater near the central axis of the tube, the effect being enhanced for the Newtonian case as supported by the density profile graph; see Figure 33.

[1] N. Martys, Study of a Dissipative Particle Dynamics Based Approach for Modeling Suspensions, *Journal of Rheology* **49**:2 (2005), 401-424.

[2] P. J. Hoogerbrugge and J. M. V. A. Koelman, Simulating Microscopic Hydrodynamic Phenomena with Dissipative Particle Dynamics, *Europhysics Letters* **19** (1992), 155-160.

[3] J. J. Monaghan, Smoothed Particle Hydrodynamics, *Reports on Progress in Physics* **68** (2005), 1703-1759.

[4] M. Liard, N. S. Martys, W. L. George, D. Lootens and P. Hebraud, Scaling laws for the flow of generalized Newtonian suspensions, *Journal of Rheology* **58** (2014), 1993.

[5] N. S. Martys, M. Khalil, W. George, D. Lootens, and P. Hebraud, Stress Propagation in a Concentrated Colloidal Suspension under Shear, *The European Physical Journal E* **35**:3 (2012), 20.

[6] P. Hebraud, D. Lootens, and N. Martys, "Stress Organization in an Attractive Concentrated Colloidal Suspension under Flow", XVIth International Conference on Rheology, Lisbon, Portugal, Aug-2012.

[7] C. Ferraris and L. Brower, eds., Comparison of Concrete Rheometers: International Tests at LCPC (Nantes, France) in October 2000, NISTIR 6819, September 2001.

[8] C. Ferraris and L. Brower, eds., Comparison of Concrete Rheometers: International Tests at MB (Cleveland OH, USA) in May 2003, NISTIR 7154, September 2004

[9] N. S. Martys, C. F. Ferraris and W. L. George, Modeling of Suspension Flow in a Pipe Geometry and Rheometers, in review.

[10] S. Satterfield, N. Martys, W. George, J. Hagedorn and J. Terrill, Suspension Flow in Pipe Systems: Comparison of Newtonian and Shear Thinning Fluid, movie presented at the NIST Booth at SC15, The International Conference for High Performance Computing, Networking, Storage and Analysis, November 15-20, 2015.

HydratiCA: A Parallelized Numeric Model of Cement Hydration

John Hagedorn
Judith Terrill
Wesley Griffin
Steven Satterfield
Jeffrey Bullard (NIST EL)
Joshua Arnold (NIST EL)

http://www.nist.gov/itl/math/hpcvg/hydrationhpc.cfm
http://www.nist.gov/itl/math/hpcvg/hydrationvis.cfm

HydratiCA is a stochastic reaction-diffusion model of cement hydration. The hydration that occurs after cement powder is mixed with water transforms the paste from a fluid suspension into a hardened solid. This process involves complex chemical and microstructural changes. Understanding and predicting the rates of these changes is a longstanding goal. Computational modeling of the hydration of cement is challenging because it involves a large number of coupled nonlinear rate equations that must be solved in a highly irregular three-dimensional spatial domain. HydratiCA addresses these challenges with a computational model that has several advantages over other models of cement hydration.

Parallelization of the model and the visualization of the output data are important components of this project. With parallelization we can simulate systems that are large enough to be realistic, avoiding finite size effects, and still be able to complete the simulations in a reasonable amount of time. Visualization of the data volumes produced by HydratiCA is important both for validation and for understanding of the results.

HydratiCA discretizes space into a three-dimensional lattice of computational sites, with the material composition described at each site. The simulation occurs in a series of time steps, which are typically on the order of 1 msec. During each time step, material at a site may migrate to a neighboring site to simulate diffusion, or react with other materials at the same site to produce other materials. Each of these types of events is modeled stochastically, assigning a probability to each event based on the mobility or the reaction rate constant and driving force. Each site is visited during each time step, and the material amounts are updated accordingly.

This year we continued work on HydratiCA with significant improvements to the algorithm, the parallel implementation, and visualization. We obtained new results from large-scale runs on the Stampede supercomputer at the Texas Advanced Computing Center. We also made substantial strides in our visualization results. In the next year, we will perform much larger simulations on Stampede, a supercomputer housed at the Texas Advanced Computing Center (TACC) through a grant from the NSF Extreme Science and Engineering Discovery Environment (XSEDE) program.

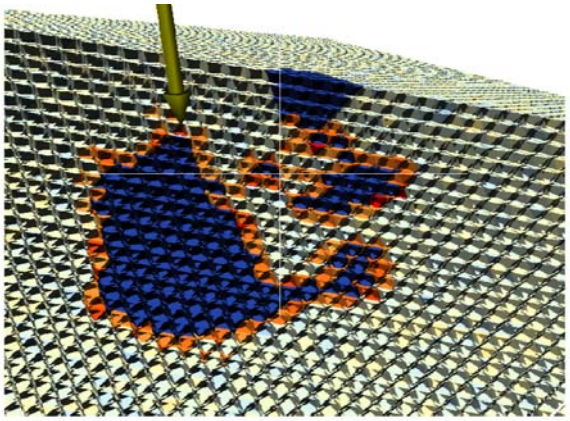

Figure 34. *Immersive display of the growth of C3S particles (blue) hydrating in a calcium hydroxide solution. Regions of orange are where hydration reactions have produced solid calcium hydrate reaction product.*

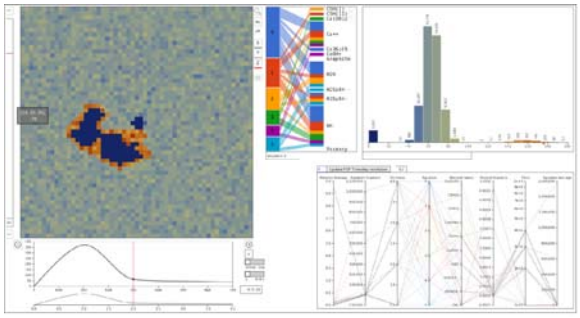

Figure 35. *An example of the 2D quantitative visualization of C3S hydration metrics. This display and all interactions are within a web browser.*

Parallel Implementation. HydratiCA has been parallelized using a spatial block decomposition of the three-dimensional array of computational sites. Each block is handled by a single processor. Communication between processors is necessary for several operations, most importantly for the diffusion step during which materials migrate to neighboring sites. All interprocess communication is accomplished through use of the Message Passing Interface (MPI).

During this year, various changes have been made to improve both the accuracy of the algorithm and the functionality of the implementation. Algorithm changes have centered around the proper handling of problems that result from the discretization of space and time. Changes to the parallel implementation include bug fixes, improvement to the communication schemes, and various performance optimizations. In addition, the parallel checkpointing scheme was substantially improved both in usability and in robustness.

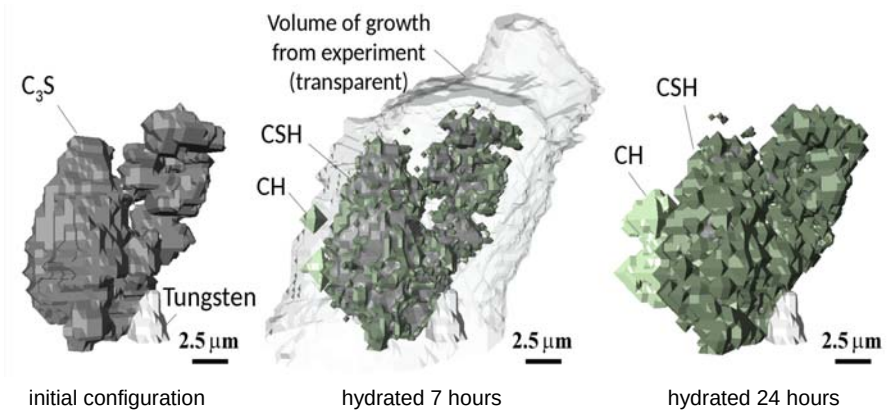

Figure 36. *A comparison of the results of the HydratiCA simulation to experimental results. The volume of growth of CSH that was found experimentally after seven hours is represented in the center image by the transparent surface.*

Visualization. Substantial improvements have been made to our visualization software that enables us to understand and interact with results from our HydratiCA runs. The current visualization tool is a hybrid 3D immersive and 2D quantitative visualization. Figure 34 and Figure 35 show the immersive 3D display and the quantitative 2D display respectively. This hybrid tool enables one to track the spatial evolution of phases and solution composition. The 2D quantitative graphs are displayed in NIST's immersive visualization environment at the same time as the 3D visualization. The graphs and 3D visualization change with the time step in sync. The 3D and 2D visualizations communicate bi-directionally under user control. Geometric clipping and parameter clipping are enabled. One can also probe the data dependencies to begin establishing kinetic relationships among members of the reaction network. This is invaluable for discovering new physio-chemical relationships during hydration, and will become more powerful for analyzing more complicated cement systems.

Results. Last year we received a grant of computer time from NSF's XSEDE program, enabling us to do large scale runs on Stampede at TACC. We have used this resource to do direct comparisons between time-resolved 3D nanoscale observations of the hydration of tricalcium silicate (C3S) and simulations of the same system using HydratiCA. In particular, we compared nano-computed tomography (nCT) observations of C3S particles hydrating in a calcium hydroxide (CH) solution to HydratiCA simulations that duplicate, as nearly as possible, the thermal and chemical conditions of the experiment. Note that one of the principal products of this hydration is calcium silicate hydrate (CSH).

Figure 36 shows a comparison of the results of the experiment with the results of the simulation. The initial configuration of materials for the simulation is derived directly from the initial nCT 3D image. HydratiCA captures the general trends observed in the nCT experimental data, but the experiment shows a much more voluminous hydration product. After seven hours of simulated time, the volume of CSH is not nearly as large as that observed in the nCT image after seven hours. After 24 hours of simulated time, the CSH volume has increased but has still not as large that the seven-hour experimental observation. Possible reasons for this differences are:

- CSH has a much larger effective molar volume than previously indicated by experiments.
- In the experiment, CSH from hydrating particles outside the field of view (which are not included in the simulation) is migrating to the particles that are in the field of view.

In addition to investigating these discrepancies, our future work will be focused on calculating the time-dependent rate of heat release, and on the development of the percolating solid network that is responsible for the hardening of concrete. We have mapped out a sequence of simulations that use realistic particle size and shape distributions that have been measured experimentally. This enables us to closely approximate the initial conditions of real cementitious systems so that simulation results and experimental measurements can be meaningfully compared. These runs will be accomplished through a grant of an additional 743K CPU-hours on Stampede through the NSF XSEDE program.

[1] J. Bullard, T. Ley, J. Hagedorn, R. Desaymons, W. Griffin, J. Terrill, Q. Hu, S. Satterfield and P. Gough, Direct Comparisons of 3D Hydration Experiments and Simulations, *6th Advances in Cement-Based Materials Conference*, July 2015.

[2] J. Hagedorn, J. Bullard, R. Desaymons, W. Griffin, J. Terrill, T. Ley, Q. Hu, S. Satterfield and P. Gough, HydratiCA: A Parallelized Numeric Model of Cement Hydration, *XSEDE 2015*, July 2015.

[3] W. Griffin, D. Catacora, S. Satterfield, J. Bullard and J. Terrill, Incorporating D3.js Information Visualization into Immersive Virtual Environments, *VR2015 IEEE Virtual Reality*, March 2015.

[4] J. Stoian, T. Oey, J. W. Bullard, J. Huang, A. Kumar, M. Balonis, J. E. Terrill, N. Neithalath and G. Sant, New Insights into the Prehydration of Cement and its Mitigation, *Cement and Concrete Research*, **70**, 94-103, April 2015.

Network Simulation Visualization

Sandy Ressler
Phil Gough (CSIRO)
Kevin Mills (NIST ITL)
Christopher Dabrowski (NIST ITL)

http://www.nist.gov/itl/math/hpcvg/infovis.cfm

Recent work by Mills and Dabrowski [1] has produced a network simulation that examines the effect of realistic parameter changes on network performance. NIST guest researcher Phil Gough produced an interactive visualization tool for network simulation data produced by this simulation. This tool allows researchers to closely examine the results of simulations and to easily identify conditions such as network congestion. Produced using D3, a JavaScript based information visualization library, it is available online[31].

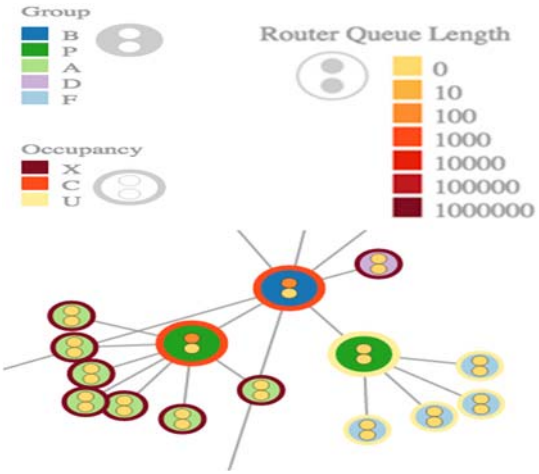

Figure 37. *Network simulation visualization tool details. There are five groups or types of nodes (indicated by color of interior of circle). Node congestion or occupancy is indicated by color of border of circle. Two small circles inside of node indicates queue length of up (top) or down (bottom) queue. This work is effectively complete however we anticipate producing some animations illustrating the behavior of the network simulations.*

[1] K. L. Mills and C. E. Dabrowski, The Influence of Realism on Congestion in Network Simulations, NIST TN 1905, January 2016.

[2] P. Gough, "Comparing Visualization Approaches to Communicating Science to Non-Scientists," ACM SIGGRAPH, Los Angeles, Aug. 9, 2015.

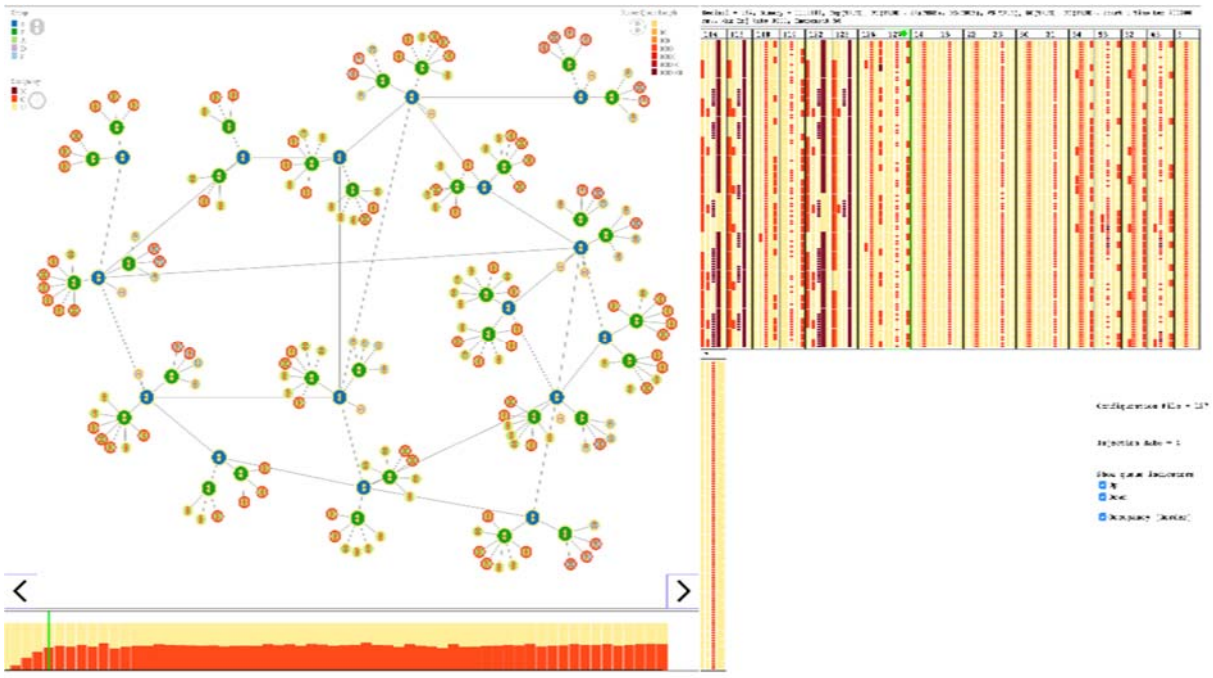

Figure 38. *Network simulation visualization tool. Topology on the left side of the display illustrates queue lengths and congestion state. Column type displays on the right side allows a user to select parameter input to simulation and displays congestion for each type of node group. The graph on bottom displays congestion and lets user step through the time of simulation. Currently two datasets are available one with 250 time steps, the other with 3000 time steps. Simply use the desired number in the URL.*

[31] http://math.nist.gov/~SRessler/pjg4/networkVis/?dataset=250

Image-based WebVR Graphics

Sandy Ressler
Tomasz Bednarz (CSIRO)
Kyle Davis (The College of New Jersey)
Steve Satterfield

WebVR is a form of virtual reality (VR) that displays in a web page. Everyone has a web browser and given a location (a URL), access to information is straightforward and virtually unlimited. Graphics presented in web pages has become enhanced with the arrival and support of WebGL, a web based version of the time-tested OpenGL[32] specification. Simply put, if you go to a page with WebGL 3D graphics it will be displayed correctly in your web browser without the need for any browser plug-ins. This means that complex 3D graphics can be placed into web pages, and the rich capabilities of these graphics can be used within a web page. Similarly, VR environments can now be placed into web pages via the WebVR extension.

One of the big differences from the VR of 20 years ago is the ability to create and use 360-degree video environments. These image-based environments offer a simple method to bring users and the public to places that are inaccessible, dangerous or simply forbidden. Our first taste of a widely used method of pseudo image-based VR is an application such as Google Streetview. People have modified Streetview to work with Oculus Rift headsets[33]. Clearly this is just the beginning of more image based VR on the web.

We can work with three types of images: computer generated graphics, image-based environments, and combinations of the two (which leads to a type of augmented reality). Each of these has different authoring and interaction requirements. Placing these images into web pages presents both opportunities and challenges. Much of our web-based 3D graphics has been built using the X3D graphics standard. Given our desire to work with this material using an immersive head-mounted display such as the Oculus Rift [1], our summer SURF student Kyle Davis created a tool to convert X3D files to files that are usable by the Rift; see Figure 39. This tool is able to take X3D files of computer graphic scenes and make them viewable as stereo pairs with WebGL code that allows for the personal adjustment of stereo separation[34]. In addition, there are user interface issues when wearing a helmet. Your hand effectively disappears and keyboard actions become difficult. One solution is to use additional devices such as the Leap motion tracking device which monitors your hands and can interpret gestures[35]; see Figure 40.

Figure 39. *X3D to Oculus tool*

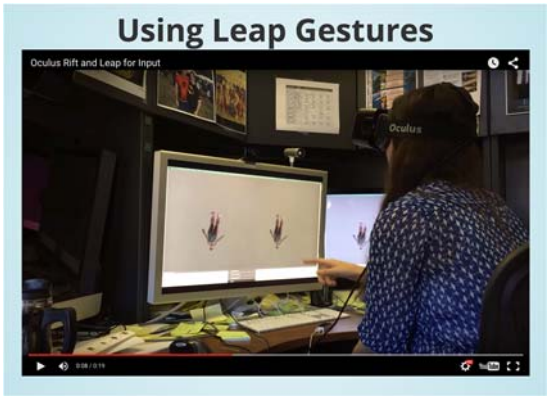

Figure 40. *Leap gestures in use.*

Figure 41. *Producing 360-degree video for embedding to web page.*

As a guest scientist at Australia's Commonwealth Scientific and Industrial Research Organization (CSIRO) [2,3] for a month in Brisbane Australia, Sandy Ressler worked with Tomaz Benarz on immersive 3D web based video. They produced a prototype workflow and demonstrations of 360-degree videos using CSIRO equipment to photograph some interior scenes[36]. See Figure 41.

A near term goal is to create a set of tools and a production path to allow people to author 360-degree image based environments with interactive areas. See Figure 42. Given appropriately indicated "hot-spots" users will be able to obtain additional information about objects in the scene, all within a web page. The end user

[32] https://www.opengl.org/
[33] http://oculusstreetview.eu.pn/
[34] http://math.nist.gov/~SRessler/kmd3/Oculus/X3DToRiftTool.html
[35] http://math.nist.gov/~SRessler/kmd3/
[36] http://math.nist.gov/~SRessler/w3d/CSIROwebvr.html#/

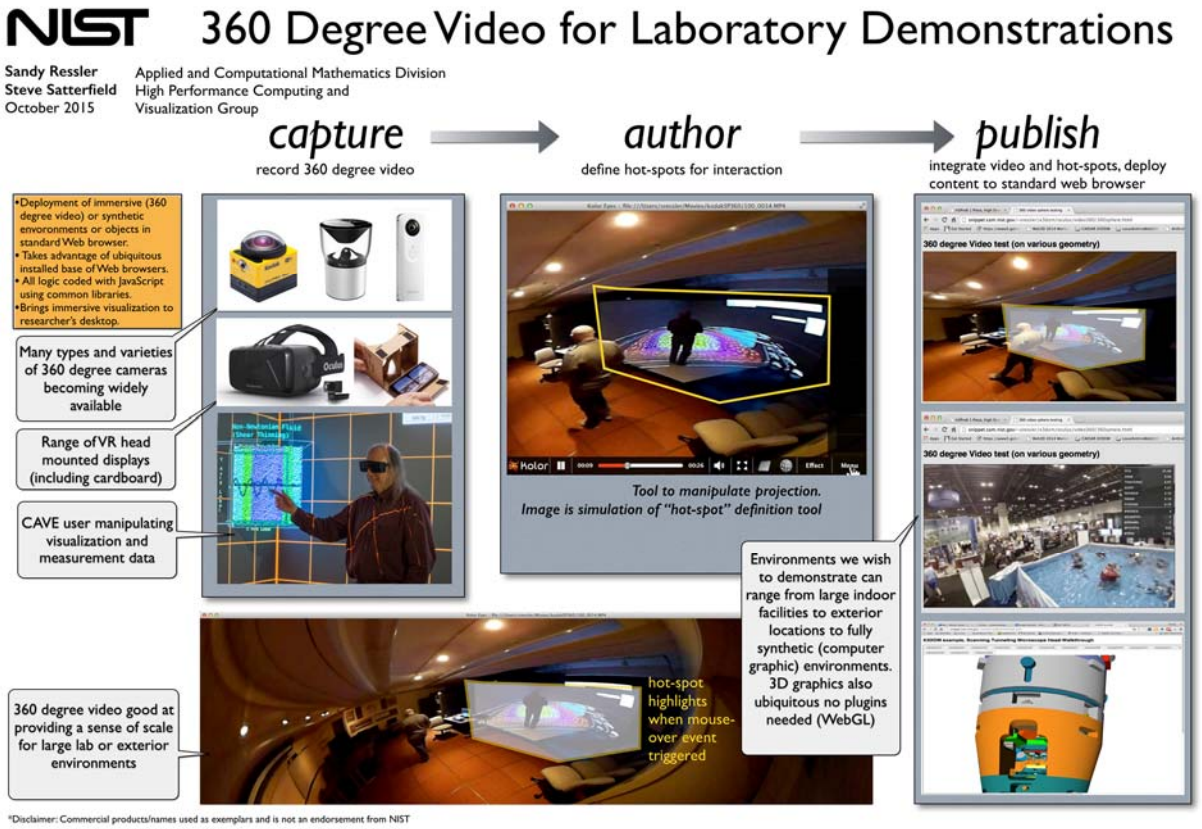

Figure 42. *Hypothetical production path for web-based immersive video content.*

will simply go to a URL and (while wearing a VR headset) look around the environment selecting points of interest. For example, an environment of a clean room for semiconductor manufacturing, a place with normally restricted access, can be explored with the user clicking on pieces of equipment getting additional information, including supplementary video, about the items of interest.

[1] S. Ressler "Using Oculus Rift with your Web Browser for Science," SIGGRAPH 2015 Birds of a Feather, August 9-13, Los Angeles CA. http://slides.com/sressler/oculusweb-siggraph2015/

[2] S. Ressler, T. Bednarz, "Image Based WebVR: Creating and Publishing Environments for Browsers and HMDs," CSIRO Seminar, Canberra, Australia, February 25, 2015. http://math.nist.gov/~SRessler/w3d/CSIROwebvr.html

[3] S. Ressler, "WebVR or What's That 3D Environment doing in my Web Browser," Computational and Simulation Sciences Conference, Melbourne, Australia, February 13, 2015. http://math.nist.gov/~SRessler/w3d/aus2015keynote.html/

High End Visualization Software: Software Tests to Maintain System Reliability

Steven Satterfield
Judith Terrill
Alauna Jackson (Bowie State University)
Aleksander Psurek (Thomas Wootton High School)
Rael Youseff (UMBC)
Jason Zimmerman (Millersville University)
John Hagedorn
Wesley Griffin
Terence Griffin

The High Performance Computing and Visualization Group (HPCVG) has operated an immersive virtual environment (IVE) since 2000 in support of its mission of advanced visualization of scientific data. In our applications, the 3D immersive environment functions as an interactive measurement laboratory. HPCVG collaborates with researchers across all areas of NIST to apply the IVE and virtual measurement techniques.

System availability is very important for ongoing collaborations and the need to do demonstrations on short notice. We have a proactive approach to system reliability through the development of our own hardware

Figure 43. *HPCVG SURF student interns during the summer of 2015.*

tests as well as additional tests obtained as part of the recent upgrade of the virtual environment (CAVE). Equally important is system and application software reliability in the context of evolving software such as operating system upgrades, security patches, changing requirements of NIST research, as well as GPU and driver upgrades. During 2015, we began designing and implementing a software testing capability to maintain software reliability and correctness.

Software Stack. The application creation framework software for the HPCVG CAVE is named HEV (High End Visualization). It consists of a stack of vendor-supplied, Open Source, and in-house developed software. At the lowest level, the vendor-supplied OpenGL library and Linux device driver renders and displays graphics in the graphics cards producing images displayed on the CAVE screens. Open SceneGraph (OSG) is the next level. It is an open source high performance 3D graphics toolkit and library for organizing graphics data in a hierarchical structure, allowing models to be built, manipulated and rendered using OpenGL.

IRIS (Interpreted Runtime Immersive Scenegraph) is above OSG in the stack. It is an HPCVG-developed C++ software library. IRIS controls the hardware elements of the IVE, reading the tracking data to build the user view, and updating the projected images in real time. For a CAVE, different 3D stereo images are built for each screen such that they combine for the user into a 3D immersive view. A key feature of IRIS is the displayed scene graph can be modified at run-time by external processes (programs and scripts) communicating via a standard Linux/Unix facility know as a *named pipe* or a FIFO (first-in first-out). The functionality of the FIFO is implemented in a set of ASCII commands written to the FIFO. These commands can be stored in a file, known as an iris file. Another feature of IRIS and HEV as a whole is device independence. By isolating the display characteristics into specific display shared objects (DSOs), the same HEV binary code can run on a full range of devices from CAVES to non-immersive desktop and laptop displays.

IDEA (IRIS Development Environment for Applications) is the level above IRIS. It is an HPCVG-developed collection of commands, scripts and file formats. This collection of software tools, locally known as the *Army of Ants* follows in the tradition of the Unix philosophy. Each of the pieces generally focus on one simple task useful for a wide variety of applications.

Applications complete the stack, typically implementing an interactive visualization in a specific area. These applications are often built with very little programming by combining existing ants. When new tools are required, they are typically generalized as much as possible and added back into the HEV software.

Source Control and Continuous Integration. A significant step implemented during 2015 for this project was to transfer the HEV source code into the Git version control system. HPCVG now maintains a single consistent code repository for building the production HEV software used for the CAVE and all supporting staff workstations. Utilizing Git, all developers have a private working copy for creating and testing without stepping on each other's work. Once new features are ready, Git merges the changes back into the production software. System reliability is enhanced because a CAVE application never depends on a special case version of HEV. The introduction of continuous integration (CI) further improved reliability development. Here, the full HEV source is rebuilt twice a day to ensure newly merged changes haven't introduced any compile time errors.

The implementation of software testing involved the design and implementation of a software-testing infrastructure that allowed all tests to be run with a single command. Each individual test required one or more baseline results as well as individual analyses to be run to yield a composite *pass* or *fail* result.

This year we completed the design and implementation of the software-testing infrastructure. We also completed a number of tests, primarily with SURF students. See Figure 43. These tests are implemented as scripts, named timeline files, that direct the system to navigate through a scene, issue modification directives (such as on/off directives for objects in the scene), and save images all at specific times. Following a test, analyses are run and the *pass / fail* output for the tests is issued. Initial results indicate that repeated tests with the same GPU, driver, and software configuration give the same results, though images generated on different GPUs can differ. Most of the differences are slight (one RGB color unit at one or two channels), however, some can vary wildly. In the coming year, we will continue to implement tests.

Optical Characterization for Advanced Immersive Displays

Judith E. Terrill
John Penczek (NIST EL)
Paul A. Boynton (NIST EL)

The human visual system (HVS) is the dominant means by which we collect information; it consumes the majority of our brainpower in processing input. The accurate visualization of datasets leverages the power of the HVS for better understanding, discovery, and innovation. The rendering of a data visualization is limited by current display technologies, which typically cannot take full advantage of HVS capabilities.

We aim to measure the performance of displays in order to better understand their limitations. As display technologies make rapid advances, they often require new characterization methods. We are developing optical methods that evaluate how well immersive display technologies perform. As the display industry migrates from large immersive multi-screen systems to relatively compact head-worn devices, we are creating new characterization methods that adjust to the unique attributes of these new technologies.

In our previous work, we developed optical characterization methods for immersive Cave Automatic Virtual Environment (CAVE) systems [1]. These large systems are well suited for team members to interact and collaborate inside a data visualization. In order to enhance the visual experience of these large screens, the display industry is driving toward brighter images with a greater range of colors by turning to light emitting diodes (LED) and laser light sources [2]. But the narrow spectral bandwidth of these light sources are substantially different than the incandescent and fluorescent sources used in the past. (Previous studies have demonstrated the sensitivity of some light-measuring devices to narrow-band filtered light sources [3].) Therefore, it is necessary to evaluate the impact of these sources on the typical optical detectors used to measure display performance. This work was conducted in support of the International Electrotechnical Commission (IEC) standardization work on laser projectors [4].

There are currently a wide range of commercial detectors available, with varying capability. Since immersive display systems often use 3D front- or rear-projections displays, we limited our study to non-contact detectors. Optical detectors that measure the spectral radiance, tristimulus values, or luminance of a small area on the screen can be used to measure most of the basic display performance characteristics. High performance portable spectroradiometers are available that offer absolute spectral measurements, but at substantial cost. Filtered colorimeters are a lower cost option, but may not be appropriate for new display technologies that use narrow band light emitting diode (LED) and laser light sources. We compared a variety of commercial spectral and filter-based detectors from two manufacturers.

Our results demonstrate that it is necessary to consider the color and spectral bandwidth when choosing the appropriate detector for display measurements. In addition, the light produced by the display can have other characteristics, such as varying polarization, laser speckle, spatial non-uniformity, and temporal modulation, all of which should be considered when choosing the appropriate detector. Our results will be included in a NIST IR, which will be an expanded version of [1].

There is currently strong interest in providing an immersive experience to the user by placing a head-worn display right in front of the eye. A transparent display can provide the viewer with an augmented reality experience that is also immersive. The transparent attribute of these devices creates some metrology challenges in evaluating their performance. We investigated this aspect in a complimentary project that involved conventional transparent displays, and supports IEC standardization work on transparent liquid crystal display (LCD) and organic light emitting diode (OLED) displays [5,6]. Our investigation developed new measuring methods for determining the transmission properties of these displays, and established a general framework for evaluating the transparent display performance under ambient lighting conditions [7,8]. This work will be incorporated into an industry measurement standard [9].

Going forward, we will leverage our work on transparent displays to develop optical metrology for see-

through near-eye displays. This augmented reality technology is expected to experience considerable growth for medical and industrial applications, but will need sound measurement methods to achieve high quality and user acceptance.

These studies on new light sources, transparent displays, and near-the-eye displays lay the groundwork for collaborations focused on virtual reality, augmented reality and usability.

[1] J. Penczek, S. G. Satterfield, E. F. Kelley, T. Scheitlin, J. E. Terrill and P. A. Boynton, Evaluating the Visual Performance of Stereoscopic Immersive Display Systems, *Presence*, to appear.

[2] *Parameter Values for Ultra-High Definition Systems for Production and International Programme Exchange,* ITU-R BT.2020-2*,* International Telecommunications Union, Geneva, 2015.

[3] P. A. Boynton and E. F. Kelley, Assessment of Colour Measurement Systems Using Interference Filters, in *Proceedings of the CIE Expert Symposium on Colour Standards for Imaging Technology* (CIE x014-1998), November 1997, 22-27.

[4] *Laser Display Devices—Part 5-1: Measurement of Optical Performance for Laser Front Projectors*, IEC 62906-5-1*,* International Electrotechnical Commission, Geneva, under development.

[5] *Organic Light Emitting Diode (OLED) Displays—Part 6-4: Measuring Methods of Transparent Properties*, IEC 62341-6-4, International Electrotechnical Commission, Geneva, under development.

[6] *Liquid Crystal Display Devices—Part 5: Optical Measuring Methods of Transmissive Transparent LCD Display Panels*, IEC 61747-30-5, International Electrotechnical Commission, Geneva, under development.

[7] J. Penczek, E.F. Kelley and P.A. Boynton, Optical Measuring Methods for Transparent Displays, *SID Symposium Digest of Technical Papers* **46** (June 2015), 731-734.

[8] J. Penczek, E.F. Kelley and P.A. Boynton, General Metrology Framework for Determining the Ambient Performance of Flat Displays, *SID Symposium Digest of Technical Papers* **46** (June 2015), 727-730.

[9] *Information Display Measurements Standard*, V1.03, International Display Metrology Committee, Society of Information Display, 2012.

Texture Compression Evaluation and Optimization

Wesley Griffin
Marc Olano

http://www.nist.gov/itl/math/hpcvg/texture_compression.cfm

Texture compression is widely used in real-time rendering to reduce storage and bandwidth requirements. Hardware-based texture compression has not fundamentally changed since its introduction in 1999. Recently, however, interest has grown in improving hardware-based texture compression.

Our research has explored new techniques for reducing the bit rate for current fixed bit rate algorithms, as well as new variable bit rate algorithms that can be efficiently decoded in graphics hardware. This work benefits the rendering and visualization communities by providing a methodology for evaluating and optimizing texture compression. It also can be directly applied to existing applications to improve the quality of compressed textures.

In evaluating texture compression, the most common approach is to use some combination of the mean square error (MSE), peak signal-to-noise ratio (PSNR), or visual image inspection of the compressed texture. Last year we introduced a new evaluation methodology that accounts for the two ways in which textures are used in rendering for which the MSE and PSNR measures cannot account. Our evaluation approach combines final image rendering with objective image comparison metrics.

This year we extended our evaluation work to incorporate additional datasets and also further analysis and published these results [1,2]. The most useful insight from this study is that the type of texture, combined with how it is used, has an impact on perceived quality when rendering with compressed textures. Leveraging our evaluation approach, we implemented an optimization framework using a first-choice hill climbing algorithm to search the multi-dimensional state space of a modern texture compression algorithm. The hill-climbing algorithm attempts to minimize an energy function that is a combination of bitrate and two objective image comparison metrics. This research prototype proves the feasibility of objectively optimizing texture compression using our new evaluation methodology. It should also enable automatic texture compression optimization in real-time rendering asset pipelines.

[1] W. Griffin and M. Olano, Objective Image Quality Assessment of Texture Compression, in *Proceedings of the 2014 ACM SIGGRAPH Symposium on Interactive 3D Graphics and Games* (I3D), San Francisco, CA, March 2014, 119-126.

[2] W. Griffin and M. Olano, Evaluating Texture Compression Masking Effects using Objective Image Quality Assessment Metrics, *IEEE Transactions on Visualization and Computer Graphics*, **21**:8 (2015), 970-979.

Quantum Information

An emerging discipline at the intersection of physics and computer science, quantum information science is likely to revolutionize science and technology in the same way that lasers, electronics, and computers did in the 20th century. By encoding information into quantum states of matter, one can, in theory, exploit the seemingly strange behavior of quantum systems to enable phenomenal increases in information storage and processing capability, as well as communication channels with high levels of security. Although many of the necessary physical manipulations of quantum states have been demonstrated experimentally, scaling these up to enable fully capable quantum computers remains a grand challenge. We engage in (a) theoretical studies to understand the power of quantum computing, (b) collaborative efforts with the multi-laboratory experimental quantum science program at NIST to characterize and benchmark specific physical implementations of quantum information processing, and (c) the demonstration and assessment of technologies for quantum communication.

Quantum Information Science

Scott Glancy
Emanuel Knill
Peter Bierhorst
Adam Keith
Karl Mayer
Jim van Meter
Peter Wills
Kevin Coakley (NIST ITL)
Sae Woo Nam (NIST PML)
Dietrich Leibfried (NIST PML)
David Wineland (NIST PML)
David Pappas (NIST PML)
Gerardo Ortiz (Indiana University)
Paul Kwiat (U. of Illinois at Urbana Champaign)

A primary goal of quantum information science (QIS) is to devise and implement algorithms and protocols that exploit quantum mechanical effects to gain an advantage over purely classical techniques. Striking examples of such advantages are efficient quantum factoring of large numbers with quantum computers, information-theoretically secure quantum communication, and quantum measurement strategies with precision scaling as N^{-1} rather than the standard $N^{-1/2}$. The insights from QIS are having a growing influence on other fields, most notably fundamental and condensed-matter physics. Our work contributes to QIS by developing protocols and analysis tools for verifying the performance of quantum devices, devising statistical certification strategies for trust in quantum information, investigating our ability to control quantum systems for storage and computation, and exploring the boundaries of quantum advantages when confronted with fundamental physical reality.

There is a wide variety of protocols to demonstrate features of QIS with a small number of qubits. We investigate protocols for testing protection against noise, establishing information subsystems and demonstrating quantum advantages. One such protocol involves preparing and manipulating a "noiseless" qubit subsystem in three physical spin-half systems. This qubit is completely immune to uniform magnetic field noise and has three non-trivial robust gates that can be applied by simply swapping the spin-halfs. A clear demonstration of this qubit would be a first for non-trivial protected subsystems. We hope to realize this in ions and atoms. This has become possible because of remarkable improvements in one and two ion control over the last few years. For more on our contributions to protocols and analysis of experimental qubits, see page 67.

In many settings, high-quality quantum control of a small number of qubits is limited to operations and evolutions that cannot distinguish between the qubits. An example is the typical experimental configuration in our ion traps where there are two or three ions in one trap. Easily implementable evolutions are those that involve each ion equally. This constraint still permits implementation of non-trivial two and three qubit gates such as the unitary evolution that changes the sign of only the $|111\rangle$ state, also known as the doubly-controlled sign flip. This is a version of the famous doubly-controlled not gate (Toffoli gate), which is critical to reversible computations. We have studied the question of how many steps of J_u^2 evolution are needed to implement this gate. A J_u^2 evolution symmetrically couples each pair of qubits and can be viewed as a parallel implementation of commuting gates. The known decompositions of the Toffoli gate require six canonical two-qubit gates, so one might hope that fewer than six J_u^2 evolutions might be required. But we found numerical evidence that six is necessary and sufficient. We hope to prove this observation.

We continued our work on using so-called test martingales [1] for rejecting hypotheses such as local realism and separability in quantum experiments. These experiments aim to show that simple classical descriptions do not suffice for explaining the observations. Our adaptive test martingale methods involve multiplying positive random variables (RVs) of a sequence of trials. These RVs have the property that, conditional on the past and given the hypotheses to be tested, they have expectations bounded by 1. We have previously shown this

to be a very effective method for certifying failure of local realism in Bell tests [2]. We developed and applied a version of this strategy [3] for Bell tests involving long (in time) trials, of which there were several well-publicized examples last year; see [4]. With this strategy, we obtained strong certificates from data that was previously thought to be useless due to the so-called coincidence loophole [5].

We started an exploratory project to expand the application of the test martingale methods from hypothesis testing to confidence interval determination. For this purpose, we are exploring the behavior of the method on the toy problem of identifying the bias of a coin flipped in sequence many times. We obtained a closed form for a particular version of our adaptive test martingale strategy, which enables efficient computations of expected performance and direct comparison to traditional methods based on "exact" *p*-values and Chernoff-Hoeffding bounds [6]. This work is still in progress.

A fundamental issue in quantum information and quantum measurement science is how the known fundamental physics based on relativistic quantum field theory and its variants affects the future performance of quantum devices and achievable measurement precision. Our initial investigations of these issues led to the reconsideration of arguments [7] suggesting that there are general uncertainty principles limiting the achievable precision for measuring features of space-time. Such principles could affect the ultimate usable precision of atomic clocks, laser interferometers and gravitational wave detection, for example. We further developed the mathematical approach based on a category-theoretical definition of quantum fields on a fixed gravitational background familiar from algebraic quantum field theory. This confirmed and made more precise the relevant uncertainty principles.

There have been many proposals to harvest entanglement from the vacuum, thus exploiting a fundamental feature of relativistic quantum fields: any bounded region of space-time is necessarily entangled with the rest of space-time. A popular effect related to this is the Unruh effect whereby an accelerating observer experiences thermal radiation when coupled to the vacuum. In fact, the standard proposal for harvesting entanglement involves two oppositely accelerating observers, but the accelerations required are unrealistically high. A recent study [8] suggests that acceleration can be simulated with stationary detectors having strongly "chirped" energies and/or reference pulses. Motivated by this study, we initiated an investigation of how one can measure general modes of free (non-interacting) quantum fields. The study is still in progress, but we expect to determine the practicality of verifying the presence of vacuum entanglement by using stationary detection systems based on homodyne measurements. This is a precondition for practical entanglement harvesting.

[1] G. Shafer, A. Shen, N. Vereshagin, and V. Vovk, Test Martingales, Bayes Factors and *p*-Values, *Statistical Science* **26** (2011), 84-101.

[2] J. S. Bell, On the Einstein-Podolsky-Rosen Paradox, *Physics* **1** (1964), 195-200.

[3] E. Knill, S. Glancy, S. W. Nam, K. Coakley and Y. Zhang, Bell Inequalities for Continuously Emitting Sources, *Physical Review A* **91** (2015), 032105, 17 pages.

[4] B. Christensen, A. Hill, P. G. Kwiat, E. Knill, S. W. Nam, K. Coakley, S. Glancy, L. K. Shalm and Y. Zhang, Analysis of Coincidence-Tie Loopholes in Experimental Bell Tests, *Physical Review A* **92** (2015), 032130, 13 pages.

[5] M. Sandberg, E. Knill, E. Kapit, M. R. Vissers and D. P. Pappas, Efficient Quantum State Transfer in an Engineered Chain of Quantum Bits, *Quantum Information Processing*, to appear.

[6] W. Hoeffding, Probability Inequalities for Sums of Bounded Random Variables, *Journal of the American Statistical Association* **58** (1963), 13-30.

[7] T. G. Downes, G. J. Milburn and C. M. Caves, Optimal Quantum Estimation for Gravitation, arXiv:1108.5220 (2012).

[8] T. Ralph and N. Walk, Quantum Key Distribution Without Sending a Quantum Signal, arXiv:1409.2061 (2014).

Quantum Estimation Theory and Applications

Peter Bierhorst
Scott Glancy
Adam Keith
Emanuel Knill
Jose Aumentado (NIST PML)
Manuel Castellanos (NIST PML)
Kevin Coakley (NIST ITL)
Michael DeFeo (NIST PML)
John Gaebler (NIST PML)
Yiheng Lin (NIST PML)
Ting Rei Tan (NIST PML)
Yong Wan (NIST PML)
George Barbosa da Silva (Federal U. of Ceara)
Hilma Vasconcelos (Federal U. of Cearal)

Many emerging technologies will exploit quantum mechanical effects to enhance metrology, computation, and communication. Developing these technologies requires improved methods to measure the states of quantum systems. Quantum estimation is a statistical problem of estimating an underlying quantum state, measurement, or process by using a collection of measurements made on independently prepared copies of the state or applications of the measurement or process. Accurate quantum estimation allows experimentalists to answer the question "What is happening in my quantum experiment?" and to characterize uncertainty in that answer.

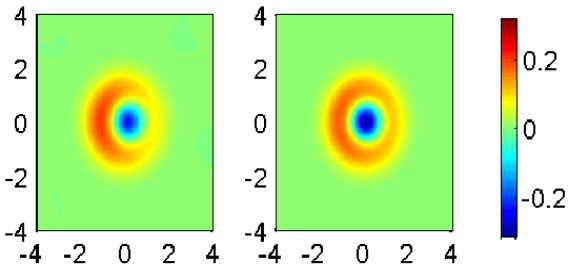

Figure 44. *Reconstruction of quantum states produced in a superconducting microwave cavity. The figures show estimated Wigner functions of two different superpositions of 0 and 1 photon states. Negative regions demonstrate quantum character of the states.*

Full quantum estimation can be a demanding task, requiring a large number of different measurements to be performed on (independently prepared copies) of the quantum system and large amounts of computation to perform the estimation. One method for reducing these costs is to exploit pre-existing knowledge about the state being measured. For example, the state could be restricted to a smaller subset of all quantum states, such as those states that have Gaussian probability distributions for measurement results. Existing algorithms for estimation of Gaussian states often return unphysical estimates that violate the Heisenberg Uncertainty Principle. ACMD developed an algorithm that constrains estimated states to those that obey the uncertainty principle, and implemented this algorithm in tomography software [1]. Enforcing the uncertainty principle constraint allows faithful estimation of states produced in high fidelity experiments.

The NIST/PML Ion Storage Group has pioneered one of the world's most successful quantum computer development projects. With their recent advances in qubit preparation, logical operation, and measurement fidelities, more advanced statistical techniques are required to characterize the resulting trapped ion quantum states. (NIST trapped ion experiments have reported a fidelity of 99.9998 % for single qubit logic operations [2].) This year, in collaboration with the Ion Storage Group, ACMD researchers developed tools to estimate properties of quantum states for experiments with extremely high fidelity. These include a protocol for placing a lower bound on the fidelity with which a single qubit state can be prepared given minimal assumptions and a single procedure for both calibrating measurements (using data from qubits with known states) and estimating the quantum state (of a collection of qubits in an unknown state) [3]. Because both measurements and the unknown state are estimated together, systematic errors are avoided, statistical uncertainty is reduced, and higher fidelity states can be analyzed reliably. These algorithms were used to analyze data from a new trapped ion experiment demonstrating entangled state fidelities above 0.99 [4].

In many quantum experiments, the state can be only partially inferred from the available measurements. However, the available measurements may be able to place useful bounds on parameters of interest, even if they cannot be inferred exactly. ACMD researchers are exploring algorithms to obtain such bounds. Researchers in the PML's Quantum Electronics and Photonics Division are preparing various exotic quantum states with new superconducting microwave-cavity technology. ACMD researchers provided software and consultation on the analysis of these experiments [5].

Maximum likelihood quantum state estimation is known to suffer from bias. However, the amount and direction of the bias has been poorly understood. In collaboration with researchers from the Federal University of Ceara, Brazil, ACMD researchers have used a series of numerical experiments to characterize this bias, finding clear evidence of significant bias for more pure quantum states and finding that some measurement schemes can significantly reduce the bias [6].

[1] S. Glancy, N. Kravitz and E. Knill, Efficient Estimation of Gaussian Quantum States, in preparation.

[2] K. R. Brown, A. C. Wilson, Y. Colombe, C. Ospelkaus, A. M. Meier, E. Knill, D. Leibfried and D. J. Wineland, Single-Qubit-Gate Error Below 10^{-4} in a Trapped Ion, *Physical Review A* **84** (2011), 030303(R).

[3] A. C. Keith, S. Glancy and E. Knill, Partial Quantum Tomography using Maximum Likelihood Estimation, in preparation.

[4] Y. Lin, J. P. Gaebler, F. Reiter, T. R. Tan, R. Bowler, Y. Wan, A. Keith, E. Knill, S. Glancy, K. Coakley, A. S. Sørensen, D. Leibfried and D. J. Wineland, Preparation of Entangled States by Hilbert Space Engineering, in preparation.

[5] M. Castellanos, M. P. DeFeo, S. Glancy and J. Aumentado, Tomographic Reconstruction of Itinerant Quantum Microwave States of Light, in preparation.

[6] G. B. Silva, S. Glancy and H. M. Vasconcelos, Investigating Bias in Maximum Likelihood Quantum State Tomography, in preparation.

Phase Retrieval and Quantum Tomography

Yi-Kai Liu
Shelby Kimmel (University of Maryland)
Felix Krahmer (Technical University of Munich)

Phase retrieval is the task of learning an unknown n-dimensional vector x from measurements of the form

$$y_i = |\langle a_i, x\rangle|^2, \qquad i = 1,2,\dots,m,$$

where the vectors a_i are chosen by the observer. Such measurements arise in a variety of applications, including optical imaging (where one measures the intensity

of the light field, but not the phase), and quantum tomography (where one measures the probability, but not the complex amplitude, of the wave function).

Recently, there has been a great deal of work on PhaseLift, an algorithm for phase retrieval that was inspired by ideas from compressed sensing. PhaseLift works by "lifting" the phase retrieval problem to a rank-one matrix recovery problem, and then solving a convex relaxation of this problem. In certain situations — for instance, when the measurement vectors a_i are chosen at random from a Gaussian distribution, PhaseLift is guaranteed to recover the unknown vector x, using $m = O(n)$ measurements.

Unfortunately, in real experiments, it is often difficult to perform measurements using Gaussian random vectors a_i. Instead, one must use vectors a_i that have some additional structure. How well does PhaseLift perform when one uses these structured measurements? This is the question we have sought to answer.

Broadly speaking, we found that for certain vectors x, the use of structured measurements prevents PhaseLift from recovering x correctly; but these choices of x are rare and in some sense pathological. For most choices of x, PhaseLift with structured measurements performs well.

More precisely, we studied two classes of structured measurements: so-called Bernoulli random vectors sampled from the hypercube $\{1, -1\}^n$, and vectors sampled from spherical and unitary 2-designs.

Bernoulli random measurements are of theoretical interest, as they are perhaps the simplest alternative to Gaussian random measurements. When using Bernoulli random measurements, we showed that PhaseLift can reconstruct all "flat" vectors, i.e., all vectors x that satisfy the condition $\|x\|_\infty \leq c\|x\|_2$, where c is some small constant [1,2]. Our result also holds more generally, for random measurements sampled from sub-Gaussian product distributions.

Measurements using spherical and unitary 2-designs are of interest in quantum tomography, as they can be implemented easily in many experimental setups, by using stabilizer states and Clifford operations. When using these 2-design measurements, we showed that PhaseLift can approximately reconstruct almost all vectors x, where the approximate reconstruction holds up to constant additive error, and the restriction to "almost all vectors x" is with respect to Haar measure [3].

As an application of this result, we have developed a method for quantum process tomography that is robust to state preparation and measurement (SPAM) errors, and is quadratically faster than conventional tomography in the case where the unknown process is a generic (Haar-random) unitary.

[1] F. Krahmer and Y.-K. Liu, Phase Retrieval Without Small-Ball Probability Assumptions: Stability and Uniqueness, in *Proceedings of the 2015 International Conference on Sampling Theory and Applications (SampTA)*, Washington, DC, May 25-29, 2015, 411-414.

[2] F. Krahmer and Y.-K. Liu, Phase Retrieval Without Small-Ball Probability Assumptions: Recovery Guarantees for PhaseLift, in *Proceedings of the 2015 International Conference on Sampling Theory and Applications (SampTA)*, Washington, DC, May 25-29, 2015, 622-626.

[3] S. Kimmel and Y.-K. Liu, Quantum Compressed Sensing Using 2-Designs, arXiv:1510.08887, October 2015.

Device Independently Secure Randomness from Loophole-Free Bell Tests

Peter Bierhorst
Scott Glancy
Stephen Jordan
Emanuel Knill
Paulina Kuo
Yi-Kai Liu
Alan Mink
Xiao Tang
Michael S. Allman (NIST PML)
Lawrence Bassham (NIST ITL)
Joshua C. Bienfang (NIST PML)
Harold Booth (NIST ITL)
Kevin J. Coakley (NIST ITL)
Shellee D. Dyer (NIST PML)
Thomas Gerrits (NIST PML)
Carson Hodge (NIST PML)
Michaela Iorga (NIST ITL)
John Kelsey (NIST ITL)
Adriana E. Lita (NIST PML)
Camilla Lambrocco (NIST PML)
Alan L. Migdall (NIST PML)
Richard P. Mirin (NIST PML)
Murugiah Souppaya (NIST ITL)
Sae Woo Nam (NIST PML)
René Peralta (NIST ITL)
Andrew Rukhin (NIST ITL)
Lynden K. Shalm (NIST PML)
Martin J. Stevens (NIST PML)
Edward Tortorici (NIST PML)
Varun B. Verma (NIST PML)
Michael A. Wayne (NIST PML)
Carlos Abellán (Barcelona Inst. of Sci. and Tech.)
Waldimar Amaya (Barcelona Inst. of Sci. and Tech.)
Bradley G. Christensen (University of Illinois)
William H. Farr (Jet Propulsion Laboratory)
Michael Fischer (Yale University)
Deny R. Hamel (University of Moncton)
Thomas Jennewein (University of Waterloo)
Daniel R. Kumor University of Illinois)
Paul G. Kwiat (University of Illinois)

Francesco Marsili (Jet Propulsion Laboratory)
Evan Meyer-Scott (University of Waterloo)
Morgan W. Mitchell (Barcelona Inst. of Sci. and Tech.)
Valerio Pruneri (Barcelona Inst. of Sci. and Tech.)
Matthew D. Shaw (Jet Propulsion Laboratory)
Jeffrey A. Stern (Jet Propulsion Laboratory)
Yanbao Zhang (University of Waterloo)

Before the invention of quantum theory, theories of physics obeyed the principle of local realism. In theories that obey realism, all possible measurement results are determined and fixed before the measurement occurs, though that result might be random and hidden. In local realistic theories, the hidden measurement results cannot be communicated between entities faster than the speed of light. The principle of local realism constrains the probability distributions that can be produced by local realistic systems. In 1964, John S. Bell described those constraints with a system of inequalities involving probabilities of measurement outcomes.

ACMD researchers have studied the properties of this system of inequalities, describing any system that violates an inequality as a mixture of a small set of deterministic local realistic distributions and a single maximally violating distribution [1]. Bell also showed that some entangled quantum systems can violate these inequalities, so quantum physics does not obey local realism. During the last 50 years, various experiments have demonstrated violation of Bell's inequalities, but all previous experiments have suffered from loopholes that would allow local realistic systems to appear to violate Bell's inequalities.

This year, ACMD researchers participated in a NIST led team that achieved a loophole-free test of local realism [2]. The experiment required generation of high fidelity entangled photon pairs, distributing each photon in opposite directions to its own detector system located approximately 100 meters from the source, featuring fast switching between polarization measurements and high efficiency detection. To ensure that communication between the measurement stations is impossible, measurements choices were made, photons detected, and measurements recorded in less than 400 ns. ACMD developed statistical analysis techniques with which *p*-values (measures of statistical evidence) for local realism were computed. P-values as small as 2.3×10^{-7} were reported, constituting a rejection of local realism with very high statistical significance.

In 2006 it was discovered that Bell tests could be used to generate random bits for cryptographic applications in a device-independent secure manner [3]. This means that, given a secure random seed, trust in the unpredictability of the secure string of bits can be derived solely from the outcomes of the Bell experiment, without needing to trust the internal workings of the hardware, even under the most pessimistic assumption that the hardware was provided by an untrustworthy adversary.

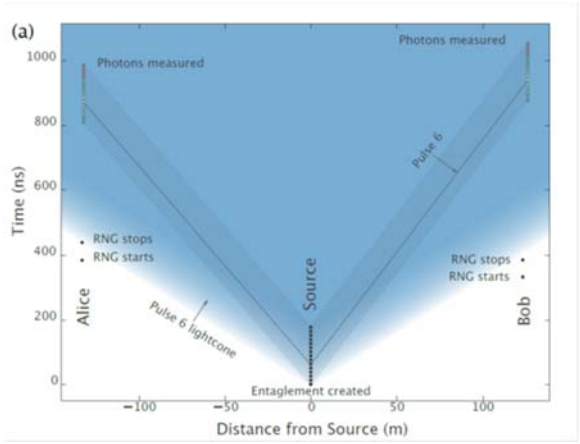

Figure 45. *Spacetime diagram of test of local realism. An entangled photon pair is created at the source, and each photon is sent to measurement stations ≈120 m from the source. Measurement choices are made by random number generators (RNG) at each measurement location. The separation of measurement stations ensures that no signal traveling at light speed from the source can influence a measurement and no light speed signal traveling from one station's RNG can influence the other station's measurement result.*

Potential future work at NIST includes doing the necessary engineering to develop the Bell test technology used in [2] into a reliable device that can be operated continuously for long periods without human oversight. Such a device could be integrated into the NIST Randomness Beacon[37], a cryptographic service currently being run by the ITL Computer Security Division using conventional hardware random bit generators. Some of the necessary tools for randomness production using Bell tests, such as randomness extraction software for postprocessing the experimental data, have already been developed as part of this project.

The NIST Beacon posts bit-strings in blocks of 512 bits every 60 seconds. Each such value is time-stamped and signed, and includes the hash of the previous value to chain the sequence of values together. This prevents all parties, even the source, from retroactively changing an output packet without being detected. The NIST Beacon keeps all output packets. At any point in time, the full history of outputs is available to users. These features ensure that the Beacon-generated numbers cannot be predicted before they are published and a user application can prove to anybody that it used truly random numbers not known before a certain point in time. Furthermore, this proof can be presented offline and at any point in the future. A number of beacon-based cryptographic protocols for e-commerce and privacy

[37] http://www.nist.gov/itl/csd/ct/nist_beacon.cfm

protection have been proposed in the cryptographic theory literature. These can now be put into practice using the NIST Beacon.

As of this writing, the NIST Beacon has been functioning without interruption for more than two years. The current generation beacon achieves (conventional, device-dependent) security using two independent, commercially available sources of randomness, each with an independent hardware entropy source and NIST Special Publication 800-90 approved components. NIST encourages the community at large to research and publish novel ways in which this tool can be used. A few examples of applications are unpredictable sampling, new authentication mechanisms, and secure multi-party computation.

[1] P. Bierhorst, Geometric Decompositions of Bell Polytopes with Practical Applications, arXiv:1511.04127 (2015).

[2] L. K. Shalm, E. Meyer-Scott, B. G. Christensen, P. Bierhorst, M. A. Wayne, M. J. Stevens, T. Gerrits, S. Glancy, D. R. Hamel, M. S. Allman, K. J. Coakley, S. D. Dyer, C. Hodge, A. E. Lita, V. B. Verma, C. Lambrocco, E. Tortorici, A. L. Migdall, Y. Zhang, D. R. Kumor, W. H. Farr, F. Marsili, M. D. Shaw, J. A. Stern, C. Abellán, W. Amaya, V. Pruneri, T. Jennewein, M. W. Mitchell, P. G. Kwiat, J. C. Bienfang, R. P. Mirin, E. Knill and S. W. Nam, A Strong Loophole-free Test of Local Realism, *Physical Review Letters* **115** (2015) 250402.

[3] R. Colbeck, Quantum and Relativistic Protocols for Secure Multiparty Computation, PhD Thesis, University of Cambridge, arXiv:0911.3814 (2006).

Performance of Adiabatic Optimization Algorithms

Stephen Jordan
Michael Jarret (University of Maryland)

It is firmly established that quantum computers, if built, could factor integers and simulate the dynamics of quantum many-body systems exponentially faster than conventional, classical computers. More recently, there has been much interest in applying quantum computers to a wide variety of optimization problems, ranging from job shop scheduling to machine learning. Such algorithms could be run on general-purpose digital quantum computers, or they could be run on specialized hardware such as is being developed by D-Wave Systems. However, the idea that quantum computers may offer an advantage for optimization problems presently rests on extremely shaky theoretical foundations.

Most of the research into quantum optimization focuses on adiabatic quantum computation. This is a scheme, somewhat similar in spirit to simulated annealing, in which the solutions to combinatorial optimization problems are encoded into the low energy states of a physical system. The only rigorously established upper bound on the runtime of quantum adiabatic optimization algorithms scales as one over the square of the gap between the smallest and second-smallest eigenvalues of the system's Hamiltonian.

The Hamiltonian of a system with n qubits is a $2^n \times 2^n$ matrix. Thus, numerically computing the eigenvalues becomes very rapidly intractable. In this project, we seek to develop mathematical tools for proving rigorous analytic bounds on the eigenvalue gaps of Hamiltonians with the ultimate goal of gaining a better understanding as to which optimization problems, if any, are amenable to faster solution by quantum adiabatic computation.

Over the past year we have adapted powerful new mathematical techniques from the theory of differential operators to the context of the discrete Hamiltonians relevant to quantum adiabatic optimization. In 2011, Andrews and Clutterbuck developed a new method for analyzing the spectrum of differential operators using the heat equation, and using this method proved the "fundamental gap conjecture." Proving this conjecture had been an open problem for more than twenty years. We have now developed a discrete analogue to this method and applied it to some example problems. While we have not yet obtained results directly applicable to the analysis of adiabatic optimization algorithms for computational problems of practical interest, we believe the introduction of these powerful mathematical techniques to this topic represents a first step toward understanding the performance of these algorithms.

[1] M. Jarret and S. P. Jordan, Modulus of Continuity Eigenvalue Bounds for Homogeneous Graphs and Convex Subgraphs with Applications to Quantum Hamiltonians, arXiv:1506.08475 (2015).

Computational Complexity of Quantum Field Theory

Stephen Jordan
Keith Lee (University of Toronto)
John Preskill (Caltech)
Hari Krovi (BBN)

Quantum field theory is needed to describe relativistic quantum systems, and forms the basis for theoretical particle physics. Unfortunately, quantum field theory is notoriously difficult to simulate. Millions of CPU hours per year are spent on simulations of quantum field theories in order to yield better understanding of nuclear physics and make predictions to compare against experimental results from particle accelerators. However, for strongly coupled quantum field theories such as quantum chromodynamics (QCD), which describes nuclei, no tractable method is known for computing dynamical

quantities such as scattering probabilities. Instead, computations are limited to static quantities such as mass ratios of composite particles.

It is natural to ask whether the lack of efficient methods for computing dynamical quantities in quantum field theories is due to a fundamental barrier, or whether we simply haven't discovered the right algorithm yet. In recent work, we have shown that, in certain regimes, there are fundamental barriers to the efficient computation of dynamical quantities in quantum field theories, which are unlikely ever to be overcome by conventional supercomputers. To show that quantum field theories are hard to simulate, we have devised a method by which arbitrary quantum computations can be encoded into the outcomes of scattering processes in quantum field theories. Thus, if the outcomes of these scattering processes could be efficiently computed by conventional computers, this would allow classical computers to efficiently compute the outcomes of all quantum computations.

There is a lot of mathematical evidence that classical and quantum computation are not equivalent. In particular, there are several problems that quantum computers can solve in polynomial time, such as integer factorization, which are not believed to be solvable in polynomial time by classical computers. This and other evidence has led to a widely-believed mathematical conjecture, known as BQP≠P, which states that the set of problems solvable in polynomial time by a quantum computer is strictly larger than the set of problems solvable in polynomial time by a classical computer. (Note that this is a strictly mathematical statement about idealized models of computation, independent of the practical construction of quantum computers.) Thus, assuming the BQP≠P conjecture, our encoding implies that efficient classical algorithms do not exist for certain problems regarding scattering in quantum field theories; the problem is not merely that we haven't discovered such algorithms. Interestingly, these difficulties arise even for very simple quantum field theories involving a single species of particles in only one spatial dimension.

[1] S. P. Jordan, H. Krovi, K. S. M. Lee and J. Preskill. BQP-completeness of Scattering in Scalar Quantum Field Theory, in preparation.

Knot Theory and Quantum Physics

Stephen Jordan
Gorjan Alagic (University of Copenhagen)
Michael Jarret (University of Maryland)

In topology, a knot is an embedding of the circle into three dimensional space. If one knot can be smoothly transformed into another without any cutting and regluing of the string, then the knots are said to be equivalent. Deciding equivalence of knots is the central problem in computational knot theory. No efficient (i.e., polynomial-time) algorithm is known for this problem. A partial solution is given by knot invariants. These are functions that take knots as inputs, and produce as output some easy-to-distinguish objects such as numbers or polynomials. For such a function to be a knot invariant, equivalent knots taken as input must produce identical outputs. The definition does not require distinct knots to produce distinct outputs. A knot invariant that takes the same value on all knots is said to be trivial, and an invariant that takes distinct values on all distinct knots is said to be complete. Known knot invariants lie at various places between these extremes.

Remarkably, many of the strongest knot invariants arise within quantum physics. In particular, solutions to the Yang-Baxter equation, which arose originally in statistical and quantum physics, can be used to construct many of the most important knot invariants, including both the Alexander and Jones polynomials. The solutions to the Yang-Baxter equation are matrices, which may be interpreted as quantum logic gates with two inputs and two outputs. We recently proved that, for the resulting knot invariant to be nontrivial, it is necessary that the corresponding quantum gate generate quantum entanglement. Thus we find an intriguing connection between quantum entanglement and topological entanglement, which remains to be further explored.

[1] G. Alagic, M. Jarret and S. P. Jordan. Yang-Baxter Operators Need Quantum Entanglement to Distinguish Knots, *Journal of Physics A*, to appear. [arXiv:1507.05979]

One-Time Programs Using Isolated Qubits

Yi-Kai Liu

One-time programs are a class of tamper-resistant computing devices, which have applications in cryptography and computer security. Essentially, a one-time program is a computer program that can run once, and then stops working. One-time programs can be used to restrict access to information that is under the physical control of an adversary such as personal information stored on a smartphone that has been subsequently lost or stolen.

In previous work, we showed that a key component of a one-time program, called a one-time memory, can be constructed using certain kinds of quantum systems, called isolated qubits. Isolated qubits are qubits that can be accessed individually, but cannot be entangled.

We are working to extend this result in various ways. First, we would like to construct one-time programs (not just one-time memories) from isolated qubits, and prove that they are secure. We have taken one step in this direction, by developing privacy amplification techniques that work for one-time memories

based on isolated qubits [1]. Crucially, these techniques are non-interactive, as required for tamper-resistant hardware.

The next step will be to show that our one-time memories can be composed securely. This is a difficult open problem, as it involves parallel (not sequential) composition in the isolated qubits model. In addition, we are studying quantum protocols for other cryptographic tasks, such as password-based identification, which might also be achievable in the isolated qubits model.

Finally, we are studying possible experimental implementations of isolated qubits. Solid-state nuclear spins are one attractive option, as they can be engineered so that they have long coherence times, while making it difficult to perform entangling gates. In addition, it may be possible to demonstrate one-time memories using other physical systems, such as trapped ions or semiconductor quantum dots, albeit with weaker security guarantees.

[1] Y.-K. Liu, Privacy Amplification in the Isolated Qubits Model, in *Advances in Cryptology – EUROCRYPT 2015*, Sofia, Bulgaria, April 26-30, 2015, 785-814.

Post-Quantum Cryptography

Stephen Jordan
Yi-Kai Liu
Lily Chen (NIST ITL)
Dustin Moody (NIST ITL)
Rene Peralta (NIST ITL)
Ray Perlner (NIST ITL)
Daniel Smith-Tone (NIST ITL)

Public-key cryptography is a fundamental building block of the Internet today. It is an essential technology for electronic commerce and cybersecurity. However, the development of quantum computers poses a potential threat to the security of the public-key cryptosystems we use today. Thus, it is desirable to develop and deploy new cryptosystems that will be secure against quantum attacks, well before any large quantum computers are built.

ACMD is collaborating with the ITL Computer Security Division on several aspects of this problem. First, we are reviewing ongoing research on quantum algorithms and quantum cryptanalysis [1]. It is well known that Shor's algorithm can factor integers and compute discrete logarithms in polynomial time, thus breaking the RSA cryptosystem, Diffie-Hellman key exchange, and elliptic curve cryptography. However, further research is needed to understand the power of quantum computers to solve other hard problems of interest to cryptography, such as finding short vectors in high-dimensional lattices, solving multivariate quadratic systems of equations, and computing isogenies of elliptic curves.

In addition, we are studying different theoretical techniques for modeling a quantum adversary when proving the security of a cryptographic protocol. In most previous security proofs, only classical adversaries are considered. Models that allow quantum adversaries, such as the quantum random oracle model, are not as well understood.

We are also reviewing ongoing progress in experimental implementations of quantum computers, using technologies such as ion traps and superconducting qubits. There have been some predictions that cryptographically-relevant quantum computers could be built by the year 2031 [2]. This informs our planning for when new post-quantum cryptosystems need to be deployed.

Finally, we are contributing to ongoing research on quantum-resistant public-key cryptosystems, including schemes based on lattices, error-correcting codes, multivariate systems of polynomial equations, and one-time hash-based signatures. Many of these schemes look quite promising, but they still have drawbacks with regard to security, efficiency and usability. NIST researchers have contributed several new results in this area [3-5].

NIST is also taking concrete steps towards standardizing post-quantum cryptography. In the past year we have engaged with the broader community, including industry, academic and government organizations. In April 2015 we organized a workshop on *Cybersecurity in a Post-Quantum World*[38], and in September 2015 we participated in discussions at a Dagstuhl workshop on *Quantum Cryptanalysis*. We have also collaborated with the Joint Center for Quantum Information and Computer Science (QuICS) at the University of Maryland.

Presently, we are in the process of writing a short report describing the current status of post-quantum cryptography, and we are making plans for an open and public process for developing standards in this area. Members of our team will discuss these plans at the Post Quantum Cryptography (PQCrypto) conference in February 2016.

[1] S. Jordan, Quantum Algorithm Zoo, http://math.nist.gov/quantum/zoo/.

[2] M. Mosca, Cybersecurity in an Era with Quantum Computers: Will We Be Ready? Cryptology ePrint Archive, Report 2015/1075, International Association for Cryptologic Research.

[38] http://www.nist.gov/itl/csd/ct/post-quantum-crypto-workshop-2015.cfm

[3] D. Moody and R. Perlner, Vulnerabilities of "McEliece in the World of Escher," *PQCrypto 2016*, Fukuoka, Japan, February 2016, to appear.

[4] R. Cartor, R. Gipson, D. Smith-Tone and J. Vates, On the Differential Security of the HFEv- Signature Primitive, *PQCrypto 2016*, Fukuoka, Japan, February 2016, to appear.

[5] R. Perlner and D. Smith-Tone, Security Analysis and Key Modification for ZHFE, *PQCrypto 2016*, Fukuoka, Japan, February 2016, to appear.

High-Speed Error Correction Codes for Quantum Key Distribution

Alan Mink
Anastase Nakassis (NIST ITL)

Quantum information science incorporates quantum mechanics into information technology. It is an emerging field thought to have the potential to cause revolutionary advances. One promising early area is quantum cryptography, specifically quantum key distribution (QKD), which is a protocol that uses a pair of unsecured communication channels, a quantum channel, and a classical channel, to establish a shared secret between two parties, Alice and Bob. This shared secret is then used to encrypt messages between Bob and Alice. QKD has been proven information theoretically secure, unlike classical key distribution which relies on computational complexity.

There are four stages to the QKD protocol. The first stage involves quantum mechanics, the other three are classical processing. Stage 1 is the transmission of randomly encoded single photons over a lossy quantum channel to be measured by Bob to form the initial raw random sequence. Stage 2 is where Alice and Bob exchange information over the classical channel to "sift" their bit sequences to achieve a common sequence. But, that sequence may have errors. Stage 3 is where Alice and Bob exchange information over the classical channel to correct errors between their bit sequences without exposing the value of their bits. Finally, Stage 4 is where Alice and Bob privacy amplify their now identical bit sequences through the application of a hash function to eliminate any leaked information, yielding a smaller set of secret bits between Alice and Bob. The last two stages are referred to as post-processing.

There is a large body of information about error correction (EC) codes, but QKD presents a different environment than conventional communication. For example, expected QKD error rates (1 % to 11 % vs. 0.1 % or below) are higher, error correction information is sent separately over an error free channel, the amount of information that the EC code leaks about the data must be minimized and, in particular, kept below a given limit to extract a secret, and quantum data retransmission is not possible.

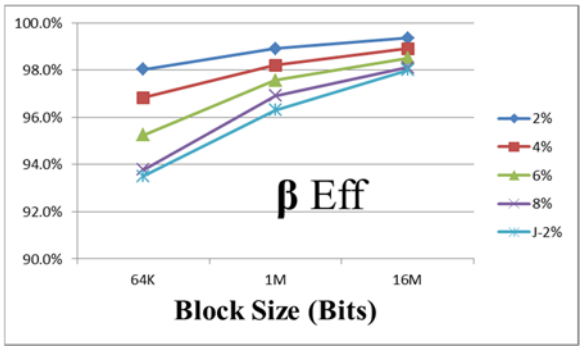

Figure 46. *Polar code β efficiency as a function of block size.*

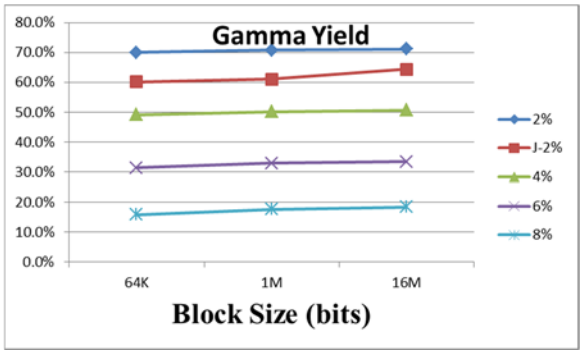

Figure 47. *QKD secure (Gamma) yield as a function of block size.*

Our previous work has focused on high speed QKD reconciliation and we have obtained a processing rate of up to 200 Mbit/s for low density parity check (LDPC) one-way EC algorithms [1] implemented on a single GPU. Our more recent work has focused on polar EC codes and how they can be adapted to QKD protocols [2]. While investigating efficient approaches to designing polar codes we developed an interactive version of a successive cancellation polar decoder that yielded significantly better EC performance. This was obtained by improvement in the frame error rate (FER), which is the code failure rate, and in its Shannon efficiency. An additional benefit of our interactive algorithm is that it eliminates the need for an initial code design (i.e., the selection of a predefined frozen bit set) since the algorithm decides what information is needed as it decodes. The downside of such an interactive code is the added communication overhead, although parallel and efficient implementations may limit the impact of this overhead. Moreover, QKD environments that don't require high speed reconciliation are appropriate applications, such as satellite QKD where the post-processing time period is much longer than the quantum exchange period.

Our error correction performance yields FERs of less than 10^{-4} compared to 1 % to 10 % as reported in the QKD literature. Our Shannon efficiency results are also

better as shown in Figure 46, where the top curve (2 %) is comparable to the bottom curve (J-2 %). The percentages in the legend refer to quantum bit error rate (QBER), so the 2 % curve refers to the results for a 2 % QBER. Furthermore, the QKD secure yield, where p=QBER, is defined as

$$\text{Gamma yield} = (1\text{-FER})(\beta(1-h(p)) - h(p)),$$

is a metric normalized across code block sizes, resulting in the fraction of secure bits extractable from the initial total. Figure 47 shows the improved overall QKD performance (Gamma yield) resulting from using our interactive polar decoder algorithm compared to the literature. The top curve (2 %) is comparable to the second curve (J-2 %).

[1] A. Mink and A. Nakassis, LDPC Error Correction for Gbit/s QKD, in *Proceedings of the SPIE: Defense Security and Sensing* **9123**, Baltimore, MD, May 2014.

[2] A. Nakassis and A. Mink, Polar Codes in a QKD Environment, in *Proceedings of the SPIE: Defense Security and Sensing* **9123**, Baltimore, MD, May 2014.

Towards a Quantum Repeater

Xiao Tang
Oliver Slattery
Lijun Ma
Paulina Kuo
Barry Hershman
Alan Mink

Future quantum computers will efficiently solve certain problems that cannot be solved with even the most powerful classical computers. Just as classical computers are linked to form large-scale networks, so too will quantum computers be linked to form large-scale quantum networks. Single photons will carry information traveling in such networks. Quantum repeaters are needed to extend transmission distances beyond single links limited by unavoidable transmission losses. Such repeaters must maintain the fidelity of the quantum information carried by the photon. Although some essential components for a quantum repeater (such as quantum memory, narrow linewidth entangled photon sources, and frequency conversion between atomic and telecom wavelengths) have been demonstrated in principle, no practical quantum repeater has yet been implemented.

The quantum communication research project in ITL was established in 2000 as a part of a NIST-wide quantum key distribution (QKD) collaboration that resulted in the fastest QKD systems in the world at that time, as well as the demonstration of a 3-node QKD network [1]. The team then developed novel single photon frequency conversion systems based on engineered nonlinear materials. These systems can be used, in principle, for entangled photon pair generation, single photon detection and as an interface between the wavelengths of transmission and storage, which are essential components for quantum repeaters [2].

In FY 2015 we extended this work, focusing on the quantum memory and entangled photon pair sources suitable for a future quantum repeater. In particular, we studied quantum memories based on electromagnetically-induced transparency (EIT), and narrow linewidth photon sources, including those at 894.6 nm and 1310 nm, as well as a polarization entangled photon source near 1550 nm.

Quantum memory is a key component in the implementation of quantum repeaters for quantum communications and quantum networks. We have demonstrated an EIT quantum memory scheme in a warm cesium (Cs) atomic vapor cell. The Cs D1 line at 894.6 nm corresponds to photon pairs (895 nm and 1310 nm) generated by our spontaneous parametric down conversion (SPDC) source. An EIT quantum memory with Cs atomic vapor provides an inexpensive and scalable scheme for quantum repeaters. Our preliminary results show photon state storage and retrieval efficiency to be similar to that of quantum memories of other groups [3]. This will provide the basis for further experiments on quantum communication, such as photon interference with quantum memory. We have reduced the noise level in our system to a level where we can do single-photon-level experiments. We expect this noise performance to be further improved, with less noise corresponding to higher fidelity of the quantum system.

Another ingredient necessary for a quantum repeater is a special entangled photon pair source. To ensure high transmission efficiency, the wavelength of one photon should be in the low-loss telecommunication band (1310 nm in our case), and the other photon should match an atomic system of the quantum memory, in terms of both linewidth and wavelength. For example, the quantum memory we developed this year works at the Cs D1 transition (around 894.6 nm), and has sub-MHz operating bandwidth. The development of such a photon source is a very challenging task because (1) the required photon bandwidth is extremely narrow; (2) its central wavelength must be locked on the atomic transition line for long term stabilization; and (3) the wavelengths of the two photons in a pair are far apart.

In FY 2015, we demonstrated a photon pair source at 1310 and 894.6 nm with a linewidth of 28 MHz. The wavelength at 894.6 nm is locked on the Cs D1 line for long term stabilization. Figure 48 shows a part of our experimental setup. The detailed results have been published [4]. However, a linewidth of 28 MHz is still broad relative to the desired range of a few MHz or even sub MHz. To address this, we have initiated another experiment, in which a micro-toroid with an ultra-high quality factor will be used to generate photon pairs based on a third-order nonlinear effect, so called spontaneous four-

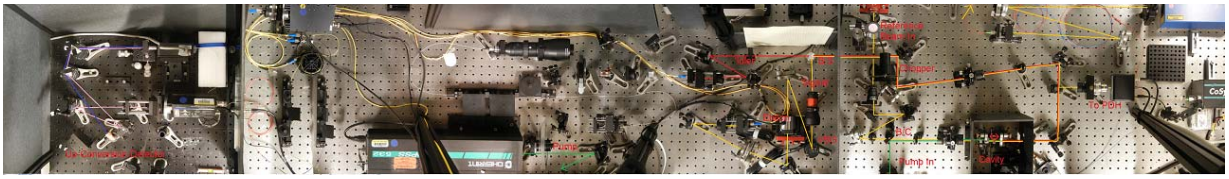

Figure 48. *Experimental setup for quantum repeater development.*

wave mixing (SFWM). The micro-toroid, developed at Washington University in St. Louis, is a very promising configuration due to its small mode volume and ultra-high quality factor.

The team has also been developing a polarization-entangled photon pair source near 1550 nm by using a domain-engineered, type-II, periodically poled nonlinear crystal combined with a 775 nm pump. Preliminary results were reported in [5]. This source will serve as a testbed for studying polarization entanglement visibility and the effects of spectral and temporal distinguishability. We are also working on devices for low-noise quantum frequency upconversion of 1550 nm photons that can be used to characterize and manipulate the 1550 nm entangled photon source. We envision the source for future use in a quantum repeater and in random number generation based on the violation of Bell's inequality.

In FY 2015, the team also worked on a few additional tasks.

- One of our team members participated in the worldwide standardization activity for QKD coordinated by the European Telecommunications Standards Institute (ETSI) QKD industry specification group (ISG). The activities were reported at a workshop in December 2014 [6].
- In recent years, diamond based single photon sources have shown great potential for quantum information science and technology applications. In FY 2015, we observed single photon emitting spectra from various defect centers, including nitrogen vacancies, silicon vacancies and Ni-doped defects in diamond films by using a confocal microscope built in our lab. The team also initiated a related collaboration with the Center for Integrated Quantum Materials at Howard University. This initial study may open up new opportunities for our future research.

[1] L. Ma, A. Mink and X. Tang, High Speed Quantum Key Distribution over Optical Fiber Network System, *Journal of Research of the National Institute of Standards and Technology* **114**:3 (2009), 149.

[2] L. Ma, O. Slattery and X. Tang, Single Photon Frequency Up-conversion and its Applications, *Physics Reports* **521**:2 (2012), 69-94.

[3] L. Ma, O. Slattery, P. Kuo and X. Tang, EIT Quantum Memory with Cs Atomic Vapor for Quantum Communication, *Proceedings of the of SPIE* **9615** (2015), 96150D–1.

[4] O. Slattery, L. Ma, P. Kuo, and X. Tang, Narrow-Linewidth Source of Greatly Non-Degenerate Photon Pairs for Quantum Repeaters from a Short Singly Resonant Cavity, *Applied Physics B* **121** (2015), 413-419.

[5] P. Kuo, J. Pelc, O. Slattery, L. Ma and X. Tang, "Domain-engineered PPLN for Generation of Polarization-entangled Photons," *SPIE Photonics West*, 9377-34, San Francisco, CA, February 7-12, 2015.

[6] R. Alléaume, T. Chapuran, C. Chunnilall, I. Degiovanni, N. Lutkenhaus, V. Martin, A. Mink, M. Peev, M. Lucamarini, M. Ward and A. Shields, Worldwide Standardization Activity for Quantum Key Distribution, in *Proceedings of the IEEE GlobeCom Workshop on Telecomm Standards – From Research to Standards*, Austin, TX, December 8 ,2014, 741-746.

Joint Center for Quantum Information and Computer Science

Dianne P. O'Leary
Ronald F. Boisvert
Jacob Taylor (NIST PML)
Carl Williams (NIST PML)
Andrew Childs (University of Maryland)

https://quics.umd.edu/

NIST and the University of Maryland (UMD), with the support and participation of the Research Directorate of the National Security Agency/Central Security Service (NSA/CSS), inaugurated a new joint venture, The Joint Center for Quantum Information and Computer Science (QuICS) on October 31, 2014. Scientists at the center will conduct basic research to understand how quantum systems can be effectively used to store, transport and process information.

The new center complements the fundamental quantum research performed at the Joint Quantum Institute (JQI), which was established in 2006 by UMD, NIST and the NSA. Focusing on one of JQI's original objectives, to fully understand quantum information, QuICS will bring together computer scientists—who have expertise in algorithm and computational complexity theory and computer architecture—with quantum information scientists and communications scientists. In particular, the center will bring together researchers from the University of Maryland Institute for Advanced

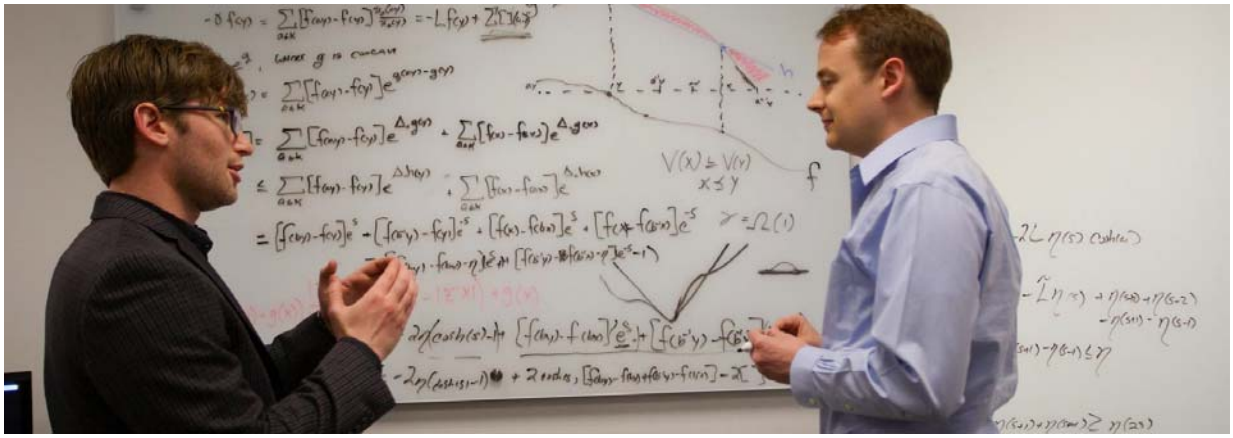

Figure 49. *Michael Jarrett (left), a doctoral student at the University of Maryland, is the recipient of the first Booz Allen Hamilton Quantum Information Fellowship at QuICS. Jarrett is working with QuICS Fellow, and ACMD researcher, Stephen Jordan (right) to understand the computational power of quantum adiabatic optimization algorithms.* *(See page 71.)*

Computer Studies (UMIACS); the UMD Departments of Physics and Computer Science with NIST's Information Technology and Physical Measurement Laboratories. An orientation for QuICS stakeholders, held on Feb. 9, 2015, was attended by some 30 staff members from UMD, NIST and the NSA.

Some of the topics QuICS researchers will initially examine include understanding how quantum mechanics informs computation and communication theories, determining what insights computer science can shed on quantum computing, investigating the consequences of quantum information theory for fundamental physics, and developing practical applications for theoretical advances in quantum computation and communication.

QuICS is also expected to train scientists for future industrial and academic opportunities and provide U.S. industry with cutting-edge research results. By combining the strengths of UMD and NIST, it is hoped that QuICS will become an international center for excellence in quantum computer and information science.

Dianne O'Leary, a Professor of Computer Science at UMD and a long-time faculty appointee in ACMD, served as a founding Director of QuICS, along with Jacob Taylor of the NIST PML. Andrew Childs, a recent hire at UMD, took over as Co-Director upon O'Leary's recent retirement. Stephen Jordan and Yi-Kai Liu, both of ACMD, have been named QuICS Fellows.

QuICS has quickly established itself as a substantial research presence in quantum information science. Two postdocs given the distinction of Hartree Postdoctoral Fellows, as well as two additional outstanding postdoctoral researchers, also began their tenures in the fall of 2014. QuICS Fellows have recruited a total of 11 graduate students into the Center. The Center has also developed a robust visitor program, with more than 50 external speakers presenting in the QuICS Seminar series since October 2014. On September 28 – October 2, 2015 QuICS hosted a Workshop on the Frontiers of Quantum Information and Computer Science. The workshop featured 24 lectures by leading quantum information researchers including Seth Lloyd, Edward Farhi and Scott Aaronson (MIT) and Daniel Gottesman (Perimeter Institute), as well as a poster session with more than 30 contributed posters. QuICS has also been selected as the host of the 6th International Conference on Quantum Cryptography to be held in Washington, DC on September 12-16, 2016. QuICS Fellow and ACMD researcher Yi-Kai Liu is the lead local organizer of the event and Chair of its international Steering Committee.

The technical work of QuICS has also seen a strong start, with 65 papers released in calendar year 2015 alone. QuICS has indeed made an impressive start.

Foundations of Measurement Science for Information Systems

Modern information systems are astounding in their complexity. Software applications are built from thousands of interacting components. Computer networks interconnect millions of independently operating nodes. Large-scale networked applications provide the basis for services of national scope, such as financial transactions and power distribution. In spite of our increasing reliance on such systems, our ability to build far outpaces our ability to secure. Protocols controlling the behavior of individual nodes lead to unexpected macroscopic behavior. Local power anomalies propagate in unexpected ways leading to large-scale outages. Computer system vulnerabilities are exploited in viral attacks resulting in widespread loss of data and system availability. The actual resilience of our critical infrastructure is simply unknown. Measurement science has long provided a basis for the understanding and control of physical systems. Such deep understanding and insight is lacking for complex information systems. We seek to develop the mathematical foundations needed for a true measurement science for complex networked information systems.

Graph Theoretic Applications to Network Security and Security Metrics

Assane Gueye
Richard J. La
Peter Mell (NIST ITL)
Rich Harang (Army Research Laboratory)
Desire Banse (NIST ITL)
Yannick Congo

In this project, we have identified and proposed graph-theoretic metrics to quantify the resilience of network topologies under an adversarial environment. Using these metrics, we have considered three application problems:

1. Resilience of the internet over time,
2. Defense-in-depth approach for IPv6 network, and
3. Connectivity of the African network.

Internet Resilience. The apparent robustness of Internet networking hides underlying weaknesses. In this work, using data available from the Center for Applied Internet Data Analysis (CAIDA), we have revealed a class of such weaknesses in the form of the ability of colluding countries to deliberately filter out other countries.

We analyzed the ability of a group of countries to disconnect two other countries, to isolate a set of countries from the Internet, or to break the Internet into non-communicative clusters. We find that, despite the potential for these attacks, the Internet as a whole has become increasingly resilient over the period of examination from 2008 to 2013. However, the gains in robustness and resilience were primarily concentrated in well-connected countries, which form a very resilient core. We found that less connected countries formed new links largely with well-connected countries, and not to each other, maintaining the centrality of the well-connected countries in the paths between the less connected countries on the fringe. Because of this, the resilience of these less connected countries did not increase significantly over the time period studied. The result is that a small set of countries is able to isolate significant portions of the Internet or to divide it up into clusters. Individual well connected countries are often able to unilaterally isolate network-dependent neighbors.

These weaknesses could be addressed through a focus on establishing links between poorly connected countries (e.g., through grants to poorer countries or through collaboration between coalitions of physically adjacent countries). This would move the poorly connected countries away from dependence on the infrastructure of the more highly connected countries. It would also move the Internet as a whole towards a more resilient architecture through the provision of alternate geographically diverse pathways.

Defense-in-Depth. Networks securely configured with Internet Protocol version 6 can be made resistant to network scanning, forcing attackers to propagate along existing benign communication paths. We leverage this limitation of attacker movements to propose a chokepoint-based defensive approach in which heightened security measures are deployed on a selected group of chokepoint hosts in order to constrain attacker propagation. Chokepoints are chosen such that, together, they connect small isolated clusters of the communication graph. Hence, attackers attempting to propagate through the network are limited to a small set of potential targets or have to penetrate one or more chokepoints.

To choose the chokepoints, we consider two metrics to optimize: (i) minimizing the maximal cluster size and (ii) maximizing the mean of the minimum number of chokepoints that lie between pairs of nodes. The former metric aims to constrain the attacker to as small a cluster as possible, and the second seeks to maximize the number of chokepoints that an attacker must penetrate on average in order to reach a particular high-value network target. The optimal placement of such chokepoints is an

NP-hard problem and, as a consequence, we have used a set of heuristics to approximate the solution. We have tested our approach and algorithms using the data from a large operational network consisting of over 15500 nodes. Our experiments have shown that enhanced security solutions have to be deployed to only 0.65 % of the nodes to limit the propagation of a random attack to less than 15 % of the nodes in the network. Thus, our approach enables a novel defense-in-depth approach that complements traditional security approaches.

African Connectivity. The development of the African Internet has lagged behind more developed continents. However, in the period from 2010 to 2014, significant growth has been observed. In this study, we use data available from CAIDA to measure and document the growth of Internet connectivity in Africa from 2010 to 2014 with a focus on inter-country relationships. We evaluate both intra-continent connectivity as well as connectivity to other continents. An initial analysis reveals a modest increase in the number of participating countries but an explosive increase in the number of routers and network links. We then form the first country level topology maps of the African Internet and evaluate the robustness of the network. This includes a study of raw connectivity, pairwise shortest paths, and betweeness centrality. We then suggest how improvements can be made to the inter-country African connectivity to enhance its robustness without reliance on paths traversing multiple continents.

At a deeper level, our connectivity metrics also reveal a highly scale free nature in the country to country Africa connectivity graph. There are many countries of low degree and a few of high degree. There is a negative assortativity whereby the low degree nodes tend to connect to the high degree nodes and not to each other. The connectivity within the center of Africa tends to be low. The problem with this model is that it is susceptible to node failure. The majority of African countries are dependent upon just a few other African countries for their intra-continental Internet access. However, we have seen that judicious placement of additional links can reduce the fragility induced by the scale free nature. In particular, links among the low degree nodes are needed. This translates into the need for direct Internet links between countries with less Internet infrastructure in order to make the African Internet stronger as a whole.

[1] A. Gueye, P. Mell, R. Harang and R. La, Defensive Resource Allocations with Security Chokepoints in High-risk IPv6 Networks, in *Lecture Notes in Computer Science* **9149** (2015), Data and Applications Security and Privacy XXIX, Springer, 261-276.

[2] P. Mell, R. Harang and A. Gueye, Measuring Limits on the Ability of Colluding Countries to Partition the Internet, *International Journal of Computer Science: Theory and Application* **3**:3 (2015), 60-73.

[3] P. Mell, R. Harang and A. Gueye, The Resilience of the Internet to Colluding Country Induced Connectivity Disruptions, in review.

[4] A. Gueye, P. Mell, D. Banse and Y. Congo, On the Internet Connectivity in Africa, in review.

[5] P. Mell, R. Harang and A. Gueye, Linear Time Vertex Partitioning on Massive Graphs, in review.

A Game Theoretic Model of Zero-Day Attack Propagation

Assane Gueye
Richard J. La
Peter Mell (NIST ITL)

The goal of this project is to understand the progress of an attacker inside a network, who can use both known exploits as well as zero-day exploits. The network is protected by a defender (and a defense system) which aims to prevent the attacker from reaching a high-value target inside the network. Both the attacker and the defender have only partial information/observation about their interaction and the progress of the attack. We use a Markov Decision (MD) process approach to model the attacker and defender's dynamic decision making and use a stochastic game model to study their interaction.

Partial results of our study show that an optimal strategy for the attacker is a threshold policy in which the attacker starts by using zero-day exploits until it achieves a certain level of success or reaches some point along the attack and switches to known exploits to complete the attack. For the defender, our numerical analysis suggests that an optimal strategy is also a threshold policy that requires the defender to monitor the number of alarms generated by the defense systems (employed for known and unknown exploits). When the number of alarms is smaller than the threshold value, the defender keeps improving its defense systems. When the number of alarms exceeds the threshold, the defense performs a full system reset.

Our game-theoretic model can be used to enhance attack graph-based analysis. For instance, by using our attack process model, one can determine the most likely paths in the attack graph.

Security of Complex, Interdependent Systems

Richard J. La

Understanding the security of large, complex interconnected networks and systems has emerged as one of the key challenges information system engineers face today. Examining the system-level security of complex networks or systems is hindered by the fact that security measures adopted by various agents or organizations, or lack thereof, produce either positive or negative network externalities on others, leading to so-called *interdependent security* (IDS).

Many, if not most, of existing studies on IDS focus on how the infection of a few agents may spread to a large number of other agents through networks (e.g., computer networks or social networks). Furthermore, they mostly consider scenarios where the agents are passive in that their security measures are pre-selected independently of the perceived risks and threats. In many scenarios of interest, e.g., cybersecurity and disease outbreaks, however, agents can employ security measures that are best suited for their risks, including the likelihood of infection.

In the past two years, our efforts have been aimed at examining scenarios where nodes are strategic entities interested in optimizing their own objectives. We model the interdependence in security among agents, which is caused by network externalities, using a dependence graph. In this graph, the nodes/vertices are the agents/organizations and an edge between two vertices indicates interdependence between them. The goal of this project is to understand how the underlying network structure and properties affect the choices made by strategic agents and influence the network-level security.

In the first year, we focused on understanding how the (weighted) node degree distribution of the dependence graph shapes the security choices of strategic agents. To this end, we adopted population game models and their Nash equilibria as reasonable approximations to expected operating points. Our key finding was that as the weighted node degree distribution, where the weights are the degrees, becomes stochastically larger, the *local* security measured by the risks seen from a neighbor improves in that the average number of attacks propagating via a single edge decreases [1]. At the same time, somewhat surprisingly, the *global* network security measured by cascade probability, i.e., the likelihood that a single initial infection will lead to a large number of infected nodes over time, deteriorates [2]. Moreover, the price of anarchy, which measures the worst-case inefficiency of Nash equilibria with respect to the system optimum, increases as the weighted node degree distribution gets larger.

In the past year, we continued our efforts along two main directions. First, in our past studies, we assumed that the dependence graph was neutral, i.e., there is no correlation between the degrees of two interdependent nodes. It is well known that many natural and engineered networks exhibit non-negligible correlations in the degrees of end nodes. We investigated how *network mixing* or *assortativity* affects the network-level security with strategic agents [3]. Our finding suggests that the effects of assortativity are similar to those of the weighted node degree distribution studied in the first year. To be more precise, it is the effective node degree distribution seen by the nodes, which is determined by both the actual node degree distribution and network mixing, that shapes the security choices of the nodes.

Secondly, we investigated the issue of convergence to Nash equilibria. Many existing studies, including our previous studies, assume that the agents can reach a (pure-strategy) Nash equilibrium, and hence they focus on the properties of Nash equilibria. However, in many cases, including our own, it is not immediately clear how and/or when the agents will be able to arrive at Nash equilibria even when they can interact with each other many times. To this end, we examined the convergence to a Nash equilibrium when the agents adopt the well-known better-reply dynamics, i.e., when an agent finds at least one better reply that reduces its cost, it switches to one of the better replies. We showed that, in a large class of games called generalized weakly acyclic games, the better-reply dynamics ensure almost certain convergence to a Nash equilibrium, even when the agents revise their actions based on delayed, sometimes outdated, payoff information in an asynchronous manner [4, 5].

[1] R. J. La, Effects of Degree Distributions on Network Security and Internalization of Externality, in review.

[2] R. J. La, Interdependent Security with Strategic Agents and Global Cascades, *IEEE/ACM Transactions on Networking*, to appear.

[3] R. J. La, Network Mixing – Is it Good or Bad for Network Security?, in preparation.

[4] S. Pal and R. J. La, A Simple Learning Rule in Games and its Convergence to Pure-Strategy Nash Equilibria, in *Proceedings of the American Control Conference*, Chicago, IL, July 2015.

[5] S. Pal and R. J. La, A Simple Learning in Weakly Acyclic Games and Convergence to Nash Equilibria, in *Proceedings of the 53rd Annual Allerton Conference*, Monticello (IL), September 30 – October 2, 2015.

Measurement Science for Systemic Risk

Vladimir Marbukh

The economic and convenience benefits of interconnectivity have driven the current explosive emergence and growth of networked systems. However, numerous recent systemic failures in various systems suggest that a market economy has difficulty in the accurate estimation and pricing of the drawbacks and systemic risks of interconnectivity. Our modeling efforts have the goal of developing recommendations on the systemic risk/benefit tradeoff of interconnectivity, where benefits are due to local risk mitigation, and systemic risk is due to risk exposure to cascading failure.

We model contagion in networked systems as a Markov process with locally interacting components, where system "topology" is encoded as a directed graph with nodes representing system components, and links representing the contagion flow [1-2]. In applications, some internal node states represent component failure, e.g., overload, and thus can be deemed "vulnerable/ undesirable." This motivates the definition of the individual node risk as the probability of this node being in such a state, and systemic risk as the individual risk averaged over all the nodes in the system.

We assume that an increase in the node risk exposure immediately drives adjacent nodes towards higher risk exposure, creating a possibility of contagion and undesirable cascades. Direct solution of the Kolmogorov equations for the underlying Markov "micro-process" with a large number of interacting components N is computationally infeasible due to the astronomically high dimension of the Kolmogorov system. This high dimension of micro-description on the one hand, and systemic risk being inherently a macroscopic phenomenon on the other, suggest the possibility of a macro-description of systemic risk.

Our first step in realizing this possibility is developing mean-field and fluid approximations for the corresponding Kolmogorov microscopic equations. For low exposure to the exogenous risk, the approximate closed systems of non-linear, fixed-point equations have a "normal/operational" system equilibrium with a low systemic risk. As the exogenous risk exposure adiabatically, i.e., "slowly," increases, the approximate equations may experience bifurcation, which results in emergence of a high systemic risk solution. Following the conventional approach, we interpret multiple solutions of the approximate equations as describing the metastable, i.e., persistent, system states.

Since for heterogeneous networked systems, the dimensions of the corresponding approximate descriptions grow with N, further dimension reduction is required. We suggest a possibility of a Perron-Frobenius-based "macro-description" near the stability boundary of the operational system equilibrium inside the system parameter space. The importance of this region is due to economics, which drives networked systems towards the stability boundary of the normal/operational equilibrium. We demonstrate that the proposed macro-description is instrumental for classification and management of the emerging instability. In particular, we suggest that while maximizing economic and convenience benefits of interconnectivity, networked system designers and operators should limit the systemic risk of abrupt/discontinuous instability in favor of gradual/continuous instability.

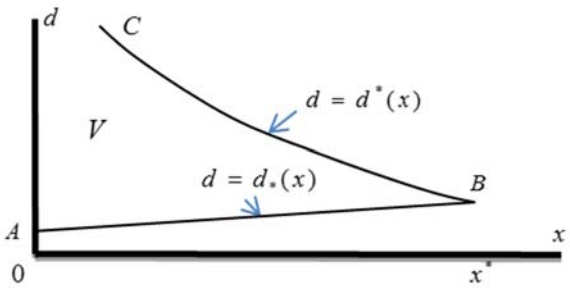

Figure 50. *A typical system phase diagram. Here x is average investment in node "antifragility," and d is the average node degree.*

Currently we are extending these results by considering the effect of system topology [3-5]. In particular, we compare the following two systemic risk mitigation techniques: (a) investing in the component "antifragility," e.g., by adding extra capacity to withstand adverse effects of demand bursts, capacity outages, etc., and (b) investing in additional interconnectivity allowing for more risk diversification. Figure 50 depicts typical system phase diagram in variables (x,d), where x is a properly defined average investment in the node "antifragility," and d is the average node degree.

The operational regime without systemic risk is unstable within region V, and is at least locally stable outside V. We assume that costs/benefits of system connectivity per node can be quantified by an increasing and concave utility function of the average node degree d, $u(d)$, and consider the optimization problem

$$\max_{(x,d)\notin V} u(d) - x.$$

The solution to this problem defines the optimal balance between the connectivity $d = d^{\text{opt}}$ and investment in the component antifragility $x = x^{\text{opt}}$ subject to systemic risk avoidance. In particular, our results indicate that $(x^{\text{opt}},d^{\text{opt}})$ lies on the boundary BC in Figure 50.

[1] V. Marbukh, Towards Unified Perron-Frobenius Framework for Managing Systemic Risk in Networked Systems, in *Proceedings of the annual European Safety and Reliability Conference* (ESREL), Zurich, Switzerland, September 7-10, 2015.

[2] V. Marbukh, Towards Managing Systemic Risk in Networked Systems, in *Proceedings of the International*

Conference on Operations Research, Vienna, Austria, September 1-4, 2015.

[3] V. Marbukh, "On Managing Cost/Benefit Connectivity Tradeoff in a Networked Infrastructure Susceptible to Adverse Cascades," International Conference on Network Science (NetSci), Zaragoza, Spain, June 1-5, 2015.

[4] V. Marbukh, "SDN: Systemic Risks due to Dynamic Load Balancing," Internet Research Task Force, Software Defined Networking Research Group, *IETF 91*, Honolulu, Hawaii, USA, 2014.

[5] V. Marbukh, "Network Evolution by Preferential Rewiring with Infection Risk Mitigation: Work in Progress," Workshop on Dynamics of and on Networks, Santa Fe Institute, Santa Fe, NM, December 2, 2014.

Identifying the Best Nodes in a Network for Fast Communication

Fern Y. Hunt

The identification of nodes in a network that enable the fastest spread of information is an important if not fundamental problem in network control and design. It is applicable to the optimal placement of sensors, the design of more secure networks, and the problem of network control when network resources are limited. Our research centers on a model problem where communication is represented mathematically by random walks on an undirected graph. The problem of selecting the best nodes is then posed in terms of finding the set of nodes on the graph (subject to constraints on the set size) that minimizes a random walk hitting time function, representing the time it takes for information to reach the entire network. In recent years, research on methods for solving combinatorial optimization problems like this have centered on the development of solution methods when the function to be optimized is bounded and submodular (supermodular).

F. Hunt has been developing methods for identifying optimal and near optimal sets that use the supermodular properties of the hitting time function as well as information about the network topology [1]. This work is intended to be part of the ongoing modeling and simulation research on communication networks and protocols going on in ITL. Developments of the past year include [3]

- showing that these methods are polynomial time in the number of nodes,
- rigorous comparison of the set obtained by our method with the exact solution (performance ratio),
- a proof that our approximation is as least as good as the result of the classic greedy algorithm (frequently used for such problems) and improves the results of the greedy algorithm by a quantity that can be calculated once the approximation is known, and
- an analysis of computational complexity that quantifies the tradeoff between the quality of the solution and computation required to achieve it.

Our ongoing research involves the development of methods based on an understanding of the structure of optimal sets and its near optimal subsets. We believe the results of this effort are key to making the approach feasible for realistic networks.

[1] F.Y. Hunt, The Structure of Optimal and Near Optimal Target Sets in Consensus Models*, NIST Special Publication 500-303*, August 2014

[2] F.Y. Hunt, Optimal Spread in Network Consensus Models, in review

[3] F. Y. Hunt, An Algorithm for Identifying Optimal Spreaders in a Random Walk Model of Network Communication, in preparation.

Measuring Networks: Monte Carlo Sampling to Approximate the Chromatic Polynomial

Yvonne Kemper
Isabel Beichl

At its heart, a network (or graph) is a collection of points (vertices) connected by lines (edges). Networks can be used to represent a variety of physical and abstract objects, and measuring characteristics of networks allows researchers to uncover and understand information encoded in the network, as well as study the systems it represents.

One example of this relates to a particular labeling of a graph G called a coloring: a proper k-coloring of the graph is an assignment of the numbers 1, 2 …, k to the vertices so that vertices connected by an edge receive different numbers. Amazingly, there exists a polynomial, the chromatic polynomial, $X_G(x)$, that evaluates to the number of k-colorings when $x=k$. The chromatic polynomial (as well as its largest integral root) has received much attention as a result of the now-resolved four-color problem, but $X_G(x)$ is also central in multiple applications, such as scheduling and assignment problems and the q-state Potts model in statistical physics. Scheduling problems occur in a variety of contexts, from algorithm design to factory procedures, and with an approximation of $X_G(x)$ it is possible to estimate the number of possible solutions given specific parameters. For the latter, the relationship between $X_G(x)$ and the Potts model connects statistical mechanics and graph theory, allowing researchers to study phenomena such as the behavior of ferromagnets. The complex roots of $X_G(x)$ are particularly useful in this area of research.

Unfortunately, computing $X_G(x)$ for a general graph G is known to be #*P*-hard, and deciding whether or not a graph is k-colorable is NP-hard; the best known algorithm for computing $X_G(x)$ for an arbitrary graph G with n vertices has complexity $O(2^n n^{O(1)})$ [1].

Approximation methods, however, have received little attention. The goal of these methods is to provide an evaluation close to the true answer in a fraction of the time. In the last year, we have adapted a Monte Carlo method of sequential importance sampling to be the basis of two approximation algorithms [2]. After implementing our algorithms in both MATLAB and C, we were able to compute approximations of $X_G(x)$ for graphs of much larger size than previously possible. Before, the best exact algorithms were limited to $2|E(G)| + |V(G)| < 950$ and $|V(G)| < 65$, where $|E(G)|$ is the number of edges, and $|V(G)|$ is the number of vertices. Our largest so far had 500 vertices and 62 323 edges, and larger computations are possible. We have shown our methods to have small relative error in the cases where we were able to compare to the exact polynomial. Moreover, as the expected value of our approximation is the precise value, we may further reduce error by performing further computations.

[1] A. Bjorklund, T. Husfeldt and M. Kolvisto, Set Partitioning via Inclusion-exclusion, *SIAM Journal of Computing* **39** (2009), 546-563.

[2] Y. Kemper and I. Beichl, Monte Carlo Methods to Approximate the Chromatic Polynomial, *Congressus Numerantium* **125** (2015), 127-152.

Fast Sequential Network Model Building

Brian D. Cloteaux
Zoe Park (Georgetown University)

Creating degree-based models is an important first step in the modeling of networks. Until recently, the only way to create a random model with a given a degree sequence would be to first create an instance using the Havel-Hakimi algorithm, and then perform a walk on a Markov chain, i.e. Markov chain Monte Carlo (MCMC), of edge switches in the graph. This method is fast, but since the entire graph must be kept in memory, the size of the graph that can be generated is severely limited. In addition, little is known about bounds on the mixing time of this walk. Finally, this algorithm is difficult to modify for creating graphs with additional given characteristics.

In 2010, Blitzstein and Diaconis published a sequential importance sampling (SIS) method for selecting random graphs with a given degree distribution [1]. Unfortunately, their method is very slow compared to the MCMC approach. While there has been some work to speed up the general algorithm, the usefulness of the algorithm is limited to small networks.

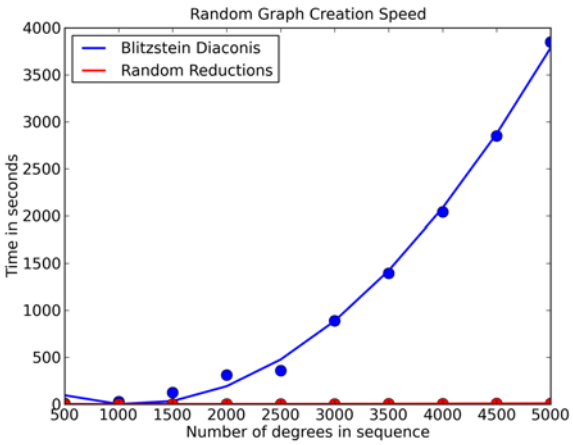

Figure 51. *Comparison of generation times for models.*

We proposed a new SIS method for constructing random graphs based on degree values [2]. Our algorithm chooses a set of possible edges (or a reduction) for a vertex in the graph, and then if that set is not viable, adjusts the selection in order to choose a new set. This selection process is done iteratively, and is guaranteed to converge to a viable selection set. This new result gives us the advantages of using SIS, while approaching the speed of the MCMC method; see Figure 51.

Zoe Park, a SURF student, has coded this algorithm and we are preparing it for release. Work on how to quickly test whether a degree sequence is graphical was also published [3].

For the Blitzstein-Diaconis algorithm, the main bottleneck in time is a requirement to check whether an edge is not allowed in order to create a viable realization. We call these edges that are not allowed in any realization of a degree sequence a *forbidden sequence*. Conversely, an edge that must appear in every realization is called a *forced edge*.

The presence of forced or forbidden edges for a degree sequence has important structural implications for graphs. We have been able to show several new results such as the set of forced edges for a degree sequence is isomorphic to some threshold graph [4]. Also, if a sequence has forbidden edges, that implies the presence of forced edges also. Finally, we showed that the diameter of every graph that is a realization of a degree sequence with forced edges is no more than 3.

These results have important algorithmic applications, but additionally they help us to understand the forced structure in models that depend on a given degree sequence.

[1] J. Blitzstein and P. Diaconis, A Sequential Importance Sampling Algorithm for Generating Random Graphs with Prescribed Degrees. *Internet Mathematics* **6**:4 (2010), 489.

[2] B. Cloteaux, Fast Sequential Creation of Random Realizations of Degree Sequences, in review.

[3] B. Cloteaux, Is This for Real? Fast Graphicality Testing, *Computing in Science and Engineering*, **17**:6 (2015), 91.

[4] B. Cloteaux. Forced and Forbidden Edges for Degree Sequences, in review.

An Algebraic Formulation for the Analysis and Visualization of Network Graphs

Roldan Pozo

Characterizing the topological structure of large graphs remains an important problem in network science. While it is straightforward to visualize small networks of hundreds or a few thousands of vertices and edges using conventional graph visualization packages, attempting to render large real networks is nearly impossible. This is particularly true for information networks and social networks, where the graph sizes number into the millions and billions. And with the amount of data being generated and gathered from large social media sites ever increasing, characterizing larger and larger networks is only becoming more challenging.

Conventional algorithms for graph visualization result in a rendering of very large networks as a solid blot of color from which it is difficult to obtain meaningful information. This difficulty is strongly influenced by the sheer volume of nodes and edges which makes rendering into a reasonable image size for viewing and printing impractical. It is exacerbated by the presence of high-degree nodes (hubs) which entangle many parts of the graph with itself.

An alternate approach is to visualize important network properties, rather than the actual network itself. Such network portraits attempt to capture interesting attributes of a large graph, such as degree distribution, or its connective properties. In this research area, we focus on a particular type of information: the distribution of "fringe" communities, i.e., connected components of a graph in the absence of high-degree hubs. In a social science context, for example, they represent independent or rogue groups, highly connected amongst themselves, but which are often lost with the inclusion of more popular nodes.

Our approach, the Q-matrix of a network, in its fundamental form, is a connected component size distribution matrix for a series of degree-limited subgraphs of the original network (or weakly-connected component for directed networks.) Thus, $Q(i,j)$ is the number of connected components of size j in a subgraph where the maximum degree is equal to or less than i. Consider, for example, a Web graph, where nodes are individual pages, and edges are directed hyperlinks between two web pages. Figure 52, for example, illustrates connected components of the math.nist.gov Web graph, where nodes of degree greater than 25 have been removed. The result is a collection of non-trivial components of math.nist.gov web graph, restricted to nodes with combined degree less than or equal to 25. The image reveals various structures, such as ladder, star, and cluster patterns, representing tightly coupled webpages. These form the nucleus of fringe communities of web pages, and by varying the degree parameter we can direct the size and granularity of groups revealed.

As the degree threshold is increased from 1 to the largest degree in the original graph, we can form a connected component size distribution, which can be encoded as a row of a matrix. This sparse matrix may still be too large to view directly, but can be compactly

Figure 52. *Non-trivial components of math.nist.gov web graph, restricted to nodes with combined degree less than or equal to 25.*

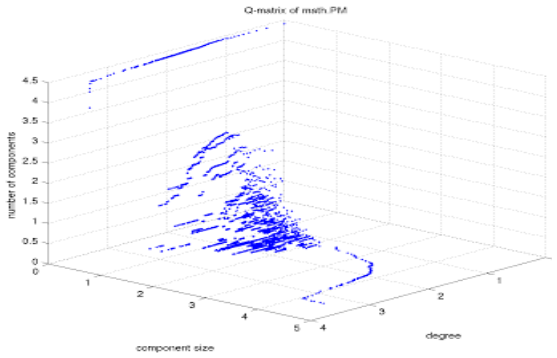

Figure 53. *Q-matrix plot of math.nist.gov webgraph (29K vertices, 62K edges) showing the component size distribution of degree-limited subgraphs.*

rendered by projecting its nonzero values onto the *z*-axis and displaying it as a three-dimensional plot, as shown in Figure 53. This Q-matrix plot of the math.nist.gov webgraph (29K vertices, 62K edges) shows the component size distribution of degree-limited subgraphs.

The Q-matrix of a graph can be considered as a generalization of its degree-distribution. However, it encodes other properties, such as the formation and growth of its giant component, its connected subparts, as well as its size parameters. In fact, common network metrics (e.g., degree distribution, number of connected components, number of vertices and edges) can be extracted from the Q-matrix using simple linear algebra operations.

Among the interesting characteristics of the Q-matrix formulation is that network graphs from similar application areas (e.g., social networks, email networks, web graphs, peer-to-peer networks, road networks, citation graphs) share similar visual characteristics, creating a potential framework for network identification and classification. Indeed, we have used the Q-matrix formulation to generate meaningful thumbnail images for network data collections. The computation of the Q-matrix is relatively efficient; graphs with millions of vertices and edges can be processed in less than one minute.

This year we extended this framework by developing an important generalized measure that compares Q-matrices of networks in varying sizes and scale. This is critical in developing the theory as it allows one to compare vastly different networks and provide a numerical similarity between them, and establish a taxonomy classification based on these characteristics. We have also provided an extended measure formulated on second and third-generation degree distributions, which provides a refined fingerprint of network graphs. To each vertex we assign not just its degree (d), but the average degree of all its neighbors (d_1), average degree of all its neighbor's neighbors (d_2), and so on. This replaces a single vertex value with a finite vector (d, d_1, $d2$, …, d_k). Such vectors can be arranged in a lexicographical along one dimension, creating a much richer profile than the conventional degree distribution.

[1] R. Pozo, Q-matrix: An Algebraic Formulation for the Analysis and Visual Characterization of Network Graphs, J*ournal of Research of NIST* **121**:1, 16 pages.

Counting the Number of Linear Extensions of a Partially Ordered Set

Isabel Beichl
Francis Sullivan

Given a partially ordered set (P,lt), a linear extension is a linear ordering (P,<) of the elements of P that is consistent with (P,lt), i.e., if p_1.lt.p_2 then $p_1 < p_2$. The ability to count the number of linear extensions of (P,lt) is central to the theory of sorting, which in turn is extremely important in the design of algorithms for advanced computers. A count of linear extensions is also important in ranking alternatives in scheduling problems where one might want to keep options open as long as possible, and in applications that arise in the social sciences where one wants to rank products or job candidates from a given partial order. It also appears in big data applications where one might need to set priorities and yet keep as many options open as possible.

The number of linear extensions is a measure of the entropy of a graph. While it is computationally easy to generate a single linear extension of (P,lt) it is known that counting the number of linear extensions is #P-complete and so one must resort to approximation. One Monte Carlo technique, called Monte Carlo Markov Chain (MCMC), has been devised and investigated extensively in the literature of theoretical computer science [1]. It has been proved that the method does give an accurate approximation. However, the method is not helpful for practical computation because it requires work (n^5) for an n-element partially ordered set.

To enable more practical computation, we investigated another Monte Carlo method that has been used with success in other #P-hard counting problems. The alternate method, called sequential importance sampling (SIS) uses non-uniform sampling based on an importance function. In this case, the importance is derived from the famous Moebius inversion formula. We have found the SIS-based algorithm to work extremely well in test cases. In addition, it has led to a combined SIS-MCMC method that improves the MCMC method from $O(n^5)$ to $O(n^3)$.

[1] G. Brightwell and P Winkler, Counting Linear Extensions, *Order* 8 (1991), 225-242.

Extremal Theorems for Degree Sequence Packing and the 2-Color Discrete Tomography Problem

James Shook
Jennifer Diemunsch (St. Vincent College)
Michael J. Ferrara (University of Colorado at Denver)
Sogol Jahanbekam (University of Colorado at Denver)

In tomography, three-dimensional objects are reconstructed using data acquired from two-dimensional projections. Tomography has uses in medical imagining, data security problems, computer assisted engineering, and electron microscopy. For computational purposes, the tomography problem is reformulated as the k-color discrete tomography problem which in turn can be stated as a coloring problem. The goal of the k-color discrete tomography problem is that of coloring the entries of an $m \times n$ matrix using k colors so that each row and column receive a prescribed number of entries of each color. This problem is equivalent to packing the degree sequences of k-bipartite graphs with parts of sizes m and n. The case of practical interest is k=2. Two graphs pack if there is a bijection of the vertices so that there are no common edges after the vertices of the two graphs have been identified with each other. The degree of a particular vertex is the number of edges incident with that vertex. A degree sequence is an ordered list of the degrees of all the vertices of the graph. A realization of a given degree sequence is a graph that has that degree sequence.

We approached the 2-color discrete tomography problem by proving a more general related result in graph packing. We found non-trivial conditions for when two degree sequences have realizations that pack. We then modified our techniques to prove several theorems that have direct applications to the 2-color discrete tomography problem. The first part of our work appears in [1]. We are now modifying and improving our techniques for better results.

[1] J. Diemunsch, M. Ferrara, S. Jahanbekam and J. M. Shook, Extremal Theorems for Degree Sequence Packing and the Two-Color Discrete Tomography Problem, *SIAM Journal on Discrete Mathematics* **29**:4 (2015), 2088-2099.

Combinatorial Methods in Software Testing

Raghu N. Kacker
D. Richard Kuhn (NIST ITL)
Yu Lei (University of Texas at Arlington)
James F. Lawrence
Jose Torres-Jimenez (CINVESTAV)
Itzel Dominguez-Mendoza (CENAM)

Combinatorial testing (CT) is an approach to detecting interaction faults, which cause a software-system to fail when certain values of some factors occur together. Many critical system failures in recent times have been traced to interaction faults in the underlying software. Combinatorial testing is based on an empirical result, referred to as the *interaction rule*, that while the behavior of a software system may be affected by a large number of factors, only a few factors are involved in a failure-inducing fault. Analysis of actual faults have demonstrated that most involved one or two factors; however, some may involve three, four or more factors (a fault involving more than six factors has not been reported yet).

NIST has taken the lead to advance technology from pair-wise to higher strength interaction testing, to make available research tools and techniques for US industry, and to help promote their effective use. CT is a versatile and broadly applicable methodology that is helping to reduce testing costs in software-based systems for science, commerce, defense and security, and electronic medical systems. CT is useful for hardware testing as well. CT is now included in software engineering courses taught in more than fifteen U.S. universities. A NIST special publication [1] on CT has been downloaded more than 30 000 times.

ACTS is a research tool, developed by NIST and the University of Texas at Arlington (UTA), to generate high strength test suites for CT. More than 2 200 users have downloaded an executable version of the ACTS tool from the NIST CT website[39]. We allow further distribution of the ACTS tool by its recipients. We are now distributing version 2.93 of the ACTS tool. The ACTS tool is optimized to support constraints among test settings; in particular, avoiding forbidden combinations of test settings efficiently.

CCM (for Combinatorial Coverage Measurement), a new research tool developed jointly by NIST and guest researcher Itzel Dominguez-Mendoza, from the Center for Metrology of Mexico (CENAM), determines combinatorial coverage of a test suite that may not have been developed from a CT viewpoint. The latest version of CCM supports constraints. A parallel processing version of CCM is also available. The most important use of CCM is to assess the coverage of the input space of a test suite. Combinatorial deficiency of a test suite can

[39] http://csrc.nist.gov/groups/SNS/acts/index.html

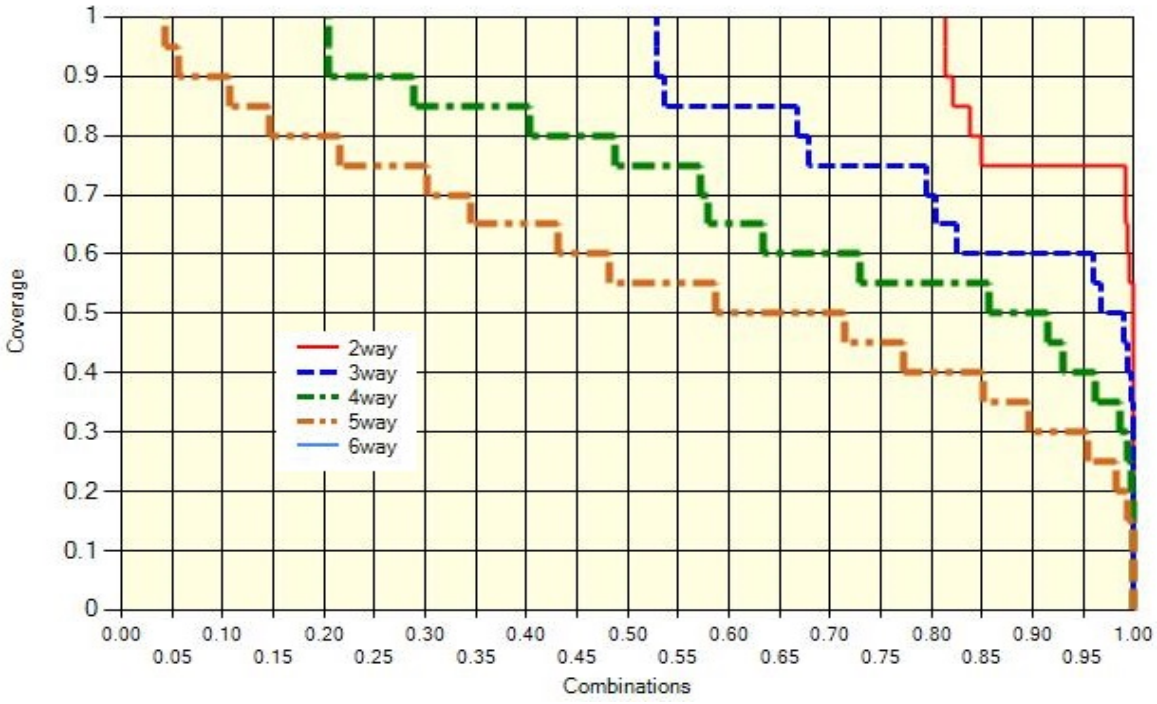

Figure 54. *Combinatorial t-way coverage of a test suite of 7489 tests of 82 variables for t=2, 3, 4, and 5.*

be remedied by additional tests, so CCM can help expand a test suite to satisfy stated combinatorial requirements. A graph of combinatorial coverage depicts the percentage (*y* axis) of the fraction (*x* axis) of all *t*-way combinations that are covered by the test suite. Figure 54 shows combinatorial *t*-way coverage of a test suite of 7489 tests of 82 factors for $t = 2, 3, 4,$ and 5. The area under a curve represents the proportion of combinations that are covered by the test suite. Thus, the area above the curve represents input values for which correct operation has not been verified.

On April 13-17, 2015 NIST co-organized 4th International Workshop on Combinatorial Testing (IWCT), held in conjunction with the 8th IEEE International Conference of Software Testing, Verification and Validation (ICST) in Graz, Austria, to bring together researchers, developers, users, and practitioners to exchange ideas and experiences with CT methods and tools. IWCT-2015 received 29 submissions of which 15 papers were selected by the Program Committee [5-9]. IWCT-2016 is scheduled to be held in conjunction with ICST-2016 on April 10-15, 2016 in Chicago, IL.

Test suites for CT are based on mathematical objects called covering arrays. Jose Torres-Jimenez of the Mexican National Polytechnic Institute Center for Research and Advanced Studies (CINVESTAV) spent his sabbatical year (July 1, 2014 to June 30, 2015) at NIST as a member of the CT team, where he worked on optimizing covering arrays [2,6].

SBA-Research[40] is a leading Austrian research center for information security. It is a consortium of companies and universities which receives half of its funding from industry and the rest from the Austrian government for research on cybersecurity. We are jointly investigating research issues in using combinatorial test methods for cyber-security applications. For example, SBA-Research has used the NIST CCM tool to analyze the combinatorial coverage of test inputs of some open-source cryptographic suites. In most cases, combinatorial coverage was low; suggesting that standard test sets for these widely used cryptographic packages may provide insufficient testing.

[1] D. R. Kuhn, R. N. Kacker and Y. Lei, Practical Combinatorial Testing, NIST Special Publication 800-142, October 2010.

[2] J. Torres-Jimenez, I. Izquierdo-Marquez, R. N. Kacker and D. R. Kuhn, Tower of Covering Arrays, *Discrete Applied Mathematics* **190–191** (2015), 141–146.

[3] D. R. Kuhn, R. N. Kacker and Y. Lei, Combinatorial Coverage as an Aspect of Test Quality, *Crosstalk: The Journal of Defense Software Engineering* **28** (March/April 2015), 19-23.

[4] J. D. Hagar, T. L. Wissink, D. R. Kuhn and R. N. Kacker, Introducing Combinatorial Testing in a Large Organization, *IEEE Computer* **48**:4 (April 2015), 64-72.

[5] D. R. Kuhn, R. Bryce, F. Duan, L. Ghandehari, Y. Lei and R. N. Kacker, Combinatorial Testing: Theory and

[40] https://www.sba-research.org/

Practice, in *Advances in Computers* **99**, (A. Memon, ed.), Elsevier, 2015, 1-66.

[6] D. R. Kuhn, R. N. Kacker, Y. Lei and J. Torres-Jimenez Efficient Verification of Equivalence Classes and Simultaneous Testing Using Two-layer Covering Arrays, in *Proceedings of 4th International Workshop on Combinatorial Testing*, Graz, Austria, April 13-18, 2015.

[7] F. Duan, L. Yu, Y. Lei, R. N. Kacker and D. R. Kuhn Improving IPOG's Vertical Growth Based on a Graph Coloring Scheme, in *Proceedings of 4th International Workshop on Combinatorial Testing*, Graz, Austria, April 13-18, 2015.

[8] L. Ghandehari, J. Chandrasekaran, Y. Lei, R. N. Kacker and D. R. Kuhn, BEN: A Combinatorial Testing-Based Fault Localization Tool, in *Proceedings of 4th International Workshop on Combinatorial Testing*, Graz, Austria, April 13-18, 2015.

[9] L. Yu, F. Duan, Y. Lei, R. N. Kacker and D. R. Kuhn Constraint Handling in Combinatorial Test Generation Using Forbidden Tuples, in *Proceedings of 4th International Workshop on Combinatorial Testing*, Graz, Austria, April 13-18, 2015.

[10] V. Hu, D. F. Ferraiolo, D. R. Kuhn, R. N. Kacker and Y. Lei, Implementing and Managing Policy Rules in Attribute Based Access Control, in *Proceedings of 16th IEEE International Conference on Information Reuse and Integration* (IRI), San Francisco, CA, August 13-15, 2015.

Can Micro Energy Harvesters Be Used to Power Up Wearable Sensors?

Kamran Sayrafian
Dora Budić (University of Zagreb)
Dina Simunić (University of Zagreb)

Wearable sensors are considered to be a key component of next generation health-IT systems. These sensors, which enable real-time physiological monitoring, will provide interfaces between human and future information and communication technology devices. Sophisticated wearable sensors capable of measuring neurological or physiological signals, as well as associated wireless communications are emerging daily. However, as complexity of these sensors increase, so does their energy consumption. Given the small size constraints for these sensors, limited energy sources (e.g., small batteries) will become a bottleneck in their functionality. Therefore, any technology that can prolong the lifetime of these sensors or reduce charging frequency will positively impact their market adoption.

Energy harvesting refers to the process of capturing and storing energy from the ambient environment. Light, body heat, and body movement all can be harvested for use in a wearable device. Kinetic energy harvested from the human body motion seems to be one of the most convenient and attractive solutions for wearable wireless sensors [1,2].

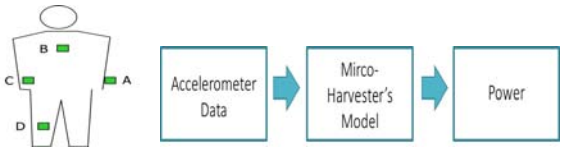

Figure 55. *Placement of the accelerometer on the body: A: Wrist, B: Chest, C: Hip, D: Leg, and Block diagram of the measurement system.*

	Average power (μW)		
Axis	Walking	Running	Rollerblading
X	19.6	351.6	11.6
Y	1.2	350.5	1.3
Z	1.3	32.6	9.0
X+Y+Z	22.2	734.7	21.9

Figure 56. *Harvested power from wrist motion for 300 sec measurement intervals (MSD dimension: 15×15×1.5 mm^3, and F = 17.25×10^{-3}).*

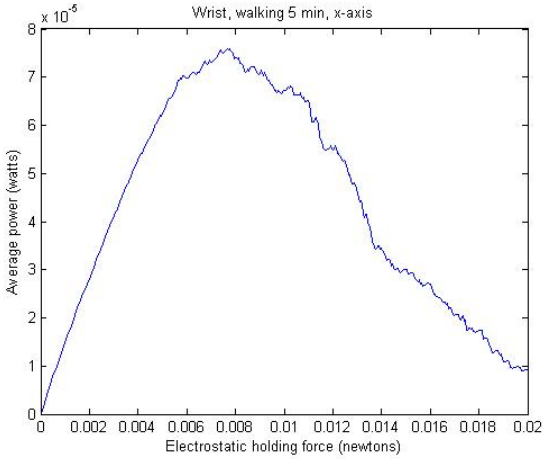

Figure 57. *Average harvested power from the human wrist motion versus the electrostatic force F in a CFPG architecture.*

Miniaturized energy harvesting devices, also known as micro-generators, consist of a mass-spring-damper (MSD), a transducer, and an interfacing power-processing circuit. The transducer converts mechanical power into electrical energy. Kinetic micro-generators either utilize direct application of force on the device, or make use of inertial, ambient forces acting on a proof mass. These forces are captured within the MSD component. Unlike micro-generators that utilize a direct application of force, their inertial-based counterparts require only one point of attachment to the moving structure, allowing for greater mounting flexibility and miniaturization that is ideal for wearable devices.

In [3] a miniature triaxial accelerometer has been used to measure acceleration from human motion during various activities. Figure 55 shows the placement of the accelerometer on the body where measurements were obtained. Measurements were done for several short (i.e., 5 min) and long (one hour) intervals during the day. Data from these measurements were used as input to a Simulink-based micro-harvester model in order to generate output instantaneous power as shown in Figure 56. The triaxial accelerometer is capable of measuring acceleration in all 3 axes as defined by the placement of the device on the body. Although the current micro-harvester technology can only use one axis for energy conversion, in our study we investigated the possible amount of average power in each direction. This information will be useful to identify which axis is most appropriate for harvesting kinetic energy. We have also provided the resulting power from all three axes combined, which is just the summation of the estimated power in each direction. Also, as the intended use of these harvesters is in very small wearable sensors, we only considered micro-harvesters with small sizes (i.e., from 100 mm^3 to 800 mm^3) to estimate the average power. Figure 57 shows sample results for a sensor that is attached to the wrist (e.g. a smart watch) during various activities like walking, running or rollerblading.

In our previous study [4], we showed that there exists an optimal value for the electrostatic force *F,* a parameter in the internal architecture of the CFPG micro-harvester. Figure 57 shows the impact of this electrostatic force on the average power. Almost a factor of 10 increase in the generated power can be expected when a proper value for *F* is chosen. Although Figure 57 uses the measurement data obtained through wrist motion during walking to demonstrate the dependency on *F*, similar behavior is also observed for other input data. With knowledge of the optimal values of the electrostatic force, a lot more power from the same body motions can potentially be harvested.

The preliminary results in this paper point to the promising application of the micro-harvesting technology in wearable sensors [5]. The power consumption of a popular wrist-worn device such as a smart watch can be as low as 1 mW. Our results show that up to 0.5 mW of power can be generated by natural human wrist motion. Therefore, integration of a small micro-harvester in a smart watch can increase its battery lifetime up to 50 %. This is a significant gain which basically leads to longer operation of the device or equivalently 50 % less frequency of recharge. The power consumption of general wearable sensors heavily depends on their functionality, and could range from nanowatt to several milliwatts. Sensor location on the human body, its size, and typical activity of the person wearing the sensor could determine the optimized design and integration of the micro-harvester. We plan to continue this research by focusing on methodologies that can adaptively optimize the architectural parameters of a micro energy harvester based on the input acceleration.

[1] N. Yarkony, K. Sayrafian and A. Possolo, Energy Harvesting from the Human Leg Motion, in *Proceedings of the 8th International Conference on Pervasive Computing Technologies for Healthcare* (Pervasive Health 2014), Oldenburg, Germany, May 20-23, 2014.

[2] N. Yarkony, K. Sayrafian and A. Possolo, Statistical Modeling of Harvestable Kinetic Energy for Wearable Medical Sensors, in *Proceedings of the IEEE International Symposium on World of Wireless Mobile and Multimedia Networks* (WoWMoM), 2010.

[3] D. Budic, *Applicability of Kinetic-Based Energy Harvesting for Mobile Phones*, Thesis No. 3868, Faculty of Electrical Engineering and Computing, University of Zagreb, July 2015.

[4] M. Dadfarnia, K. Sayrafian, P. Mitcheson and J. Baras, Power of a CFPG Micro Energy-Harvester for Wearable Medical "Maximizing Output Sensors", in *Proceedings of the 4th International Conference on Wireless Mobile Communication and Healthcare*, MobiHealth 2014, Athens, Greece, November 2014

[5] D.Budic, D. Simunic and K. Sayrafian, Kinetic-Based Micro Energy-Harvesting for Wearable Sensors, in *Proceedings of the 6th IEEE International Conference on Cognitive Infocommunications*, October 19-21, 2015.

A Study of the Energy Detection Threshold in the Body Area Network Standard CSMA/CA Protocol

Martina Barbi
Vladimir Marbukh
John Hagedorn
Kamran Sayrafian
Mehdi Alasti

A body area network (BAN) consists of multiple wearable (or implantable) sensors that can establish two-way wireless communication with a controller node that is located in the vicinity of the body. Considering the mobile nature of BANs, these networks are expected to coexist with other wireless devices that are operating in their proximity. However, interference from coexisting wireless networks or other nearby BANs could create problems with the reliability of the network operation. For example, when several body area networks are within close proximity of each other, inter-BAN interference may occur since no coordination across multiple networks exists in general. For these scenarios, several mitigation strategies that are applicable to the PHY layer have been proposed and studied [2,3]. In this project, we focus on the MAC layer and specifically the operation of the CSMA/CA protocol.

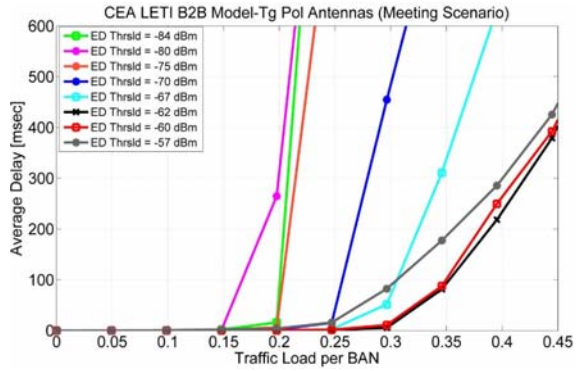

Figure 58. *Average Packet Delay versus Traffic Load for the meeting scenario.*

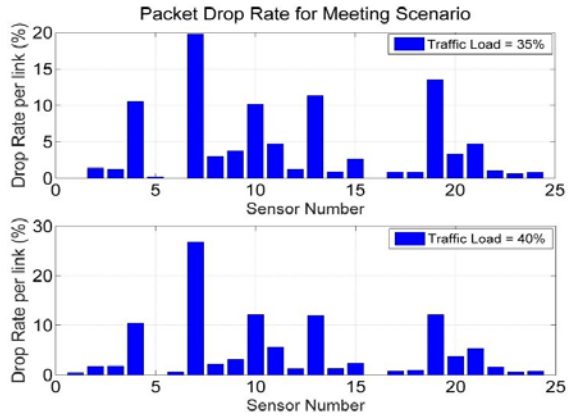

Figure 59. *Packet Drop Rate per link for different Traffic Loads.*

Consider a system comprised of several adjacent BANs. Each BAN consists of one coordinator and several sensor nodes in a star topology as outlined in the IEEE 802.15.6 standard[41] [1]. A CSMA/CA transmission protocol based on the standard is used for communication between the coordinator and the body sensors. At each BAN, the access to the channel is managed by the coordinator through the establishment of a SuperFrame (SF). According to the IEEE 802.15.6 CSMA MAC protocol, time in a SF is divided into slots with duration of 145 μsec. When a node needs to transmit a data packet, a back-off counter (BC) is chosen randomly within the interval [1 CW], where CW ∈ [CWmin CWmax]. Then, the channel is sensed for a time period pSIFS (Short Inter Frame Spacing) of 75 μsec to determine whether it is idle. If the channel is determined to be idle for this period, the BC (corresponding to the node) is decremented by one for each idle slot that follows. Once the BC has reached zero, the node transmits the corresponding data packet. On the other hand, if the channel is sensed to be busy, the BC is locked until the channel becomes idle again for the entire duration of a pSIFS.

A node assessment of the transmission channel (i.e., idle/free) is done according to the Clear Channel Assessment (CCA) Mode 1 described in the standard document [1]. It involves the use of an Energy Detection (ED) threshold. If the node's receiver detects any energy in the selected frequency channel above the ED threshold, the channel is determined to be busy; conversely, the idle channel status corresponds to no energy detection above the ED threshold. According to the standard, the minimum ED threshold should be set to values such that the received power is no less than 10 dB above the receiver sensitivity for the lowest data rate within the band of interest.

Consider a simulation scenario consisting of eight BANs (each having three on-body sensors and one coordinator node) that are static and at a fixed distance from each other [5]. This is intended to emulate eight people (each wearing a BAN) sitting around an oval-shaped table. Similar static scenarios such as people sitting in a bus may also be considered, and it can be shown that our results are easily applicable to those scenarios as well. Figure 58 shows the average packet delay as a function of the traffic load per BAN for this system. Here it has been assumed that there are no hidden node problems within each BAN. Therefore, simultaneous transmissions within the same BAN may occur only if sensor nodes set their BC to the same random value. On the other hand, simultaneous transmissions at different adjacent BANs may indeed occur, and this in fact depends on the ED threshold that has been set for the sensor nodes. As observed, the value of an ED threshold could have a significant impact on the system performance. For low threshold values (corresponding to the range -84 dBm to -75 dBm in our example), the average packet delay tends to rapidly increase for relatively lower values of the traffic load. This is due to the fact that the low values of the ED thresholds make transmitting nodes be more conservative, and therefore, hold off on any possible transmissions if they sense even a slight amount of inter-BAN interference. This could result in large delays (i.e., waiting time in the queue) that each packet experiences before it even gets the chance to be transmitted. Similarly, for high values of the ED threshold, nodes will become more aggressive and could transmit their waiting packets irrespective of the high existing inter-BAN interference. This, in turn, will increase the possibility of unsuccessful receptions (e.g., collisions) at the receiver which means further retransmissions will be required. Obviously, this will add to the total delay experienced by the packet.

As the results in Figure 58 show, the optimal value of the ED threshold is -62 dBm. In general, this optimal value depends on the exact scenario details including the relative position of each sensor at each BAN, the number of nodes, the channel conditions, etc. However, our

[41] http://standards.ieee.org/findstds/standard/802.15.6-2012.html

argument is that the choice of this value could make a significant impact on the quality of service experienced by a node. If we consider a bound for the number of times that a given packet is allowed to be retransmitted, we can see the impact of a static ED threshold on packets drop rate. Figure 59 shows this drop rate for the sensor nodes in the system when the maximum number of retransmissions is 3. The large standard deviation of the packet drop rates across sensors is indicative of the non-uniform quality of service experienced by the nodes.

The focus of our study is the potential significant impact of the ED threshold in the IEEE 802.15.6 standard on the quality of service performance of various links across multiple adjacent BANs. We show that there exists an optimal choice for the value of this threshold for the example of several adjacent BANs. We have observed that this optimal value is heavily scenario-dependent. So, in normal operation of a BAN, it would be impossible to estimate and adjust the static value of this threshold in order to guarantee the optimal performance of all links in the system. This is a fundamental problem that is caused by having the same fixed ED threshold to sense the channel and make decisions on whether to go ahead with packet transmissions. We believe that the solution to this problem is through an intelligent adaptive threshold scheme for energy detection, where each node can modify their corresponding ED threshold based on their assessment of their own channels. Several adaptive strategies are currently under investigation. Further results have been provided in [4].

[1] 802.15.6 – IEEE Standard for Local and Metropolitan Area Networks – Part 15.6: Wireless Body Area Networks, IEEE Standards Association.

[2] M. Barbi, K. Sayrafian and M. Alasti, Uncoordinated Scheduling Strategies for BAN-to-BAN Interference Mitigation, in *Proceedings of the 3rd International Black Sea Conference on Communications and Networking*, Constanta, Romania, May 18-21, 2015.

[3] V. Marbukh, K. Sayrafian, M. Barbi and M. Alasti, A Regret Matching Strategy Framework for Inter-BAN Interference Mitigation, in *Proceedings of the IFIP 8th Wireless and Mobile Networking Conference*, Munich, Germany, October. 5-7, 2015, 231-234.

[4] M. Barbi, K. Sayrafian and M. Alasti, Impact of the Energy Detection Threshold on Performance of the IEEE 802.15.6 CSMA/CA, in *Proceedings of the 2015 IEEE Conference on Standards for Communications and Networking*, Tokyo, Japan, October 28-30, 2015.

[5] K. Sayrafian, J. Hagedorn, M. Barbi, J. Terrill and M. Alasti, A Simulation Platform to Study Inter-BAN Interference, in *Proceedings of the 4th IEEE International Conference on Cognitive Infocommunicaitons*, Budapest, Hungary, December 2-5, 2013.

Mathematical Knowledge Management

We work with researchers in academia and industry to develop technologies, tools, and standards for representation, exchange, and use of mathematical data. Of particular concern are semantic-based representations which can provide the basis for interoperability of mathematical information processing systems. We apply this to the development and dissemination of reference data for applied mathematics. The centerpiece of this effort is the Digital Library of Mathematical Functions, a freely available interactive and richly linked online resource, providing essential information on the properties of the special functions of applied mathematics, the foundation of mathematical modeling in all of science and engineering.

Digital Library of Mathematical Functions

Barry I. Schneider
Daniel W. Lozier
Adri B. Olde Daalhuis (University of Edinburgh)
Bruce R. Miller
Ronald F. Boisvert
Charles W. Clark (NIST PML)
Bonita V. Saunders
Marjorie A. McClain
Howard S. Cohl
Brian Antonishek (NIST EL)
Neil Agrawal (Poolesville High School)
Nina Agrawal (Poolesville High School)
Hannah Cohen (Colonel Z. Magruder High School)

Progress in science has often been catalyzed by advances in mathematics. More recently, developments in the physical sciences, such as investigations into string theory, have had influence in pure mathematics. This symbiotic relationship has been extremely beneficial to both fields. Mathematical developments have found numerous applications in practical problem-solving in all fields of science and engineering, while cutting-edge science has been a major driver of mathematical research**.** Often the mathematical objects at the intersection of mathematics and physical science are mathematical functions. Effective use of these tools requires ready access to their many properties, a need that was capably satisfied for more than 50 years by the 1964 National Bureau of Standards (NBS) *Handbook of Mathematical Functions with Formulas, Graphs, and Mathematical Tables* [1].

The 21st century successor to the NBS Handbook, the online Digital Library of Mathematical Functions (DLMF)[42] together with the accompanying book, *NIST Handbook of Mathematical Functions* [2], both issued in 2010, are collectively referred to as the DLMF. The DLMF continues to remain the gold standard reference for the properties of what are termed the special functions of mathematical physics. The DLMF has considerably extended the scope of the original handbook, as well as improved accessibility to the worldwide community of scientists and mathematicians. To cite a few examples, the new handbook contains more than twice as many formulas as the old one, coverage of more functions, in more detail, and an up-to-date list of references. The website covers everything in the printed NIST Handbook and much more: additional formulas and graphics, live zooming and rotation of 3D graphs, interactive search, internal links to symbol definitions and cross-references, and external links to online references and sources of software. In order to help assess the impact of the DLMF project, the NIST library has undertaken a project to track citations to the DLMF, as well as to the original NBS Handbook. While the original Handbook still receives an enormous number of citations (2421 in 2014 alone), citations to the DLMF are steadily growing, with 374 citations in 2014. As of February 2016, Google Scholar has identified 2087 total citations to the new NIST Handbook.

Today's DLMF is the product of many years of effort by more than 50 expert contributors. Its appearance in 2010, however, was not the end of the project. Corrections to errors, clarifications, bibliographic updates, and addition of important new material all continually need to be made, and new chapters covering emerging subject areas need to be added, so as to assure the continued vitality of the DLMF deep into the 21st century.

Developments Currently in Progress. During the past year, the DLMF project has seen continued progress on several fronts. During that period there was only a single new release of the DLMF (version 1.0.10). This was a consequence of the large number of changes required for this update, which took more time than anticipated.

An important effort initiated during the current year was the verification, completeness and traceability of proofs for DLMF formulae. One of the goals of the DLMF was to ensure that each equation had either a

[42] http://dlmf.nist.gov/

Principal Editors	
Barry Schneider	General Editor
Daniel Lozier	General Editor
Adri Olde Daalhuis	Mathematics Editor *University of Edinburgh*
Bruce Miller	Information Technology Editor
Bonita Saunders	Graphics Editor
Ronald Boisvert	Editor-at-Large
Charles Clark	Applications Editor
Contributing Developers	
Marjorie McClain	Bibliography, LaTeX
Howard Cohl	Mathematics
Brian Antonishek	Graphics
Senior Associate Editors	
Mark Ablowitz	*University of Colorado*
George Andrews	*Penn State University*
Michael Berry	*University of Bristol*
Annie Cuyt	*University of Antwerp*
Mourad Ismail	*University of Central Florida*
James Pitman	*University of California at Berkeley*
William Reinhardt	*University of Washington (retired)*
Simon Ruijsenaars	*University of Leeds*
Nico Temme	*CWI Amsterdam (retired)*
Stephen Watt	*University of Waterloo*

Figure 60. *DLMF Management and Organization Structure*

short proof for the formula or a reference to a proof for the formula, and that each definition also was linked to a source. Unfortunately, gaps have been observed in this coverage. A systematic audit of Chapters 25 and 27, aided by a group of capable high school interns, is now underway to determine the extent of the problem, as well as to fill in all missing information. We plan to extend this effort to the entire DLMF.

We continue to pursue enhancement to the online graphics provided in the DLMF. That work is described on 93.

The past year also saw changes in the Editorial Board and a restructuring of the management of the project in order to ensure active maintenance and development of the DLMF for the future. Figure 60 lists the roles of the current principal DLMF editors and developers. Also listed is the revitalized set of Senior Associate Editors (SAE), who will advise NIST management on the future evolution of the project. Finally, an Associate Editor (AE) has been identified for each existing DLMF chapter. AEs will work with the Mathematics Editor in responding to user queries about current chapter content, as well as developing minor updates.

On November 9-10, 2015 the SAEs assembled at NIST to discuss the possibility of a second edition of the DLMF with significant new content and features. Among the items discussed were

- Chapters that need major expansions,
- Potential topics for new chapters,
- The merits of online versus print,
- Numbering of formulae and relation to the first edition,
- Raising awareness of the DLMF,
- Licensing issues,
- New semantic-based technologies, and
- Application programmer interfaces to data.

A good deal of useful input was obtained, and project staff are now beginning to act on it.

The DLMF has spawned a number of related efforts within the Division, which are described elsewhere in this document, including the DLMF Standard Reference Tables on Demand (page 93), the Digital Repository of Mathematical Formulae (page 97), as well as a robust research effort on the natural language processing of mathematics (page 96).

[1] M. Abramowitz and I. Stegun, eds., *Handbook of Mathematical Functions with Formulas, Graphs and Mathematical Tables*, Applied Mathematics Series 55, National Bureau of Standards, Washington, DC 1964.

[2] F. Olver, D. Lozier, R. Boisvert and C. Clark, eds. *NIST Handbook of Mathematical Functions*, Cambridge University Press, 2010.

Visualization of Complex Functions Data

Bonita Saunders
Brian Antonishek (NIST EL)
Qiming Wang
Bruce Miller
Sandy Ressler

Though originally motivated by a desire for clear, informative graphs in the NIST Digital Library of Mathematical Functions (DLMF), our work has produced cutting edge 3D visualizations that have evolved in tandem with technologies for creating and viewing 3D graphics on the Web. Our first visualizations were created using VRML, a special 3D file format for displaying graphics on the Web, but by the release of the DLMF in 2010, we also offered X3D, an XML-based format touted as the successor to VRML. At the Web3D conference in June 2015, Johannes Behr of Fraunhofer IGD, one of the developers of X3D, noted that he was so impressed with our implementation of cutting planes that it motivated him to incorporate a clipping plane feature into the specifications for X3D.

Unfortunately, both VRML and X3D require users to install a special plugin in order to view visualizations. However, by taking advantage of work on WebGL by the Khronos Group[43] and the development of X3DOM by Behr et al. [4], we were able to create

[43] https://www.khronos.org/webgl/

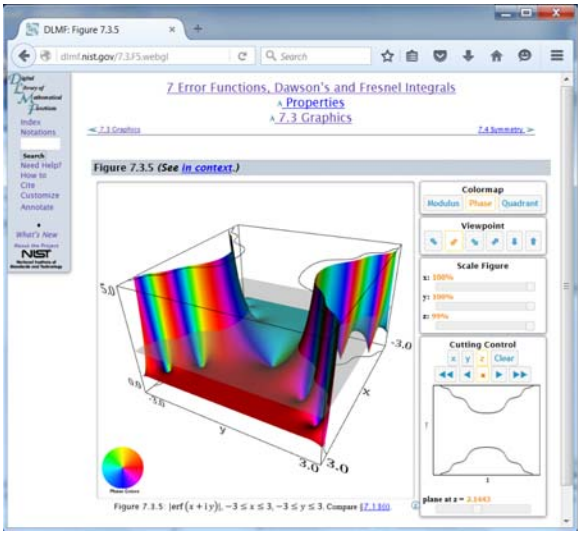

Figure 61. *DLMF webpage with an embedded visualization of* $|\mathrm{erf}(x + iy)|$.

X3DOM/WebGL visualizations for the DLMF that all but eliminated the plugin problem. WebGL is a JavaScript application program interface (API) for rendering 3D graphics in a web browser without a plugin. X3DOM is a special framework for creating graphics applications on the Web. Basing our WebGL code on X3DOM allowed us to build our WebGL applications around our X3D codes. Our visualizations can now be viewed in any WebGL-enabled browser on Windows, Mac, and Linux platforms as well as on many mobile devices.

The new X3DOM/WebGL visualizations were released in version 1.0.7 of the DLMF in March 2014. Figure 61 shows the graph of the modulus of the error function, $|\mathrm{erf}(x + iy)|$, displayed with a phase, or argument, color map. In the new visualizations, color maps are more vibrant, cutting plane curves clearer, and the interactive movement of surfaces faster and smoother. While X3DOM/WebGL is now the default, we continue to offer VRML and X3D for users who prefer to continue viewing the graphs in those formats.

Some of our work is now focused on the creation of a continuous surface spin option in our X3DOM/WebGL visualizations. This feature would permit a user to create a continuous spin in any direction by touching and flicking the surface. The speed of the spin would vary according to how fast the surface is flicked. This would be an effective tool for drawing interest during a talk or for creating an instant animation in an exhibit. The feature was available in the early CosmoPlayer VRML plugin designed by Silicon Graphics, but it was implemented in few VRML or X3D plugins developed subsequently. X3DOM developers have expressed an interest in making the feature part of their standard if our work is successful. Sandy Ressler has completed preliminary work, first implementing the feature by coding directly in WebGL and then successfully creating a rough X3DOM version by modifying codes pieced together from software freely shared by a designer at Shapeways, a 3D printing firm[44]. A substantial amount of work is still needed to streamline, restructure, and integrate the code into our visualizations.

We are also working on the reduction of graphics file sizes using adaptive grid generation, looking at 2D visualization possibilities, and exploring the feasibility of developing an accurate zoom.

We continually search for opportunities to increase the visibility of our work. In version 1.0.10 of the DLMF released in August 2015 a List of Figures entry was added to the table of contents to give users quicker access to the nearly 600 graphs and visualizations available in the DLMF. An animation on the table of contents page and a Wikipedia reference are also being explored. We published a proceedings paper based on our talk given at Web3D 2015 [1] and presented numerous invited and contributed talks throughout the year [5-9].

[1] B. Saunders, B. Antonishek, Q. Wang and B. Miller, Dynamic 3D Visualizations of Complex Function Surfaces Using X3DOM and WebGL, in *Proceedings of the 20th International Conference on 3D Web Technology* (Web3D 2015), Crete, Greece, 2015, 219-225.

[2] B. Saunders, Q. Wang and B. Antonishek, Adaptive Composite B-Spline Grid Generation for Interactive 3D Visualizations, *IMACS Series in Computational and Applied Mathematics* **18** (2014), Proceedings of MASCOT/ISGG 2012, Las Palmas de Gran Canaria, Spain, October 22-26, 2012, 241-250.

[3] S. Ressler and B. Antonishek, "New WebGL Graphics in the NIST DLMF," Web3D Emerging Technology Showcase, Virginia Tech Research Center, Arlington, VA, March 25, 2014.

[4] J. Behr, P. Eschler, Y. Jung and M. Zollner, 2009. X3DOM: a DOM-based HTML5/X3D Integration Model, in *Proceedings of the 14th International Conference on 3D Web Technology* (Web3D '09), ACM, S. N. Spencer, Ed., 127–135.

[5] B. Saunders, "Slices of 3D Surfaces on the Web Using Tensor Product B-Spline Grids," SIAM Conference on Geometric and Physical Modeling (GD/SPM15), Salt Lake City Utah, Utah, October 12, 2015.

[6] B. Saunders, "Cutting Edge Information Technology Applied to the NIST Digital Library of Mathematical Functions," Mathematical Association of America MathFest 2015, Washington, D.C., August 8, 2015.

[7] B. Saunders, "X3DOM/WebGL Visualizations in the NIST DLMF," Web3D Showcase, 20th International Conference on 3D Web Technology (Web3D 2015), Heraklion, Crete, Greece, June 20, 2015.

[44] http://www.shapeways.com/

[8] B. Saunders, B. Antonishek, Q. Wang and B. Miller, "State of the Art Visualizations of Complex Function Data," 2015 International Conference on Orthogonal Polynomials, Special Functions and Applications, NIST, Gaithersburg, MD, June 4, 2015.

[9] B. Saunders, "Adaptive Grid Generation, 3D Graphics on the Web, and a Digital Library," Infinite Possibilities Conference, Oregon State University, Corvallis, Oregon, March 2, 2015.

DLMF Standard Reference Tables on Demand

Bonita Saunders
Bruce Miller
Marjorie McClain
Daniel Lozier
Andrew Dienstfrey
Annie Cuyt (University of Antwerp)
Stefan Becuwe (University of Antwerp)
Franky Backeljauw (University of Antwerp)
Chris Schanzle

During the development of the NIST Digital Library of Mathematical Functions (DLMF) http://dlmf.nist.gov/ [1,2] the inclusion of a computational component was seen as a desirable goal, but its creation was deferred for the future. To begin meeting this objective, and to bring the value of reliable computing to the attention of a broader audience, NIST and the University of Antwerp are collaborating to develop the DLMF Standard Reference Tables (DLMF Tables), an online service that allows users to create their own tables of special function values with an error certification. ACMD is building the front end user interface while the University of Antwerp Computational Mathematics Research Group (CMA) is developing the back end computational engine based on their MpIeee library.

Of course, there are many numerical routines for evaluating special functions in widely used mathematical software libraries, packages, and systems, but none of these produce results with guaranteed error-bounds. For a real valued function, the error bound determines an interval within which the exact function value is guaranteed to lie [3]. Reliable results of this type, while typically too computationally intensive to use directly in modeling and simulation, are valuable references for the testing and evaluation of mathematical software libraries and systems.

MpIeee is an IEEE 754/854 compliant C++ library for mixed precision floating point arithmetic in base 2^n or 10^m. IEEE compliance implies, among other things, that basic arithmetic operations as well as remainder and square root operations are rounded according to specification: round-to-nearest (even), round toward ∞, round toward $-\infty$, round toward 0, round away from 0. This means the result of the operation is the floating point value that would be obtained by first computing the exact mathematical value and then rounding it to its floating point representation. IEEE compliance provides the foundation for building reliable software.

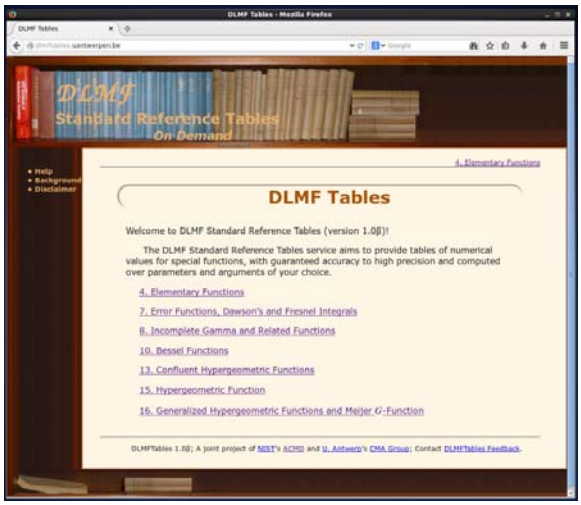

Figure 62. *Table of contents for DLMF Tables website.*

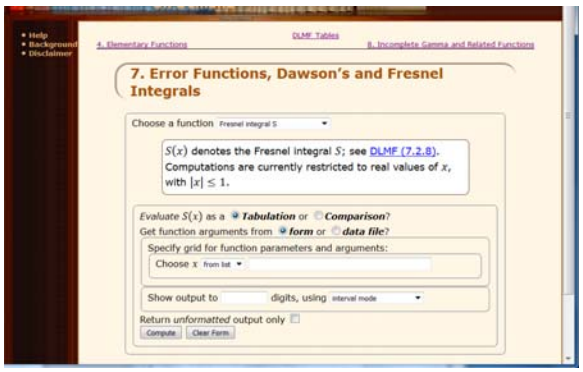

Figure 63. *Input screen for Fresnel integral S(x).*

MpIeee contains a selection of special functions, using algorithms based on series and continued fraction representations, in conjunction with a detailed analysis of the rounding errors, to compute results that lie within an arbitrarily prescribed relative error. Currently, MpIeee covers real variables only, but CMA is actively working to expand its coverage to more functions and eventually to complex variables [3-7].

A beta version of the site is already in place.[45] As shown in Figure 62, the table of contents lists the chapters available, with all entries currently corresponding to chapters in the DLMF. After a chapter is selected, the input screen (Figure 63) for that chapter appears; the

[45] http://dlmftables.uantwerpen.be/

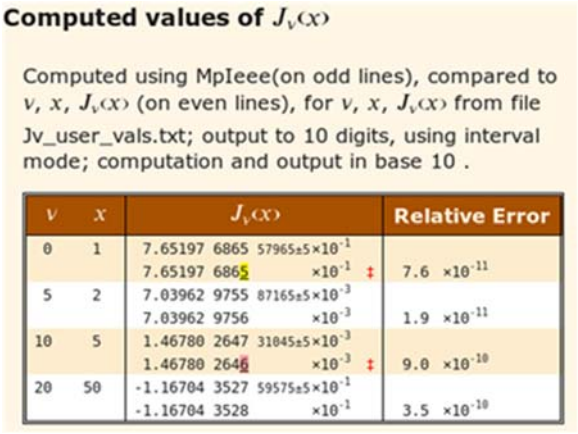

Figure 64. *Output for comparison of DLMF Tables computations with table of function values submitted by the user.*

user chooses a function and requests either a tabulation or comparison. This selection determines what additional user input will be required. Each function description contains a link to the definition of the function in the DLMF.

For a tabulation, a user may request up to 500 output digits and choose an output mode for computation. The default is interval mode, where a strict high-precision enclosure (lower and upper bound) is displayed for each requested function value. Alternatively, the user may choose an exact output rounded to the requested number of digits according to one of the standard rounding modes indicated earlier.

If the user requests a comparison, a user-supplied data file must be uploaded. The output table displays the reference values, computed in one of the user selected output modes, alternated with the values provided by the user. The approximate relative error is also shown. Differences between reference values and uploaded values are highlighted in either yellow (warning) or red (error) as shown in Figure 64.

The release of the beta version marks the completion of the first phase of the project. More functions are in the pipeline, and additional site enhancements are currently in progress. Links to relevant papers will be added along with more user documentation, and the possibility of more extensive documentation for programmers is being considered. Testing of the site has also begun, but the sparsity of systems and software of this type and quality make comprehensive testing a challenging task. We are in the process of developing a formal structure where test results can be duplicated when necessary to address problems identified either through our own work or from user feedback. Several talks were presented throughout the year [8,9] and a paper on the DLMF Tables is in review [10].

[1] NIST Digital Library of Mathematical Functions. http://dlmf.nist.gov/, Release 1.0.10 of 2015-08-07. Online companion to [2].

[2] F. W. J. Olver, D. W. Lozier, R. F. Boisvert and C. W. Clark, eds., *NIST Handbook of Mathematical Functions*. Cambridge University Press, New York, NY, 2010. Print companion to [1].

[3] F. Backeljauw, S. Becuwe, A. Cuyt, J. Van Deun and D. Lozier, Validated Evaluation of Special Mathematical Functions, *Science of Computer Programming* **10** (2013), 1016.

[4] M. Colman, A. Cuyt and J. Van Deun, Validated Computation of Certain Hypergeometric Functions, *ACM Transactions on Mathematical Software* **38**:2 (January 2012), 11.

[5] F. Backeljauw, A Library for Radix-independent Multiprecision IEEE-compliant Floating-point Arithmetic, Technical Report 2009-01, Department of Mathematics and Computer Science, Universiteit Antwerpen, 2009.

[6] A. Cuyt, V. B. Petersen, B. Verdonk, H. Waadeland and W. B. Jones, *Handbook of Continued Fractions for Special Functions*. Springer, New York, 2008.

[7] A. Cuyt, B. Verdonk and H. Waadeland, Efficient and Reliable Multiprecision Implementation of Elementary and Special Functions, *SIAM Journal of Scientific Computing* **28** (2006), 1437-1462.

[8] B. Saunders, B. Miller, M. McClain, D. Lozier, A. Dienstfrey, A. Cuyt, S. Becuwe and F. Backeljauw, "DLMF Standard Reference Tables on Demand (DLMF Tables)," Minisymposium on Orthogonal Polynomials and Special Functions: Computational Aspects, 2015 International Conference on Orthogonal Polynomials, Special Functions and Applications, NIST, Gaithersburg, MD, June 1, 2015.

[9] B. Saunders, "NIST Projects: Graphics in the Digital Library of Mathematical Functions (DLMF) and DLMF Standard Reference Tables on Demand (DLMF Tables)," Careers in Mathematical Sciences Workshop for Underrepresented Groups, IMA, University of Minnesota, Minneapolis, MN, March 29, 2015.

[10] B. Saunders, B. Miller, F. Backeljauw, S. Becuwe, M. McClain, D. Lozier, A. Cuyt and A. Dienstfrey, DLMF Tables: A Computational Resource Inspired by the NIST Digital Library of Mathematical Functions, in review.

Natural Language Processing of Mathematics

Abdou Youssef
Bruce Miller
Howard Cohl

Natural language processing (NLP) has made significant strides in recent years, with practical applications and deployed software such as part-of-speech tagging (e.g., Stanford POS tagger), language translation (e.g. Google translate), text analysis, and question answering systems. Mathematics literature, however, presents unique challenges due to its abstract nature and its inclusion of

mathematical equations and expressions. While mainstream NLP applies to some extent to processing math texts, considerable changes must be made and new techniques developed to address uniquely mathematical challenges and applications.

This project is a natural next step to the math search work that we pioneered at NIST, and that resulted in a search system that is deployed as part of the online Digital Library of Mathematical Functions. This project is broader than math search, spans several years, and involves many components and applications, which we describe below.

Part-of-Math Tagging. Much as part-of-speech (POS) tagging is a fundamental early stage of many NLP tasks, part-of-math (POM) tagging is expected to be an essential early stage of many math-NLP tasks. A POM tagger will read any math expression/equation, identify its tokens, and label each token as to its math role (e.g., variable, function, relation, operation/operator, derivative, integral, logical quantifier, logical connective, delimiter, sub/super-scripts, "accent", etc., along with additional attributes that enrich the description of tokens). One key problem is token-sense disambiguation.

- Techniques: We will use techniques from machine learning, standard NLP and text mining, and mathematical parsing, to achieve POM tagging.
- Potential applications: Automated annotation of math documents; richer math search; mathematical text-to-speech readers; semantic extraction; etc.
- Timeline: We have already mapped out the main parts of POM tagging, and fully determined the classes of math tokens (and their attributes). In the next 18 months (on a part-time basis), the essential POM tagging algorithms will be developed. Refinements and extensions will take a little longer.

Mathematical Semantic Extraction (MSE). Using POM tagging, MSE aims to extract semantics about the various components of math expressions and related (surrounding) texts in math documents. For example, if a token is determined by POM to be a function, the MSE module will determine what kind of function it is (e.g., its functional class), its mathematical definition, (possibly) its properties and constraints, etc. Similarly, if it is a variable, the MSE module will attempt to determine its data type, what it signifies if any (e.g., time variable, positional variable), its range, etc. If it is a superscript, the semantic module will determine if it is a power, a mere index, a derivative, the order of a derivative, etc.

- Techniques: We will use POM tagging, and machine learning techniques for deriving the meaning of each mathematical symbol, exploiting textual correlations and mathematical notational practices, and mining definitions embedded in texts.
- Potential Applications: Automated annotation of math documents; richer semantic search; math question answering; math document summarization; proof checking; proof assistants; etc.
- Timeline: About 12 to18 months after POM tagging.

Mathematical Question Answering (MQA). Using semantic extraction, we will develop an MQA application that can ultimately answer questions like: (1) Given a math document D and a math symbol X, is X defined in the given document? If so, what is the definition of X? If not explicitly defined in D, what is the likely implicit meaning of X? (2) Given a math document D, a corpus C, and a formula E, Is formula E proved in document D? If not, is E proved in the corpus? If so, what/where is the proof? Under what constraints does E hold? (3) What is the relationship between concept A and concept B in a given math document/corpus? (e.g., A could be a special case, a generalization, or a prerequisite of B.)

- Techniques: Semantic extraction; machine learning; AI; text mining; and various NLP techniques.
- Potential Applications: Online math help systems/math assistants for students, mathematicians, and scientists; an efficient time-saving way for examining/interrogating large collections of math documents; Knowledge discovery in general; etc.
- Timeline: About 1 to 2 years after the MSE part.

[1] M. Schubotz, A. Youssef, V. Markl and H. S. Cohl, Challenges of Mathematical Information Retrieval in the NTCIR-11 Math Wikipedia Task, 38th Annual ACM SIGIR Conference, Santiago, Chile, August 9-13, 2015.

[2] M. Schubotz, A. Youssef, V. Markl, H. Cohl, and J. Li, Evaluation of Similarity-Measure Factors for Formulae based on the NTCIR-11 Math Task, 11th NTCIR Conference and Evaluation of Information Access Technologies, Tokyo, Japan, December 9-12, 2014.

NIST Digital Repository of Mathematical Formulae

Howard S. Cohl
Marjorie A. McClain
Bonita V. Saunders
Moritz Schubotz (Technische Universität Berlin)
Alan P. Sexton (University of Birmingham)
Ankita Sharma (Poolesville High School)
Cherry Zou (Poolesville High School)
Sabrina Zou (Montgomery Blair High School)
Shraeya Madhu (Poolesville High School)
Divya Gandla (Poolesville High School)
Azeem Mohammed (Poolesville High School)
Jimmy Li (Richard Montgomery High School)
Yusuf Ameri (Quince Orchard High School)
Akash Shah (Northwest High School)
Claude Zou (Poolesville High School)
Yash Kapoor (Clarksburg High School)
Rahul Shah (Clarksburg High School)

The NIST Digital Repository of Mathematical Formulae (DRMF) is designed for a mathematically literate audience to (1) facilitate interaction among a community of mathematicians and scientists interested in compendia of formulae data for orthogonal polynomials and special functions (OPSF); (2) be expandable, allowing the input of new formulae from the literature; (3) provide information about related open data projects; (4) represent the context-free full semantic information concerning individual formulas; (5) have a user friendly, consistent, and hyperlinkable viewpoint and authoring perspective; (6) contain easily searchable mathematics; and (7) take advantage of modern MathML tools for easy to read, scalably rendered, content driven mathematics.

Our DRMF implementation is built using MediaWiki, the software used by Wikipedia. See Figure 66 for a sample DRMF formula home page. The DRMF has been described in a series of publications and talks [1-3].

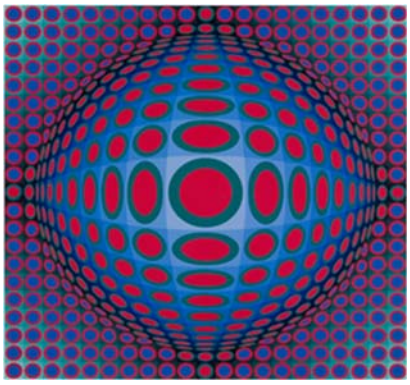

Figure 65. *The DRMF logo.*

A key asset in the development of DRMF context-free semantic content is the utilization of a set of LaTeX macros originally created for the NIST Digital Library of Mathematical Functions (DLMF)[46]. These macros were invented by Bruce Miller of ACMD to achieve the encapsulation of semantic information within the NIST DLMF. These macros give us the capability to tie LaTeX commands unambiguously to mathematical functions defined in an OPSF context. There are currently 533 DLMF LaTeX macros, as well as an additional 156 which have been created specifically for the DRMF. All DLMF macros have at least one DLMF web page associated with them, and the goal is to have definition pages for all additional DRMF macros. The committed use of DLMF and DRMF macros guarantees a mathematical and structural consistency throughout the DRMF.

DRMF formula seeding is currently focused on

- DLMF chapters 5 (Gamma Functions), 15 (Hypergeometric Function), 16 (Generalized Hypergeometric Functions and Meijer G-Function), 17 (q-Hypergeometric and Related Functions), 18 (Orthogonal Polynomials), and 25 (Zeta and Related Functions);
- Koekoek, Lesky, and Swarttouw chapters 1 (Definitions and Miscellaneous Formulas), 9 (Hypergeometric Orthogonal Polynomials), and 14 (Basic Hypergeometric Orthogonal Polynomials) [4];
- Koornwinder KLS addendum LaTeX data [5];
- Bateman Manuscript Project (BMP) books [6]; and
- the Wolfram Computational Knowledge of Continued Fractions Project (eCF).[47]

In August, 2014, the DRMF Project obtained permission to use BMP material as seed content for the DRMF from Caltech. Alan Sexton of the Scientific Document Analysis Group, School of Computer Science, University of Birmingham, UK has scanned a copy of the BMP (loaned to us by Caltech) and is developing software to perform mathematical optical character recognition to obtain LaTeX source code.

For the first seed project, the DLMF source already has DLMF macros inserted. However, for the remaining seed projects we are developing Python and node.JS software to incorporate DLMF and DRMF macros into the corresponding LaTeX source. Our coding efforts have also focused on extracting formula data from LaTeX source as well as generating DRMF Wikitext. We are developing Python software for the seeding of the eCF project which involves conversion from Mathematica format to DLMF and DRMF macro incorporated LaTeX.

Current and future DRMF MediaWiki development projects include the production of formula output representations (such as semantic LaTeX, MathML,

[46] http://dlmf.nist.gov

[47] http://blog.wolframalpha.com/2013/05/16/computational-knowledge-of-continued-fractions

Mathematica, Maple, and Sage); incorporation of sophisticated DLMF and DRMF macro-related formula search; and the development of capabilities for user community formula input. Our current DRMF servers, both public and development instances, have been deployed using the Wikitech server of the Wikimedia Foundation in San Francisco. We use Labs Vagrant and Puppet to upload our Wikitext pages quickly using PHP importDump.

The DLMF Chapter 25 source has been uploaded to the Wikitech instances as well as the KLS and KLSadd datasets, for a total of 1842 Wikitext pages [7]. This includes one main page, one bibliography page, one common.css page, one DRMF requirements page, two table of contents pages, 76 lists of formulas pages, 124 definition pages, and 1636 formula home pages.

By working with the Artists Rights Society of New York, we have received permission from Foundation Vasarely, to use an image of one of Victor Vasarely's paintings as a DRMF logo; see Figure 65.

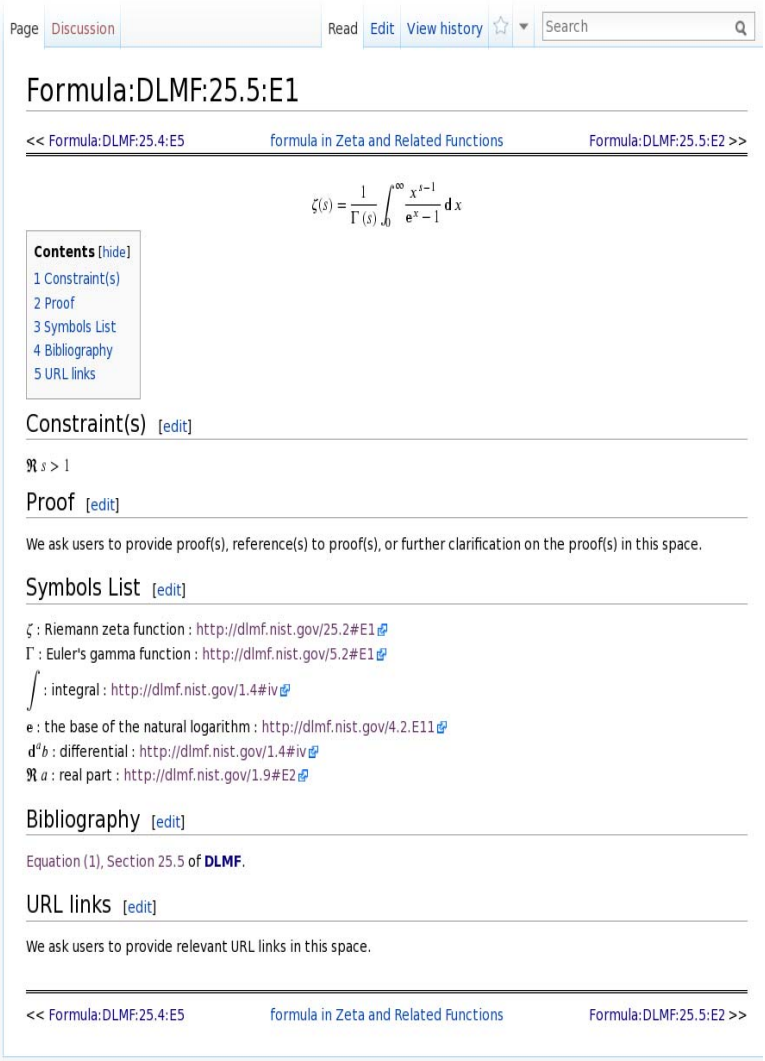

Figure 66. *Sample DRMF formula home page.*

[1] H. S. Cohl, M. A. McClain, B. V. Saunders, M. Schubotz and J. C. Williams, Digital Repository of Mathematical Formulae, *Lecture Notes in Artificial Intelligence* **8543** (2014), Proceedings of the Conferences on Intelligent Computer Mathematics 2014, (S. M. Watt, J. H. Davenport, A. P. Sexton, P. Sojka and J. Urban, eds.), Coimbra, Portugal, July 7-11, 2014, 419-422.

[2] H. S. Cohl, M. A. McClain, B. V. Saunders and M. Schubotz, "Outgrowths of the Digital Library of Mathematical Functions Project, Part II: NIST Digital Repository of Mathematical Formulae," Workshop on Challenges in 21st Century Experimental Mathematical Computation, Institute for Computational and Experimental Research in Mathematics, Providence, Rhode Island, July 2014[48].

[3] H. S. Cohl, M. A. McClain, B. V. Saunders, M. Schubotz, A. Danoff, J. Li, J. Migdall, A. Liu, C. Zou, A. Mohammed and S. Madhu, "XSEDE and the NIST Digital Repository of Mathematical Formulae," XSEDE Science Gateways Community Series, August 2014[49].

[4] R. Koekoek, P. A. Lesky and R. F. Swarttouw, *Hypergeometric Orthogonal Polynomials and their q-Analogues*, Springer Monographs in Mathematics, Springer-Verlag, Berlin, 2010.

[5] T. H. Koornwinder, Additions to the Formula Lists in "Hypergeometric Orthogonal Polynomials and their q-analogues" by Koekoek, Lesky and Swarttouw, arXiv:1401.0815, January 2014.

[6] A. Erdelyi, W. Magnus, F. Oberhettinger and F. G. Tricomi, *Higher Transcendental Functions*, Vols. I, II, III, Robert E. Krieger Publishing Co., Melbourne, FL, 1981.

[7] H. S. Cohl, M. Schubotz, M. A. McClain, B. V. Saunders, C. Y. Zou, A. S. Mohammed and A. A. Danoff, Growing the Digital Repository of Mathematical Formulae with Generic LaTeX Sources, *Lecture Notes in Artificial Intelligence* **9150** (2015), Conference on Intelligent Computer Mathematics, (M. Kerber, J. Carette, C. Kaliszyk and V. Sorge, eds.), 280-287.

[48] http://icerm.brown.edu/video_archive, see Programs and Workshops 2014 → Summer 2014 → Challenges in 21st Century

[49] https://www.youtube.com/watch?v=gAGqr_4AjkI&list=UU6ulv87KV32afXMLv6uWTW

Fundamental Solutions and Expansions for Special Functions and Orthogonal Polynomials

Howard S. Cohl
Roberto S. Costas-Santos (University of Alcalá)
Hans Volkmer (University of Wisconsin-Milwaukee)
Gestur Olafsson (Louisiana State University)
Michael A. Baeder (Citigroup Inc.)
Rebekah M. Palmer (Johns Hopkins University)
Jessica E. Hirtenstein (American University)
Philbert R. Hwang (University of Maryland)
Wenqing Xu (Caltech)
Sean J. Nair (Montgomery Blair High School)

The concept of a function expresses the idea that one quantity (the input) completely determines another quantity (the output). Our research concerns special functions and orthogonal polynomials. A special function is a function that has appeared in the mathematical sciences so often that it has been given a name. Green's functions (named after the British mathematician George Green, who first developed the concept in the 1830s) describe the influence of linear natural phenomena such as electromagnetism, gravity, heat and waves. For example, in electrostatics, a Green's function describes the influence of a point charge, called the source, over all of space. The inputs for Green's functions are all of space (with the exception of a singular region), and the output is the "force" exerted from the point throughout space. Green's functions are fundamental to the study of partial differential equations and provide a powerful mechanism for obtaining their solutions.

We investigate fundamental solutions (Green's functions) of linear partial differential equations on highly symmetric Riemannian manifolds (harmonic, rank-one symmetric spaces) such as real, complex, quarternionic, and octonionic Euclidean, hyperbolic, and projective spaces. Our recent focus has been on applications of fundamental solutions for linear elliptic partial differential operators on spaces of constant curvature. For instance, we have recently submitted a paper which derives fundamental solution expansions (azimuthal Fourier and Gegenbauer) with applications to Newtonian potential theory on d-dimensional spaces of constant positive curvature, namely hyperspherical geometry [1]. We have also recently had success in constructing closed-form expressions of a fundamental solution for the Helmholtz equation is d-dimensional spaces of constant negative curvature, namely the hyperboloid model of hyperbolic geometry, in terms of associated Legendre functions. We continue our ongoing discussion on the harmonic analysis of fundamental solutions for Laplace's equation on rank one symmetric spaces of compact and noncompact type with Gestur Olafsson (Louisiana State University).

In [2] we derived eigenfunction expansions for a fundamental solution of Laplace's equation in 3-dimensional Euclidean space in one of the most general orthogonal asymmetric confocal cyclidic coordinate systems which admit solutions through separation of variables, 5-cyclide coordinates. The harmonics in this coordinate system are given by products of solutions of second-order Fuchsian ordinary differential equations with five elementary singularities. The Dirichlet problem for the global harmonics in this coordinate system is solved using multiparameter spectral theory in the regions bounded by the asymmetric confocal cyclidic coordinate surfaces.

In the following sequence of papers, we derive specializations and generalizations of generalized and basic hypergeometric orthogonal polynomial generating functions as well as corresponding definite integrals using orthogonality.

- In [3] we derive generalized generating functions for continuous hypergeometric orthogonal polynomials, namely Wilson, continuous Hahn, continuous dual Hahn, and Meixner-Pollaczek polynomials.
- In [4] we presented an open problem on a very-well-poised ${}_9F_8$ generalized hypergeometric series which was presented at OPSFA12.
- In [6] we present the power collection method for hypergeometric orthogonal polynomials, and summarize for which orthogonal polynomials in the Askey and q-Askey schemes, it can be applied. We apply the power collection method to Meixner polynomials and compute a series of connection and connection-type relations for these orthogonal polynomials. We also apply these connection and connection-type relations to generating functions for Meixner and Krawtchouk polynomials.
- In [7] we present contour integral orthogonality relations for the Al-Salam-Carlitz polynomials which is valid for arguments in the complex plane and complex-valued parameters. We also compute generalized generating functions for the Al-Salam-Carlitz polynomials using connection relations for these polynomials.
- In [8] we derive definite integrals for Bessel functions of the first kind by applying the method of integral transforms (Hankel transform) to know definite integrals which are found in famous compendia of definite integrals.
- In [9] we derive explicit bounds of convergence for an integral addition theorem due to Magnus which expresses a Kummer confluent hypergeometric function of the second kind $U(x+y)$ as an integral over a product of U with argument x and U with argument y. We also show how this integral addition theorem can also be expressed in terms of modified parabolic cylinder functions, Hankel, Macdonald, and Bessel

functions of the first and second kind with order zero and one.

There are several connections with conferences for this project. For instance, Cohl served on both the scientific and local organizing committees for the 13th International Symposium on Orthogonal Polynomials, Special Functions and Applications which was held on June 1-5, 2015 at NIST. Cohl is also serving on the Scientific and Local Organizing committees for the Orthogonal Polynomials and Special Functions Summer School 6 (OPSF-S6) workshop to be held on June 17-23, 2016 at the Norbert Wiener Center for Harmonic Analysis and Applications at the University of Maryland. The OPSF-S6 summer school is being co-organized with Daniel Lozier, Mourad Ismail, Kasso Okoudjou, John Benedetto, Stephen Casey, Erik Koelink, Ahmed Zayed and Willard Miller, Jr.

[1] H. S. Cohl and R. M. Palmer, Fourier and Gegenbauer Expansions for a Fundamental Solution of Laplace's Equation in Hyperspherical Geometry, *Symmetry, Integrability and Geometry: Methods and Applications*, **11**:015 (2015).

[2] H. S. Cohl and H. Volkmer, Expansions for a Fundamental Solution of Laplace's Equation on $\mathbf{R}^3$ in 5-cyclidic Harmonics, *Analysis and Applications* **12**:6 (2014), 613-633. (Special Issue Dedicated to the Memory of Frank Olver).

[3] M. A. Baeder, H. S. Cohl and H. Volkmer, Generalizations of Generating Functions for Higher Continuous Hypergeometric Orthogonal Polynomials in the Askey Scheme, *Journal of Mathematical Analysis and Applications* **427**:1 (2015), 377-398.

[4] C. Berg, M. J. Atia and H. S. Cohl, A. Swaminathan and W. Van Assche, Open problems at OPSFA-12 Sousse, Tunisia, *Integral Transforms and Special Functions* **26**:2 (2015), 90-95.

[5] H. S. Cohl, R. S. Costas-Santos and P. R. Hwang, Generalizations of Generating Functions for Basic Hypergeometric Orthogonal Polynomials, in review.

[6] H. S. Cohl, R. S. Costas-Santos, and W. Xu, The Power Collection Method for Connection Relations: Meixner Polynomials, in review.

[7] H. S. Cohl, R. S. Costas-Santos and W. Xu, The orthogonality of Al-Salam-Carlitz Polynomials for Complex Parameters, in review.

[8] H. S. Cohl, S. J. Nair and R. M. Palmer, Some Dual Definite Integrals for Bessel Functions, in review.

[9] H. S. Cohl, J. E. Hirtenstein and H. Volkmer, Convergence of Magnus Integral Addition Theorems for Confluent Hypergeometric Functions, in preparation.

Part IV

Activity Data

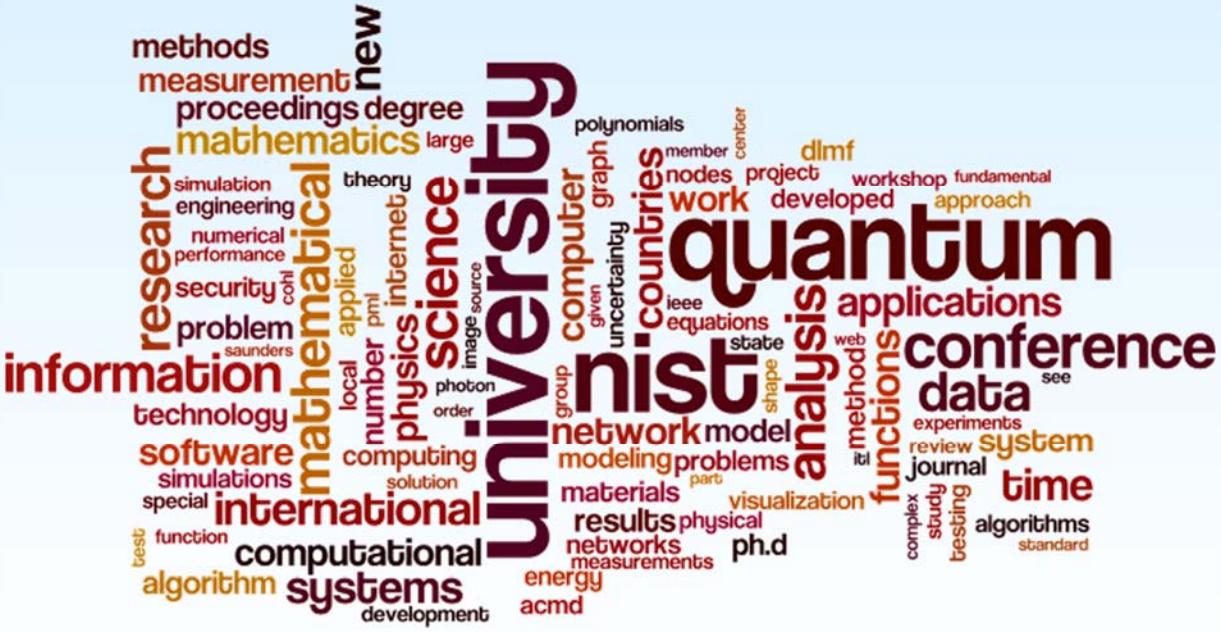

Publications

Note: Names of (co-)authors with a Division affiliation during this reporting period are underlined.

Appeared

Refereed Journals

1. B. Alpert, M. Balata, D. Bennett, M. Biasotti, C. Boragno, C. Brofferio, V. Ceriale, D. Corsini, P.K. Day, M. De Gerone, R. Dressler, M. Faverzani, E. Ferri, J. Fowler, F. Gatti, A. Giachero, J. Hays-Wehle, S. Heinitz, G. Hilton, U. Köster, M. Lusignoli, M. Maino, J. Mates, S. Nisi, R. Nizzolo, A. Nucciotti, G. Pessina, G. Pizzigoni, A. Puiu, S. Ragazzi, C. Reintsema, M. Ribeiro-Gomes, D. Schmidt, D. Schumann, M. Sisti, D. Swetz, F. Terranova and J. Ullom, HOLMES: The Electron Capture Decay of ^{163}Ho to Measure the Neutrino Mass with sub-eV Sensitivity, *European Physics Journal C* **75**:3 (2015), 112. DOI: 10.1140/epjc/s10052-015-3329-5

2. D. A. Anderson, J. D. Benson, A. J. Kearsley, Foundations of Modeling in Cryobiology-I: Concentration, Gibbs Energy, and Chemical Potential Relationships, *Cryobiology,* **69** (2015), 349-360. DOI: 10.1016/j.cryobiol.2014.09.004

3. A. Anandkumar, D. P. Foster, D. Hsu, S. M. Kakade and Y.-K. Liu, A Spectral Algorithm for Latent Dirichlet Allocation, *Algorithmica* **72**:1 (2015), 193-214. DOI: 10.1007/s00453-014-9909-1

4. M. A. Baeder, H. S. Cohl and H. Volkmer, Generalizations of Generating Functions for Higher Continuous Hypergeometric Orthogonal Polynomials in the Askey Scheme, *Journal of Mathematical Analysis and Applications* **427**:1 (2015), 377-398. DOI: 10.1016/j.jmaa.2015.01.074

5. C. Berg, M. J. Atia, H. S. Cohl, A. Swaminathan and W. Van Assche, Open Problems, Special Issue on OPSFA12, Sousse, Tunisia, *Integral Transforms and Special Functions* **26**:2 (2015), 90-95. DOI: 10.1080/10652469.2014.973193

6. I. Brezinova, A. U. J. Lode, A. I. Streltsov, L. S. Cederbaum, O. E. Alon, L. A Collins, B. I. Schneider and J. Burgdörfer, Elastic Scattering of a Bose-Einstein Condensate at a Potential Landscape, *Journal of Physics: Conference Series* **488** (2014), 012032. DOI: 10.1088/1742-6596/488/1/012032

7. T. Burns, S. P. Mates, R. L. Rhorer, E. P. Whitenton and D. Basak, Inverse Method for Estimating Shear Stress in Machining, *Journal of the Mechanics and Physics of Solids,* **86** (2016), 220-236. DOI: 10.1016/j.jmps.2015.10.008

8. A. S. Carasso, Stable Explicit Time Marching in Well-posed or Ill-posed Nonlinear Parabolic Equations. *Inverse Problems in Science and Engineering*, 2015, 21 pages. DOI: 10.1080/17415977.2015.1110150

9. B. G. Christensen, A. Hill, P. G. Kwiat, E. Knill, S. W. Nam, K. Coakley, S. Glancy, L. K. Shalm and Y. Zhang, Analysis of Coincidence-time Loopholes in Experimental Bell Tests, *Physical Review A* **92**:3 (2015), 032130. DOI: 10.1103/PhysRevA.92.032130

10. H. S. Cohl and R. M. Palmer, Fourier and Gegenbauer Expansions for a Fundamental Solution of Laplace's Equation in Hyperspherical Geometry, *Symmetry, Integrability and Geometry: Methods and Applications* **11**:015 (2015). DOI: 10.3842/SIGMA.2015.015

11. H. S. Cohl and H. Volkmer, Expansions for a Fundamental Solution of Laplace's Equation on R^3 in 5-cyclidic Harmonics, *Analysis and Applications* **12**:6 (2014), 613-633. DOI: 10.1142/S0219530514500407

12. J. Diemunsch**,** M. Ferrara**,** S. Jahanbekam and J. Shook, Extremal Theorems for Degree Sequence Packing and the Two-Color Discrete Tomography Problem, *SIAM Journal on Discrete Mathematics* **29**:4 (2015), 2088-2099. DOI: 10.137/140987912

13. A. Eberle, N. Martys, L. Porcar, S. Kline, W. George, J. Kim, P. Butler and N. Wagner, Shear Viscosity and Structural Scalings in Model Adhesive Hard-Sphere Gels, *Physical Review E*, **89**, 050302R (2014). DOI: 10.1103/PhysRevE.89.050302

14. S. Fackler, M. Donahue, T. Gao, P. N. A. Nero, S. W. Cheong, J. Cumings and I. Takeuchi, Locally Controlled Magnetic Anisotropy in Transcritical Permalloy Thin Films Using Ferroelectric, *Applied Physics Letters* **105** (2014), 212905. DOI: 10.1063/1.4902809

15. C. Ferraris, N. Martys and W. George, Development of Standard Reference Materials for Rheological Measurements of Cement-Based Materials, *Cement and Concrete Composites* **54** (2014), 29-33. DOI: 10.1016/j.cemconcomp.2014.01.008

16. J. W. Fowler, B. Alpert, W. B. Doriese, D. A. Fischer, C. Jaye, Y. I. Joe, G. C. O'Neil, D. S. Swetz and J. N. Ullom, Microcalorimeter Spectroscopy at High Pulse Rates: a Multi-Pulse Fitting Technique, *Astrophysical Journal Supplement Series* **219** (2015), 35. DOI: 10.1088/0067-0049/219/2/35

17. Z. Gimbutas and L. Greengard, Computational Software: Simple FMM Libraries for Electrostatics, Slow Viscous Flow, and Frequency-Domain Wave Propagation, *Communications in Computational Physics*, **18:2** (2015), 516-528. DOI: 10.4208/cicp.150215.260615sw

18. Z. Gimbutas and L. Greengard, A Fast Multipole Method for The Evaluation of Elastostatic Fields in a Half-Space with Zero Normal Stress, *Advances in Computational Mathematics*, **42:**1 (2016), 175 - 198. DOI: 10.1007/s10444-015-9416-1

19. Z. Gimbutas, L. Greengard and S. Veerapaneni, Simple and Efficient Representations for the Fundamental Solutions of Stokes Flow in a Half-space, *Journal of Fluid Mechanics*, **776** (2015), R1, 10 pages. DOI: 10.1017/jfm.2015.302

20. W. Griffin and M. Olano, Evaluating Texture Compression Masking Effects Using Objective Image Quality Assesment Metrics, *IEEE Transactions on Visualization and Computer Graphics*, **21**:8 (2015), 970-979. DOI: 10.1109/TVCG.2015.2429576

21. X. Guan, K. Bartschat, L. Koesterke and B. I. Schneider, Effects of Autoionizing States on Two-Photon Double Ionization of the H_2 Molecule, *Journal of Physics: Conference Series* **488** (2014), 032015. DOI: 10.1088/1742-6596/488/3/032015

22. R. Kacker, Probability Distributions and Coverage Probability in GUM, JCGM Documents and Statistical Inference, *Measurement* **65** (2015), 61-70. DOI: 10.1016/j.measurement.2014.12.056

23. A. J. Kearsley, Y. Gadhyan, W. E. Wallace, Stochastic Regression Modeling of Chemical Spectra, *Chemometrics and Intelligent Laboratory Systems* **139**, pp. 26-32 (2015). DOI: 10.1016/j.chemolab.2014.08.002

24. Y. Kemper and I. Beichl, Monte Carlo Methods to Approximate the Chromatic Polynomial, *Congressus Numerantium* **125** (2015), 127-152.

25. E. Knill, S. Glancy, S. W. Nam, K. Coakley and Y. Zhang, Bell Inequalities for Continuously Emitting Sources, *Physical Review A* **91**:3 (2015), 032105. DOI: 10.1103/PhysRevA.91.032105

26. H. S. Ku, W. F. Kindel, F. Mallet, S. Glancy, K. D. Irwin, G. C. Hilton, L. R. Vale and K. W. Lehnert, Generating and Verifying Entangled Itinerant Microwave Fields with Efficient and Independent Measurements, *Physical Review A* **91**:4 (2015), 042305. DOI: 10.1103/PhysRevA.91.042305

27. J. Lawrence, R. Kacker, R. Kessel, Obtaining a Trapezoidal Distribution, *Communications in Statistics Theory and Methods* **44**:21 (2015), 4586 - 4599. DOI: 10.1080/03610926.2013.833239

28. M. Liard, N. Martys, W. George, D. Lootens and P. Hebraud, Scaling Laws for the Flow of Generalized Newtonian Suspensions, *Journal of Rheology* **58** (2014), 1993-2015. DOI: 10.1122/1.4896896

29. A. Luna, G. B. McFadden, M. I Aladjem and K. W. Kohn, Predicted Role of NAD Utilization in the Control of Circadian Rhythms During DNA Damage Response, *PLOS Computational Biology*, **11** (2015), 1004144. DOI: 10.1371/journal.pcbi.1004144

30. H. Mahboubi, K. Moezzi, A. Aghdam and K. Sayrafian, Distributed Deployment Algorithms for Efficient Coverage in a Network of Mobile Sensors with Nonidentical Sensing Capabilities, *IEEE Transactions of Vehicular Technology*, **63**:8 (2014), 3998-4016. DOI: 10.1109/TII.2013.2280095

31. P. Mell, R. Harang and A. Gueye, Measuring Limits on the Ability of Colluding Countries to Partition the Internet, *International Journal of Computer Science: Theory and Application* **3**:3 (2015), 60-73.

32. Y. Mishin, G. B. McFadden, R. F. Sekerka and W. J. Boettinger, A Sharp Interface Model of Creep Deformation in Crystalline Solids, *Physical Review* **B 92** (2015), 064113. DOI: 10.1103/PhysRevB.92.064113

33. W. F. Mitchell and M. A. McClain, A Comparison of *hp*-Adaptive Strategies for Elliptic Partial Differential Equations, *ACM Transactions on Mathematical Software* **41**:1 (2014). DOI: 10.1145/2629459

34. J. L. Molaro, S. Byrne, S. A. Langer, Grain-scale Thermoelastic Stresses and Spatiotemporal Temperature Gradients on Airless Bodies, Implications for Rock Breakdown, *Journal of Geophysical Research: Planets*, **120**:2 (2015), 255-277. DOI: 10.1002/2014JE004729

35. A. K. Nurse, S. Colbert-Kelly, S. R. Coriell and G. B. McFadden, Equilibrium and Stability of Axisymmetric Drops on a Conical Substrate under Gravity, *Physics of Fluids* **27** (2015), 084101. DOI: 10.1063/1.4927697

36. J. Penczek, S. Satterfield, E. Kelley, T. Scheitlin, J. Terrill and P. Boynton, Evaluating the Visual Performance of Stereoscopic Immersive Display Systems, *Presence: Teleoperators and Virtual Environments*, **24**:4 (2015).

37. A Reiman, A. Cerfon, G. B. McFadden, et al., A Cross-Benchmarking and Validation Initiative for Tokamak 3D Equilibrium Calculations, *Nuclear Fusion* **55** (2015), 063026. DOI: 10.1088/0029-5515/55/6/063026

38. L. K. Shalm, E. Meyer-Scott, B. G. Christensen, P. Bierhorst, M. A. Wayne, M. J. Stevens, T. Gerrits, S. Glancy, D. R. Hamel, M. S. Allman, K. J. Coakley, S. D. Dyer, C. Hodge, A. E. Lita, V. B. Verma, C. Lambrocco, E. Tortorici, A. L. Migdall, Y. Zhang, D. R. Kumor, W. H. Farr, F. Marsili, M. D. Shaw, J. A. Stern, C. Abellán, W. Amaya, V. Pruneri, T. Jennewein, M. W. Mitchell, P. G. Kwiat, J. C. Bienfang, R. P. Mirin, E. Knill, S. W. Nam, A

Strong Loophole-free Test of Local Realism, *Physical Review Letters* **115**:25 (2015), 250402. DOI: 10.1103/PhysRevLett.115.250402

39. J. Sifuentes, Z. Gimbutas and L. Greengard, Randomized Methods for Rank-Deficient Linear Systems, *Electronic Transactions on Numerical Analysis*, **44** (2015), 177-188. URL: http://etna.mcs.kent.edu//vol.44.2015/pp177-188.pdf

40. J. Sims and S. Hagstrom, Mathematical and Computational Science Issues in High Precision Hylleraas-Configuration Interaction Variational Calculations: III Four-Electrol Integrals, *Journal of Physics B: Atomic, Molecular and Optical Physics* **48**:17 (2015), 175003. DOI: 10.1088/0953-4075/48/17/175003

41. O. Slattery, L. Ma, P. Kuo and X. Tang, Narrow-linewidth Source of Greatly Non-degenerate Photon Pairs for Quantum Repeaters from a Short Singly Resonant Cavity, *Applied Physics B* **121** (2015), 413-419. DOI: 10.1007/s00340-015-6198-6

42. J. Stoian, T. Oey, J. Huang, A. Kumar, J. Bullard, M. Balonis, S. Satterfield, J. Terrill, N. Neithalath and G. Sant, New Insights into the Prehydration of Cement and its Mitigation, *Cement and Concrete Research*, **70** (2015), 94–103. DOI: 10.1016/j.cemconres.2015.01.012

43. A. Streib, N. Streib, I. Beichl and F. Sullivan, Stratified Sampling for the Ising Model – A Graph Theoretic Approach, *Computer Physics Communications* **191** (2015), 1-8. DOI: 10.1016/j.cpc.2015.01.005

44. J. Torres-Jimenez, I. Izquierdo-Marquez, R. Kacker and D. R. Kuhn, Tower of Covering Arrays, *Discrete Applied Mathematics* (2015), 141–146. DOI: 10.1016/j.dam.2015.03.010

45. J. Torres-Jimenez, N. Rangel-Valdez, R. Kacker and J. Lawrence, Combinatorial Analysis of Diagonal, Box, and Greater-Than Polynomials as Packing Functions, *Applied Mathematics and Information Sciences* **9** (2015), 2757-2766.

46. J. Torres-Jimenez, I. Izquierdo-Marquez, A. Garcia-Robledo, A. Gonzalez-Gomez, J. Bernal and R. Kacker, A Dual Representation Simulated Annealing Algorithm for the Bandwidth Minimization Problem on Graphs, *Information Sciences* **303** (2015), 33–49. DOI: 10.1016/j.ins.2014.12.041

47. F. Vico, M. Ferrando, L. Greengard and Z. Gimbutas, The Decoupled Potential Integral Equation for Time-Harmonic Electromagnetic Scattering, *Communications on Pure and Applied Mathematics*, (2015), 42 pages. DOI: 10.1002/cpa.21585

48. S. Weiss, A. Boliong and H. S. Cohl, Measurement and Analysis of the Lowest Resonant Mode of a Spherical Annular-Sector Patch Antenna, *IET Microwaves, Antennas & Propagation* **9**:2 (2015), 95-100. DOI: 10.1049/iet-map.2014.0163

49. D. H. Yeo and F. A. Potra, Sustainable Design of Reinforced Concrete Structures Through CO2 Emission Optimization, *Journal of Structural Engineering* **141**:3-4 (2015), B4014002, 07015002. DOI: 10.1061/(ASCE)ST.1943-541X.0000888

Journal of Research of NIST

1. J. Bernal and J. Torres-Jimenez, SAGRAD: A Program for Neural Network Training with Simulated Annealing and the Conjugate Gradient Algorithm, *Journal of Research of the NIST* **120** (2015), 113-128. DOI: 10.6028/jres.120.009

2. A. S. Carasso and A. E. Vladar, Recovery of Background Structures in Nanoscale Helium Ion Microscope Imaging, *Journal of Research of the NIST* **119** (2014), 683-701. DOI: 10.6028/jres.119.030

3. A. K. Nurse, S. R. Coriell and G. B. McFadden, On the Stability of Rotating Drops, *Journal of Research of the NIST* **120** (2015), 74-101. DOI: 10.6028/jres.120.007

Book Chapters

1. R. Datla and R. Kacker, Calibration Traceability, Measurement Uncertainty, and Verification and Validations, Chapter 3 in *NIST Handbook 157: Guidelines for Radiometric Calibration of Electro-Optical Instruments for Remote Sensing,* (J. Tansock, ed.), April 2015, 17-30. DOI: 10.6028/NIST.HB.157

2. H. Mahboubi, A. Aghdam and K. Sayrafian, Area Coverage in a Fixed-Obstacle Environment Using Mobile Sensor Networks, *Control and Systems Engineering: A Report on Four Decades of Contributions*, Springer Publishing, 2015.

3. D. Richard Kuhn, R. Bryce, F. Duan, L. Ghandehari, Y. Lei and R. Kacker, Combinatorial Testing: Theory and Practice, Chapter 1 in *Advances in Computers*, Vol. 99, (A. Memon, ed.) Academic Press, Elsevier Inc., 2015.

4. B. I. Schneider, L. A. Collins, X. Guan, K. Bartschat and D. Feder, Time-Dependent Computational Methods for Matter Under Extreme Conditions, in *Advances in Chemical Physics* **157**, Proceedings of the 240 Conference: Science's Great Challenges (A. Dinner, ed.), John Wiley and Sons, 2015.

5. R. F. Sekerka, S. R. Coriell and G. B. McFadden, Morphological Stability, Chapter 14 in *Handbook*

of Crystal Growth, 2nd ed. (T. Nishinaga, ed.), Elsevier, 2015, 595-630.

In Conference Proceedings

1. R. Alléaume, T. Chapuran, C. Chunnilall, I. Degiovanni, N. Lutkenhaus, V. Martin, A. Mink, M. Peev, M. Lucamarini, A. Shields and M. Ward, Worldwide Standardization Activity for Quantum Key Distribution, in *Proceedings of IEEE GlobeCom Workshop on Telecomm Standards, From Research to Standards*, Austin, TX, December 8, 2014, 741-746. DOI: 10.1109/GLOCOMW.2014.7063507
2. M. Barbi, K. Sayrafian and M. Alasti, Inter-BAN Interference Mitigation Using Uncoordinated Transmission Scheduling Strategies, in *Proceedings of COST IC1004*, TD(15), Dublin, Ireland, January 28-30, 2015, 12035.
3. M. Barbi, K. Sayrafian and M. Alasti, Uncoordinated Scheduling Strategies for BAN-to-BAN Interference Mitigation, in *Proceedings of the 2015 IEEE International Conference on Communications and Networking* (BlackSeaCom), Constanta, Romania, May 18-21, 2015. DOI: 10.1109/BlackSeaCom.2015.7185121
4. M. Barbi, K. Sayrafian and M. Alasti, Impact of the Energy Detection Threshold on Performance of the IEEE 802.15.6 CSMA/CA, in *Proceedings of the IEEE Conference on Standards for Communications & Networking* (CSCN'15), Tokyo, Japan, October 28-30, 2015.
5. T. Bednarz, J. Taylor, W. Huang, W. Griffin, S. Satterfield, J. Hagedorn and J. Terrill, High-Performance Visualization in Science and Research, in *Electronic Proceedings of the IEEE Vis 2014*, Paris, France, November 9-14, 2014.
6. D.Budic, D. Simunic and K. Sayrafian, Kinetic-Based Micro Energy-Harvesting for Wearable Sensors, in *Proceedings of the 6th IEEE International Conference on Cognitive infocommunications*, (IEEE CogInfocom), Gyor, Hungary, October 19-21, 2015.
7. J. Bullard, M. Ley, J. Hagedorn, R. Desaymons, W. Griffin, J. Terrill, Q. Hu, S. Satterfield, and P. Gough, Direct Comparisons of 3D Hydration Experiments and Simulations, in *Proceedings of the 6th Advances in Cement-based Materials: Characterization, Processing, Modeling and Sensing*, Manhattan, Kansas, July 20, 2015.
8. S. D. Casey and H. S. Cohl, UWB Signal Processing: Projection, B-Splines, and Modified Gegenbauer Bases, in *Proceedings of the 11th International Conference on Sampling Theory and Applications* (SampTA), 2015.
9. H. S. Cohl, M. Schubotz, M. A. McClain, B. V. Saunders, C. Y. Zou, A. S. Mohammed and A. A. Danoff, Growing the Digital Repository of Mathematical Formulae with Generic LaTeX Sources in *Proceedings of the Conference on Intelligent Computer Mathematics*, *Lecture Notes in Artificial Intelligence* **9150** (2015), (M. Kerber, J. Carette, C. Kaliszyk and V. Sorge, eds.), 280-287.
10. J. Chen, H. Zhao, W. Griffin, J. Terrill and G. Bryant, Validation of SplitVector Encoding and Steroscopy for Quantitative Visualization fo Quantum Physics Data in Virtual Environments, in *Proceedings of the IEEE Virtual Reality 2015 Conference*, Arles, France, March 23 – 27, 2015.
11. M. Dadfarnia, K. Sayrafian, P. Mitcheson and J. Baras, Maximizing Output Power of a CFPG Micro Energy-Harvester for Wearable Medical Sensors, in *Proceedings of the 4th International Conference on Wireless Mobile Communication and Healthcare* (MobiHealth 2014), Athens, Greece, November 2014.
12. G. Dogan, An Efficient Curve Evolution Algorithm for Multiphase Image Segmentation, in *Proceedings of the 10th International Conference of Energy Minimization Methods in Computer Vision and Pattern Recognition* (EMMCVPR'15), Hong Kong, January 2015.
13. G. Dogan, An Efficient Curve Evolution Algorithm for Multiphase Image Segmentation, in *Proceedings of the 5th International Conference on Scale Space and Variational Methods in Computer Vision* (SSVM'15), Bordeaux, France, May 2015.
14. G. Dogan, J. Bernal and C. Hagwood, A Fast Algorithm for Elastic Shape Distances between Closed Planar Curves, in *Proceedings of CVPR 2015* (IEEE Conference on Computer Vision and Pattern Recognition), Boston, MA, June 7-12, 2015, 4222-4230.
15. G. Dogan, J. Bernal and C. Hagwood, FFT-based Alignment of 2D Closed Curves with Application to Elastic Shape Analysis, in *Proceedings of 1st International Workshop on Differential Geometry in Computer Vision for Analysis of Shapes, Images and Trajectories* (DIFF-CV) 2015, British Machine Vision Conference (BMVC) 2015, Swansea, Wales, UK, September 7-10, 2015, 12.1-12.10.
16. F. Duan, L. Yu, Y. Lei, R. Kacker and D. R. Kuhn, Improving IPOG's Vertical Growth Based on a Graph Coloring Scheme, in *Proceedings of 4th International Workshop on Combinatorial Testing in*

Junction with 8th IEEE International Conference on Software Testing, Verification and Validation (ICST 2015), Graz, Austria, April 13-18, 2015.

17. J. T. Fong, J. J. Filliben, N. A. Heckert, P. V. Marcal and R. Rainsberger, Uncertainty Quantification of Stresses in a Cracked Pipe Elbow Weldment using a Logistic Function Fit, a Nonlinear Least Squares Algorithm, and a Super-parametric Method, in *Proceedings of the 14th International Conference on Pressure Vessel Technology (ICPVT-14)*, Shanghai, China, September 23-26, 2015.
18. J. T. Fong, N. A. Heckert, J. J. Filliben, P. V. Marcal and R. Rainsberger, Uncertainty of FEM Solutions Using a Nonlinear Least Squares Fit Method and a Design of Experiments Approach, *Proceedings of the 2015 International COMSOL Users' Conference*, Boston, MA, Oct. 7-9, 2015.
19. L. Ghandehari, J. Chandrasekaran, Y. Lei, R. Kacker and D. R. Kuhn, BEN: A Combinatorial Testing-Based Fault Localization Tool, in *Proceedings of 4th International Workshop on Combinatorial Testing in Junction with 8th IEEE International Conference on Software Testing, Verification and Validation (ICST 2015)*, Graz, Austria, April 13-18, 2015.
20. W. Griffin, D. Catacora, S. Satterfield, J. Bullard and J. Terrill, Incorporating D3.js Information Visualization into Immersive Virtual Environments, in *Proceedings of the IEEE Virtual Reality 2015 Conference*, Arles, France, March 23-27, 2015.
21. A. Gueye, P. Mell, R. Harang, R. La. Defensive Resource Allocations with Security Chokepoints in High-risk IPv6 Networks, in *Proceedings of the 29th Annual IFIP WG 11.3 Working Conference on Data and Applications Security and Privacy*, Fairfax, VA, July 13-15, 2015.
22. J. Hagedorn, J. Bullard, R. Desaymons, W. Griffin, J. Terrill, T. Ley, Q. Hu, S. Satterfield and P. Gough, HydratiCA: A Parallelized Numeric Model of Cement Hydration, in *Proceedings of the Extreme Science Engineering Discovery Environment 2015 Conference* (XSEDE'15), St. Louis, Missouri, July 26-30, 2015.
23. V. Hu, D. F. Ferraiolo, D. R. Kuhn, R. Kacker and Y. Lei, Implementing and Managing Policy Rules in Attribute Based Access Control, in *Proceedings of 16th IEEE International Conference on Information Reuse and Integration (IRI 2015)*, San Francisco, CA, August 13-15, 2015.
24. F. Krahmer and Y. K. Liu, Phase Retrieval Without Small-Ball Probability Assumptions: Stability and Uniqueness, in *Proceedings of the 2015 International Conference on Sampling Theory and Applications (SampTA)*, Washington, DC, May 25-29, 2015.
25. D. R. Kuhn, R. Kacker, Y. Lei and J. Torres-Jimenez, Efficient Verification of Equivalence Classes and Simultaneous Testing Using Two-layer Covering Arrays, in *Proceedings of 4th International Workshop on Combinatorial Testing in Junction with 8th IEEE International Conference on Software Testing, Verification and Validation (ICST 2015)*, Graz, Austria, April 13-18, 2015.
26. R. J. La, Role of Network Topology in Cybersecurity, in *Proceedings of the IEEE Conference on Decision and Control* (CDC), Los Angeles, CA, December 15-17, 2014.
27. M. Liard, N. Martys, W. George, D. Lootens and P. Hebraud, Scaling Laws for the Flow of Non-Newtonian Suspensions, in *Proceedings of the 86th Annual Meeting of the Society of Rheology*, Philadelphia, Pennsylvania, October 5-9, 2014.
28. Y. K. Liu, Privacy Amplification in the Isolated Qubits Model, *Advances in Cryptology - EUROCRYPT 2015*, Sofia, Bulgaria, April 26-30, 2015.
29. Li Ma, M. Stoudt, L. Levine and J. T. Fong, Effect of Grain Size and Grain Boundary Microstructure on Fatigue Crack Nucleation in FCC Polycrystalline Materials, *Proceedings of the 2015 Three Materials Society (TMS) 144th Annual Meeting and Exhibition*, Walt Disney World, FL, March 15-19, 2015.
30. Lijun Ma, O. Slattery, P. Kuo and X. Tang, EIT Quantum Memory with Cs Atomic Vapor for Quantum Communication, in *Proceedings of SPIE*, Vol. 9615, 96150D–1 (2015).
31. Li Ma, J. T. Fong, B. Lane, S. Moylan, J. J. Filliben, N. A. Heckert and L. Levine, Using Design of Experiments in Finite Element Modeling to Identify Critical Variables for Laser Powder Bed Fusion, in *Proceedings of the 26th Annual International Solid Freeform Fabrication Symposium: An Additive Manufacturing Conference*, University of Texas, Austin, Texas, August 10-12, 2015.
32. V. Marbukh, Towards Managing Systemic Risk in Networked Systems, in *Proceedings of the International Conference on Operations Research*, Vienna, Austria, September 1-4, 2015.
33. V. Marbukh, Towards Unified Perron-Frobenius Framework for Managing Systemic Risk in Networked Systems, in *Proceedings of the annual European Safety and Reliability Conference (ESREL)*, Zurich, Switzerland, September 7-10, 2015.

34. V. Marbukh, K. Sayrafian, M. Barbi and M. Alasti, A Regret Matching Strategy Framework for Inter-BAN Interference Mitigation, in *Proceedings of 8th IFIP Wireless and Mobile Networking Conference (WMNC)*, Munich, Germany, October 5-7, 2015.

35. P. V. Marcal, J. T. Fong, R. Rainsberger and L. Ma, Finite Element Analysis of a Pipe Elbow Weldment Creep-Fracture Problem Using an Extremely Accurate 27-node Tri-Quadratic Shell and Solid Element Formulation, in *Proceedings of the 14th International Conference on Pressure Vessel Technology (ICPVT-14)*, Shanghai, China, September 23-26, 2015.

36. P. Mell, R. Harang and A. Gueye, The Resilience of the Internet to Colluding Country Induced Connectivity Disruptions, in *Proceedings of the Workshop on Security of Emerging Networking Technologies* (SENT), San Diego CA, February 8, 2015.

37. W. F. Mitchell, How High a Degree is High Enough for High Order Finite Elements? in *Proceedings of the 2015 International Conference on Computational Science*, Reykjavík, Iceland, June 1-3, 2015. DOI: 10.1016/j.procs.2015.05.235

38. S. Pal and R. J. La, A Simple Learning Rule in Games and Its Convergence to Pure-Strategy Nash Equilibria, in *Proceedings of the American Control Conference*, Chicago, IL, July 1-3, 2015.

39. S. Pal and R. J. La, A Simple Learning in Weakly Acyclic Games and Convergence to Nash Equilibria, in *Proceedings of the Annual Allerton Conference on Communication, Control, and Computing,* Monticello, IL, September 30 – October 2, 2015.

40. B. Saunders, B. Antonishek, Q. Wang and B. Miller, Dynamic 3D Visualizations of Complex Function Surfaces Using X3DOM and WebGL, in *Proceedings of the 20th International Conference on 3D Web Technology (Web3D 2015)*, Crete, Greece, ACM and New York, 2015.

41. M. Schubotz, A. Youssef, V. Markl, H. S. Cohl and J. J. Li, Evaluation of Similarity Measure Factors for Formulae based on the NTCIR-11 Math Task, in *Proceedings of the 11th NTCIR Conference, Tokyo, Japan, December 9-12*, 2014.

42. M. Schubotz, A. Youssef, V. Markl, and H. S. Cohl, Challenges of Mathematical Information Retrieval in the NTCIR-11 Math Wikipedia Task, 2015, in *Proceedings of the 38th Annual ACM Special Interest Group on Information Retrieval Conference* (SIGIR 2015), Santiago, Chile, August 9-13, 2015.

43. O. Slattery, L. Ma, P. Kuo and X. Tang, Comparing the Linewidths from Single-Pass SPDC and Singly-Resonant Cavity SPDC, in *Proceedings of SPIE*, Vol. 9615, 961507–1 (2015).

44. L. Yu, F. Duan, Y. Lei, R. Kacker and D. R. Kuhn, Constraint Handling in Combinatorial Test Generation Using Forbidden Tuples, in *Proceedings of 4th International Workshop on Combinatorial Testing in Junction with 8th IEEE International Conference on Software Testing, Verification and Validation (ICST 2015)*, Graz, Austria, April 13-18, 2015.

Technical Magazine Articles

1. B. Cloteaux, Is This for Real? Fast Graphicality Testing, *Computing in Science & Engineering* **17**:6 (2015), 91-95. DOI: 10.1109/MCSE.2015.125

2. B. I. Schneider, The Impact of Heterogenous Computer Architectures on Computational Physics, *Computing in Science & Engineering* **17**:2 (2015), 9-13. DOI: 10.1109/MCSE.2015.39

3. D. R. Kuhn, R. Kacker and Y. Lei, Combinatorial Coverage as an Aspect of Test Quality, *Crosstalk: the Journal of Defense Software Engineering*, **28**, (March/April 2015), 19-23.

4. J. D. Hagar, T. L. Wissink, D. R. Kuhn and R. Kacker, Introducing Combinatorial Testing in a Large Organization, *IEEE Computer* (April 2015), 64-72. DOI: 10.1109/MC.2015.114

Technical Reports

1. J. Bernal, NEURBT: A Program for Computing Neural Networks for Classification using Batch Learning, NISTIR 8037, February 2015. DOI: 10.6028/NIST.IR.8037

2. R. F. Boisvert (ed.), Applied and Computational Mathematics Division, Summary of Activities for Fiscal Year 2014, NISTIR 8056, April 2015. DOI: 10.6028/NIST.IR.8056

3. S. Kimmel and Y. K. Liu, Quantum Compressed Sensing Using 2-Designs, Arxiv preprint, October 2015. DOI: 1510.08887v1

4. S. A. Langer, A. C. E Reid, F. Y. Congo, R. Lua, V. R. Coffman, gtklogger: A Tool for Systematically Testing Graphical User Interfaces, NIST TN 1862, August 2015. DOI: 10.6028/NIST.TN.1862

Accepted

1. B. Alpert, E. Ferri, D. Bennett, M. Faverzani, J. Fowler, A. Giachero, J. Hays-Wehle, M. Maino, A. Nucciotti, A. Puiu, D. Swetz and J. Ullom, Algorithms for Identification of Nearly-Coincident

Events in Calorimetric Sensors, *Journal of Low Temperature Physics*. DOI: 10.1007/s10909-015-1402-y

2. A. S. Carasso, Stable Explicit Stepwise Marching Scheme in Ill-Posed Time-Reversed Viscous Wave Equations, *Inverse Problems in Science and Engineering*. DOI: 10.1080/17415977.2015.112429
3. J. W. Fowler, B. Alpert, W. B. Doriese, Y. I. Joe, G. C. O'Neil, J. N. Ullom, D. S. Swetz, The Practice of Pulse Processing, *Journal of Low Temperature Physics*. DOI: 10.1007/s10909-015-1380-0
4. R. J. La, Interdependent Security with Strategic Agents and Global Cascades, *IEEE/ACM Transactions on Networking*. DOI: 10.1109/TNET.2015.2408598
5. J. Lawrence, R. Kacker and R. Kessel, Obtaining a Trapezoidal Distribution, *Communications in Statistics: Theory and Methods*. DOI: 10.1080/03610926.2013.833239
6. F. A. Potra, Sufficient Weighted Complementarity Problems, *Computational Optimization and Applications*. DOI: 10.1007/s10589-015-9811-z
7. K. Sayrafian and K. Yazdandoost, Toward 5G Emerging Technologies: Selected Papers from IEEE PIMRC 2014, *International Journal of Wireless Information Networks*.
8. R. Rossini and K. Sayrafian, MAC and Upper Layers in Body Area Networks, in *Cooperative Radio Communications for Green Smart Environments*.
9. K. Sayrafian, Implant Channel Models in Body Area Networks, in *Cooperative Radio Communications for Green Smart Environments*.
10. B. I. Schneider, X. Guan and K. Bartschat, Time Propagation of Partial Differential Equations Using the Short Iterative Lanczos Method and Finite-Element Discrete Variable Representation, *Advances in Quantum Chemistry*.
11. J. C. Wu, A. F. Martin and R. Kacker, Validation of Nonparametric Two-sample Bootstrap in ROC Analysis on Large Datasets, *Communications in Statistics: Simulation and Computation*. DOI: 10.1080/03610918.2015.1065327

In Review

1. D. Anderson, J. Benson, A. Kearsley, Foundations of Modeling in Cryobiology-II: Heat and Mass Transport in Bulk and at Cell Membrane and Ice-Liquid Interfaces.
2. D. Anderson, J. Benson, A. Kearsley, Foundations of Modeling in Cryobiology-III: Heat and Mass Transport in a Ternary System.
3. B. Cloteaux, Fast Sequential Creation of Random Realiozations of Degree Sequences.
4. B. Cloteaux, Forced and Forbidden Edges for Degree Sequences.
5. H. S. Cohl, J. Hirtenstein and H. Volkmer, Convergence of Magnus Integral Addition Theorems for Confluent Hypergeometric Functions.
6. H. S. Cohl, R. S. Costas-Santos and P. R. Hwang, Generalizations of Generating Functions for Basic Hypergeometric Orthogonal Polynomials.
7. H. S. Cohl, R. S. Costas-Santos and W. Xu, The Power Collection Method for Connection Relations: Meixner Polynomials.
8. H. S. Cohl, S. J. Nair and R. M. Palmer, Some Dual Definite Integrals for Bessel Functions.
9. H. S. Cohl, R. S. Costas-Santos and W. Xu, The Orthogonality of Al-Salam-Carlitz Polynomials for Complex Parameters.
10. S. Colbert-Kelly, G. B. McFadden, D. Phillips and J. Shen, A Spectral-Galerkin Method for a Generalized Ginzburg-Landau Equation in a Circular Geometry.
11. S. Fu, W. Cui, M. Hu, R. Chang, M. Donahue, and V. Lomakin, Finite Difference Micromagnetic Solvers with Object Oriented Micromagnetic Framework on Graphics Processing Units.
12. A. Gueye, P. Mell, D. Banse and Y. Congo, On the Internet Connectivity in Africa.
13. F. Y. Hunt, Optimal Spread in Network Consensus Models.
14. F. Y. Hunt, An Algorithm for Identifying Optimal Spreaders in a Random Walk Model of Network Communication.
15. R. Kacker, R. Kessel and J. Lawrence, Removing Divergence of JCGM Documents from the GUM (1993).
16. R. J. La, Effects of Degree Distributions on Network Security and Internalization of Externality.
17. J. Lawrence and R. Kacker, The Pair of Distributions that Brackets a Trapezoidal Distribution.
18. F. Maggioni, F. A. Potra and M. Bertocchi, A Scenario-Based Framework for Supply Planning Under Uncertainty: Stochastic Programming Versus Robust Optimization Approaches.
19. H. Mahboubi, W. Masoudimansour, A. Aghdam and K. Sayrafian, An Energy-Efficient Target Tracking Strategy for Mobile Sensor Networks.

20. H. Mahboubi, W. Masoudimansour, A. Aghdam and K. Sayrafian, Maximum Lifetime Strategy for Target Monitoring with Controlled Node Mobility in Sensor Networks with Obstacles.
21. H. Mahboubi, A. Aghdam and K. Sayrafian, Toward Autonomous Mobile Sensor Networks Technology.
22. P. Mell, R. Harang and A. Gueye, Linear Time Vertex Partitioning on Massive Graphs.
23. S. Mitropoulos, V. Tsiantos, K. Ovaliadis, D. Kechhhrakos and M. Donahue, Stiff Modes in Spin-valve Simulations with OOMMF.
24. S. Pal and R.J. La, Better Reply Dynamics – Convergence under Information Delays and Erroneous Payoff Information.
25. P. N. Patrone, A. Dienstfrey, A. R. Browning, S. Tucker and S. Christensen, Uncertainty Quantification in Molecular Dynamics Studies of the Glass Transition Temperature.
26. P. N. Patrone, T. W. Rosch and F. R. Phelan, Bayesian Calibration of Coarse-Grained Forces: Efficiently Addressing Transferability.
27. C. G. Petra and F. A. Potra, A Homogeneous Model for Monotones Mixed Horizontal Linear Complementarity Problems.
28. R. Pozo, Q-matrix: An Algebraic Formulation for the Analysis and Visual Characterization of Network graphs.
29. B. Saunders, B. Miller, F. Backeljauw, S. Becuwe, M. McClain, D. Lozier, A. Cuyt and A. Dienstfrey, DLMF Tables: A Computational Resource Inspired by the NIST Digital Library of Mathematical Functions.
30. H. Zhao, G. Bryant, W. Griffin, J. Terrill and J. Chen, Validation of SplitVector Encoding and Stereoscopy for Quantitative Visualization of Quantum Physics Data.

Presentations

Invited Talks

1. R. F. Boisvert, "The Role of Publishers in Reproducibility," Panel on Reporting Results and Sharing Study Data, Workshop on Statistical Challenges in Assessing and Fostering the Reproducibility of Scientific Results, National Research Council Committee on Applied and Theoretical Statistics, Washington, DC, February 27, 2015.
2. R. F. Boisvert, "Reproducibility in Computing: The Role of Professional Societies," Bluenose Applied and Computational Mathematics Days Workshop, St. Mary's University, Halifax, NS, Canada, July 11, 2015.
3. A. S. Carasso, "Stabilized Explicit Time-Marching Schemes in Ill-Posed Nonlinear Backward Parabolic Equations," 2015 Inverse Problems Symposium, Michigan State University, East Lansing, MI, May 31 - June 2, 2015.
4. H. S. Cohl, "Fundamental Solutions, Generalized Expansions, and Formulae for Orthogonal Polynomials and Special Functions at NIST," Department of Mathematics, University of Macau, Macau, December 9, 2014.
5. G. Dogan, J. Bernal and C. R. Hagwood, "Fast Algorithms for Shape Analysis of Planar Objects," SIAM Conference of Comptuational Science and Engineering, Salt Lake City, UT, March 14, 2015.
6. G. Dogan, "Lagrangian Shape Optimization for Segmentation of Mulitphase Images," AMMCS-CAIMS Congress of Applied Mathematics, Modeling and Computational Science, Waterloo, Canada, June 11, 2015.
7. M. Donahue, "An Introduction to Micromagnectic Modeling," Orlando, Florida, March 15, 2015.
8. J. T. Fong, "Optimal Design of a Magnetic Resonance Imaging (MRI) Radio Frequency (RF) Coil using Finite Element Method (FEM) and Statistical Design of Experiments (DOE)," Department of Electrical Engineering Seminar, University of Northern Texas, Denton, TX, October 3, 2014.
9. J. T. Fong, "A Design-of-Experiments Approach to FEM Uncertainty Analysis for Optimizing Magnetic Resonance Imaging RF Coil Design," 2014 International COMSOL Users' Conference, Boston, MA, October 9, 2014.
10. J. T. Fong, "Introduction to Statistical Design of Experimetns with a Software Tool," Department of Electrical Engineering, University of Northern Texas, Denton, TX, January 28-30, 2015.
11. J. T. Fong, "Experience in Uncertainty Estimation of FEM Solutions using COMSOL Structural Mechanics, MEMS, and RF Modules," COMSOL Government Symposium, McLean, VA, May 6, 2015.
12. J. T. Fong, "Model-based POD and Fatigue Life Modeling using Modern Statistical Tool," 2015 IEEE 12th Far East Forum on Nondestructive Evaluation and Testing (FENDT), Zhuhai, China, May 29, 2015.

13. J. T. Fong, "Multiaxial Composites Failure Criteria, Uncertainty Propagation, and Estimation of A-basis and B-basis Design Allowables," ASME Applied Mechanics and Materials Division Joint Conference, McMat2015, Seattle, WA, July 1, 2015.
14. J. T. Fong, "Structural Reliability Theory and Software Tools for Composites Design," 10th Composites Design Workshop (CDW-10), Department of Aeronautics and Astronautics, Stanford University, Stanford, CA, July 17, 2015.
15. J. T. Fong, "Uncertainty Quantification of Finite Element Simulations for Creep, Fracture, Fatigue and Crystal Viscoplasticity," Metallurgy Research Laboratories of the French Atomic Energy Commission (CEA), Saclay, France, July 31, 2015.
16. J. T. Fong, "A Fail-Safe Design and Operation Methodology based on a Near-Zero Failure Probability and NDE-informed Damage Tolerance Limit Approach," International Structural Mechanics in Reactor Technology (SMiRT) Conference, Manchester, United Kingdom, August 11, 2015.
17. J. T. Fong, "Uncertainty Quantification of Stresses in a Cracked Pipe Elbow Weldment using a Logistic Function Fit, a Nonlinear Least Squares Algorithm, and a Super-parametric Method, 14th International Conference on Pressure Vessel Technology (ICPVT-14), Shanghai, China, September 24, 2015.
18. Z. Gimbutas and A. Dienstfrey, "A Fast Algorithm for Decaying Complex Exponential Sums," Applied Mathematics & Statistics Colloquium, Colorado School of Mines, Golden, Colorado, March 20, 2015.
19. S. Glancy, "Quantum Information and Statistics at NIST Boulder," US-Korea Workshop on Quantum Information Applications, Los Angeles, CA, November 17, 2014.
20. S. Glancy, "Analysis of Coincidence-Time Loopholes in Experimental Bell Tests," Quantum Theory: from Foundations to Technologies, Växjö, Sweden, June 8, 2015.
21. S. Glancy, "Bell Inequalities for Continuously Emitting Sources," Joint Center for Quantum Information and Computer Science Seminar, College Park, MD, October 28, 2015.
22. F.Y. Hunt, "An Algorithm for Identifying Optimal Spreaders in a Random Walk Model of Network Communication," Probability Seminar, Mathematics Department, University of Delaware, November 1, 2015.
23. A. J. Kearsley, "Measurement Science at NIST," SIAM Mid-Atlantic Regional Conference, George Mason University, March 21, 2015.
24. Y. Kemper, "Approximating the Chromatic Polynomial," George Mason University, February 20, 2015.
25. Y. Kemper, "From Broken Circuits to Monte Carlo: Approximating the Chromatic Polynomial and its Friends", Workshop on New Directions for the Tutte Polynomial: Extensions, Interrelations, and Applications, Royal Holloway University of London, Egham, England, July 11, 2015.
26. R. J. La, "Convergence of a Class of Simple Learning Rules to Pure-strategy Nash Equilibria," Department of Electrical Engineering, University of Southern California, Los Angeles (CA), January 2015.
27. R. J. La, "Convergence to Pure-Strategy Nash Equilibria under Simple Learning Rules and Selection of Resilient Pure-Strategy Nash Equililbria," Department of Electrical Engineering and Computer Science, University of Michigan, Ann Arbor (MI), April 2015.
28. Y. K. Liu, "Tamper-Resistant Cryptographic Hardware in the Isolated Qubits Model," US-Korea Workshop on Quantum Information, Los Angeles, CA, November 17-19, 2014.
29. Y. K. Liu, "Tamper-Resistant Cryptographic Hardware in the Isolated Qubits Model," Southwest Quantum Information and Technology (SQuInT) workshop, Berkeley, CA, February 20, 2015.
30. Lijun Ma, O. Slattery, P. Kuo and X. Tang, "EIT Quantum Memory with Cs Atomic Vapor for Quantum Communication", SPIE: Optics and Photonics, Quantum Communications and Quantum Imaging Xlll, San Diego, CA. August 09, 2015.
31. Li Ma and J. T. Fong, "Effect of Grain Size and Grain Boundary Microstructure on Fatigue Crack Nucleation in FCC Polycrystalline Materials," The 2015 Three Materials Society (TMS) 144th Annual Meeting and Exhibition, Walt Disney World, FL, March 16, 2015.
32. V. Marbukh, "SDN: Systemic Risk Due to Dynamic Load Balancing," Software Defined Networking Internet Research Task Force Working Group (SDN IRTF WG), Honolulu, Hawaii, November 9-14, 2014.
33. W. F. Mitchell, "The NIST Adaptive Mesh Refinement Benchmark Suite", Mathematics Department Numerical Analysis Seminar, University of Maryland, College Park, MD, February 24, 2015.
34. W. F. Mitchell, "30 Years of Newest Vertex Bisection", Thirteenth International Conference of Numerical Analysis and Applied Mathematics, Rhodes, Greece, September 23, 2015.

35. D. G. Porter, "State of Tcl", 21st Annual Tcl/Tk Conference, Portland, OR, November 13, 2014.
36. R. Pozo, "A Network Measure the Analysis and Visualization of Large-scale Graphs," SIAM Workshop on Network Science, Snowbird, UT, May 17, 2015.
37. S. Ressler, "360 Image Creation," CSIRO Conference, Brisbane, Australia, March 2, 2015.
38. S. Ressler, "Image Based WebVR: Creating and Publishing Environments for Browsers and HMDs," Queensland University of Technology, School of Design, February 27, 2015.
39. S. Ressler, "Image Based WebVR: Creating and Publishing Environments for Browsers and HMDs," CSIRO, Canberra and Brisbane, Australia, 2015.
40. B. Saunders, B. Miller, M. McClain, D. Lozier, A. Dienstfrey, A. Cuyt, S. Becuwe and F. Backeljauw, "DLMF Standard Reference Tables on Demand (DLMF Tables)," Minisymposium on Orthogonal Polynomials and Special Functions: Computational Aspects, 2015 International Conference on Orthogonal Polynomials, Special Functions and Applications, NIST, Gaithersburg, MD, June 1, 2015.
41. B. Saunders, "NIST Projects: Graphics in the Digital Library of Mathematical Functions (DLMF) and DLMF Standard Reference Tables on Demand (DLMF Tables)," Careers in Mathematical Sciences Workshop for Underrepresented Groups, IMA, University of Minnesota, Minneapolis, MN, March 29, 2015.
42. B. Saunders, "A Historical Perspective on the 2015 Winner of the Dr. Etta Z. Falconer Award for Mentoring and Commitment to Diversity—Dr. Genevieve Knight," Infinite Possibilities Conference, Oregon State University, Corvallis, Oregon, March 2-3, 2015.
43. K. Sayrafian, "Internet of Things – How to Break the Barriers for Business Development?" IEEE BlackSeaCom, Constanta, Romania, May 20, 2015.
44. J. Shook, "Matrix Scaling: A New Heuristic for the Directed Feedback Vertex Set Problem", Institute for Defense Analysis Center for Computing Sciences, Bowie, MD, November 11, 2014.
45. O. Slattery, L. Ma, P. Kuo and X. Tang, "A Narrowband Source of Correlated Non-degenerate Photon Pairs," SPIE: Optics and Photonics, Quantum Communications and Quantum Imaging Xlll, San Diego, CA. August 09, 2015.
46. O. Slattery, "Status of Narrow Linewidth Source for Quantum Communication Applications," University of Limerick, Department of Physics and Energy, Limerick, Ireland. July 19th, 2015.

Conference Presentations

1. T. J. Burns and B. W. Rust, "Estimation of Shear Stress in Machining by Approximating the Solution of a Volterra Integral Equation of the First Kind," ASME 2015 Applied Mechanics and Materials Conference, McMAT2015, Seattle, WA, June 2015.
2. S. D. Casey and H. S. Cohl, "UWB Signal Processing: Projection, B-Splines, and Modified Gegenbauer Bases," Sampling Theory and Applications 2015 (SampTA 2015), American University, Washington DC, May 25, 2015.
3. H. S. Cohl, "Overview of Digital Mathematics Libraries and the NIST Digital Repository of Mathematical Formulae," 13th International Symposium on Orthogonal Polynomials, Special Functions and Applications, National Institute of Standards and Technology, Gaithersburg, Maryland, June 4, 2015.
4. H. S. Cohl, "Generalizations of generating functions for hypergeometric and q-hypergeometric orthogonal polynomials," International Conference on Applied Mathematics, in honour of Professor Roderick S. C. Wong's 70th birthday, City University of Hong Kong, Hong Kong, China, December 1, 2014.
5. H. S. Cohl, "Newtonian Potential Theory on Hyperspheres," International Conference on Applied Mathematics, in honour of Professor Roderick S. C. Wong's 70th birthday, City University of Hong Kong, Hong Kong, China, December 4, 2014.
6. H. S. Cohl, "Newtonian Potential Theory and Superintegrable Potentials on Hyperspheres," International Conference on Orthogonal Polynomials and q-Series, University of Central Florida, Orlando, Florida, May 10, 2015.
7. G. Dogan, J. Bernal and C. Hagwood, "FFT-based Alignment of 2D Closed Curves with Application to Elastic Shape Analysis," 1st International Workshop on Differential Geometry in Computer Vision for Analysis of Shapes, Images and Trajectories (DIFF-CV) 2015, British Machine Vision Conference (BMVC) 2015, Swansea, Wales, UK, September 10, 2015.
8. G. Dogan, "An Efficient Curve Evolution Algorithm for Muliphase Image Segmentation," 10th International Conference of Energy Minimization

Methods in Computer Vision and Pattern Recognition (EMMCVPR'15), Hong Kong, January 13, 2015.

9. G. Dogan, J. Bernal, C. R. Hagwood, "A Fast Algorithm to Compute Shape Dissimilarity of 2d Curves," DelMar Numerics Day, US Naval Academy, Annapolis, MD, May 9, 2015.
10. M. Donahue, "Implementation of a Localized Fourth Order Demagnetization Tensor," Magnetism and Magnetic Materials Conference, Honolulu, Hawaii, November 5, 2014.
11. A. Gueye, P. Mell, R. Harang and R. La, "Defensive Resource Allocations with Security Chokepoints in High-risk IPv6 Networks," 29th Annual IFIP WG 11.3 Working Conference on Data and Applications Security and Privacy, Fairfax, VA, July 13-15, 2015.
12. Y. Kemper, "Approximating the Chromatic Polynomial", 46th Southeastern International Conference on Combinatorics, Graph Theory, and Computing, March 2, 2015.
13. M. Liard, N. Martys, W. George, D. Lootens and P. Hebraud, "Scaling Laws for the Flow of Non-Newtonian Suspensions," 86th Annual Meeting of the Society of Rheology, Philidelphia, Pennsylvania, October 5-9, 2014.
14. V. Marbukh, "Network Evolution by Preferential Rewiring with Infection Risk Mitigation: Work in Progress," Dynamic Off & On Networks workshop, Santa Fe Complex Systems Institute, December 1-5, 2014.
15. V. Marbukh, "Towards Managing Systemic Risk in Networked Systems, International Conference on Operations Research," Vienna, Austria, September 1-4, 2015.
16. V. Marbukh, "Towards Unified Perron-Frobenius Framework for Managing Systemic Risk in Networked Systems, Annual European Safety and Reliability Conference (ESREL)", Zurich, Switzerland, September 7-10, 2015.
17. S. Mates, E. Vax, R. Rhorer, M. Kennedy, E. Whitenton, S. Banovic, T. Burns, "Dynamic Flow Stress Measurements for Machining Applications", 2014 Annual Conference on Experimental and Applied Mechanics, Greenville, SC, June 2-5, 2014.
18. W. F. Mitchell, "Using Space Filling Curves to Find an Element That Contains a Given Point", SIAM Conference on Computational Science and Engineering, Salt Lake City, UT, March 18, 2015.
19. W. F. Mitchell, "How High a Degree is High Enough for High Order Finite Elements?", International Conference on Computational Science, Reykjavík, Iceland, June 2, 2015.
20. P. N. Patrone, "A Method for Simulated Annealing of Cross-linked Polymers," The Composites and Advanced Materials Expo (CAMX 2015), Dallas Texas, October 28, 2015.
21. S. Ressler, "WebVR What's It All About," Web3D 2015, Heraklion, Greece, June 18-21, 2015.
22. S. Ressler, "Web3D Cultural and Natural Heritage Working Group," Web3D 2015, Heraklion, Greece, June 18-21, 2015.
23. S. Ressler, "Web3D 20 Year History," Web3D 2015, Heraklion, Greece, June 18-21, 2015.
24. S. Ressler, "Web3D Cultural and Natural Heritage Working Group," SIGGRAPH 2015, Los Angeles, California, August 9-13, 2015.
25. S. Ressler, "Using Oculus Rift with your Web Browser for Science," SIGGRAPH 2015, Los Angeles, California, August 9-13, 2015.
26. B. W. Rust, "The Metrology of Type Ia Supernova Lightcurves," 225th Meeting of the American Astronomical Society, Seattle, WA, January 5, 2015.
27. B. W. Rust, M. Pruzhinskaya and B. J. Thijsse, "Calibrating the Decline Rate – Peak Luminosity Relation for Type Ia Supernovae," XXIX General Assembly fo the International Astroniomical Union, Honolulu, HI, August 2015.
28. B. Saunders, "Slices of 3D Surfaces on the Web Using Tensor Product B-Spline Grids," SIAM Conference on Geometric and Physical Modeling (GD/SPM15), Salt Lake City, Utah, October 12, 2015.
29. B. Saunders, "Cutting Edge Information Technology Applied to the NIST Digital Library of Mathematical Functions," MAA MathFest 2015, Washington, D.C., August 8, 2015.
30. B. Saunders, B. Antonishek, Q. Wang and B. Miller, "Dynamic 3D Visualizations of Complex Function Surfaces Using X3DOM and WebGL," 20th International Conference on 3D Web Technology (Web3D 2015), Crete, Greece, June 20, 2015.
31. B. Saunders, "X3DOM/WebGL Visualizations in the NIST DLMF," Web3D Showcase, 20th International Conference on 3D Web Technology (Web3D 2015), Crete, Greece, June 20, 2015.
32. B. Saunders, B. Antonishek, Q. Wang and B. Miller, "State of the Art Visualizations of Complex Function Data," 2015 International Conference on

Orthogonal Polynomials, Special Functions and Applications, NIST, June 4, 2015.

33. B. Saunders, "Adaptive Grid Generation, 3D Graphics on the Web and a Digital Library," Infinite Possibilities Conference, Oregon State University, Corvallis, Oregon, March 2, 2015.
34. K. Sayrafian, "Kinetic-Based Micro Energy-Harvesting for Wearable Sensors," 6th IEEE International Conference of Cognitive Infocommunications, Gyor, Hungary, October 19-21, 2015.
35. K. Sayrafian, "A Regret Matching Strategy Framework for Inter-BAN Interference Mitigation," 8th Wireless and Mobile Networking Conference, Munich Germany, October 5-7, 2015.
36. K. Sayrafian, "Impact of the Energy Detection Threshold on Performance of the IEEE 802.15.6 CSMA/CA," 2015 IEEE Conference of Standards for Communications & Networking, Tokyo, Japan, October 28-30, 2015.
37. K. Sayrafian, "Inter-BAN Interference Mitigation Using Uncoordinated Transmission Scheduling Strategies," COST IC1004, Dublin, Ireland, January 28-30, 2015.
38. K. Sayrafian, "Uncoordinated Scheduling Strategies for BAN-toBAN Interference Mitigation," IEEE BlackSeaCom 2105 Conference, Constanta, Romania, May 18-21, 2015.
39. K. Sayrafian, "Maximizing Output Power of a CFPG Micro Energy-Harvester for Wearable Medical Sensors," 4th International Conference on Wireless Mobile Communication and Healthcare, November 2-5, 2014.
40. B. I. Schneider, "Novel Numerical Approaches to Solving the Time-Dependent Schrödinger's Equation," Concepts of Mathematical Physics in Chemistry, Playa del Carmen, Quintana Roo, México, December 10, 2014.
41. M. Schubotz, H. S. Cohl, M. A. McClain, B. V. Saunders, C. Y. Zou, A. S. Mohammed and A. A. Danoff, "Growing the Digital Repository of Mathematical Formulae with Generic LaTeX Sources," Conference on Intelligent Computer Mathematics, Washington DC, July 17, 2015.
42. J. Shook, "Matrix Scaling: A New Heuristic for the Directed Feedback Vertex Set Problem," 2015 Joint Mathematics Meetings, San Antonio, Texas, January 13th, 2015.

Poster Presentations

1. B. Alpert, E. Ferri, D. Bennett, M. Faverzani, J. Fowler, A. Giachero, J. Hays-Wehle, M. Maino, A. Nucciotti, A. Puiu and J. Ullom, "Algorithms for Identification of Nearly-Coincident Events in Calorimetric Sensors," 16th International Workshop on Low Temperature Detectors, July 21, 2015, Grenoble, France.
2. T. Bednarz, J. Taylor, W. Huang, W. Griffin, S. Satterfield, J. Hagedorn and J. Terrill, High-Performance Visualization in Science and Research, IEEE Vis 2014, Paris, France, November 9-14, 2014.
3. J. Bullard, T. Ley, J. Hagedorn, R. Desaymons, W. Griffin and J. Terrill, "Direct Comparisions of 3D Hydration Experiments and Simulations," 6th Advances in Cement Based Materials Conference, Manhattan, KS, July 20-22, 2015.
4. G. Dogan, "A Pyton Toolbox for Shape Optimization in Image Processing," 10th International Conference on Energy Minimization Methods in Computer Vision and Pattern Recognition (EMMCVPR'15), Hong Kong, January 13, 2015.
5. G. Dogan, "A Python Toolbox for Shape Optimization in Imaging and Data Analysis," SIAM Conference on Computational Science and Engineering, Salt Lake City, UT, March 14, 2015.
6. G. Dogan, J. Bernal and C. Hagwood, "Fast Computation of Elastic Shape Distances between 2D Objects," Bioimage Informatics Conference 2015, NIST, October 15, 2015.
7. G. Dogan, "Fast Minimization of Region-based Active Contours Using Shape Hessian," 5th International Conference of Scale Space and Variational Methods in Computer Vision (SSVM'15), Bordeaux, France, June 3, 2015.
8. G. Dogan, J. Bernal and C. R. Hagwood, "A Fast Algorithm for Elastic Shape Distances Between Closed Planar Curves," IEEE Conference on Computer Vision and Pattern Recognition (CVPR'15), Boston, MA, June 9, 2015.
9. S. Glancy, "Maximum Likelihood Estimation of Gaussian Quantum States," Southwest Quantum Information Technology Workshop, Berkeley, CA, February 19, 2015.
10. W. Griffin, D. Catacora, S. Satterfield, J. Bullard and J. Terrill, "Incorporating 3D Information Visualization into Immersive Virtual Environments," VR2015 IEEE Virtual Reality, Arles, Camargue, Provence France, March 23-27, 2015.
11. J. Hagedorn, J. Bullard, R. Desaymons, W. Griffin, J. Terrill, T. Ley, Q. Hu, S. Satterfield and P. Gough, "HydratiCA: A Parallelized Numeric

Model of Cement Hydration," XSEDE 2015 Extreme Science Engineering Discovery Environments, St. Louis, MO, July 26-30, 2015.

12. F. Y. Hunt, "An Optimization Problem Arising from a Random Walk on an Undirected Graph," Workshop on Convexity and Optimization: Theory and Applications, Institute for Mathematics and its Applications, University of Minnesota, Minneapolis, MN, February 24, 2015.
13. P. Kuo, J. S. Pelc, O. Slattery, L. Ma and X. Tang, "Domain-engineered PPLN for Generation of Polarization-entangled Photons," 2015 SPIE Photonics West, San Francisco, CA, February 11, 2015.
14. V. Marbukh, "On Managing Cost/Benefit Connectivity Tradeoff in a Networked Infrastructure Susceptible to Adverse Cascades," International Conference on Network Science (NetSci), Zaragoza, Spain, June 1-5, 2015.
15. W. F. Mitchell, "NIST AMR Benchmarks", SIAM Conference on Computational Science and Engineering, Salt Lake City, UT, March 15, 2015.
16. O. Slattery, L. Ma, P. Kuo and X. Tang "Narrow Source of Greatly Non-degenerate Correlated Photon Pairs from a Singly Resonant Cavity," 7th Single Photon Workshop, University of Geneva, Geneva, Switzerland, July 14, 2015.
17. X. Tang, "An Overview of Quantum Repeater Research at NIST," Workshop for Quantum Repeaters and Networks, Pacific Grove, California, May 15-17, 2015.
18. X. Tang, O. Slattery, L. Ma, P. Kuo, A. Mink, "Quantum Repeater Research at NIST", SPIE Optics and Photonics 2015, (9615-32) San Diego, California, 9-13 August 2015.

Web Services

1. *Adaptive Mesh Refinement Benchmark Problems*[50]: a collection of partial differential equations suitable for testing and benchmarking adaptive mesh refinement algorithms and software.
2. *Digital Library of Mathematical Functions*[51]: a repository of information on the special functions of applied mathematics.
3. *DLMF Standard Reference Tables on Demand*[52]: an online service providing tables of values for special functions, with guaranteed accuracy to high precision.
4. *Guide to Available Mathematical Functions*[53]: a virtual repository of mathematical software components. (dormant)
5. *Matrix Market*[54]: a repository of matrices for testing of algorithms and software for numerical linear algebra. (dormant)
6. *μMAG*[55]: a collection of micromagnetic reference problems and submitted solutions
7. *Quantum Algorithm Zoo*[56]: a comprehensive catalog of quantum algorithms
8. *SciMark*[57]: a benchmark for scientific computing in Java. (dormant)

Software Released

1. *CCM Combinatorial coverage measurement*[58]: Java version with support of constraints. D. R. Kuhn, R. Kacker
2. *PHAML*[59]: Solution of elliptic partial differential equations using finite elements, hp-adaptive refinement, and multigrid methods. Version 1.15.0. W. F. Mitchell
3. *OOF2*[60]: Two dimensional finite element analysis of materials with complex microstructures. Version 2.1.12. S.A. Langer, A.C.E. Reid, F.Y. Congo, L. Zhang.
4. *OOF3D*[61]: Three dimensional finite element analysis of materials with complex microstructure. Version 3.0.1. S.A. Langer, A.C.E. Reid, F.Y. Congo, L. Zhang.
5. *OOMMF*[62]: Micromagnetics software suite. Version 1.2a6. M. Donahue and D. G. Porter
6. *Tcl/Tk*[63]: Extensible scripting language and GUI toolkit. Versions 8.5.17, 8.5.18, 8.6.3, 8.6. D. G. Porter

[50] http://math.nist.gov/amr-benchmark
[51] http://dlmf.nist.gov/
[52] http://dlmftables.uantwerpen.be/
[53] http://gams.nist.gov/
[54] http://math.nist.gov/matrixmarket/
[55] http://www.ctcms.nist.gov/~rdm/mumag.org.html
[56] http://math.nist.gov/quantum/zoo/
[57] http://math.nist.gov/scimark/
[58] http://csrc.nist.gov/groups/SNS/acts/coverage_measure.html
[59] http://math.nist.gov/phaml/
[60] http://www.ctcms.nist.gov/oof/oof2/
[61] http://www.ctcms.nist.gov/oof/oof3d/
[62] http://math.nist.gov/oommf
[63] https://www.tcl.tk/software/tcltk/

7. *Itcl*: C++ inspired Object Oriented commands for Tcl. Versions 3.4.2, 4.0.2, 4.0.3. D. G. Porter.
8. *Thread*[64]: Thread management commands for Tcl. Version 2.7.2. D. G. Porter.
9. *TDBC*: Database connection commands for Tcl. Versions 1.0.2, 1.0.3. D. G. Porter.
10. *sqlite3*[65]: Bindings to the SQLite database engine for Tcl. Versions 3.8.7.1, 3.8.8.3, 3.8.9, 3.8.10, 3.8.11.1. D. G. Porter
11. *trofs*[66]: Read-only archive system for Tcl virtual filesystems. Version 0.4.8 D. G. Porter

Conferences, Minisymposia, Lecture Series, Courses

ACMD Seminar Series

Brian Cloteaux served as Chair of the ACMD Seminar Series. There were 36 talks presented during this period; all talks are listed chronologically.

1. J. Edmonds, University of Waterloo, "The Traveling Salesman Problem and P vs. NP: Some 1960s Theoretical Work at NIST On the Complexity of Mathematical Algorithms," October 10, 2015.
2. S. Hartke, University of Nebraska-Lincoln, "Computational Combinatorics: Uniquely Kr-saturated Graphs," October 20, 2014.
3. D. Kahaner, Asian Technology Information Program, "High Performance Computing Development in China," October 21, 2014.
4. Y. Li, Old Dominion University, "Revisit of Monte Carlo Methods on Solving Large-Scale Linear Systems," November 4, 2015.
5. E. Gobet, Ecole Polytechnique, "Rare Event Simulation Using Reversible Shaking Transformations," November 13, 2014.
6. D. Kelly, Courant Institute of Mathematical Sciences, New York University, "Filter divergence and EnKF," December 11, 2014.
7. B. Schneider, ACMD, "The Finite Element Discrete Variable Method (FEDVRM) for Solving the Time-Dependent Schroedinger Equation (TDSE)," December 16, 2014.
8. J. E. Johnson, University of South Carolina, "A Proposed Standard for Representing Numerical Information & A Mathematical Foundation for Networks with Clustering Analysis," January 13, 2015.
9. W. Keyrouz, NIST/ITL Software and Systems Division, "A Hybrid CPU-GPU System for Stitching Large Scale Optical Microscopy Images," February 3, 2015.
10. R. Nochetto, University of Maryland, "Discrete ABP Estimate and Rates of Convergence for Linear Elliptic PDEs in Non-Divergence Form," February 18, 2015.
11. V. Braverman, Johns Hopkins University, "Approximating Large Frequency Moments with $O(n^{1-2/k})$ Bits," February 24, 2015.
12. V. Lomakin, University of California San Diego, "High-Performance Micromagnetic Simulators," March 2, 2015.
13. K. K. Irikura, NIST/MML Chemical Sciences Division, "Attaching Uncertainties to Predictions from Quantum Chemistry Models," March 3, 2015.
14. S. Rump, Hamburg University of Technology, "INTLAB - The Matlab Toolbox for Reliable Computing," March 12, 2015.
15. F. Hunt, ACMD, "A New Approach to Finding Influential Spreaders in a Network," March 24, 2015.
16. R. Mullen, University of South Carolina, "Uncertainty Quantification of Structures with Unknown Probabilistic Dependency," April 3, 2015.
17. S. Margulies, US Naval Academy, "Hilbert's Nullstellensatz and Linear Algebra: An Algorithm for Determining Combinatorial Infeasibility," April 7, 2015.
18. W. Cai, UNC Charlotte, "A Highly Scalable Communication-free Domain Decomposition BIE-WOS (Boundary Integral Equation-Walk on Spheres) Method for Laplace Equations," April 16, 2015.
19. H. Elman, University of Maryland, "Reduced Basis Collocation Methods for Partial Differential Equations with Random Coefficients," April 22, 2015.
20. J. Shook, ACMD, "Degree Sequence Packing with Applications to Discrete Tomography," April 28, 2015.
21. E. Otarola, University of Maryland, "A PDE

[64] https://www.tcl.tk/

[65] http://sf.net/projects/tcl/files/Tcl/

[66] http://math.nist.gov/~DPorter/tcltk/trofs/

Approach to Fractional Diffusion," May 7, 2015.

22. M. Ferrara, University of Colorado Denver, "Realization Problems for Graphic and Hypergraphic Sequences," May 12, 2015.
23. R. Costas-Santos, Universidad de Alcala, "Discovering Discrete Classical Polynomials: First Steps," May 19, 2015.
24. A. Bertozzi, UCLA, "Geometric Graph-Based Methods for High Dimensional Data," May 26, 2015.
25. S. Flammia, University of Sydney, Sparse Quantum Codes with (Almost) Good Distance," June 18, 2015.
26. C. Puelz, Rice University, "Reduced Blood Flow Models: Numerical Methods and Applications," June 25, 2015.
27. M. Mascagni, ACMD, "Convergence Analysis of Monte Carlo Linear Solvers Using the Ulam-Von Neumann Algorithm: Necessary and Sufficient Conditions," June 30, 2015.
28. A. Moorthy, University of Guelph, "Guts, Bugs, and Dietary Fiber - A Mathematical Approach to Studying a Complex Biophysical System," June 17, 2015.
29. P. Diniz, USC Information Science Institute, "Managing Application Resilience: A Programming Language Approach," July 21, 2015.
30. M. Schubotz, Technische Universitat Berlin, "The NIST Digital Repository of Mathematical Formulae and Scalable Math Search," July 24, 2015.
31. C. Witzgall, ACMD, "Determining Primitive Roots," September 15, 2015.
32. D. Simos, SBA Research, "Combinatorial Security Testing: Combinatorial Testing Meets Information Security," September 22, 2015.
33. P. Krajcevski, University of North Carolina, "GPU Focused Image Compression Techniques," October 19, 2015.
34. A. S. Carasso, ACMD, "Taming Explosive Computational Instability: Compensated Explicit Time-Marching Schemes in Multidimensional, Nonlinear, Well-Posed or Ill-Posed Initial Value Problems for Partial Differential Equations," October 29, 2015.
35. R. Evans, Department of Mathematical Sciences, University of Delaware, "Multiple-Component Reactions in Optical Biosensors," November 17, 2015.
36. K. Mills, NIST/ITL Advanced Network Technologies Division, "The Influence of Realism on Congestion in Network Simulations," December 1, 2015.

Shortcourses

1. T. Achim, Summer Lectures in Machine Learning, NIST, Gaithersburg, MD, July-August 2015.

Conference Organization

Leadership

1. H. S. Cohl and D. Lozier, Co-Organizers, Orthogonal Polynomials and Special Functions Summer School 6 (OPSF-S6), Norbert Wiener Center for Harmonic Analysis and Applications, University of Maryland, July 11-15, 2016.
2. W. Griffin, Chair, 2015 ACM SIGGRAPH Symposium on Interactive 3D Graphics and Games, San Francisco, CA, February 27 – March 1, 2015.
3. R. Kacker, Co-Organizer, 4th International Workshop on Combinatorial Testing (IWCT 2015) in Conjunction with ICST 2015, Graz, Austria April 13-18, 2015.
4. Y.-K. Liu, Chair, Steering Committee, International Conference on Quantum Cryptography (QCrypt), 2016.
5. D. Lozier, Co-Chair, Scientific Committee, 13th International Symposium on Orthogonal Polynomials, Special Functions, and Applications (OPSFA-13), Gaithersburg, MD, June 1-5, 2015.
6. B. Miller and A. Youssef, Co-Organizers, 3th International Symposium on Orthogonal Polynomials, Special Functions and Applications (OPSFA), Washington, DC. July 13-17, 2015.
7. P. Patrone and A. Dienstfrey, Co-Organizers, Workshop on Uncertainty Quantification in Materials Modeling[67], Purdue University, West Lafayette, IN. July 28-31, 2015.
8. S. Ressler, Chair and Member, Organizing Committee, Web3D 2015, Crete, Greece, June 18 – 21, 2015.

Committee Membership

9. H. S. Cohl, Member, Scientific Committee, 13th International Symposium on Orthogonal

[67] http://www.ima.umn.edu/2014-2015/SW7.28-31.15/

Polynomials, Special Functions, and Applications (OPSFA-13), Gaithersburg, MD, June 1-5, 2015.

10. F. Y. Hunt, Member, Organizing and Awards Committees, Infinite Possibilities Conference, Oregon State University, Corvallis, OR, March 1-3, 2015.
11. R. Kacker, Member, Program Committee, 8th IEEE International Conference on Software Testing, Verification and Validation, (ICST 2015), Graz, Austria, April 13-18, 2015.
12. P. Kuo, Member, Program Committee (CLEO S&I 4: Nonlinear Optical Technologies), CLEO Conference, May 10-15, 2015.
13. Y.-K. Liu, Member, Program Committee, International Conference on Post-Quantum Cryptography (PQCrypto), 2016.
14. W. F. Mitchell, Member, Scientific Committee, Thirteenth International Conference of Numerical Analysis and Applied Mathematics, (ICNAAM), Rhodes, Greece, September 23-29, 2015.
15. X. Tang, Member, Program Committee, SPIE Conference 9615: Quantum Communications and Quantum Imaging XIII, San Diego, CA. August 09, 2015.

Session Organization

16. T. Bednarz and J. Terrill, Co-Organizers, Bird's of a Feather Session on Immersive Visualization for Science and Research International, 42nd International Conference and Exhibition on Computer Graphics and Interactive Technologies, Los Angeles, CA, August 10, 2015.
17. Y. Parker and J. Terrill, Co-Organizers, NIST Booth, 2014 International Conference for High Performance Computing, Networking, Storage and Analysis, New Orleans, LA, November 17-20, 2014.
18. B. Saunders, Chair, Session on Spline Surfaces, SIAM Conference on Geometric and Physical Modeling (GD/SPM15), Salt Lake City, Utah, October 12, 2015.

Other Professional Activities

Internal

1. R. Boisvert, Member, ITL Diversity Committee.
2. B. Cloteaux, Member, Washington Editorial Review Board.
3. C. Schanzle, Member, Scientific Computing Steering Group.
4. I. Beichl, ITL Co-Director, NIST Summer Undergraduate Research Fellowship Program.
5. S. Glancy, Member, NIST Boulder SURF Committee.
6. S. Glancy, Member, ITL Diversity Committee.

External

Editorial

1. R. F. Boisvert, Associate Editor, *ACM Transactions on Mathematical Software*.
2. R. F. Boisvert, Area Editor (Numerical Analysis, Mathematical Software, and Computational Engineering, Finance, and Science), *Computing Research Repository*.
3. I. Beichl, Member, Editorial Board, *Computing in Science & Engineering*.
4. H. S. Cohl, Co-Editor, OP-SF NET, The Electronic News Net of the SIAM Activity Group on Orthogonal Polynomials and Special Functions.
5. H. S. Cohl, Guest Editor, Special Issue on Orthogonal Polynomials, Special Functions and Applications, *Symmetry, Integrability and Geometry: Methods and Applications*.
6. Z. Gimbutas, Member, Editorial Board, *Advances in Computational Mathematics*.
7. W. F. Mitchell, Editor, *Journal of Numerical Analysis, Industrial and Applied Mathematics.*
8. D. P. O'Leary, Editor-in-Chief, *SIAM Journal on Matrix Analysis and Applications*.
9. D. P. O'Leary, Department Editor, Your Homework Assignment column, *Computing in Science & Engineering*.
10. F. A. Potra, Regional Editor for the Americas, *Optimization Methods and Software*
11. F. A. Potra, Associate Editor, *Journal of Optimization Theory and Applications*
12. F. A. Potra, Associate Editor, *Numerical Functional Analysis and Optimization*
13. F. A. Potra, Associate Editor, *Optimization and Engineering*
14. K. Sayrafian, Associate Editor, *International Journal of Wireless Information Networks*
15. K. Sayrafian, Section Editor, *Cooperative Radio Communications for Green Smart Environments*

16. K. Sayrafian, Guest Editor, *IEEE Wireless Communications*, Special Issue: Mobile Wearable Communications.
17. K. Sayrafian, Guest Editor, *International Journal on Wireless Information Networks*, Special Issue: Toward 5G Emerging Technologies: Selected Papers from IEEE PIMRC 2014.
18. B. I. Schneider, Department Editor (Computer Simulations), *Computing in Science & Engineering.*

Boards and Committees

1. R. F. Boisvert, Member, ACM Publications Board.
2. R. F. Boisvert, Member, International Federation for Information Processing (IFIP) Working Group 2.5 (Numerical Software).
3. R. F. Boisvert, Member, External Advisory Committee, Department of Computer Science, George Washington University.
4. W. George, Member, Argonne National Laboratory, Leadership Computing Facility User Advisory Committee.
5. G. B. McFadden, Member, SIAM Kleinman Prize Selection Committee.
6. G. B. McFadden, Member-at-Large, SIAM Council.
7. D. P. O'Leary, Founding Co-Director, Joint University of Maryland and NIST Center for Quantum Information and Computer Science (QuICS), 2013-2015.
8. D. G. Porter, Member, Tcl Core Team.
9. S. Ressler, Member, Web3D Consortium.
10. S. Ressler, Member, W3C, Declaritive 3D for the WebArchitecture Community Group.
11. B. Saunders, Member, Advisory Board for Degree Programs in Mathematics and Statistics, American University, Washington, D.C.
12. B. Saunders, Member, NSF Panel Selection Committee for Presidential Awards for Excellence in Mathematics and Science Teaching.
13. B. Saunders, Member, MAA Business, Industry, and Government (BIG) Committee.
14. B. Saunders, Webmaster, SIAM Activity Group on Orthogonal Polynomials and Special Functions.
15. B. Saunders, OP-SF Talk listserv Moderator, SIAM Activity Group on Orthogonal Polynomials and Special Functions.
16. K. Sayrafian, Co-Chair and Co-Organizer, IEEE BSN 2015.
17. K. Sayrafian, Member, Quantum Medical Device Interoperablility Project.
18. K. Sayrafian, Member, Wireless Medical Technology Working Group.
19. K. Sayrafian, Member, Advisory Board, National Center for Wearable Technology in Rehabilitation Research.
20. B. I Schneider, Chair, Division of Computational Physics, American Physical Society.
21. B. I Schneider, Member, High End Computing Interagency Working Group, Federal Networking and Information Technology R&D (NITRD) Program.
22. J. Terrill, Co-Organizer, 42nd International Conference and Exhibition on Computer Graphics and Interactive Technologies.
23. J. Terrill, Member, High End Computing Research and Development and Infrastructure Interagency Working Groups, Networking and Information Technology R & D. (NITRD) Program.

Community Outreach

1. A. J. Kearsley, Panelist, Industrial Day, SIAM Mid-Atlantic Regional Conference, George Mason University, March 21, 2015.
2. D. P. O'Leary, Mentor, Association for Women in Mathematics Mentor Network.
3. B. Saunders, Judge (Mathematics), Siemens Competition in Math, Science and Technology, October 9-11, 2015 at Discovery Communications, Silver Spring, MD.
4. B. Saunders, Organizer, Virginia Standards of Learning Tutoring Program, Northern Virginia Chapter (NoVAC) of Delta Sigma Theta Sorority, Inc. and the Dunbar Alexandria-Olympic Branch of the Boys and Girls Clubs of Greater Washington, January-May, 2015.
5. B. Saunders, Mentor, Careers in Mathematical Sciences: Workshop for Underrepresented Groups, Institute for Mathematics and Its Applications, University of Minnesota, Minneapolis, MN March 26-29, 2015.
6. B. Saunders, Mentor, International Baccalaureate Middle Years Program, Francis Scott Key Middle School, Silver Spring, MD, May 21, 2015.
7. D. P. O'Leary, Mentor, Association for Women in Mathematics Mentor Network.

Thesis Direction

1. Z. Gimbutas, Member, Ph.D. Thesis Committee, Sija Hao, Applied Mathematics, University of Colorado, Boulder. Title: *Numerical Methods for Solving Linear Elliptic PDEs: Direct Solvers and High Order Accurate Discretization*. Completed 2015.
2. K. Sayrafian, Member, Ph.D. Thesis Committee, Mehdi Dadfarnia, University of Maryland.
3. K. Sayrafian, Member, Ph.D. Thesis Committee, Bojan Lukovac, University of Zagreb.
4. K. Sayrafian, Member, Ph.D. Thesis Committee, Hamid Mahboubi, Concordia University.
5. X. Tang, Ph.D. Thesis Supervisor, Oliver Slattery, University of Limerick, Ireland.
6. J. Terrill, Member, Thesis Committee, Henan Zhao, University of Maryland Baltimore County.

Awards and Recognition

1. S. Glancy, ITL Outstanding Contribution Award, NIST Information Technology Laboratory, 2015.
2. R. Kacker, Silver Medal (joint award), Department of Commerce, December 10, 2014.
3. E. Knill, Samuel Wesley Stratton Award, NIST, December 2015.
4. Y. K. Liu, ITL Outstanding Conference Paper Award, NIST Information Technology Laboratory, June 15, 2015.
5. D. P. O'Leary, *A Celebration in Honor of Dianne P. O'Leary on the Occasion of her Retirement*, Minisymposium and Banquet, SIAM Conference on Applied Linear Algebra, Atlanta, GA, October 29, 2015.
6. B. Saunders, recognized for 12 years of service as a math tutor, Boys and Girls Clubs of Greater Washington, GEICO and the Washington Wizards, Washington Wizards Basketball game, Verizon Center, December 5, 2014.
7. K. Sayrafian, Bronze Medal, US Department of Commerce, December 2015.
8. X. Tang, O. Slattery, P. Kuo and B. Hershman, Bronze Medal, US Department of Commerce, December 2015.

Grants Received

1. W. George, M. Olano, S. Satterfield, J. Terrill, N. Martys, C. Ferraris and D. Lootens, Rheometer Design for Large-particle Dense Suspensions, DOE Advanced Scientific Computing Research Leadership Computing Challenge, 50 million hours of computer time, IBM Blue Gene Q system (Mira) at Argonne National Laboratory.
2. B. I. Schneider, K. Bartschat and X. Guan, Numerical Solutions to the Time-independent and Time-dependent Schrödinger Equation, NSF XSEDE Program, 8M service units of computer time, Texas Advanced Computer Center Stampede and San Diego Supercomputer Center Comet supercomputers.

Grants Awarded

ACMD awards a small amount of funding through the NIST Measurement Science Grants Program for projects that make direct contributions to its research programs. Often such grants support direct cooperation between an external awardee and ACMD. This year the following new cooperative agreements were initiated.

1. University of Edinburgh: *Rigorous and Presentable Asymptotics for Special Functions and Orthogonal Polynomials*, $687,640 (5 years). PI: Prof. Adri Olde Daalhuis.
2. University of Texas at Arlington: *Combinatorial Testing for Big Data Software*, $375,624 (3 years), PI: Prof. Yu Lei. (Jointly funded by the ITL Computer Security Division.)

External Contacts

ACMD staff members make contact with a wide variety of organizations in the course of their work. Examples of these follow.

Industrial Labs

ActiveState
Boeing Company
CEA Leti (France)
Center for Intergration of Medicine & Innovative Tech
Citigroup, Inc.
FlightAware
Ford Motor Company
Fraunhofer Institute for Computer Graphics Research (Germany)
Jet Propulsion Laboratory
Lockheed Martin
Mechdyne
Memorial Sloan Kettering Cancer Center

Mentor Graphics
Microsoft
One World Terrain Standards Development
Raytheon
Rockwell-Collins
SAS Institute
Schrodinger
Siemens
SIKA Technology (Switzerland)
SINTEF (Norway)
Suisse d'Electronique et Microtechnique (Switzerland)
Synopsys

Government/Non-profit Organizations

Air Force Office of Scientific Research
American Institute of Physics
Argonne National Laboratory
Army Research Laboratory
Association for Computing Machinery
Barcelona Institute of Science and Technology (Spain)
Canadian Institute for Advanced Research (Canada)
CENAM, National Metrology Center (Mexico)
Center for Research and Advanced Studies of the National Polytechnic Institute (Mexico)
Centrum Wiskunde & Informatica (Netherlands)
China Special Equipment Inspection and Res. Inst.
Commonwealth Scientific & Ind. Res. Org. (Australia)
Defense Advanced Research Projects Agency
Department of Energy
Electric Power Research Institute
Food and Drug Administration
IDA Center for Computing Sciences
IDA Center for Communications Research
IEEE Computer Society
IPCMS Strasborg (France)
Johns Hopkins University Applied Physics Lab
Lawrence Livermore National Laboratory
MIT Lincoln Labs
Montgomery County, Maryland
NASA - Cassini MSS Project
NASA Glenn Research Center
NASA Ind. Verification and Validation Facility
National Center for Scientific Research (France)
National Institutes of Health
National Oceanic and Atmospheric Administration
National Physical Laboratory (United Kingdom)
National Renewable Energy Laboratory
National Science Foundation
National Security Agency
Naval Facilities Engineering Command
Nuclear Regulatory Commission
Oak Ridge National Laboratory
Princeton Plasma Physics Laboratory
Pacific Northwest National Laboratory
Sandia National Laboratories
SBA-Research (Austria)
Leibniz-Zentrum für Informatik (Germany)
Smithsonian Institution
Southwest Research Institute
US Army Research Laboratory
U.S. Marine Corps
Web3D Consortium

Universities

American University
Arizona State University
Beijing Institute of Technology (China)
California Institute of Technology
Carnegie Mellon University
China University of Petroleum (China)
City University of Hong Kong (China)
Colorado State University
Concordia University (Canada)
Dalian University of Technology (China)
Dartmouth College
Drake University
Duke University
East Carolina University
East China University of Science and Tech. (China)
Federal University of Rio Grande do Norte (Brazil)
Federal University of Ceará (Brazil)
George Mason University
Georgetown University
George Washington University
Hampton University
Howard University
Imperial College (United Kingdom)
Indiana University
Iowa State University
Khallikote College (India)
Kings College (United Kingdom)
Lanzhou University of Technology (China)
Linköping University (Sweden)
Linnaeus University (Sweden)
Louisiana State University
Lund University (Sweden)
Mahidol University (Thailand)
McLennan Community College
Nanyang University (Singapore)
National University of Singapore (Singapore)
Naval Postgraduate School
Ningbo University (China)
New York University
Northern Illinois Univerisity
Northwestern University
Oregon State University
Oslo University (Norway)
Polytechnic University of Valencia (Spain)
Queensland University of Technology (Australia)
Rochester Institute of Technology
Shandong University (China)
Stanford University
Technical University of Berlin (Germany)
Technical University of Delft (Netherlands)

Technical University of Munich (Germany)
Three Gorges University (China)
Tohoko University (Japan)
Tsinghua University (China)
Tulane University
University of Alcala (Spain)
University of Antwerp (Belgium)
University of Bologna (Italy)
University of British Columbia (Canada)
University of California San Diego
University of California Santa Barbara
University of Campinas (Brazil)
University of Colorado
University of Copenhagen (Denmark)
University of Edinburgh (Scotland)
University of Erlangen-Nuremberg (Germany)
University of Hong Kong (China)
University of Houston
University of Illinois Urbana-Champaign
University of Indiana, Bloomington
Univeristy of Innsbruck (Austria)
University of Iowa
University of Limerick (Ireland)
University of Lisbon (Portugal)
University of Maryland, College Park
University of Maryland, Baltimore County
University of Miami
University of Michigan
University of Moncton (Canada)
University of Nebraska
University of Northern Texas
University of Oulu (Finland)
University of South Carolina
University of Surrey (United Kingdom)
University of Texas, Arlington
University of Toronto (Canada)
University of Waterloo (Canada)
University of Windsor (Canada)
University of Wisconsin-Milwaukee
University of Zagreb (Croatia)
Virginia Polytechnic Institute and State University
Washington University, St. Louis
Worcester Polytechnic University
Yale University
Yokohama National University (Japan)

Part V

Appendix

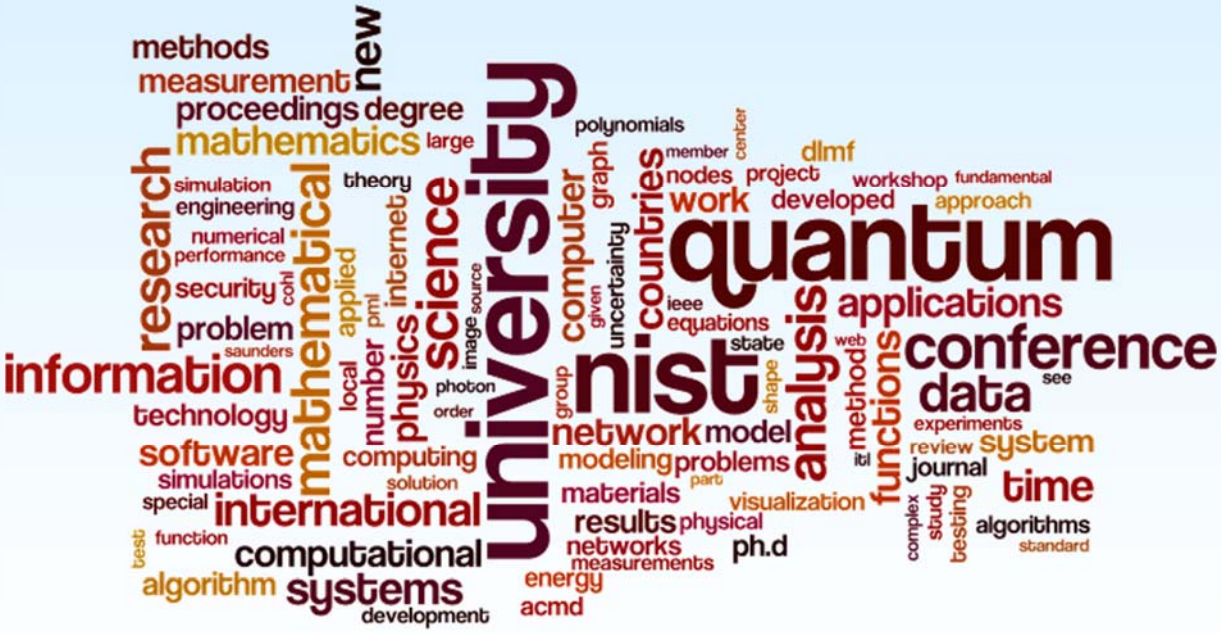

Staff

ACMD consists of full time permanent staff located at NIST laboratories in Gaithersburg, MD and Boulder, CO. This is supplemented with a variety of special appointments. The following list reflects all non-student appointments held during any portion of the reporting period (October 2014 – December 2015). For students and interns, see Staff News on page 10. (*) Denotes staff at NIST Boulder.

Division Staff

Ronald Boisvert, *Chief*, Ph.D. (Computer Science), Purdue University, 1979
Catherine Graham, *Secretary*
Ginger White, *Administrative Assistant*, M.B.A., University of Maryland, 2014.
Lochi Orr, *Administrative Assistant*, Associate (Criminal Justice), Grantham University, 2009
Alfred Carasso, Ph.D. (Mathematics), University of Wisconsin, 1968
Roldan Pozo, Ph.D. (Computer Science), University of Colorado at Boulder, 1991
Kamran Sayrafian-Pour, Ph.D. (Electrical and Computer Engineering), University of Maryland, 1999
Christopher Schanzle, B.S. (Computer Science), University of Maryland Baltimore County, 1989

Mathematical Analysis and Modeling Group

Timothy Burns, *Leader*, Ph.D. (Mathematics), University of New Mexico, 1977
*Bradley Alpert, Ph.D. (Computer Science), Yale University, 1990
*Andrew Dienstfrey, Ph.D. (Mathematics), New York University, 1998
Jeffrey Fong, Ph. D. (Applied Mechanics and Mathematics), Stanford University, 1966
*Zydrunas Gimbutas, Ph.D. (Applied Mathematics), Yale University, 1999
Fern Hunt, Ph.D. (Mathematics), New York University, 1978
Raghu Kacker, Ph.D. (Statistics), Iowa State University, 1979
Anthony Kearsley, Ph.D. (Computational and Applied Mathematics), Rice University, 1996
Geoffrey McFadden, *NIST Fellow,* Ph.D. (Mathematics), New York University, 1979
Paul Patrone, Ph.D. (Physics), University of Maryland, 2013
Bert Rust, Ph.D. (Astronomy), University of Illinois at Urbana-Champaign, 1974

Faculty Appointee (Name, Degree / Home Institution)
Daniel Anderson, Ph.D. / George Mason University
Dianne O'Leary, Ph.D. / University of Maryland College Park
Michael Mascagni, Ph.D. / Florida State University
Florian Potra, Ph.D. / University of Maryland Baltimore County

Guest Researchers (Name, Degree / Home Institution)
Sean Colbert-Kelly, Ph.D. / Noblis
Michael Cromer, Ph.D. / Rochester Institute of Technology
David Gilsinn, Ph.D. / NIST (retired)
Yu (Jeff) Lei, Ph.D. / University of Texas at Arlington
Itzel Dominquez Mendoza / Centro Nacional de Metrología, Mexico
Asha Nurse, Ph.D.
Jose Torres-Jimenez, Ph.D / CINVESTAV, Mexico
Christoph Witzgall, Ph.D. / *NIST Scientist Emeritus*

Mathematical Software Group

Michael Donahue, *Leader* Ph.D. (Mathematics), Ohio State University, 1991
Javier Bernal, Ph.D. (Mathematics), Catholic University, 1980

Howard Cohl, Ph.D. (Mathematics), University of Auckland, 2010
Stephen Langer, Ph.D. (Physics), Cornell University, 1989
Daniel Lozier, Ph.D. (Applied Mathematics), University of Maryland, 1979
Marjorie McClain, M.S. (Mathematics), University of Maryland College Park, 1984
Bruce Miller, Ph.D. (Physics), University of Texas at Austin, 1983
William Mitchell, Ph.D. (Computer Science), University of Illinois at Urbana-Champaign, 1988
Donald Porter, Ph.D. (Electrical Engineering), Washington University, 1996
Bonita Saunders, Ph.D. (Mathematics), Old Dominion University, 1985
Barry Schneider, Ph.D. (Physics), University of Chicago, 1969

Faculty Appointees (Name, Degree / Home Institution)
G.W. Stewart, Ph.D. / University of Maryland College Park
Abdou Youssef, Ph.D. / George Washington University

Guest Researchers (Name, Degree / Home Institution)
Gunay Dogan, Ph.D. / Theiss Research
Adri Olde Daalhuis, Ph.D. / University of Edinburgh
Leonard Maximon, Ph.D. / George Washington University
Mark Pederson, Ph.D. / DOE Office of Science
Jianwei Sun, Ph.D. / Temple University
Qiming Wang / NIST (retired)

Computing and Communications Theory Group

Ronald Boisvert, *Acting Leader*, Ph.D. (Computer Science), Purdue University, 1979
Isabel Beichl, *Project Leader,* Ph.D. (Mathematics), Cornell University, 1981
Brian Cloteaux, Ph.D. (Computer Science), New Mexico State University, 2007
*Scott Glancy, Ph.D. (Physics), University of Notre Dame, 2003
Barry Hershman, A.A. (Electronics Engineering), Capitol College, 1979
Stephen Jordan, Ph.D. (Physics), Massachusetts Institute of Technology, 2008
*Emanuel Knill, *NIST Fellow,* Ph.D. (Mathematics), University of Colorado at Boulder, 1991
Paulina Kuo, Ph.D. (Physics), Stanford University, 2008
Yi-Kai Liu, Ph.D. (Computer Science), University of California, San Diego, 2007
Vladimir Marbukh, Ph.D. (Mathematics) Leningrad Polytechnic University, 1986
James Shook, Ph.D. (Mathematics), University of Mississippi, 2010
Oliver Slattery, Ph.D. (Physics), University of Limerick, 2015
Xiao Tang, *Project Leader,* Ph.D. (Physics), Chinese Academy of Sciences, 1985

NRC Postdoctoral Associates
Yvonne Kemper, Ph.D. (Mathematics), University of California at Davis, 2013

Contractors (Name, Degree / Home Institution)
Alan Mink, Ph.D. / Wagner Resources

Faculty Appointees (Name, Degree / Home Institution)
James Lawrence, Ph.D. / George Mason University

Guest Researchers (Name, Degree / Home Institution)
*Peter Bierhorst, Ph.D. / University of Colorado
*Bryan Eastin, Ph.D. / Northrup Grumman
Assane Gueye, Ph.D. / University of Maryland
Richard La, Ph.D. / University of Maryland
Lijun Ma, Ph.D. / Theiss Research
Francis Sullivan, Ph.D. / IDA Center for Computing Sciences

High Performance Computing and Visualization Group

Judith Terrill, Leader, Ph.D. (Information Technology), George Mason University, 1998
Yolanda Parker, Office Manager
William George, Ph.D. (Computer/Computational Science), Clemson University, 1995
Terence Griffin, B.S. (Mathematics), St. Mary's College of Maryland, 1987
Wesley Griffin, M.S. (Computer Science), University of Maryland Baltimore County, 2010
John Hagedorn, M.S. (Mathematics), Rutgers University, 1980
Sandy Ressler, M.F.A. (Visual Arts), Rutgers University, 1980
Steven Satterfield, M.S. (Computer Science), North Carolina State University, 1975
James Sims, Ph.D. (Chemical Physics), Indiana University, 1969

Faculty Appointees (Name, Degree / Home Institution)
Marc Olano, Ph.D. / University of Maryland Baltimore County

Guest Researchers (Name, Degree / Home Institution)
Tomasz Bednarz, Ph.D. / CSIRO, Australia
Jian Chen, Ph.D. / University of Maryland Baltimore County

Glossary of Acronyms

2D	two-dimensional
3D	three-dimensional
ACM	Association for Computing Machinery
ACMD	NIST/ITL Applied and Computational Mathematics Division
ACTS	Advanced Combinatorial Testing System
AFOSR	Air Force Office of Scientific Research
ALCC	Advanced Leadership Computing Center
API	application programmer's interface
APS	American Physical Society
arXiv	preprint archive housed at Cornell University (http://arxiv.org/)
AS	autonomous system
ASCE	American Society of Civil Engineers
ASCR	Advanced Scientific Computing Research
BAN	body area network
BC	back-off counter
BGP	boarder gateway protocol
BMP	Bateman Manuscript Project
BQP	bounded-error quantum polynomial time
CAC	NIST-NTIA Center for Advanced Communications
CAIDA	Center for Applied Internet Data Analysis
Caltech	California Institute of Technology
CAVE	Cave Automatic Virtual Environment
CCA	clear channel assessment
CCM	Combiatorial Coverage Measurement
CENAM	Center for Metrology of Mexico
CFPG	Coulomb force parametric generator
CG	coarse-grained
CI	configuration interaction
CICM	Conference on Intelligent Computer Mathematics
CINVESTAV	Center for Research and Advanced Studies of the National Polytechnic Institute (Mexico)
CMA	University of Antwerp Computational Mathematics Research Group
CMOS	complementary metal-oxide semiconductor
CNRS	Centre National de la Recherche Scientifique (France)
CNST	NIST Center for Nanoscale Science and Technology
CPU	central processing unit
CSH	calcium silicate hydrate
CT	combinatorial testing
CT	computed tomography
CTL	NIST Communications Technology Laboratory
CY	calendar year
CVS	a source code control system
DLMF	Digital Library of Mathematical Functions
DNA	deoxyribonucleic acid
DOC	Department of Commerce
DOE	U.S. Department of Energy
DPD	dissipative particle dynamics
DRMF	digital repository of mathematical functions
DSO	display shared object
EC	error correction
ED	energy detection
EIT	electromagnetically induced transparency
EL	NIST Engineering Laboratory
ETSI	European Telecommunications Standards Institute
FEDVR	finite element discrete variable method

FEM	finite element method
FFT	fast Fourier transform
FIFO	first-in first-out
FY	fiscal year
GPU	graphics processing units
GUI	graphical user interface
HEC	High End Computing
HEV	high end visualization
HIM	helium ion microscope
HOLMES	a physics experiment
HPCVG	ACMD High Performance Computing and Visualization Group
HTML	hypertext markup language
HVS	human visual system
Hy-CI	Hylleraas-Configuration Interaction technique
ICA	independent component analysis
ICST	International Conference of Software Testing
IDEA	IRIS Development Environment for Applications
IDL	Interactive Data Language
IDS	interdependent security
IEC	International Electrotechnical Commission
IEEE	Institute of Electronics and Electrical Engineers
IFIP	International Federation for Information Processing
IMA	Institute for Mathematics and Its Applications
IMACS	International Association for Mathematics and Computers in Simulation
IMS	Innovations in Measurement Science
IP	internet protocol
IRIS	Interpreted Runtime Immersive Scenegraph
ISG	industry specification group
ISGG	International Society for Grid Generation
ISIMA	Institut Supérieur d'Informatique, de Modélisation et de leurs Applications (France)
ITL	NIST Information Technology Laboratory
ITM	irregular terrain model
ITS	NTIA Institute for Telecommunication Sciences
IVE	immersive visualization environment
JILA	joint NIST-University of Colorado physics research institute
JMONSEL	simulation code used to model electron scattering in materials
JQI	Joint Quantum Institute
KLS	Koekoek, Lesky and Swarttouw
LaTeX	a math-oriented text processing system
LDPC	low density parity check
LiDAR	light detection and ranging
LTE	long-term evolution
MAA	Mathematical Association of America
MathML	Mathematical Markup Language (W3C standard)
MCMC	Monte Carlo Markov Chain
MD	molecular dynamics
MEMS	micro-electro-mechanical system
MHD	magnetohydro-dynamic
MIT	Massachusetts Institute of Technology
MML	NIST Material Measurement Laboratory
MOAs	Multinational ASs
MPI	Message Passing Interface
MQA	mathematical questions answering
MRAM	magneto-resistive random access memory
MRI	magnetic resonance imaging
MSD	mass-spring damper
MSE	mean squared error

muMAG	Micromagnetic Activity Group
NASA	National Aeronautics and Space Administration
NBS	National Bureau of Standards
nCT	nano computed tomography
NIST	National Institute of Standards and Technology
NISTIR	NIST Internal Report
NITRD	Networking and Information Technology Research and Development
NLP	natural language processing
NPSC	National Physical Science Consortium
NRC	National Research Council
NSA	National Security Agency
NSF	National Science Foundation
NTIA	National Telecommunications and Information Administration
NYU	New York University
ODEs	ordinary differential equations
OLED	organic light emitting diode
OOF	Object-Oriented Finite Elements (software)
OOMMF	Object-Oriented Micromagnetic Modeling Framework (software)
OPSF	orthogonal polynomials and special functions
OSG	Open SceneGraph
PDE	partial differential equation
PHAML	Parallel Hierarchical Adaptive Multi Level (software)
PML	NIST Physical Measurement Laboratory
POM	part of math
PoPs	Points of Presence
POS	part of speech
PPLN	periodically poled lithium niobate
PSCR	NTIA Public Safety Communications Research
PSNR	peak signal-to-noise ratio
QBER	quantum bit error rate
QCD	quantum chromodynamics
QD	quantum dot
QDPD	quarternion-based dissipative particle dynamics
QIS	quantum information science
QKD	quantum key distribution
QuICS	UMD-NIST Joint Center for Quantum Information and Computer Science
R&D	research and development
RF	radio frequency
RSA	a public-key cryptosystem
SAE	senior associate editor
SDE	stochastic differential equation
SEM	scanning electron microscope
SFWM	spontaneous four-wave mixing
SHIP	NIST Summer High School Internship Program
Si	Silicon
SIAM	Society for Industrial and Applied Mathematics
SIGGRAPH	ACM Special Interest Group on Graphics
SIS	sequential importance sampling
SPAM	state preparation and measurement
SPDC	spontaneous parametric down-conversion
SPH	smoothed particle hydrodynamics
SPIE	International Society for Optical Engineering
SQUID	superconducting quantum interference device
SRM	standard reference material
SRVF	square root velocity function
SURF	Student Undergraduate Research Fellowship
TACC	Texas Advanced Computing Center

TES	transition edge sensor
TSCM	truncated singular components method
UMBC	University of Maryland Baltimore County
UMD	University of Maryland
UMIACS	University of Maryland Institute for Advanced Computer Studies
UQ	uncertainty quantification
VR	virtual reality
VRML	virtual reality modeling language
W3C	World Wide Web Consortium
WebGL	Web-based Graphics Library
X3D	Extensible 3D
X3DOM	an open-source framework for integrating X3D and HTML5
XSEDE	NSF eXtreme Science and Engineering Discovery Environment
XML	Extensible Markup Language